



Function, localization and evolution of SOSEKI polar proteins

Maritza van Dop

Propositions

1. Autocatalytic protein polymerization is useful in the context of cell polarity across kingdoms of life.
(this thesis)
2. *Arabidopsis* roots contain a radial polarity axis that can be read and interpreted by a variety of proteins.
(this thesis)
3. Gene names can have a profound impact on the public's perception of science.
4. Collection of large datasets is useless without developing methods to extract meaningful results from them.
5. Mental health education should be part of the standard curriculum in high schools.
6. People that lack visual memory learn differently, not necessarily less.

Propositions belonging to the thesis, entitled
Function, localization and evolution of SOSEKI polar proteins

Maritza van Dop
Wageningen, 7th of September 2018

Function, localization and evolution of SOSEKI polar proteins

Maritza van Dop

Thesis committee

Promotor

Prof. Dr D. Weijers
Professor of Biochemistry
Wageningen University & Research

Other members

Prof. Dr C. Testerink, Wageningen University & Research
Dr F. Quattrocchio, Amsterdam University
Prof. Dr L. Strader, Washington University, St. Louis MO, USA
Dr Y. Jaillais, Ecole Normale Supérieure, Lyon, France

This research was conducted under the auspices of the Graduate School of Experimental Plant Sciences.

Function, localization and evolution of SOSEKI polar proteins

Maritza van Dop

Thesis
submitted in fulfilment of the requirements for the degree of doctor
at Wageningen University
by the authority of the Rector Magnificus
Prof. Dr A. P. J. Mol,
in the presence of the
Thesis Committee appointed by the Academic Board
to be defended in public
on Friday 7 September 2018
at 1.30 p.m. in the Aula.

Maritza van Dop

Function, localization and evolution of SOSEKI polar proteins,
174 pages.

PhD thesis, Wageningen University, Wageningen, NL (2018)
With references, with summaries in Dutch and English

ISBN: 978-94-6343-479-9

DOI: <https://doi.org/10.18174/455753>

Table of Contents

Chapter 1

Introduction

7

Chapter 2

Control of oriented cell division in the *Arabidopsis* embryo

19

Chapter 3

SOSEKI polarity determinants reveal mechanisms of supra-cellular polarity in *Arabidopsis*

31

Chapter 4

SOSEKI loss-of-function

57

Chapter 5

Deep evolutionary origin of the polymerizing DIX domain in locally focused protein assemblies

85

Chapter 6

SOSEKI proteins form a polar scaffold that recruits interactors cell edges

115

Chapter 7

General Discussion

149

English Summary

163

Dutch Summary

165

Acknowledgements

167

Curriculum Vitae

169

Publications

170

Education Statement

171

Chapter 1

Introduction

Abstract

The evolution of plants with complex, 3-dimensional body plans required the establishment of an elaborate polarity system. On a cellular level, these polarity cues need to be established, sensed and translated into sub-cellular processes such as cell division and directional transport. Polarly localized plasma membrane (PM) proteins have been described that mark different membrane domains. Their polar localization is mediated by polar delivery, retention and local endocytosis, and may depend on cell wall properties and PM composition. Polar localization of such polarity markers is however often context-dependent and easily altered by drug treatments. Assuming that such treatments do not alter the intrinsic organismal polarity, this suggests that localization of the known polar markers is a readout of a more inert underlying polarity system. Polar cues are also required for other sub-cellular processes, such as asymmetric cell divisions. Yet, the exact mechanisms that translate polarity into sub-cellular processes remain elusive. The *Arabidopsis* embryo is an excellent model for studying cell polarity, as the first polarization events of plant life take place during early embryo development. In this thesis, we aim to gain more insight into the establishment and translation of polarity in plants. To this end, we study the novel SOSEKI (SOK) family of polar proteins that we identified in the embryo. SOK localizes robustly to cell edges in the embryo and root, and we investigate the localization, function and evolution of this family.

Introduction

The transition of plants from water to land and subsequent diversification of species went hand in hand with the evolution of a more complex body plan. The mechanisms involved in development of simple algal forms were probably no longer sufficient to create such body plans. Therefore, establishment of additional directional axes became essential to guide correct placement of cells, tissues and organs relative to the surface of the 3-dimensional organism, or to air or soil. On a cellular level, this polarity is defined as the asymmetric distribution of cellular components (reviewed in Nakamura & Grebe, 2018). Cell polarity is involved in a wide variety of processes, such as instruction of the cell division plane, initiation of local outgrowths, transport of hormones and nutrients, and organization of the cytoskeleton (reviewed in Nakamura & Grebe, 2018; Van Norman, 2016). Yet, how polarity is established, sensed and translated into sub-cellular processes remains largely unclear.

Cell polarity and plasma membrane proteins

Polar localization of plasma membrane (PM) proteins is a striking manifestation of cell polarity. Several proteins have been identified that are enriched on one cell face, while being absent from others. The most well-known and well-studied among these proteins are the PIN auxin transport regulators. PINs display a mostly apical or basal localization that is dynamically regulated (Friml et al., 2004; Gälweiler et al., 1998; Kleine-Vehn et al., 2009; Wisniewska et al., 2006). Nutrient transporters can also be found at the lateral domains of cells. For example, the BOR4 boron exporter (Miwa et al., 2007), the NIP5;1 Boric acid import channel (Takano et al., 2010) and ATP-binding cassette transporter PEN3 (Strader & Bartel, 2009) all localize to the outer membrane in the root. Borate exporter BOR1 is present at the inner face of the cell (Takano et al., 2002, 2010). Not only transporters are localized to lateral sides. The recently described SGN1 protein kinase also accumulates at the outer lateral domain (Alassimone et al., 2016). In leaf epidermal cells, BASL resides at a polar crescent of stomata lineage cells (Dong et al., 2009). Aside from localizing to cell faces, plants display some other remarkable local accumulations of PM proteins. For example, root hair development is preceded by the formation of a ROP-DRP island near the outer-basal side of the cell (Jones, 2002; Molendijk et al., 2001; Stanislas et al., 2015). Outgrowth of the root hair by polar tip growth requires accumulation of many proteins at the tip domain (reviewed in Mendrinna & Persson, 2015). In the endodermis, Caspary strip formation is mediated by the CASP proteins, which form a narrow ring around the middle of the cell (Roppolo et al., 2011).

Many polarly localized membrane proteins are specifically targeted to a face of the cell. Polar delivery is mediated by the Exocyst complex and the trans-Golgi trafficking pathway (reviewed in Nakamura & Grebe, 2018). PINs, ABCG37 and BOR1 are delivered to the middle of their polar membrane domain in a super-polar fashion (Kleine-Vehn et al., 2011; Langowski et al., 2016). Retention mechanisms may help to restrict the proteins to their polar domain. Such mechanisms may rely for example on interaction with the extracellular matrix or association with fixed or slowly moving proteins. Both CASPs and PIN2 have been shown to reside in clusters which could also help to retain or even enhance their polarity (Kleine-Vehn et al., 2011; Roppolo et al., 2011). In addition, local endocytosis and recycling can restrict or sharpen the boundaries of the polar domain (Kleine-Vehn et al., 2011).

Polar markers or polar determinants

Establishment of polar protein accumulation is often referred to as establishment of polarity itself. This is true when one strictly adheres to the definition of ‘uneven distribution of cellular components.’ However, the localization of many polar proteins is quite easily changed when transport substrates or hormones are applied (Geldner et al., 2001; Paciorek et al., 2005; Takano et al., 2010). The same happens when the proteins themselves undergo post-translational modifications (Alassimone et al., 2016; Friml et al., 2004; Michniewicz et al., 2007; Zhang et al., 2015). In addition, polar localization is often coordinated within a tissue or cell type (e.g. Abas et al., 2006), which suggests that directional information on a larger scale feeds into cell polarity. Therefore, it is likely that localization of polar membrane proteins is a readout of a, yet unknown, underlying polarity system, rather than these polar proteins being polarity determinants themselves. However, this does not exclude that (some) polar proteins can be involved in establishing or reinforcing polarity on a tissue level.

To understand how polar proteins are targeted to their specific domains, research has focused on properties of the PM and cell wall. Asymmetric distribution of lipid species in the membrane may provide a directional cue or favor interaction with some proteins over others. Indeed, tips of growing root hairs display sterol accumulation and altered sterol composition has been shown to disturb polar localization of ROP (Ovečka et al., 2010; Stanislas et al., 2015). Phosphoinositides (PIs) are lipid molecules in the membrane that can be phosphorylated on three different positions, which results in a variety of PI species. PIs have many regulatory and signalling functions, and accumulate in different combinations in different membranes. This is thought to provide information about membrane identity and location (reviewed in Noack & Jaillais, 2017). PIs are generated by PIP-kinases and PIP5Ks are involved in polar PIN localization (Ischebeck et al., 2013; Mei et al.,

2012; Tejos et al., 2014). Yet, PIN and PIP5K are polarly localized, but the level of PI polar enrichment varies greatly per line (reviewed in Armengot et al., 2016). PIs and PI Kinases may therefore be involved in PIN localization, but it is unclear if and how they could provide spatial information for all the different polar domains and proteins. An additional question would be how asymmetric lipid and kinase distributions in the membrane are established.

Aside from the PM, the cell wall has also been shown to be essential for polar protein localization. Degradation of the cell wall resulted in complete loss of polarity of PIN2, ABCG36/37 and BOR1, although membrane association was maintained (Langowski et al., 2016). Mutation of CESA3, which is involved in cell wall synthesis, also influenced PIN polarity (Feraru et al., 2011). Direct or indirect physical association with the cell wall could restrict protein movement after polar delivery. Additionally, the cell is not a straight plane, but a 3D shape that can vary greatly. Turgor pressure and the resistance of the cell wall may generate asymmetric mechanical forces on the plasma membrane, which in turn could act as polarity cues. Thus, cell wall and PM properties, as well as polar targeting, retention and recycling all play important roles in cell polarity. It is likely that many of these processes depend and feed back on each other on a cell and tissue level.

Polarity in cell division

Polarity is not only important for polar localization of proteins, but also for morphogenesis. Patterning of complex 3-dimensional plant structures relies on cell division orientation and cell growth, as a rigid wall directly fixes the cell in place. Plants do not have ways to easily move cells and correct division mistakes. Thus, strict control of cell division and growth is essential for land plant development. Research showed that the division machinery can use geometrical properties of the cell to determine division orientation for symmetric divisions (Besson & Dumais, 2011; Minc, et al., 2011; Minc & Piel, 2012; Sahlin & Jönsson, 2010). Additionally, tensile forces within tissues and cells in the shoot meristem were found to direct the position of the division plane (Louveaux et al., 2016). However, such ‘default’ mechanisms may not be enough to create the wide variety of cell patterns found in plants. Additional regulation will be required to ensure that the new cell wall appears in the right place, particularly when initiating a new growth axis, or during asymmetric division. The hormone auxin was shown to be involved in this regulation in the *Arabidopsis* embryo, but how auxin instructs division plane orientation remains to be determined (Yoshida et al., 2014). To position a new cell wall in a specific orientation, the cell division machinery must be able to distinguish apical-basal and radial sides of the cell. Cell polarity is thought to provide these directional cues, although information about how such cues are read and interpreted is still lacking.

The *Arabidopsis* embryo as a model for polarity and pattern formation

The *Arabidopsis* embryo is an excellent model for studying cellular and organismal polarity and tissue patterning. The embryo is a simple structure with few cells that divide and develop in a predictable pattern. It is encased in a seed, which in turn is protected by the silique. As such, embryos are likely less sensitive to environmental changes than other tissues. Before fertilization, the egg cell is polarized with a vacuole at the base and the nucleus at the apex (Mansfield et al., 1991). The vacuole fragments after fertilization and the nucleus loses its apical localization, which leads to a temporary symmetric state of the zygote (Faure et al., 2002; Ueda et al., 2011). Shortly afterwards, apico-basal polarity is established. It is unclear whether directional cues from the egg cell are still present or that polarity is established *de novo* (reviewed in Jeong et al., 2016). The zygote elongates and divides into a small apical cell and a large basal cell. The YODA-MAP kinase pathway has been shown to be important in repolarizing the zygote. Disruption of this pathway leads to retention of the symmetric stage of the zygote, and zygote division is almost symmetrical (Lukowitz et al., 2004; Wang et al., 2007). The transcription factor WRKY2 is also involved in repolarization and asymmetric division of the zygote. Mutants in this gene have zygotes that elongate like WT, but fail to redistribute their organelles in a polar manner (Ueda et al., 2011). As a result, the normally asymmetric first division becomes symmetric. Thus, genetic regulation and sub-cellular signaling are important for early development. Yet, how zygote repolarization and asymmetric division are accomplished exactly, and what polar cues direct cellular reorganization is a subject for further study.

The first division establishes an apical and basal fate for the two resulting cells. This apico-basal axis is maintained throughout embryogenesis and plant development. The basal cell divides symmetrically several times to create the suspensor that connects the proembryo to the maternal tissue. The proembryo divides three times symmetrically, upon which asymmetric divisions are initiated. Genetic perturbations showed that auxin is required to instruct these asymmetric divisions, yet how this hormone influences division is unknown (Yoshida et al., 2014). The first asymmetric division results in an 8-cell proembryo with an apical tier and basal tier. At 16-cell stage, a clear radial axis is established by creating an inner and outer layer. The outer layer will form the protoderm, while the inner layer of the lower tier later becomes subdivided into ground tissue and vasculature precursors. The apical tier divides in a less regular pattern and will form the shoot apical meristem and cotyledons. The most apical cell of the suspensor, the hypophysis, is recruited into the embryo and will later form the Quiescent Center (QC) and Columella of the root (Palovaara et al., 2016). As a result, the globular stage embryo has all directional axes and tissue initials in place to create a functional plant.

Polarly localized proteins are a useful tool in studying polarity establishment in the embryo. Already after the first division of the zygote, the auxin transporter PIN7 is localized towards the apical side of the basal cell (Friml et al., 2003). The establishment of an inner and outer cell layer at 16-cell stage suggests that now enough directional information should be available to guide polar protein localization to radial cell faces. Surprisingly, recent work showed that, when expressed in the embryo, the inner membrane marker BOR1 can already be targeted to the inner cell faces at 4- and 8-cell stages. Similarly, the outer membrane marker NIP1;5 is also correctly targeted to outer faces at 8 to 16-cell stage (Liao & Weijers, 2017). Thus, while there are no known markers for outer and inner faces normally expressed at this stage, these cell faces are molecularly distinct nearly as early as they are physically separated. Hence, radial subcellular polarity has very early origins in the embryo.

During globular and heart stages, the precursors of the embryonic root are formed. Finally, the mature embryo contains a miniature version of the root with QC, columella, vasculature, ground tissue and epidermal layers (reviewed in Palovaara et al., 2016). After germination of the seed, initials near the QC divide and elongate to extend the root. Periclinal divisions in for example the vasculature add more cell layers in the radial direction. Like in the embryo, the division patterns and overall structure of the root tip are relatively simple and predictable (reviewed in Slovak et al., 2016). As the root is more easily accessible, it makes a good additional model for polarity and patterning studies. Many published polar markers have been first described in the root (e.g. Alassimone et al., 2016; Miwa et al., 2007). The development of lateral roots and root hairs also provide excellent cases for polarity switching and local tip growth. Roots contain more cell layers and tissue types than the early embryo, and division and identity establishment are a continuous process rather than *de novo* events. As such, polarity establishment and integration may be more complex.

Scope of the thesis

In this thesis, we study how polarity is translated into the control of sub-cellular processes. We focus on a novel family of polarly localized membrane proteins and assess their localization mechanism, function and evolution.

In **Chapter 2**, we review how developmental regulators control cell division orientation. Default mechanisms are in place to guide the division plane during symmetric division. We focus on the *Arabidopsis* embryo and discuss that 3D cell shape is an important factor in division plane determination. To generate asymmetric divisions, additional input is required in the form of directional information and regulatory mechanisms that translate this information into oriented division.

Chapter 3 describes the discovery and initial characterization of the SOSEKI (SOK) polar proteins. We describe their unique polar edge localization patterns and behavior. We also identify two functional domains within SOK: a domain required for polar edge selection and a DIX-LIKE domain required for protein clustering. Finally, we show that SOK proteins integrate apico-basal and radial polarity to determine their polar edge localization.

1

SOKs do not have any annotated function and their biological role is unknown. Therefore, we generate mutants of SOK1 in **Chapter 4**. Loss of SOK1 function does not result in a phenotype, but reveals a feedback loop or compensation mechanism with SOK4. We further assess other potential redundancies between SOKs by studying their expression and localization patterns throughout plant development.

The results in Chapter 4 show that SOKs have fascinating and unique properties, and we asked whether these are specific to *Arabidopsis*, or represent a more general principle in plants. In **Chapter 5**, we address the evolution of SOK sequence, structure and function. We demonstrate that SOK genes arose in the first land plants. Polar edge localization is conserved in a moss SOK protein, which suggests an ancestral origin of this protein property. The DIX-LIKE domain is highly conserved in SOK proteins, and we used phylogenetic studies to investigate its evolutionary origin. Lastly, we show that DIX-LIKE is not only structurally similar to animal DIX, but also has the same polymerization behavior.

In **Chapter 6**, we explore the biochemical context of SOK protein action, to learn more about their cellular function. We identify shared and unique protein interactors of SOK1, SOK2 and SOK3, and show that protein complex formation depends on the DIX-LIKE domain. At least one interactor is recruited to the polar SOK domain in a DIX-LIKE-dependent manner. Based on our results we propose a model for SOK complex formation and two possible roles of this complex in the cell.

Finally, **Chapter 7** places our findings in a broader context and discusses their implications and potential for future research.

References

Abas, L., Benjamins, R., Malenica, N., Paciorek, T. T., Wiśniewska, J., Moulinier-Anzola, J. C. et al. (2006). Intracellular trafficking and proteolysis of the *Arabidopsis* auxin-efflux facilitator PIN2 are involved in root gravitropism. *Nature Cell Biology*, *8*, 249–256.

Alassimone, J., Fujita, S., Doblas, V. G., Van Dop, M., Barberon, M., Kalmbach, L. et al. (2016). Polarly localized kinase SGN1 is required for Caspary strip integrity and positioning. *Nature Plants*, *2*, 1–10.

Armenget, L., Marquès-Bueno, M. M., & Jaillais, Y. (2016). Regulation of polar auxin transport by protein and lipid kinases. *Journal of Experimental Botany*, *67*, 4015–4037.

Besson, S., & Dumais, J. (2011). Universal rule for the symmetric division of plant cells. *Proceedings of the National Academy of Sciences of the United States of America*, *108*, 6294–6299.

Dong, J., MacAlister, C. A., & Bergmann, D. C. (2009). BASL Controls Asymmetric Cell Division in *Arabidopsis*. *Cell*, *137*, 1320–1330.

Faure, J. E., Rotman, N., Fortuné, P., & Dumas, C. (2002). Fertilization in *Arabidopsis thaliana* wild type: Developmental stages and time course. *Plant Journal*, *30*, 481–488.

Feraru, E., Feraru, M. I., Kleine-Vehn, J., Martinière, A., Mouille, G., Vanneste, S. et al. (2011). PIN polarity maintenance by the cell wall in *Arabidopsis*. *Current Biology*, *21*, 338–343.

Friml, J., Vieten, A., Sauer, M., Weijers, D., Schwarz, H., Hamann, T. et al. (2003). Efflux-dependent auxin gradients establish the apical-basal axis of *Arabidopsis*. *Nature*, *426*, 147–153.

Friml, J., Yang, X., Michniewicz, M., Weijers, D., Quint, A., Tietz, O. et al. (2004). A PINOID-dependent binary switch in apical-basal PIN polar targeting directs auxin efflux. *Science*, *306*, 862–865.

Gälweiler, L., Guan, C., Müller, A., Wisman, E., Mendgen, K., Yephremov, A., & Palme, K. (1998). Regulation of polar auxin transport by AtPIN1 in *Arabidopsis* vascular tissue. *Science*, *282*, 2226–2230.

Geldner, N., Friml, J., Stierhof, Y. D., Jürgens, G., & Palme, K. (2001). Auxin transport inhibitors block PIN1 cycling and vesicle trafficking. *Nature*, *413*, 425–428.

Ischebeck, T., Werner, S., Krishnamoorthy, P., Lerche, J., Meijon, M., Stenzel, I. et al. (2013). Phosphatidylinositol 4,5-Bisphosphate Influences PIN Polarization by Controlling Clathrin-Mediated Membrane Trafficking in *Arabidopsis*. *The Plant Cell*, *25*, 4894–4911.

Jeong, S., Eilbert, E., Bolbol, A., & Lukowitz, W. (2016). Going mainstream: How is the body axis of plants first initiated in the embryo? *Developmental Biology*, *419*, 78–84.

Jones, M. A. (2002). The *Arabidopsis* Rop2 GTPase Is a Positive Regulator of Both Root Hair Initiation and Tip Growth. *The Plant Cell*, *14*, 763–776.

Kleine-Vehn, J., Huang, F., Naramoto, S., Zhang, J., Michniewicz, M., Offringa, R., & Friml, J. (2009). PIN Auxin Efflux Carrier Polarity Is Regulated by PINOID Kinase-Mediated Recruitment into GNOM-Independent Trafficking in *Arabidopsis*. *The Plant Cell*, *21*, 3839–3849.

Chapter 1

Kleine-Vehn, J., Wabnik, K., Martinière, A., Łangowski, Ł., Willig, K., Naramoto, S. et al. (2011). Recycling, clustering, and endocytosis jointly maintain PIN auxin carrier polarity at the plasma membrane. *Molecular Systems Biology*, 7, 1–13.

Langowski, L., Wabnik, K., Li, H., Vanneste, S., Naramoto, S., Tanaka, H., & Friml, J. (2016). Cellular mechanisms for cargo delivery and polarity maintenance at different polar domains in plant cells. *Cell Discovery*, 2.

Liao, C.-Y., & Weijers, D. (2017). A toolkit for studying cellular reorganization during early *Arabidopsis thaliana* embryogenesis. *ARPN Journal of Engineering and Applied Sciences*, 12(10), 3218–3221.

Louveaux, M., Julien, J.-D., Mirabet, V., Boudaoud, A., & Hamant, O. (2016). Cell division plane orientation based on tensile stress in *Arabidopsis thaliana*. *Proceedings of the National Academy of Sciences*, 113, E4294–E4303.

Lukowitz, W., Roeder, A., Parmenter, D., & Somerville, C. (2004). A MAPKK Kinase Gene Regulates Extra-Embryonic Cell Fate in *Arabidopsis*. *Cell*, 116, 109–119.

Mansfield, S. G., Briarty, L. G., & Erni, S. (1991). Early Embryogenesis in *Arabidopsis thaliana*. I. The Mature Embryo Sac. *Canadian Journal of Botany*, 69, 447–460.

Mei, Y., Jia, W. J., Chu, Y. J., & Xue, H. W. (2012). *Arabidopsis* phosphatidylinositol monophosphate 5-kinase 2 is involved in root gravitropism through regulation of polar auxin transport by affecting the cycling of PIN proteins. *Cell Research*, 22, 581–597.

Mendrinna, A., & Persson, S. (2015). Root hair growth: it's a one way street. *F1000Prime Reports*, 7, 1–6.

Michniewicz, M., Zago, M. K., Abas, L., Weijers, D., Schweighofer, A., Meskiene, I. et al. (2007). Antagonistic Regulation of PIN Phosphorylation by PP2A and PINOID Directs Auxin Flux. *Cell*, 130, 1044–1056.

Minc, N., Burgess, D., & Chang, F. (2011). Influence of cell geometry on division-plane positioning. *Cell*, 144, 414–426.

Minc, N., & Piel, M. (2012). Predicting division plane position and orientation. *Trends in Cell Biology*, 22, 193–200. <https://doi.org/10.1016/j.tcb.2012.01.003>

Miwa, K., Takano, J., Omori, H., Seki, M., Shinozaki, K., & Fujiwara, T. (2007). Plants tolerant of high boron levels. *Science*, 318, 1417.

Molendijk, A. J., Bischoff, F., Rajendrakumar, C. S. V., Friml, J., Braun, M., Gilroy, S., & Palme, K. (2001). *Arabidopsis thaliana* Rop GTPases are localized to tips of root hairs and control polar growth. *EMBO Journal*, 20, 2779–2788.

Nakamura, M., & Grebe, M. (2018). Outer, inner and planar polarity in the *Arabidopsis* root. *Current Opinion in Plant Biology*, 41, 46–53.

Noack, L. C., & Jaillais, Y. (2017). Precision targeting by phosphoinositides: how PIs direct endomembrane trafficking in plants. *Current Opinion in Plant Biology*, 40, 22–33.

Ovečka, M., Berson, T., Beck, M., Derksen, J., Šamaj, J., Baluška, F., & Lichtscheidl, I. K. (2010). Structural Sterols Are Involved in Both the Initiation and Tip Growth of Root Hairs in *Arabidopsis thaliana*. *The Plant Cell*, 22, 2999–3019.

Paciorek, T., Zažímalová, E., Ruthardt, N., Petrášek, J., Stierhof, Y. D., Kleine-Vehn, J. et al. (2005). Auxin inhibits endocytosis and promotes its own efflux from cells. *Nature*, 435, 1251–1256.

Palovaara, J., de Zeeuw, T., & Weijers, D. (2016). Tissue and Organ Initiation in the Plant Embryo: A First Time for Everything. *Annual Review of Cell and Developmental Biology*, 32, 47–75.

Roppolo, D., De Rybel, B., Tendon, V. D., Pfister, A., Alassimone, J., Vermeer, J. E. M. et al. (2011). A novel protein family mediates Casparyan strip formation in the endodermis. *Nature*, 473, 381–384.

Sahlin, P., & Jönsson, H. (2010). A modeling study on how cell division affects properties of epithelial tissues under isotropic growth. *PLoS One*, 5, e11750.

Slovak, R., Ogura, T., Satbhai, S. B., Ristova, D., & Busch, W. (2016). Genetic control of root growth: From genes to networks. *Annals of Botany*, 117, 9–24.

Stanislas, T., Hüser, A., Barbosa, I. C. R., Kiefer, C. S., Brackmann, K., Pietra, S. et al. (2015). Arabidopsis D6PK is a lipid domain-dependent mediator of root epidermal planar polarity. *Nature Plants*, 1, 1–9.

Strader, L. C., & Bartel, B. (2009). The Arabidopsis PLEIOTROPIC DRUG RESISTANCE8/ABCG36 ATP Binding Cassette Transporter Modulates Sensitivity to the Auxin Precursor Indole-3-Butyric Acid. *The Plant Cell*, 21, 1992–2007.

Takano, J., Noguchi, K., Yasumori, M., Kobayashi, M., Gajdos, Z., Miwa, K. et al. (2002). Arabidopsis boron transporter for xylem loading. *Nature*, 420, 337–340.

Takano, J., Tanaka, M., Toyoda, A., Miwa, K., Kasai, K., Fuji, K. et al. (2010). Polar localization and degradation of Arabidopsis boron transporters through distinct trafficking pathways. *Proceedings of the National Academy of Sciences of the United States of America*, 107, 5220–5225.

Tejos, R., Sauer, M., Vanneste, S., Palacios-Gomez, M., Li, H., Heilmann, M. et al. (2014). Bipolar Plasma Membrane Distribution of Phosphoinositides and Their Requirement for Auxin-Mediated Cell Polarity and Patterning in Arabidopsis. *The Plant Cell*, 26(5), 2114–2128. <https://doi.org/10.1105/tpc.114.126185>

Ueda, M., Zhang, Z., & Laux, T. (2011). Transcriptional Activation of Arabidopsis Axis Patterning Genes WOX8/9 Links Zygote Polarity to Embryo Development. *Developmental Cell*, 20, 264–270.

Van Norman, J. M. (2016). Asymmetry and cell polarity in root development. *Developmental Biology*, 419, 165–174.

Wang, H., Ngwenyama, N., Liu, Y., Walker, J. C., & Zhang, S. (2007). Stomatal Development and Patterning Are Regulated by Environmentally Responsive Mitogen-Activated Protein Kinases in Arabidopsis. *The Plant Cell*, 19, 63–73.

Wisniewska, J., Xu, J., Seifertova, D., Brewer, P. B., Ru, K., Scheres, B. et al. (2006). Polar PIN Localization Directs Auxin. *Science*, 312(May), 883.

Yoshida, S., Barbier de Reuille, P., Lane, B., Bassel, G. W., Prusinkiewicz, P., Smith, R. S., & Weijers, D. (2014). Genetic control of plant development by overriding a geometric division rule. *Developmental Cell*, 29, 75–87.

Zhang, Y., Wang, P., Shao, W., Zhu, J. K., & Dong, J. (2015). The BASL Polarity Protein Controls a MAPK Signaling Feedback Loop in Asymmetric Cell Division. *Developmental Cell*, 33, 136–149.

Chapter 2

Control of oriented cell division in the *Arabidopsis* Embryo

Maritza van Dop¹, Che-Yang Liao¹ and Dolf Weijers¹

1. Laboratory of Biochemistry, Wageningen University, Dreijenlaan 3, 6700 HA Wageningen, the Netherlands

This Chapter is published as:

van Dop, M., Liao, C. Y., & Weijers, D. (2015). Control of oriented cell division in the *Arabidopsis* embryo. *Current Opinion in Plant Biology*, 23, 25–30.

Abstract

Multicellular plant development requires strict control of cell division orientation. A key unanswered question is how developmental regulators interact with the generic cell division machinery to trigger oriented divisions. We discuss the *Arabidopsis* embryo as a model for addressing this question. Recent progress in 3D imaging and computation now allows sketching of a framework for the developmental control of division orientation in which the signaling molecule auxin controls oriented division by preventing a geometrically defined default plane. We expect that the identification of auxin effectors, together with the identification of novel regulators of cell division will help to link developmental regulators to the division machinery.

Introduction

Plants cannot migrate or quickly replace cells like animals do, as new cells are fixed by a rigid cell wall directly after division. This constraint makes positioning of the cell division plane a crucial factor in shaping plant tissues. During cell proliferation, the mother cell usually divides symmetrically into two daughters of approximately equal volume (Sachs, 1878, 1887). Cells can however strongly deviate their division plane and give rise to daughters of different volumes. Often, such divisions are associated with the formation of new cell layers and cell identities, and these divisions can thus be asymmetric both in volume partitioning and in developmental fate. These latter divisions are often also referred to as “formative divisions” (De Smet & Beeckman, 2011). The occurrence of these two different types of division implies that plants must have ways to control the position and orientation of the cell division plane. As cell types usually have specific modes of oriented cell division (De Smet & Beeckman, 2011), orientation of cell division must be under developmental control.

A central question in plant developmental biology is how genetic programs instruct cells to execute unique behavior like oriented division. While many developmental regulators have been identified (Smolarkiewicz & Dhonukshe, 2013) and the nuts and bolts of the division process itself are reasonably well understood (see next section), how one directs the other remains to be investigated. In this review we will discuss recent progress in understanding the developmental control of cell division orientation. Oriented cell division is studied in a variety of contexts, including meristems (De Smet & Beeckman, 2011) and stomatal complexes (Lau & Bergmann, 2012). We will focus our discussion on the *Arabidopsis* embryo, which is a relatively simple model that encapsulates many aspects of later development.

The embryo consists of very few, differently shaped cells, yet each cell has a specific fate (Wendrich & Weijers, 2013). The division pattern is not only well studied, but also nearly invariable and thus highly predictable (Jürgens & Mayer, 1994; Scheres et al., 1994). Precursors for the organs (cotyledons, hypocotyl, root), tissues (epidermis, ground tissue, vascular tissue) and their stem cells are all established during early embryogenesis, and oriented cell division lies at the base of most of these structures. All these characteristics make the embryo an excellent model for studying the regulation of cell division orientation. In the following we will first briefly describe the generic cell division process. Next, we will discuss the latest findings on the possible regulatory mechanisms for cell division orientation, with a focus on the young *Arabidopsis* embryo.

One ring to rule it all

Cell division can roughly be separated in three processes: definition of the cell division plane, mitosis and cytokinesis (Figure 1a). It is still largely unclear how cells select a division plane, but the processes following this initial event are reasonably well understood. In most cells, a cortical ring of cytoskeletal filaments called the Preprophase Band (PPB) is formed (Pickett-Heaps & Northcote, 1966). The PPB is especially enriched with microtubules (MT) and actin is necessary to restrict the width of the PPB, which is essential for a proper division orientation (Eleftheriou & Palevitz, 1992; Hoshino et al., 2003; Mineyuki & Palevitz, 1990). Several genes that interact with the cytoskeleton and that are required for PPB establishment have been identified (Figure 1a). Recent examples are SABRE, CLASP, FASS, and TONNEAU1 (TON1). SABRE has been shown to stabilize the orientation of CLASP labelled MT in the PPB, which is essential for correct division plane orientation (Pietra et al., 2013). TON1 and FASS are part of the same complex that is recruited to microtubules and regulates the transition from interphase microtubules to PPB (Drevensek et al., 2012; Spinner et al., 2013).

The PPB marks the position of the future division plane (Rasmussen et al., but is not a permanent structure: once the mitotic spindle starts to form, the PPB is broken down (Pickett-Heaps & Northcote, 1966). The long-standing question of how the cell ‘remembers’ where the PPB has been is slowly starting to be answered. The PPB leaves behind a Cortical Division Zone (CDZ) that guides the mitotic spindle and phragmoplast to the correct position. The CDZ is depleted of cortical F-actin (Mineyuki & Palevitz, 1990) and several proteins localize to this domain. For example, the highly basic MT-binding protein TANGLED (TAN) is recruited to the PPB and remains at the CDZ to guide the expanding phragmoplast after mitosis (Rasmussen et al., 2011; Walker et al., 2007). Two kinesin-12 proteins POK1 and POK2 have an important role in TAN localization and division plane maintenance. POK1 localizes to the PPB and stays at the CDZ where it functions to maintain TAN at the correct position (Lipka et al., 2014). Once mitosis is complete and the phragmoplast has been formed, the expanding cell plate has to be guided and connected to the existing cell wall. The adaptin-like TPLATE protein is recruited to the cell plate and CDZ together with Clathrin Light Chain2 (CLC2; Gadeyne et al., 2014; Van Damme et al., 2011). It was recently shown that TPLATE adaptor complexes drive clathrin-mediated endocytosis, which in turn is necessary for cell plate maturation and fusion with the cell wall (Gadeyne et al., 2014; Van Damme et al., 2011).

Shape matters

Recent research gave more insight in how the division plane is selected in symmetric

cell divisions. Such divisions can be explained by interactions of the cell division machinery with the geometric properties of the cell. It has long been accepted that during symmetric division the new cell wall is placed at a right angle to the existing cell walls (Sachs, 1878). For maximum efficiency, this new wall must be as small as possible (Errera, 1888). In order to do this, microtubules in cytoplasmic strands probe the cell and make the shortest connections between the cell wall and the nucleus (Besson & Dumais, 2011; Lloyd, 1991). As a result, the nucleus and thus the shortest cell division plane is positioned in the geometrical center of the cell. When multiple smallest walls are possible because of local minima, a stochastic process based on surface differences between optional walls selects the correct division orientation (Besson & Dumais, 2011).

Asymmetric, or oriented, division cannot be the result from mere microtubular probing, but will require additional information to turn its division site away from the minimum. This information should contain instructions for orienting the division plane in a certain way (regulation) and directional cues necessary for positioning the division machinery accordingly. An important part of the directional information is likely provided by cell polarity: the uneven distribution of cellular components and molecules in the cell and on the plasma membrane. Signaling from neighboring cells may provide additional cues of direction and could promote a specific division orientation.

Rules for early development

As a morphogenetic process that is under strict genetic control, *Arabidopsis* embryogenesis may provide better understanding of the control of oriented cell division. An important consideration is that embryogenesis is a truly three-dimensional process, and given the small size of embryos, each spatial dimension matters. However, models for oriented cell division that incorporate geometry have until recently been applied to 2D slices of cells and tissues. Lately, a developmental map has been established that shows *Arabidopsis* embryogenesis in 3D from the zygote to the late heart stage (Yoshida et al., 2014). This map greatly enhances our understanding of each cell division and its consequences for the shape and size of daughter cells. 3D analysis of division and ontogeny confirmed earlier observations on cell division orientation in 2D (Jürgens & Mayer, 1994; Scheres et al., 1994), but could also be used to derive quantitative morphological parameters, such as cell volume and cell wall surface. In contrast to what was visible in sections, most cell divisions in embryos of 8 cells and larger are asymmetric with regards to the distribution of volume over the daughter cells. For example, the cell division that separates protoderm and inner cells (Figure 1b) seems to result in cells of roughly equal size in sections. In reality, the outer cell is more than two times larger.

Interestingly, this volumetrically asymmetric cell gives rise to cells with different fates (protoderm versus inner cell types). Several other asymmetric divisions could be correlated with differences in gene expression between daughter cells (Yoshida et al., 2014), which suggests a link between volumetric difference and developmental asymmetry.

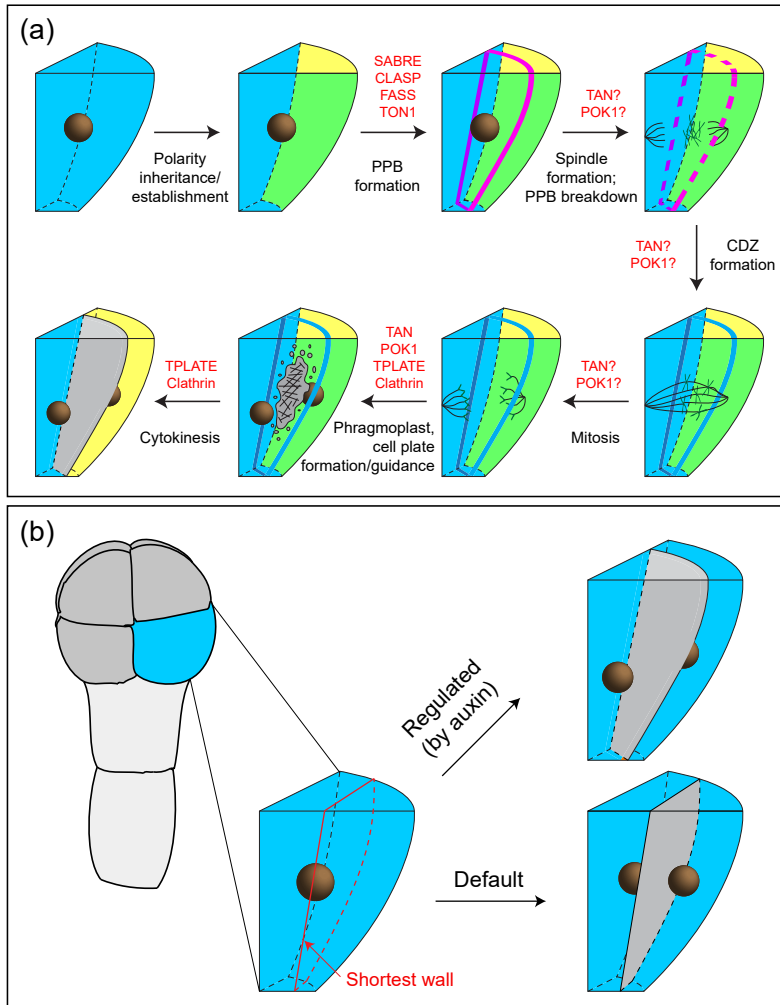


Figure 1: Oriented cell division in the *Arabidopsis* embryo. (A) The generic cell division process depicted in an asymmetrically dividing cell. Proteins whose function was recently illuminated in each step are indicated. Cell polarity (yellow) is established in the cell or inherited from the mother cell. Directional cues direct the establishment of the PPB (pink), which marks the division plane. Next, the PPB is broken down and the mitotic spindle (black) is established. The PPB leaves behind a CDZ (blue) and mitosis progresses. The phragmoplast and cell plate (grey with lines) are formed and expand until the cell plate (grey) fuses to the existing cell walls. (B) At the transition from 8 to 16 cells during embryogenesis, auxin response is required to prevent a cell division plane that approximates the 'shortest wall', and can thus create unequal daughter cells.

The 3D embryo data was also used to address geometric influence on cell division plane orientation by simulating all possible walls that could form in a pair of sister cells after division. The surface of these walls was measured, and compared to the division wall that was actually used. Classical rules (Errera, 1888; Sachs, 1878, 1887) and their modern interpretations (Besson & Dumais, 2011; Minc et al., 2011) state that the shortest path crossing the center of the cell describes the division plane. Computational simulations in 3D showed that divisions leading to the 2, 4 and 8 cell embryo indeed followed this simple “shortest wall” rule. However, the next divisions that generate the protoderm and inner cells at the 16-cell stage clearly deviated from this rule. While this might indicate that there is no “default” division rule, it could also mean that the divisions that disobey the rule are genetically instructed to do so. Indeed, cells in the 8-cell embryo could be reverted to dividing along the shortest path when the auxin transcriptional response was perturbed by misexpressing the *bdl/iaa12* transcriptional inhibitor (Yoshida et al., 2014). These findings indicate that the “default” rule translates 3D geometry into a division plane and that additional regulation by auxin-related pathways results in alternative orientation of the division plane (Figure 1b).

How to ignore the rules

It is clear that regulation is necessary for oriented division, but the key question remains what mechanisms relay the action of developmental regulators such as transcription factors to orient the division plane in the embryo. Many factors have been identified that are required for cell division (Figure 1a), and mutations in these genes cause incomplete or randomized division (e.g. Torres-Ruiz & Jürgens, 1994; Traas et al., 1995). Arguably, such factors are unlikely to directly control division orientation. Rather, one would expect regulators of oriented division to trigger a given orientation when misexpressed, and/or show consistent reversion to symmetric division along the shortest path when absent. Several mutants with such a switch in orientation have been identified in the past decades. Interestingly, most of these genes play a role in auxin-related pathways, ranging from auxin biosynthesis (Cheng et al., 2007; Stepanova et al., 2008) to transport (Friml et al., 2003) and transcriptional responses (Dharmasiri et al., 2005; Hamann et al., 2002; Hardtke & Berleth, 1998). This indicates that auxin-dependent gene regulation plays a vital role in oriented division in the embryo. In the specific example discussed above, auxin action can be interpreted as preventing the geometrically inspired default plane. An important question thus becomes HOW auxin-dependent gene regulation acts to control division orientation.

Knowledge on transcriptional auxin output is limited, but recent studies on the MONOPTEROS/AUXIN RESPONSE FACTOR5 (MP; Hardtke & Berleth, 1998)

protein have started to provide insight into auxin-dependent control of cell division. MP regulates the divisions in the lower tier of the embryo that lead to vascular tissue formation and root initiation (Berleth & Jürgens, 1993; De Rybel et al., 2013). However, since MP misexpression is not known to trigger specific division orientations (Hardtke et al., 2004; Weijers et al., 2006), it likely acts through a specific set of target genes that are more directly causal to division plane orientation. So far, the only identified transcriptional targets of MP are transcription factors (Cole et al., 2009; Donner et al., 2009; Schlereth et al., 2010). The mobile TARGET OF MONOPTEROS7 (TMO7) transcription factor was shown to be required for asymmetric hypophysis cell division (Schlereth et al., 2010). Intriguingly, recent studies showed that the TMO5 transcription factor, in complex with another bHLH transcription factor LONESOME HIGHWAY (LHW) is both necessary and sufficient for the periclinal divisions that form the vascular tissue (De Rybel et al., 2013; Ohashi-Ito et al., 2013). Since the TMO5/LHW complex appears to trigger periclinal division through promoting cytokinin biosynthesis (De Rybel et al., 2014; Ohashi-Ito et al., 2014) further research will be necessary to identify the target within the generic cell division machinery.

Even though it remains unclear which components of the cell division machinery are under control of auxin, several steps in the division process can be identified that are most likely to be affected. Productive regulation of cell division orientation would have to occur before the moment at which events become irreversible. In *Arabidopsis*, the PPB and CDZ accurately predict and guide spindle, phragmoplast and cell plate formation (Rasmussen et al., 2013). Absence of a PPB results in a lacking or misplaced CDZ and randomized divisions (Rasmussen et al., 2013). Thus, the PPB forms the essential positional cue for the division plane and is a likely target of regulation. This regulation must ensure the translation of directional cues into a specific orientation of the PPB. Therefore, auxin-regulated transcription should result in altered production of proteins that affect cell polarity, its perception or positioning of the PPB. Such proteins could be involved in for example Plasma Membrane restructuring, anchoring and organization of the cytoskeleton, endo/exocytosis or integration of signals. Identifying such downstream targets of auxin-dependent transcription will open the way to true understanding of the control of cell division orientation by auxin.

Conclusions and perspectives

Oriented cell division is key to plant development, and mutant phenotypes often manifest in altered division planes. Through genetics, many developmental regulators have been identified and dissection of gene regulatory networks is in full swing. However, one of the major unanswered questions in plant developmental

biology remains at what step and through what molecular intermediates regulators control division orientation. Further dissection of gene regulatory networks will identify hubs that connect more directly to the cell division machinery and we propose the *Arabidopsis* embryo as an attractive model for addressing this question. Recent improvements in imaging have allowed the generation of a 3D framework to address the role of cell shape and genetic regulation in oriented division. This has led to a new perspective on the role of auxin in controlling division orientation – by preventing a geometric default rule. Important future challenges will therefore be to identify the network mediating this activity. Furthermore, it is currently unclear whether this auxin activity is unique to the early embryo, or if it can be generalized to other cell types and other plant species.

Acknowledgements

We apologize to authors, whose important contributions we could not include as a consequence of space constraints and focus. Work on cell division control in the embryo in the authors' lab is supported by the Netherlands Organization for Scientific Research (NWO; Grant ALW 831.13.001 to M.v.D.) and the European Research Council (Starting Grant 'CELLPATTERN', contract no. 281573 to D.W.).

References

Berleth, T., & Jürgens, G. (1993). The role of the *monopteros* gene in organising the basal body region of the *Arabidopsis* embryo. *Development*, 118, 575–587.

Besson, S., & Dumais, J. (2011). Universal rule for the symmetric division of plant cells. *Proceedings of the National Academy of Sciences of the United States of America*, 108, 2011.

Cheng, Y., Dai, X., & Zhao, Y. (2007). Auxin synthesized by the *YUCCA* flavin monooxygenases is essential for embryogenesis and leaf formation in *Arabidopsis*. *The Plant Cell*, 19, 2430–2439.

Cole, M., Chandler, J., Weijers, D., Jacobs, B., Comelli, P., & Werr, W. (2009). DORNROSCHEN is a direct target of the auxin response factor MONOPTEROS in the *Arabidopsis* embryo. *Development*, 136, 1643–1651.

De Rybel, B., Adibi, M., Breda, A. S., Wendrich, J. R., Smit, M. E., Novak, O. et al. (2014). Integration of growth and patterning during vascular tissue formation in *Arabidopsis*. *Science*, 345, 1255215.

De Rybel, B., Möller, B., Yoshida, S., Grabowicz, I., Barbier de Reuille, P., Boeren, S. et al. (2013). A bHLH complex controls embryonic vascular tissue establishment and indeterminate growth in *Arabidopsis*. *Developmental Cell*, 24, 426–437.

De Smet, I., & Beeckman, T. (2011). Asymmetric cell division in land plants and algae: the driving force for differentiation. *Nature Reviews. Molecular Cell Biology*, 12, 177–188.

Dharmasiri, N., Dharmasiri, S., Weijers, D., Lechner, E., Yamada, M., Hobbie, L. et al. (2005). Plant development is regulated by a family of auxin receptor F box proteins. *Developmental Cell*, 9, 109–119.

Donner, T. J., Sherr, I., & Scarpella, E. (2009). Regulation of preprocambial cell state acquisition by auxin signaling in *Arabidopsis* leaves. *Development*, 136(19), 3235–3246.

Drevensek, S., Goussot, M., Duroc, Y., Christodoulidou, A., Steyaert, S., Schaefer, E. et al. (2012). The *Arabidopsis* TRM1-TON1 interaction reveals a recruitment network common to plant cortical microtubule arrays and eukaryotic centrosomes. *The Plant Cell*, 24, 178–191.

Eleftheriou, E. P., & Palevitz, B. A. (1992). The effect of cytochalasin D on preprophase band organization in root tip cells of *Allium*. *Journal of Cell Science*, 103, 989–998.

Errera, L. (1888). Über zellformen und siefenblasen. *Botanisches Centralblatt*, 34, 395–399.

Friml, J., Vieten, A., Sauer, M., Weijers, D., Schwarz, H., Hamann, T. et al. (2003). Efflux-dependent auxin gradients establish the apical-basal axis of *Arabidopsis*. *Nature*, 426, 147–153.

Gadeyne, A., Sanchez-Rodriguez, C., Vanneste, S., Di Rubbo, S., Zauber, H., Vanneste, K. et al. (2014). The TPLATE Adaptor Complex Drives Clathrin-Mediated Endocytosis in Plants. *Cell*, 156, 691–704.

Hamann, T., Benkova, E., Bäurle, I., Kientz, M., & Jürgens, G. (2002). The *Arabidopsis* *BODENLOS* gene encodes an auxin response protein inhibiting MONOPTEROS-mediated embryo patterning. *Genes & Development*, 16, 1610–1615.

Hardtke, C. S., & Berleth, T. (1998). The *Arabidopsis* gene MONOPTEROS encodes a transcription factor mediating embryo axis formation and vascular development. *The EMBO Journal*, 17, 1405–1411.

Hardtke, C. S., Ckurdumova, W., Vidaurre, D. P., Singh, S. a, Stamatiou, G., Tiwari, S. B. et al. (2004). Overlapping and non-redundant functions of the *Arabidopsis* auxin response factors MONOPTEROS and NONPHOTOTROPIC HYPOCOTYL 4. *Development*, 131, 1089–1100.

Hoshino, H., Yoneda, A., Kumagai, F., & Hasezawa, S. (2003). Roles of actin-depleted zone and preprophase band in determining the division site of higher-plant cells, a tobacco BY-2 cell line expressing GFP-tubulin. *Protoplasma*, 222, 157–165.

Jürgens, G., & Mayer, U. (1994). *Arabidopsis*. In *EMBRYOS Colour Atlas of Development*. London: Wolfe Publishing.

Lau, O. S., & Bergmann, D. C. (2012). Stomatal development: a plant's perspective on cell polarity, cell fate transitions and intercellular communication. *Development*, 139, 3683–3692.

Lipka, E., Gadeyne, A., Stöckle, D., Zimmermann, S., De Jaeger, G., Ehrhardt, D. W. et al. (2014). The Phragmoplast-Orienting Kinesin-12 Class Proteins Translate the Positional Information of the Preprophase Band to Establish the Cortical Division Zone in *Arabidopsis thaliana*. *The Plant Cell*, 26, 2617–2632.

Lloyd, C. W. (1991). How does the cytoskeleton read the laws of geometry in aligning the division plane of plant cells. *Development Supplement*, 1, 55–65.

Minc, N., Burgess, D., & Chang, F. (2011). Influence of cell geometry on division-plane positioning. *Cell*, 144, 414–426.

Mineyuki, Y., & Palevitz, B. A. (1990). Relationship between preprophase band organization , F-actin and the division site in *Allium*. *Journal of Cell Science*, 97, 283–296.

Ohashi-Ito, K., Oguchi, M., Kojima, M., Sakakibara, H., & Fukuda, H. (2013). Auxin-associated initiation of vascular cell differentiation by LONESOME HIGHWAY. *Development (Cambridge, England)*, 140, 765–769.

Ohashi-Ito, K., Saegusa, M., Iwamoto, K., Oda, Y., Katayama, H., Kojima, M. et al. (2014). A bHLH Complex Activates Vascular Cell Division via Cytokinin Action in Root Apical Meristem. *Current Biology*, 24, 2053–2058.

Pickett-Heaps, J. D., & Northcote, D. H. (1966). Organization of microtubules and endoplasmatic reticulum during mitosis and cytokinesis in wheat meristems. *Journal of Cell Science*, 1, 109–120.

Pietra, S., Gustavsson, A., Kiefer, C., Kalmbach, L., Hörstedt, P., Ikeda, Y. et al. (2013). *Arabidopsis* SABRE and CLASP interact to stabilize cell division plane orientation and planar polarity. *Nature Communications*, 4, 2779.

Rasmussen, C. G., Sun, B., & Smith, L. G. (2011). Tangled localization at the cortical division site of plant cells occurs by several mechanisms. *Journal of Cell Science*, 124, 270–279.

Rasmussen, C. G., Wright, A. J., & Müller, S. (2013). The role of the cytoskeleton and associated proteins in determination of the plant cell division plane. *The Plant Journal*, 75(2), 258–269.

Sachs, J. (1878). Über die anordnung der zellen in jungsten pflanzentheilen. *Arbeiten des Botanischen Instituts in Wurzburg*.

Sachs, J. (1887). Lecture XXVII. Relations between growth and cell-division in the embryonic tissues. *Lectures in Plant Physiology*, 431–459.

2

Scheres, B., Wolkenfelt, H., Willemsen, V., Terlouw, M., Lawson, E., Dean, C., & Weisbeek, P. (1994). Embryonic origin of the *Arabidopsis* primary root and root meristem initials, *2487*, 2475–2487.

Schlereth, A., Möller, B., Liu, W., Kientz, M., Flipse, J., Rademacher, E. H. et al. (2010). MONOPTEROS controls embryonic root initiation by regulating a mobile transcription factor. *Nature*, *464*, 913–916.

Smolarkiewicz, M., & Dhonukshe, P. (2013). Formative cell divisions: principal determinants of plant morphogenesis. *Plant & Cell Physiology*, *54*, 333–342.

Spinner, L., Gadeyne, A., Belcram, K., Goussot, M., Moison, M., Duroc, Y. et al. (2013). A protein phosphatase 2A complex spatially controls plant cell division. *Nature Communications*, *4*, 1863.

Stepanova, A. N., Robertson-Hoyt, J., Yun, J., Benavente, L. M., Xie, D.-Y., Dolezal, K. et al. (2008). TAA1-mediated auxin biosynthesis is essential for hormone crosstalk and plant development. *Cell*, *133*, 177–191.

Torres-Ruiz, R. A., & Jürgens, G. (1994). Mutations in the FASS gene uncouple pattern formation and morphogenesis in *Arabidopsis* development. *Development*, *120*, 2967–2978.

Traas, J., Bellini, C., Nacry, P., Kronenberger, J., Bouchez, D., & Caboche, M. (1995). Normal differentiation patterns in plants lacking microtubular preprophase bands. *Nature*, *375*, 676–677.

Van Damme, D., Gadeyne, A., Vanstraelen, M., Inzé, D., Van Montagu, M. C. E., De Jaeger, G., ... Geelen, D. (2011). Adapton-like protein TPLATE and clathrin recruitment during plant somatic cytokinesis occurs via two distinct pathways. *Proceedings of the National Academy of Sciences of the United States of America*, *108*, 615–620.

Walker, K. L., Müller, S., Moss, D., Ehrhardt, D. W., & Laurie, G. (2007). *Arabidopsis* Tangled Identifies the Division Plane Throughout Mitosis and Cytokinesis. *Current Biology*, *17*, 1827–1836.

Weijers, D., Schlereth, A., Ehrismann, J. S., Schwank, G., Kientz, M., & Jürgens, G. (2006). Auxin triggers transient local signaling for cell specification in *Arabidopsis* embryogenesis. *Developmental Cell*, *10*, 265–270.

Wendrich, J. R., & Weijers, D. (2013). The *Arabidopsis* embryo as a miniature morphogenesis model. *New Phytologist*, *199*, 14–25.

Yoshida, S., Barbier de Reuille, P., Lane, B., Bassel, G. W., Prusinkiewicz, P., Smith, R. S., & Weijers, D. (2014). Genetic control of plant development by overriding a geometric division rule. *Developmental Cell*, *29*, 75–87.

Chapter 3

SOSEKI polarity determinants reveal mechanisms of supra-cellular polarity in *Arabidopsis*

Saiko Yoshida^{1,2,a}, Maritza van Dop¹, Alja van der Schuren^{1,b}, Luc van Galen¹,
Shunsuke Saiga^{1,c}, Milad Adibi³, Barbara Möller^{1,d}, Peter Marhavy^{2,b}, Richard Smith³,
Jiri Friml², Dolf Weijers¹

van Dop and Van der Schuren: shared second authors

1. Laboratory of Biochemistry, Wageningen University, Stippeneng 4, Wageningen, the Netherlands
2. Institute of Science and Technology, Klosterneuburg, Austria
3. Department of Comparative Development and Genetics, Max Planck Institute for Plant Breeding Research, Cologne, Germany

a. Present address: Department of Comparative Development and Genetics, Max Planck Institute for Plant Breeding Research, Cologne, Germany

b. Present address: Department of Plant Molecular Biology, University of Lausanne, Lausanne, Switzerland

c. Present address: Department of Plant and Microbial Biology, University of Zürich, Zürich, Switzerland

d. Present address: VIB-UGent Center for Plant Systems Biology, Ghent, Belgium

Abstract

Multicellular development requires coordinated patterning of cells, tissues and organs relative to the major body axes. Plant cells have rigid cell walls and are immobile, thus oriented cell division and growth translate polarity to morphogenesis. Polarly localized proteins have been identified (Dong et al., 2009; Friml et al., 2003) and generic mechanisms of oriented cell division are well known (Cruz-Ramírez et al., 2012; Koizumi et al., 2012). However, it is unknown how organismal axes are connected to cell polarity and translated to oriented growth or division. Here, we identify the novel SOSEKI (SOK) family of polarly localized proteins. SOK proteins localize to specific edges of cells that appear to integrate apical-basal and inner-outer axial information. Polar localization is surprisingly inert to pharmacological inhibition, yet requires cell wall integrity. Using two oppositely polarized family members, we show that proteins orient to a supra-cellular coordinate field that spans all tissues, and through domain swaps and deletions we identify a small domain that directs corner localization. Misexpression demonstrated that ectopic SOK1 alters cell division planes, and we used this property to show that biological activity requires polar localization. Part of the DUF966 domain in SOK proteins structurally resembles the DIX oligomerization domain in the *Drosophila* Dishevelled polarity regulator (Ehebauer & Arias, 2009; Schwarz-Romond et al., 2007). The SOK1 DIX domain indeed mediates dimerization and is required for focused edge localization and biological activity. Our work identifies a plant compass, read by SOK proteins, as a new mechanism for supra-cellular polarity. Furthermore, it appears that cell polarity in plants and animals converge upon the same protein domain.

Results and discussion

The plant signaling molecule auxin regulates pattern formation, where defects in auxin response mutants are often manifested as changes in growth direction or cell division plane (Möller & Weijers, 2009). Auxin control over cell division plane was recently conceptualized as enabling cells to deviate from a default symmetric cell division in early *Arabidopsis* embryos (Yoshida et al., 2014). However, the effectors of auxin response that mediate its role in division orientation are unknown. We exploited the prominent function of the MONOPTEROS/AUXIN RESPONSE FACTOR5 (MP) transcription factor (Hardtke & Berleth, 1998), whose loss of function alters division planes in the early embryo causing a rootless phenotype (Schlereth et al., 2010). MP controls cell division orientation, and mediators of this function should be among its direct targets. We performed transcriptome analysis on isolated globular-stage embryos in which MP activity was locally inhibited in the lower inner cells of the embryo. We found the previously identified *TMO7* gene (Schlereth et al., 2010) as the most strongly down-regulated genes (Möller et al., 2017). We focused on the second most strongly down-regulated gene (7.5-fold), which is a gene of unknown function, containing a Domain of Unknown Function 966 (DUF966) and named *SOSEKI1* (explained below; *SOK1*; *At1g05577*). *SOK1* has 4 paralogues in the *Arabidopsis* genome: *SOK2* (*At5g10150*), *SOK3* (*At2g28150*), *SOK4* (*At3g46110*) and *SOK5* (*At5g59790*) (Fig. 1A), of which *SOK5* was also 2.4-fold down-regulated in the microarray.

To determine gene expression domains, we generated lines expressing a nuclear-localized triple GFP (n3GFP) driven by each *SOK* promoter, and found that all *SOK* genes are expressed during embryogenesis, as well as in the primary and lateral root meristem (Fig. S1). As predicted by the transcriptome data, expression of *SOK1* was nearly absent in *mp* mutant embryos (Möller et al., 2017) indicating that *SOK1* is a target of MP.

We next generated translational fusions of *SOK* proteins to YFP to observe *SOK* protein localization, and found all *SOK*-YFP proteins to mirror pSOK-n3GFP expression patterns (Fig. 1B-L; Fig. S2A-E; Fig. S3). Strikingly, all *SOK*-YFP proteins localized to unique and novel domains within the cell. *SOK1*-YFP is localized to the outer/apical edge of the youngest vascular cells and apical in columella initials in the primary root (Fig. 1C). During embryogenesis, *SOK1*-YFP protein is first detected on the apical side of inner cells of the lower tier at the early globular stage (Fig. 2A; Fig. S3). Subsequently, *SOK1* localizes to the apical and outer lateral side of vascular cells and outer corners of the hypophysis (Fig. 1B; Fig. 2A,B; Fig. S3). The pattern of *SOK1*-YFP accumulation suggests that the protein is highly unstable: Following anticlinal divisions of vascular initial cells, protein is found in only the lower daughter cell (Fig. 2F; Fig. S3). Indeed, live

imaging in lateral root primordia showed the protein to disappear during mitosis, and be re-established at polar sites following cytokinesis (Fig. 2P). At heart stage, SOK1 is expressed and localized outer apical corner of pericycle, vasculature cells and hypophysis (Fig. 2F; Fig S3). This pattern is then maintained in the post-embryonic root (Fig. 1C,H), and reiterated in newly initiated lateral roots (Fig. 2K; Fig S4A-E). The localization pattern of SOK1-tdTomato is identical to the YFP version in both roots and embryos, suggesting that properties of YFP do not contribute to this unique localization pattern (Fig. S2F-G). The protein was named SOSEKI1 (Japanese for “cornerstone”) for this unique corner localization pattern.

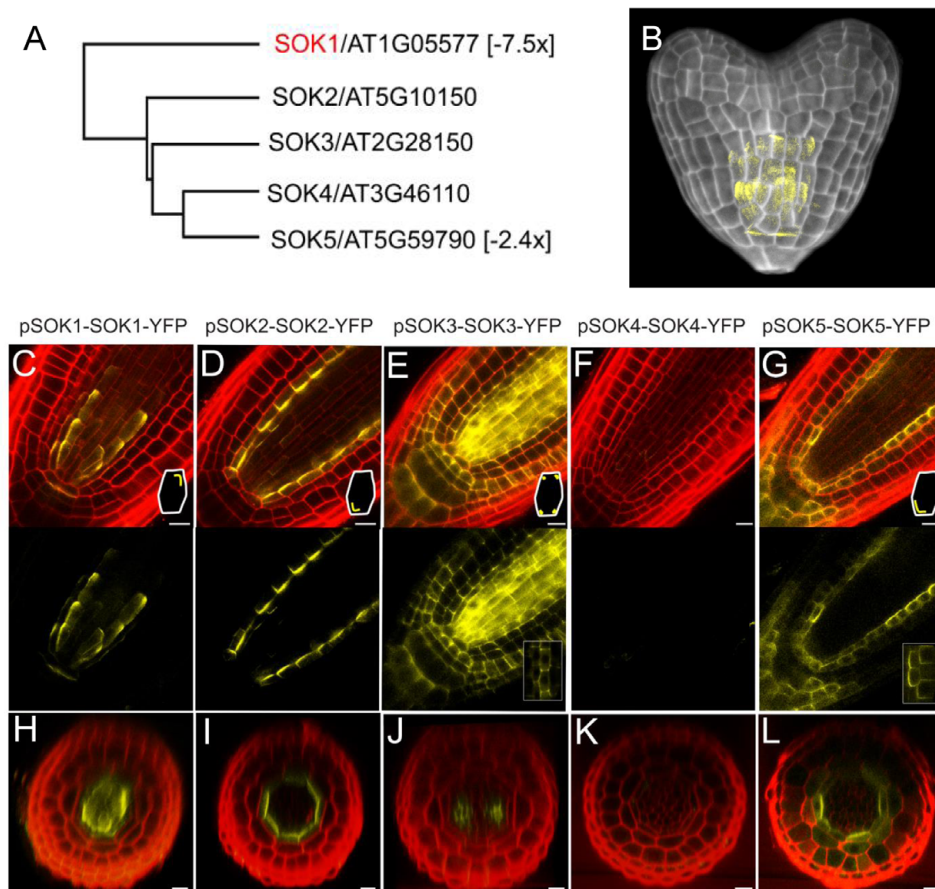


Figure 1: The SOSEKI family of polarly localized proteins. (A) Phylogenetic tree of the Arabidopsis DUF966/SOSEKI protein family. Values in brackets indicate fold-change (downregulation) in *Q0990* > > *bdl* embryos (B. K. Möller et al., 2017). (B) SOK1-YFP protein localization in a 3D maximum intensity projection of a heart-stage embryo. (C-L) Localization of SOK1-YFP (C,H), SOK2-YFP (D,I), SOK3-YFP (E,J), SOK4-YFP (F,K) and SOK5-YFP (G,L) in longitudinal cross-sections (C-G) and transverse cross-sections (H-L) of primary root tips counterstained with Propidium Iodide (red). Insets in C-G schematically show subcellular SOK protein localization. Bars 10 μ m.

Patterns of other SOK proteins were either opposite to (SOK2; Fig. 1D,I; Fig S3) or only partly overlapping (SOK3/4/5; Fig. 1E-G,J-L; Fig S3) with SOK1. SOK2-YFP localized to the inner basal edge of endodermal cells in the primary (Fig. 1D,L) and lateral (Fig. 2L; Fig S4F-I) root, and this pattern was first initiated in protodermal cells in the globular embryo (Fig. 2B; Fig S3). SOK3-YFP protein accumulated at the basal side and every corner of most cells in the primary root with highest levels in vascular cells, as well as on the apical side of root cap cells (Fig. 1E,J) a pattern that is reiterated in lateral roots (Fig. 2M; Fig. S4J-M).

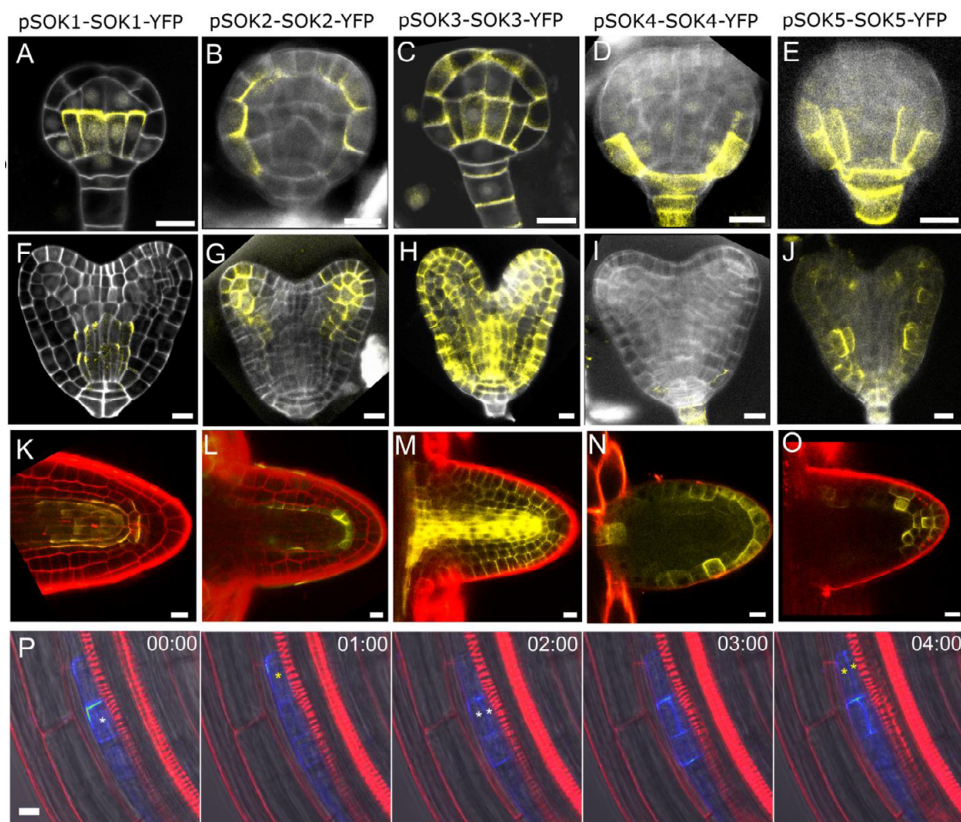


Figure 2: Diverse polar patterns of SOSEKI proteins. Localization of SOK1-YFP (A,F,K), SOK2-YFP (B,G,L), SOK3-YFP (C,H,M), SOK4-YFP (D,I,N) and SOK5-YFP (E,J,O) in globular stage embryos (A-E), heart stage embryos (F-J) and emerged lateral root primordia (K-O). (D) Stills of a time-lapse imaging series of SOK1-YFP fluorescence in an initiating lateral root. Time (in hours) is indicated in each panel and cells are marked by asterisks. Embryos in A-J are counterstained with Renaissance RS2200 (white), and roots (K-P) with Propidium Iodide (red). Bars 10 μ m.

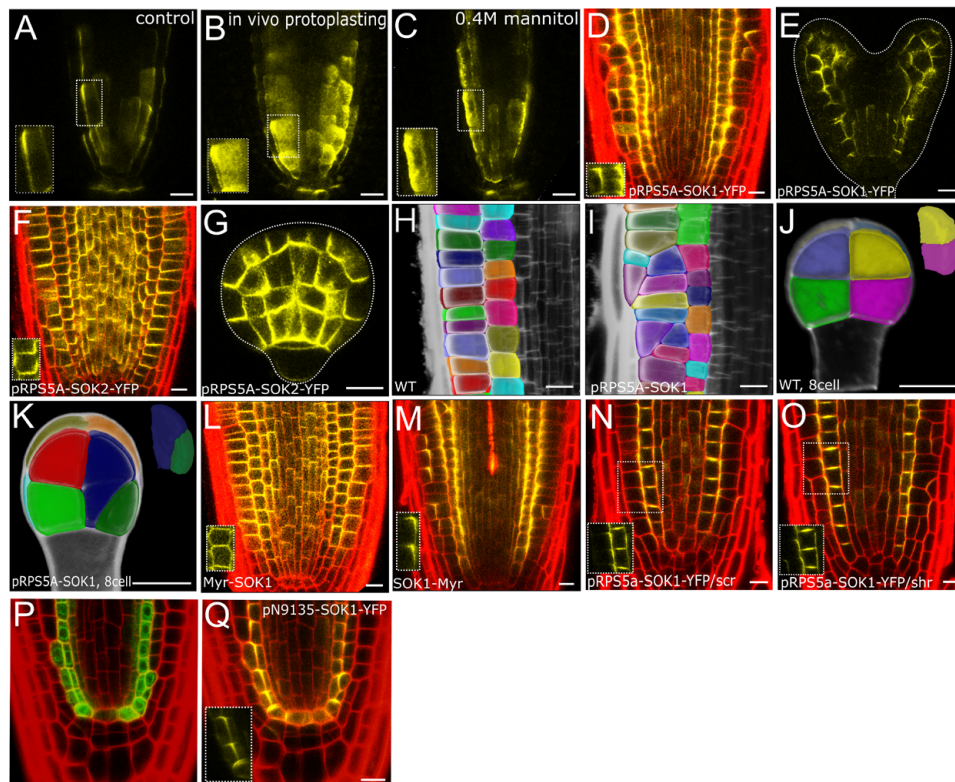
During embryogenesis, SOK3 localizes to the basal side or all corners of most cells starting at the 1-2 cell stage (Fig. S3). Expression of SOK4-YFP is weaker than other SOKs – the protein could not be detected in the primary root (Fig. 1F,K; Fig. S2D), but faint signal was found during lateral root formation (Fig. 2N; Fig. S4N-Q) and in the embryo (Fig. 2D,I; Fig. S3). Finally, SOK5-YFP strongly resembles SOK2 accumulation in its pattern in endodermis, quiescent center (QC) and lateral root cap in primary root (Fig. 1G,L; Fig. 2O), where it localizes to inner basal edges. Yet the evolution of this pattern in the embryo differs from SOK2 as it is initiated earlier (Fig. 2E,J; Fig. S3). In summary, all SOK family proteins are expressed in specific tissues during embryonic root formation and mark unique polar subcellular domains.

3 To investigate the mechanism controlling edge localization of SOK proteins, we examined the effect of various chemicals, previously shown to affect (polar) protein localization, on localization pattern of SOK1, SOK2 and SOK3. None of the hormones auxin (2,4-D), cytokinin (BA, tZ), epi-brassinolide or giberellic acid, of the trafficking or cytoskeleton inhibitors, NPA, BFA, wortmannin, monensin, concanamycin A, leptomycin B, cytochalasin B, latrunculin B, jasplakinolide, oryzalin and taxol, proteasome inhibitor MG-132 affected the edge localization of SOK1 (or SOK2 and SOK3 where tested). This suggests that polar localization follows a path that is distinct from the well-known polar proteins PIN (reviewed in Armengot et al., 2016), BOR1 (Takano et al., 2002, 2010) and NIP5 (Takano et al., 2010). We next tested if cell wall, or mechanical properties influence SOK protein localization and found that a brief (1-10 minutes) treatment with cell wall-degrading enzymes (Fig. 3A,B ; Fig. S5A-D,F-I) or with high osmotic mannitol solution (Fig. 3C; Fig. S5E,J) led to acute disappearance of SOK proteins from edges and intracellular accumulation in large clumps despite normal cellular morphology as evidenced by a plasma membrane marker (Fig. S5K-N). This indicates that cell wall integrity is critical for edge localization of SOK proteins.

To test whether differences in polar localization among SOK proteins are caused by cell type influences or intrinsic differences between proteins, we expressed YFP fusions to SOK1 or SOK2 from the ubiquitous, meristem-specific *RPS5A* promoter (Weijers et al., 2003). While SOK1 protein localizes to the outer apical edge in vascular cells, misexpressed SOK1 localizes to inner apical edge in the cortex and epidermis (Fig. 3D,E; Fig. S6B). Ectopic SOK2-YFP localizes to inner basal edges of all cells (Fig. 3F,G; Fig. S6H-J). Thus apical/basal polarity is maintained in misexpression lines and appears intrinsic to SOK1 and SOK2 proteins. Strikingly, in *RPS5A*-SOK-YFP embryos, the apical or basal localization was conserved in all cells spanning root, hypocotyl and cotyledons (Fig. 3E,G), which suggests the existence of a common supra-cellular polarity reference in the entire plant. During lateral root initiation however, localization followed the new organ axis (Fig. 2K-O; Fig. S4), suggesting that the coordinate system is autonomous to lateral organs. Interestingly,

unlike apical/basal polarity, inner/outer polarity of SOK1 was altered upon misexpression: SOK1 localized in outer apical edge in the vascular cells whereas it decorated the inner apical edge in epidermis/cortex. Therefore, SOK1 proteins always localized pointing towards the endodermis. Localization in the *shr* and *scr* mutants with impaired endodermal identity (Benfey et al., 1993; Scheres et al., 1995) caused loss of edge localization and led to apical accumulation (Fig. 3N,O; Fig. S6E,F). This suggests that edge localization integrates genetically separable apical-basal and outer-inner axes. The cortex-endodermis junction serves as a potent cue for SOK1 localization, which is confirmed by ground tissue-specific expression of SOK1-YFP using the N9135 GAL4 driver line. In the shared initial between cortex and endodermis, SOK1-YFP is apical, while the protein localized at both opposing edges toward the junction after the periclinal division that separates endodermis and cortex (Fig. 3P,Q; Fig. S6G). Thus, plant cells possess a universal coordinate system with an internal reference that is read and integrated by SOK proteins.

When analyzing SOK1 misexpression lines, we noticed that both embryos and roots showed frequent alterations in cell division orientation. In embryos, such division were found in all cell types (Fig. 3J,K), while in roots, defects were most pronounced in the endodermis, cortex and epidermis (Fig. 3D,H,I). While normal divisions in these root cell types are anticlinal to the growth axis, misexpression lines displayed either oblique or periclinal divisions that consequently generated additional cell layers. Root growth was slightly inhibited in misexpression lines (Fig. S6A). The same defects were found in lines that misexpressed either YFP-tagged or non-tagged SOK1, suggesting that this is a property of the naturally occurring SOK1 protein. This result demonstrates that ectopic SOK protein can induce altered orientations of cell division planes. We next utilized this biological activity to determine localization requirements for activity. We first tested if polar localization is required for function. To this end, we fused a Myristoylation (Myr) motif to either the N- or C-terminus of SOK1-YFP. SOK proteins do not have a signal peptide or predicted transmembrane helices (Fig. S7), and are likely peripherally membrane-associated. Both polarity and activity (as judged by oblique cell divisions) of SOK1-YFP was completely lost when the Myr motif was fused to the N-terminus of SOK1-YFP (Fig. 3L; Fig. S6C). In contrast, adding the Myr motif to the C-terminus of SOK1-YFP did not affect localization or activity (Fig. 3M; Fig. S6D). The result showed that polar localization is a requirement for SOK1 function.



3

Figure 3: Regulation of SOSEKI localization. (A-C) Localization of SOK1-YFP in control-treated root tip (A), and in root tips treated with cell wall-digesting enzymes (B) or with mannitol (C). (D,E) Localization of SOK1-YFP in RPS5A-SOK1-YFP root tip (D) and heart stage embryo (E). (F,G) Localization of SOK2-YFP in RPS5A-SOK2-YFP root tip (F) and heart stage embryo (G). (H-K) Segmented cell volumes in wild-type (H,J) and RPS5A-SOK1 (I,K) root meristem (H,I) and 8-cell embryo (J,K). (L) Myr-SOK1-YFP localization in RPS5A- Myr-SOK1-YFP root tip. (M) SOK1-Myr-YFP localization in RPS5A-SOK1-Myr-YFP root tip. (N,O) Localization of RPS5A-driven SOK1-YFP in scr (N) and shr (O) root tips. (P,Q) GAL4-driven GFP expression (P) and GAL4-driven SOK1-YFP accumulation (Q) in root tip of *N9135 >> SOK1-YFP*. Walls in (D,F,L-Q) are counterstained with Propidium Iodide (red). Insets in (A-D,F,L-O,Q) show SOK protein localization in single cells. Bars 10 μ m.

To determine whether signals in the SOK1 protein also correlate with polarity and activity, we carried out a series of N- or C-terminal deletions (Fig. 4A; Fig. S7) and misexpressed each as a YFP fusion. Deletions Δ A, Δ B, Δ C and Δ D caused SOK1 to be localized in the cytosol (Fig. 4B; Fig. S8A-E). Interestingly, the Δ E SOK1 protein localized to the apical edge (Fig. 4C; Fig. S8F), suggesting that the fragment contained in the Δ D- Δ E segment is sufficient for polar localization. Deletions Δ F, Δ G and Δ H are broadly localized to the lateral side of cells (Fig. 4D;

Fig. S8G-I), suggesting that the N-terminus is not required for localized membrane association per se, but rather for focusing to the edge. Finally, deletions ΔI , ΔJ , ΔK and ΔL were all localized to the cytosol (Fig. 4E; Fig. S8G-M), suggesting that the ΔD - ΔE segment can only direct edge localization if the N-terminus is present. Strikingly, only ΔE SOK1 protein induced altered cell divisions (Fig. 4C). Thus, SOK1 carries two function domains: one for membrane association (middle), and another (N-terminal) for focused polar localization and activity.

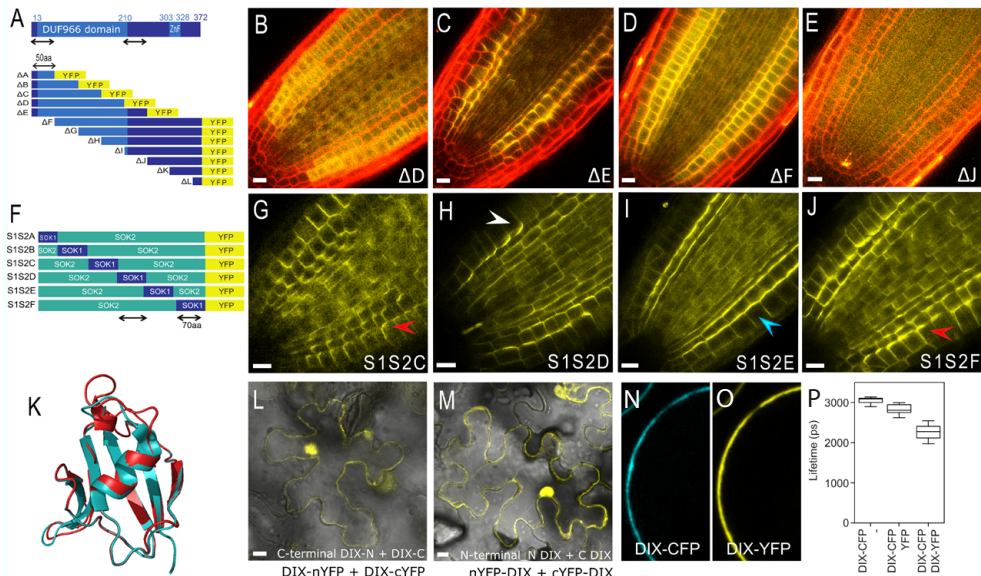


Figure 4: Protein determinants for SOK localization and activity. (A) Schematic representation of SOK1 protein domains (ZnF = Zn-finger), and outline of domain deletion constructs expressed as YFP-fusions driven from the RPS5A promoter. (B-E) Representative examples of SOK1-YFP domain deletion accumulation in root tips. (F) Outline of SOK2-SOK1 domain swaps, expressed as YFP fusions driven from the RPS5A promoter. (G-J) Representative examples of SOK1-SOK2-YFP domain swap accumulation in root tips. Red arrowheads in G and J mark basal localization, while white arrowhead in H marks apical localization and blue arrowhead in I marks lateral localization. Note that regions in A and F marked by arrows denote the regions for focused membrane localization and polarity defined by deletions and swaps. (K) Structural alignment of the DIX domain in human Dvl2 (PDB: 4WIP; Cyan) and the homology model of the SOK1 DIX-like domain (Red). (L,M) Bimolecular Fluorescence complementation (BiFC) in *Nicotiana benthamiana* epidermis of the SOK1 DIX-like domain in homo-dimeric conformation, using either N-terminal YFP fragments (L) or C-terminal YFP fragments (M). (N,O) Fluorescence of co-expressed SOK1 DIX-like domain as CFP (N) and YFP (O) fusion in protoplast. (P) Quantification of CFP Fluorescence Lifetime (ps) in SOK1-DIX-CFP/YFP pair, and the two individual fusions in protoplasts. Walls in (B-E) are counterstained with Propidium Iodide (red). Bars 10 μ m.

We next asked whether different SOK proteins use similar domains for localization and hoped to identify a minimal polarity domain. We replaced successive 50-70 amino acid segments of SOK2 by the corresponding region of SOK1 (Named S1S2A-F; Fig. 4F, Fig. S7) and localized protein chimaeras using YFP. S1S2A, S1S2B, S1S2C and S1S2F chimaeras localized to the basal edge (Fig. 4G,J; Fig. S8N,O,P,S), like wild-type SOK2-YFP protein. Interestingly, the S1S2D protein localized to the apical corner of the cell (Fig. 4H; Fig. S8Q) similar to SOK1-YFP. The S1S2E proteins showed a mixture of SOK1 and SOK2 localization and decorated the inner lateral membrane (Fig. 4I; Fig. S8R). Thus, polar localization can be transferred between SOK1 and SOK2 using a discrete domain, that overlaps with the Δ D- Δ E segment defined by deletions. We confirmed that the same domain conferred polarity changes in swaps between SOK1 and SOK5 (Fig. S9). This identifies a minimal domain for polar targeting of multiple SOK family members.

3
SOK proteins are plant-specific, and the DUF966 domain (Fig. S7) has no known function. We used structural homology modeling to identify potential homologues. This surprisingly showed that a part of the DUF966 domain resembles the DIX (Dishevelled/Axin) domain that is found in a number of animal proteins (Fig. 4K; reviewed in Bienz, 2014). The DIX domain mediates head-to-tail oligomerization and is required for clustering of the polarity regulator Dishevelled in animals (Schwarz-Romond et al., 2007). We used *in vivo* FRET and BiFC assays to show that the predicted DIX domain in SOK1 indeed mediates homodimerization (Fig. 4L-P; Fig. S8T-W). Strikingly, the DIX-like domain corresponds to the N-terminal region that is required for focused edge localization and biological activity. Thus, polar proteins in plants and animals use the same protein domain for localization and function.

Our study identified a novel plant-specific family of polar/corner localized proteins. We showed that edge localization is important for the activity of SOK1 in influencing the orientation of cell division plane. Whether SOK1 and other family members normally mediate this function, and what cellular mechanism underlies such activity remains to be determined. Yet our detailed analysis of SOK localization identified a universal coordinate system in plants, as well as a set of proteins that can read and integrate the coordinates. Consistent with this being a coordinate system, the localization mechanism is extremely robust, yet seems to rely on cell wall integrity and/or mechanical properties. We expect that further exploration of the mechanisms of SOK localization and function may help reveal the fundamental principles of organismal and cell polarity in plants. This may herald surprising analogies to animal polarity, given the adoption of the same functional protein domain in polar proteins across kingdoms.

Material and Methods

Plant material

All seeds were sterilized, sown on 1/2 MS medium with 1% sucrose and 0.8% Daishin agar (Duchefa) and vernalized for one day. Plants were grown on soil at 22°C under the long-day condition. The N9135-GAL4 enhancer trap line was generated by Jim Haseloff (University of Cambridge, UK) and obtained through the *Arabidopsis* Biological Resource Centre (ABRC). *shr-2* and *scr-4* mutants were obtained from (Fukaki et al., 1998; Helariutta et al., 2000).

Cloning

Cloning procedures were described previously (De Rybel et al., 2011). For promoter-GFP lines, 2-5 kb fragments upstream of the ATG of SOK genes were amplified and introduced into pGIIK-LIC-SV40-3xGFP-NOST (pPLV04). For protein-YFP fusion lines, genomic fragments of SOK genes excluding the stop codon (SOK1: 3.6 kb, SOK2: 3.6 kb, SOK3: 5.3 kb, SOK4: 2.6 kb, SOK5: 4.9 kb) were introduced into pGIIB-LIC-sYFP-NOST (pPLV16) and/or pGIIB-LIC- tdTomato-NOST (pPLV10). For misexpression lines, SOK cDNAs excluding the stop codon were amplified, fused with YFP sequences and introduced into pGIIB-pRPS5a-LIC-NOST (pPLV28). For gene swap experiment, cDNA fragments of SOK1, SOK2, 5 and YFP were amplified, fused by overlap extension PCR method and introduced into pGIIB-pRPS5a-LIC-NOST (pPLV28). For deletion experiments, 7 cDNA fragments with increasing length at the 3' end and 7 fragments with decreasing length at the 5' end were amplified and introduced into pGIIB-LIC-sYFP-NOST (pPLV16). For myristoylated SOK1 constructs, sequences for myristylation was added to either C-terminus or N-terminus of SOK1 cDNA sequences and introduced into pGIIB-LIC-sYFP-NOST (pPLV16). All the constructs are sequenced and transformed into wild-type Columbia and transformed by floral dip using the *Agrobacterium* strain GV3101 (pSoup). The UAS::SOK1-YFP construct was generated by amplifying SOK1-YFP from the pRPS5a::SOK1-YFP plasmid and introducing it into pGIIB-UAS::LIC-NOST (pPLV32). The construct was transformed directly into the N9135 enhancer trap line. For BiFC, the DIX sequence was amplified from a SOK1 cDNA vector and cloned into a modified pGII vector containing p35S::LIC-n/cYFP. FLIM vectors were generated by cloning the DIX cDNA into pMON 35S::LIC-sYFP or pMON 35S::LIC-sCFP3a.

Microscopic analysis

Roots were stained by PI at final concentration of 10 µg/ml. Embryos were fixed and stained by 2.2% renaissance2200 in PBS buffer at pH6.9 containing 4% paraformaldehyde, 50% glycerol, 4.2% dimethyl sulfoxide (DMSO) or stained by PI after fixation as previously described (Yoshida, Reuille, et al., 2014).

Confocal imaging was performed on a Zeiss LSM510 or Leica SP5 or SP8 with a hybrid detector. Following laser settings are used for the observation; GFP (Argon laser, excitation 488nm, emission, 500-530nm), YFP (Argon laser, excitation 524nm, emission 525-600nm), tdTomato and PI staining (DPSS 5611 laser, excitation 561nm, emission 570-600nm) and renaissance2200-staining (UV 405 diode laser, excitation 405nm, emission 430-470nm). Analysis of confocal images (3D reconstruction, 3D segmentation) was performed by MorphoGraphX (de Reuille et al., 2015).

Chemical treatments

Following chemicals were used: IAA (1 μ M), 2,4-D (1 μ M),benzyladenine (1 μ M), trans-zeatin (1 μ M), epi-brassinolide (epiBL; 1 μ M) and gibberellic acid (GA) (1 μ M), NPA (5 μ M), BFA (42 μ M), wortmannin (30 μ M), monensin (10 μ M), concanamycin A (ConcA); 0.8 μ M), leptomycin B (30 nM), cytochalasin B (50 μ M), laticulolin B (LatB; 1 μ M), oryzalin (5 μ M), taxol (100 μ M), MG-132 (50 μ M), cycloheximide (CHX; 50 μ M), hydroxyurea (HU; 2mM), Mannitol (0.4 M), and isoxaben (100 nM). Seedlings were placed on the MS plates containing each chemical for the durations mentioned in the text and were subsequently imaged by confocal microscopy.

3
Plasmolysis was performed either on the MS medium with mannitol (Sigma, M9546) at final concentration 0.4M or in 0.4M mannitol solution in miliQ water, and stained by FM4-64 at least for 2 min. For in vivo protoplasting, either 1% cellulose R10 (Yakult Honsha Co. L.T.D, Japan) and/or 0.2% macerozyme (Serva) were used. Cellulose and/or macerozyme was dissolved in a solution congaing 72.86g mannitol, 1.49g KCl and 20 mL of a 1M MES (pH 5.7) per liter. 250 μ l of CaCl₂ is added prior to the experiments. Seedlings were treated by 70 μ l of protoplasting solution, stained by FM4-64 and observed by confocal.

Structural homology modeling

SwissModel (<https://swissmodel.expasy.org/>) was used to model the structure of DIX-LIKE. To this end, the conserved N-terminal part of SOK1 was entered into the program and the software itself selected the best matching crystal structure, which was human Dvl2 (PBD: 4WIP).

BiFC

Agrobacterium containing BiFC plasmids were grown overnight in 5ml LB + 20mg/L Gentamycin, 50mg/L kanamycin, 25mg/L rifampicin and 2mg/L tetracyclin. Cultures were spun down at 4000rpm for 10 minutes and the bacterial pellet was resuspended in 1 mL MMAi (5g/L MS salts without vitamins, 2g/L MES, 20g/L sucrose, pH 5.6; and 0.2 mM Acetosyringone). The OD₆₀₀ was measured with a spectrophotometer. The infiltration samples were mixed 1:1 at a total OD₆₀₀ of 0.8. Samples were incubated at RT for 2 hours and infiltrated into the underside of

Nicotiana benthamiana leaves with a 1mL syringe. After two days, leaf samples were cut out with a razor blade and imaged with a confocal microscope.

FLIM

Protoplast transfection and FLIM measurements were performed on a Leica SP8 as described in (Rios et al., 2017). Per construct (combination), 20 protoplasts were measured.

Acknowledgments

We would like to thank Dominique Hagemans for her help with the FRET-FLIM, Vivienne Mol for creating the N9135 SOK1 line and Colette ten Hove for crossing the *shr* and *scr* mutants with SOK. Also great thanks to J.W. Borst for his help with the confocal and FRET-FLIM.

References

Benfey, P. N., Linstead, P. J., Roberts, K., Schiefelbein, J. W., Hauser, M.-T., & Aeschbacher, R. A. (1993). Root development in *Arabidopsis*: four mutants with dramatically altered root morphogenesis. *Development*, *119*, 57–70.

Biernz, M. (2014). Signalosome assembly by domains undergoing dynamic head-to-tail polymerization. *Trends in Biochemical Sciences*, *39*, 487–495.

Cruz-Ramírez, A., Díaz-Triviño, S., Blilou, I., Grieneisen, V. A., Sozzani, R., Zamioudis, C., ... Scheres, B. (2012). A bistable circuit involving SCARECROW-RETINOBLASTOMA integrates cues to inform asymmetric stem cell division. *Cell*, *150*, 1002–1015.

de Reuille, P. B., Routier-Kierzkowska, A. L., Kierzkowski, D., Bassel, G. W., Schüpbach, T., Tauriello, G. et al. (2015). MorphoGraphX: A platform for quantifying morphogenesis in 4D. *eLife*, *4*, 1–20.

De Rybel, B., van den Berg, W., Lokerse, A. S., Liao, C.-Y., van Mourik, H., Möller, B. et al. (2011). A Versatile Set of Ligation-Independent Cloning Vectors for Functional Studies in Plants. *Plant Physiology*, *156*, 1292–1299.

Dong, J., MacAlister, C. A., & Bergmann, D. C. (2009). BASL Controls Asymmetric Cell Division in *Arabidopsis*. *Cell*, *137*, 1320–1330.

Ehebauer, M. T., & Arias, A. M. (2009). The structural and functional determinants of the Axin and Dishevelled DIX domains. *BMC Structural Biology*, *9*, 1–12.

Friml, J., Vieten, A., Sauer, M., Weijers, D., Schwarz, H., Hamann, T. et al. (2003). Efflux-dependent auxin gradients establish the apical-basal axis of *Arabidopsis*. *Nature*, *426*, 147–153.

Fukaki, H., Wysocka-Diller, J., Kato, T., Fujisawa, H., Benfey, P. N., & Tasaka, M. (1998). Genetic evidence that the endodermis is essential for shoot gravitropism in *Arabidopsis thaliana*. *Plant Journal*, *14*, 425–430.

Hardtke, C. S., & Berleth, T. (1998). The *Arabidopsis* gene MONOPTEROS encodes a transcription factor mediating embryo axis formation and vascular development. *EMBO Journal*, *17*, 1405–1411.

Helariutta, Y., Fukaki, H., Wysocka-Diller, J., Nakajima, K., Jung, J., Sena, G. et al. (2000). The SHORT-ROOT Gene Controls Radial Patterning of the *Arabidopsis* Root through Radial Signaling. *Cell*, *101*(5), 555–567.

Koizumi, K., Hayashi, T., & Gallagher, K. L. (2012). SCARECROW reinforces SHORT-ROOT signaling and inhibits periclinal cell divisions in the ground tissue by maintaining SHR at high levels in the endodermis. *Plant Signaling & Behavior*, *7*:12, 1573–1577.

Möller, B. K., ten Hove, C. A., Xiang, D., Williams, N., López, L. G., Yoshida, S. et al. (2017). Auxin response cell-autonomously controls ground tissue initiation in the early *Arabidopsis* embryo. *Proceedings of the National Academy of Sciences*, *114*, E2533–E2539.

Möller, B., & Weijers, D. (2009). Auxin control of embryo patterning. *Cold Spring Harbor Perspectives in Biology*.

Rios, A. F., Radoeva, T., Rybel, B. De, Weijers, D., & Borst, J. W. (2017). FRET-FLIM for Visualizing and Quantifying Protein Interactions in Live Plant Cells, *1497*, 135–146.

Scheres, B., Dilaurenzio, L., Willemsen, V., Hauser, M. T., Janmaat, K., Weisbeek, P., & Benfey, P. N. (1995). Mutations affecting the radial organisation of the *Arabidopsis* root display specific defects throughout the embryonic axis. *Development*, *121*, 53–62.

Schlereth, A., Möller, B., Liu, W., Kientz, M., Flipse, J., Rademacher, E. H. et al. (2010). MONOPTEROS controls embryonic root initiation by regulating a mobile transcription factor. *Nature*, *464*, 913–916.

Schwarz-Romond, T., Fiedler, M., Shibata, N., Butler, P. J. G., Kikuchi, A., Higuchi, Y., & Bienz, M. (2007). The DIX domain of Dishevelled confers Wnt signaling by dynamic polymerization. *Nature Structural and Molecular Biology*, *14*, 484–492.

Takano, J., Noguchi, K., Yasumori, M., Kobayashi, M., Gajdos, Z., Miwa, K. et al. (2002). *Arabidopsis* boron transporter for xylem loading. *Nature*, *420*, 337–340.

Takano, J., Tanaka, M., Toyoda, A., Miwa, K., Kasai, K., Fuji, K. et al. (2010). Polar localization and degradation of *Arabidopsis* boron transporters through distinct trafficking pathways. *Proceedings of the National Academy of Sciences of the United States of America*, *107*, 5220–5225.

Weijers, D., vanHamburg, J. P., vanRijn, E., Hooykaas, P. J. J., & Offringa, R. (2003). Diphtheria toxin-mediated interregional communication seed development. *Plant Physiology*, *133*, 1882–1892.

Yoshida, S., Barbier de Reuille, P., Lane, B., Bassel, G. W., Prusinkiewicz, P., Smith, R. S., & Weijers, D. (2014). Genetic control of plant development by overriding a geometric division rule. *Developmental Cell*, *29*, 75–87.

Supplemental Information

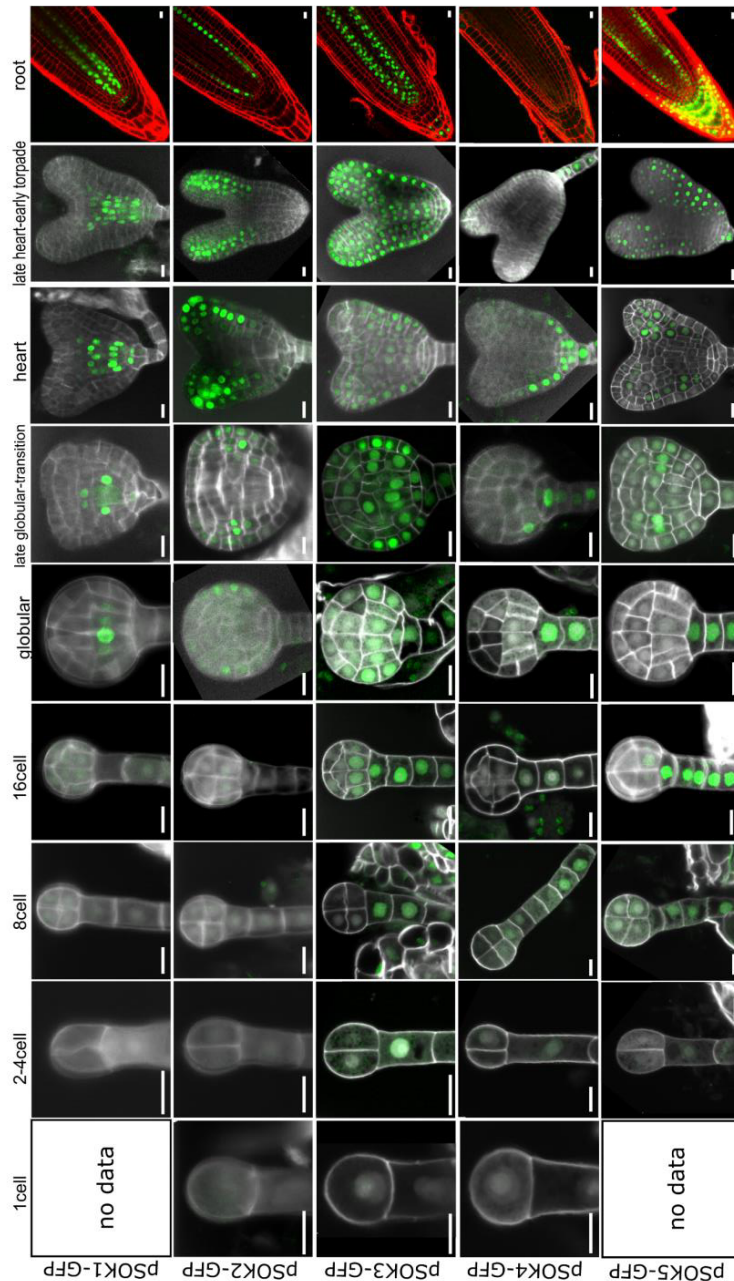


Figure S1: Expression of SOK genes in embryo and root. Fluorescence of n3GFP in successive stages of embryo development and the root meristem of lines expressing pSOK1-n3GFP, pSOK2-n3GFP, pSOK3-n3GFP, pSOK4-n3GFP and pSOK5-n3GFP. Embryos are counterstained with Renaissance RS2200 (white), and roots with Propidium Iodide (red). Bars 10 μ m.

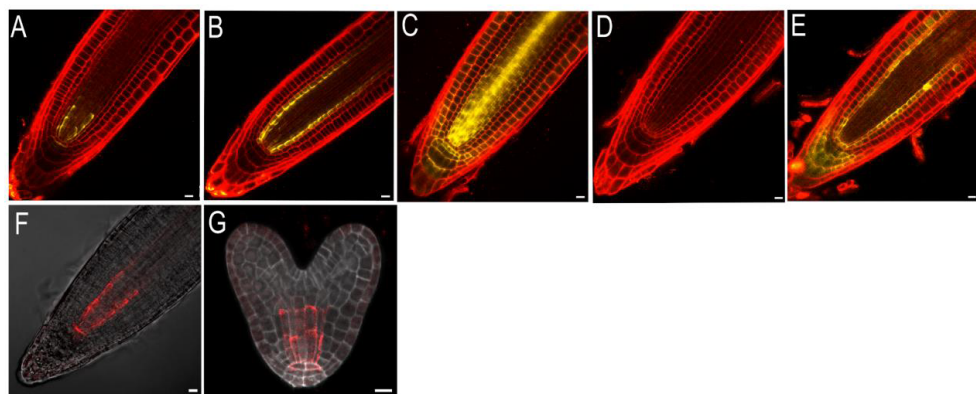


Figure S2: Localization of *SOK*-YFP and *SOK*-tdTomato in root tips. (A-E) Fluorescence of *SOK*-YFP fusion proteins in the extended root meristem, when expressed from the native promoter. (F,G) Fluorescence of *SOK1*-tdTomato in root tip (F) and heart stage embryo (G). Roots in (A-E) are counterstained with Propidium Iodide (red) and Embryo (G) with Renaissance RS2200 (white). Bars 10 μ m.

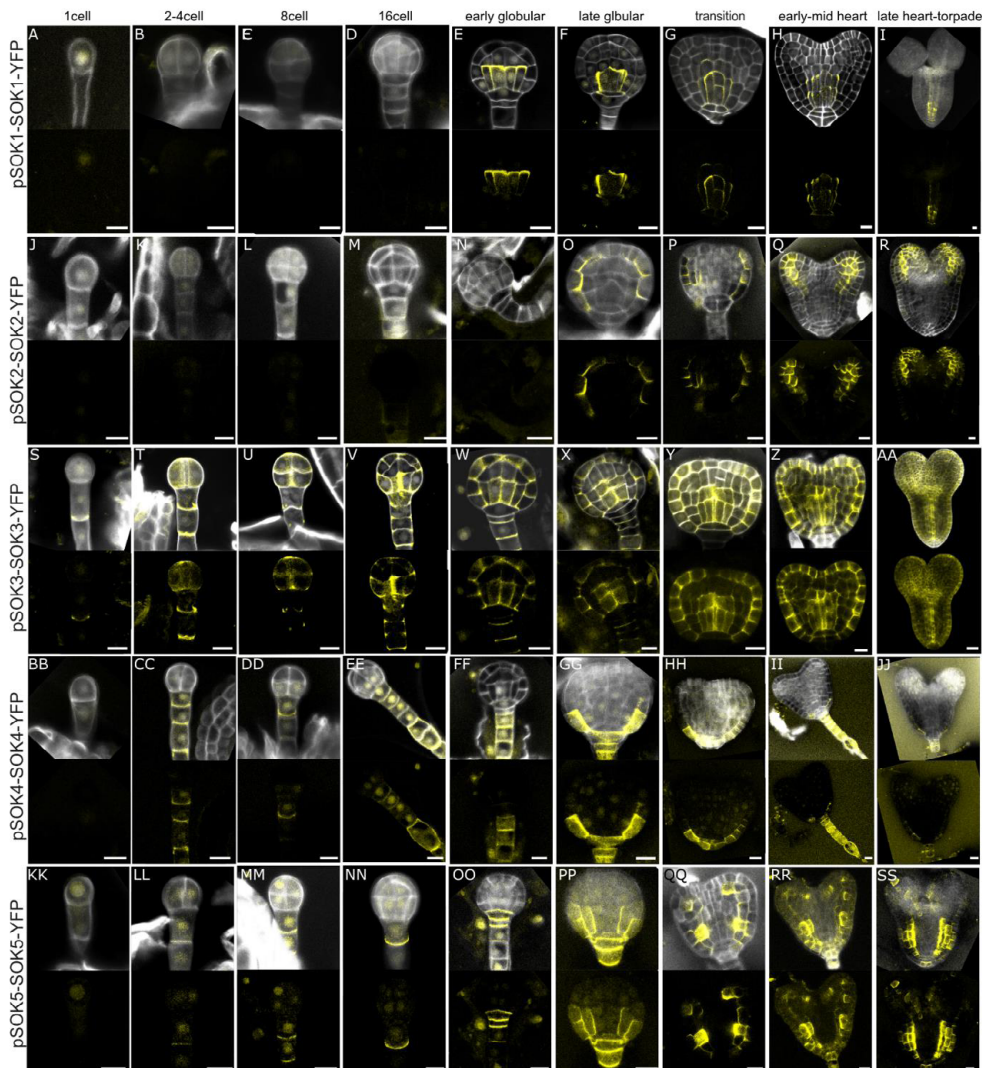


Figure S3: *SOK* protein localization during embryogenesis. *SOK*-YFP protein accumulation during successive stages of embryogenesis. Upper panels show overlay of YFP and cell wall (Renaissance RS2200 – white) signals, while lower panels show only the YFP signal. Bars 10 μ m.

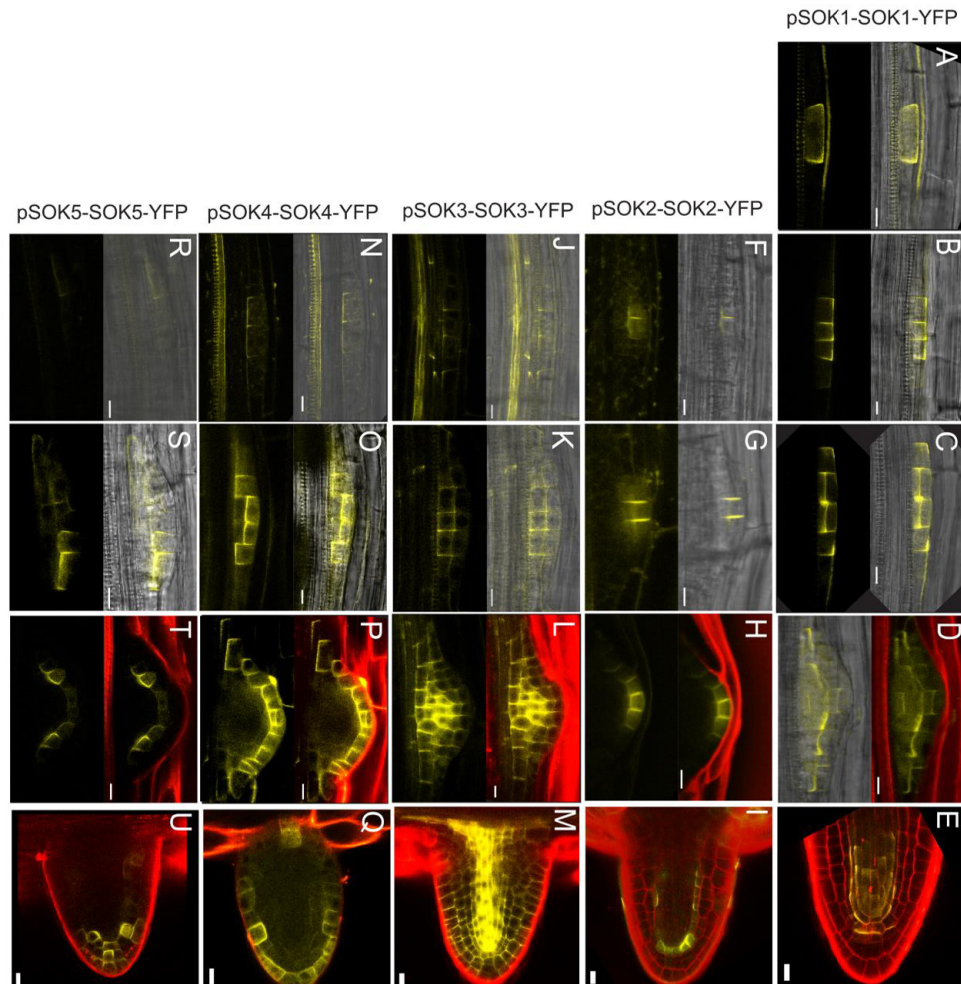
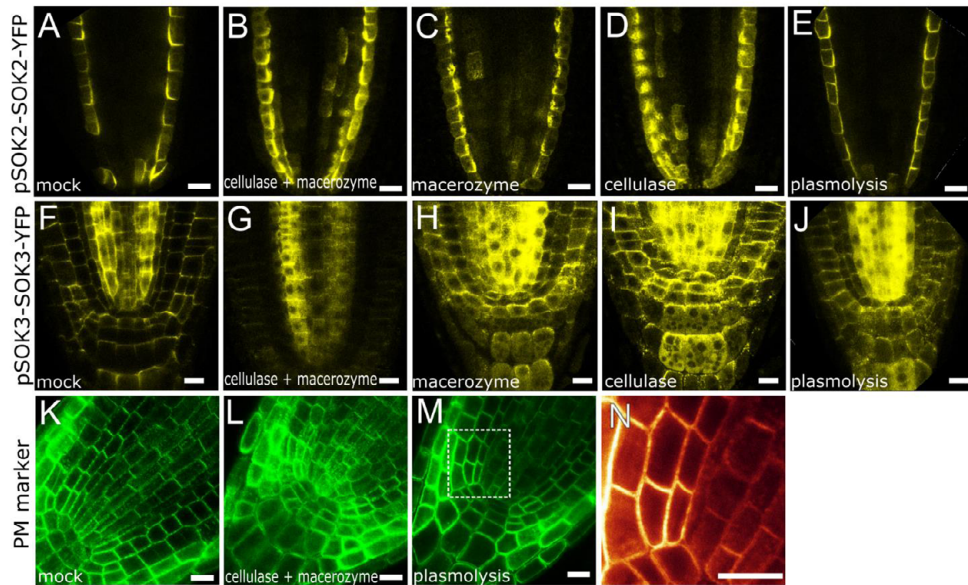


Figure S4: *SOK* protein accumulation during lateral root development. *SOK1*-YFP (A-E), *SOK2*-YFP (F-I), *SOK3*-YFP (J-M), *SOK4*-YFP (N-Q) and *SOK5*-YFP (R-U) protein accumulation during successive stages of lateral root formation. Upper panels in (A-D,F-H,J-L,N-P,R-T) are overlays of YFP signal and transmitted light images (A-C,F,G,J,K,N,O,R,S) or Propidium Iodide (D,H,L,P,T - red), while lower panels are YFP signal alone. Bars 10 μ m.



3
Figure S5: Cell wall-dependent SOK protein localization. (A-J) Localization of SOK2-YFP (A-E) and SOK3-YFP (F-J) protein in control root (A,F) and root tips treated with Cellulase and Macerozyme (B,G), Macerozyme (C,H), Cellulase (D,I) or Mannitol (E,J). (K-M) Localization of a plasma membrane-integral GFP marker in control root tip (K) and root tips treated with Cellulase and Macerozyme (L), or with Mannitol (M,N). Note that (N) is a magnification of the dashed area in (M). Bars 10 μ m.

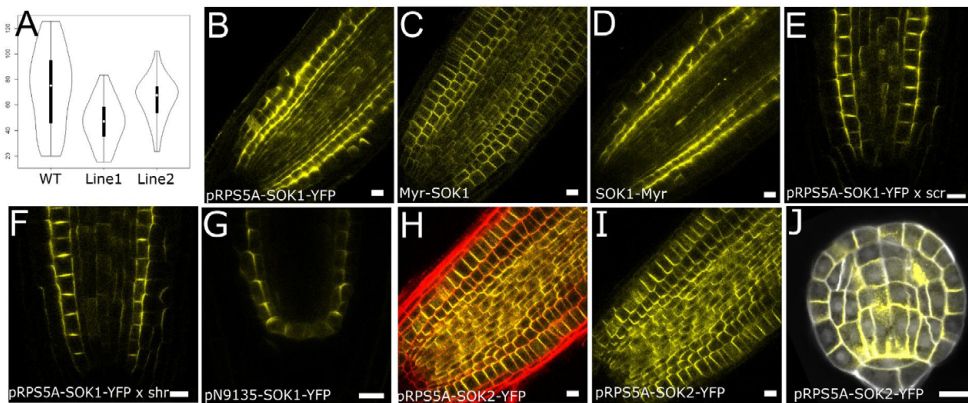


Figure S6: Regulation of SOK polar localization. (A) Root length (mm) in wild-type and two independent RPS5A-SOK1 lines. (B-D) YFP fluorescence in RPS5A-SOK1-YFP (B), RPS5A-Myr-SOK1-YFP (C) and RPS5A-SOK1-Myr-YFP (D) root tips. (E,F) YFP fluorescence in RPS5A-SOK1-YFP in scr (E) and shr (F) roots. (G,H) SOK2-YFP localization in RPS5A-SOK2-YFP root tip with (H) or without (I) Propidium Iodide counterstain (red). (J) SOK2-YFP localization in RPS5A-SOK2-YFP transition stage embryo. Bars 10 μ m.

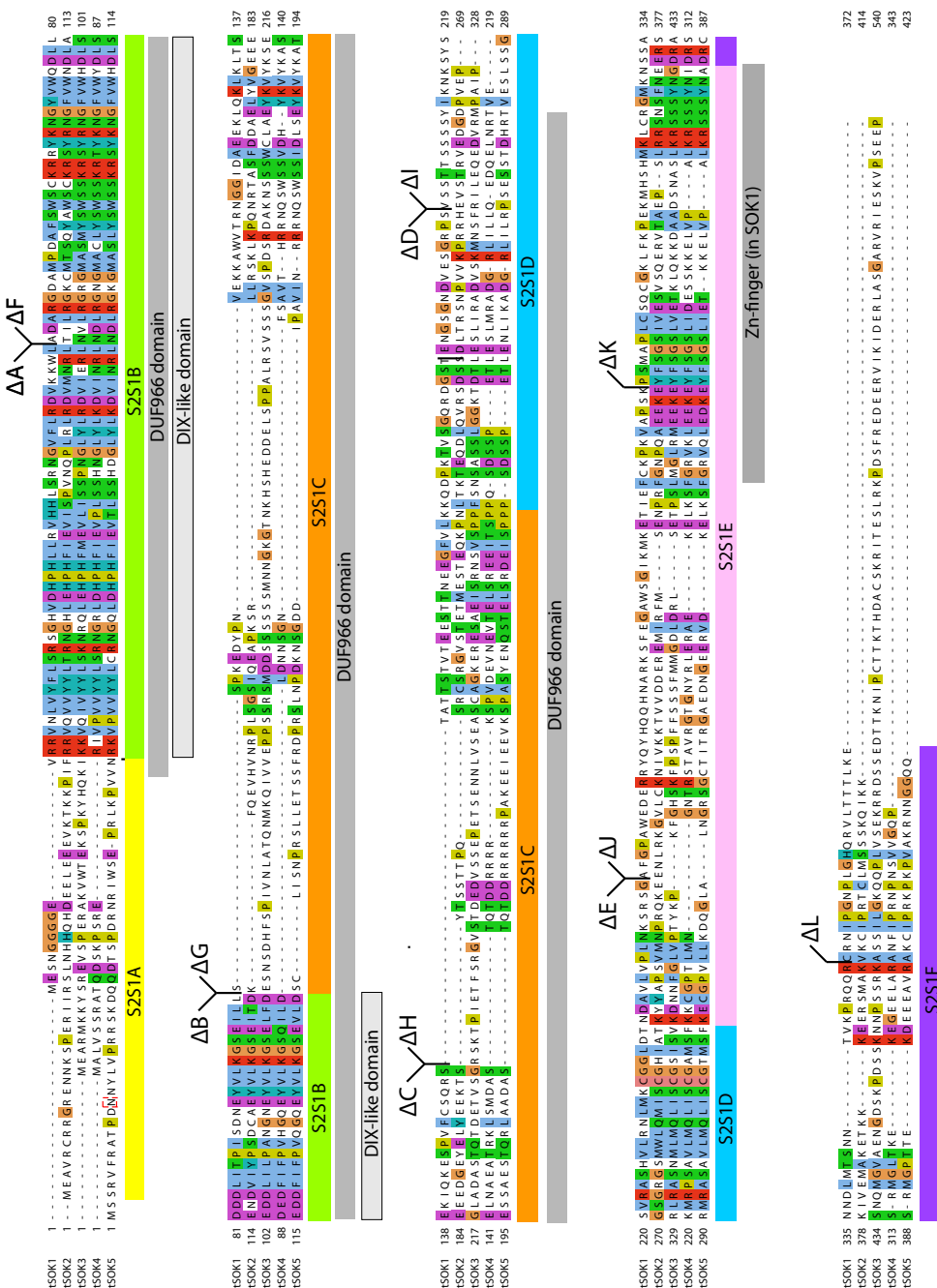


Figure S7: *SOK* protein alignment, domains, swaps and deletion fragments. Protein sequence alignment of the 5 *Arabidopsis* *SOK* proteins. The DUF966 domain, as well as the DIX-like domain and the Zinc Finger are indicated. All deletion fragment boundaries are bracketed above the sequence, and the regions swapped between *SOK1* and *SOK2* are marked underneath the alignment.

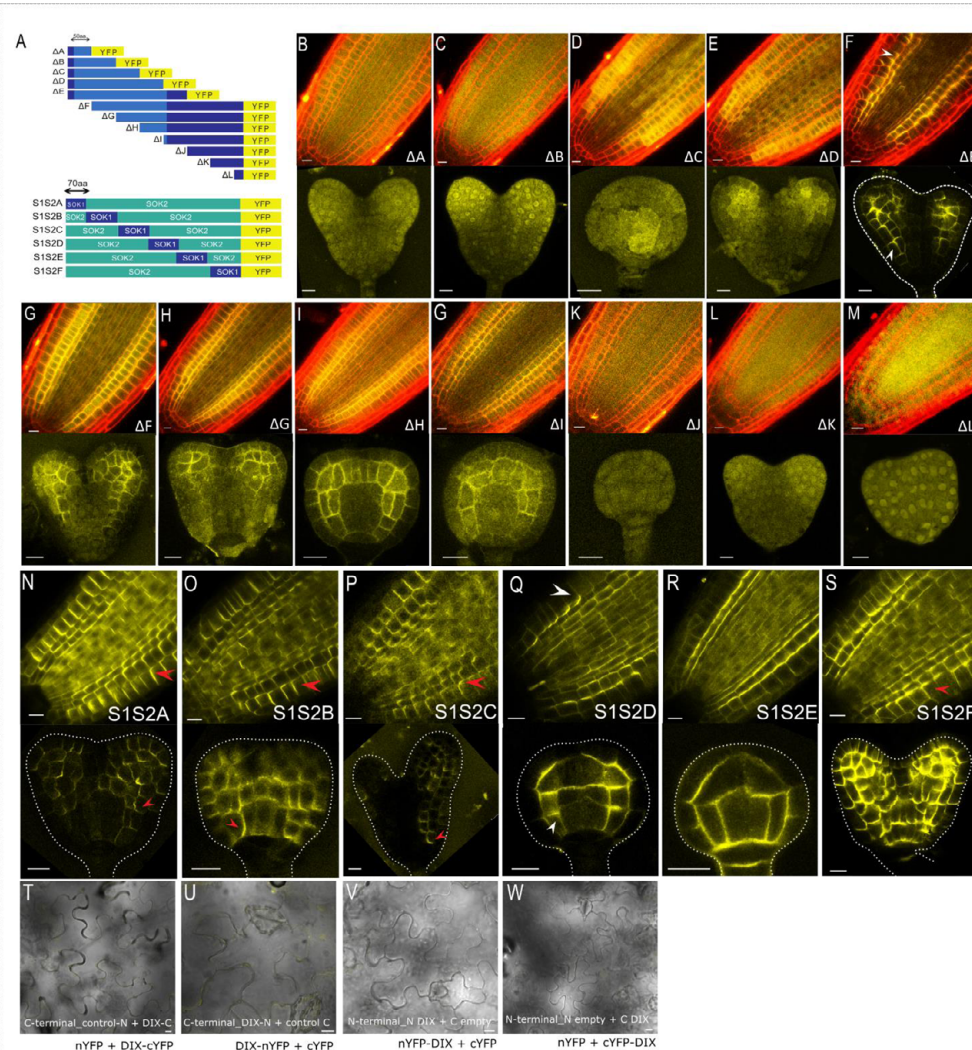


Figure S8: Details of SOK1 deletions and SOK1/2 swaps. (A) Schematic representation of SOK1 domain deletion constructs expressed as YFP-fusions driven from the RPS5A promoter, and SOK2-SOK1 domain swaps, also expressed as YFP fusions driven from the RPS5A promoter. (B-M) Complete set of SOK1-YFP domain deletion accumulation in root tips (upper panels, counterstained with Propidium Iodide – red) and heart stage embryos (lower panels). (N-S) Complete set of SOK1-SOK2-YFP domain swap accumulation in root tips (upper panels) and embryos (lower panels). (T-W) Negative BiFC controls (single SOK1 DIX-cYFP or nYFP fusions with empty vector partner) in *Nicotiana benthamiana* epidermis. Bars 10 μ m.

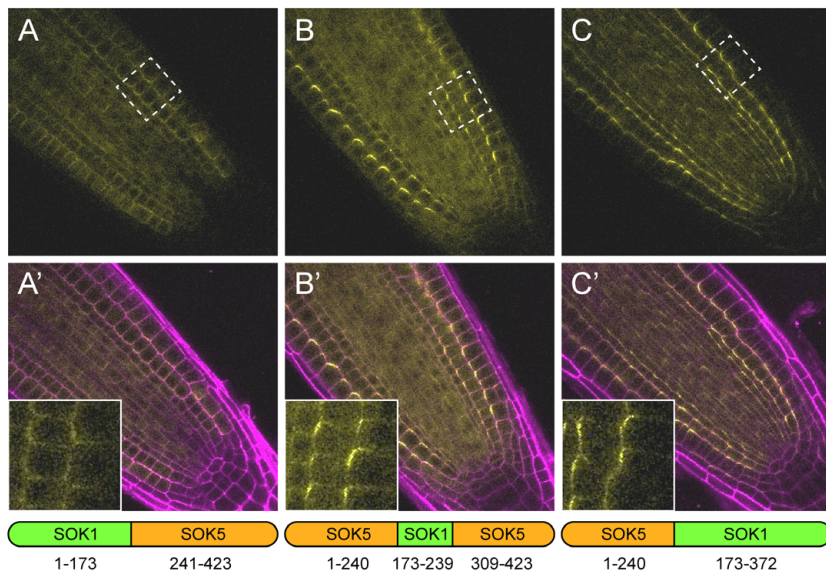


Figure S9: SOK1-SOK5 domain swaps. Fluorescence of SOK1/SOK5 chimaeras, expressed as YFP fusions from the RPS5A promoter in root tips (A-C), and counterstained with Propidium Iodide (A'-C' – magenta). Insets in (A'-C') show protein localization in individual cells at high magnification (corresponding to dashed boxes in A-C). Arrangement of SOK1 and SOK5 fragments in chimaeras are indicated underneath (A'-C').

Supplemental Table 1: Primers used in this study

Construct	F/R	Primer sequence	Purpose
SOK1-GFP	F	TAGTTGGAATGGGTTCGAACGTTCCGTGGTAATCAATG	lic-pSOK1
	R	TTATGGAGTTGGGTTCGAACCTCTCTTTGTTTGGTCT	pSOK1-lic
SOK2-GFP	F	TAGTTGGAATGGGTTCGAACGCCATTGATCTCGATAACAGAG	lic-pSOK2
	R	TTATGGAGTTGGGTTCGAACCTTTGTGTCTATAATGTCGGG	pSOK2-lic
SOK3-GFP	F	TAGTTGGAATGGGTTCGAACGTTATGGACTTACATTCTAACGATC	lic-pSOK3
	R	TTATGGAGTTGGGTTCGAACGTTATCTCGGGACCTAATTGG	pSOK3-lic
SOK4-GFP	F	TAGTTGGAATGGGTTCAACTCTCTTCTGCTCAGCTGAGTGAGATAGAG	lic-pSOK4
	R	TTATGGAGTTGGGTTCAATAATGTTCTCGGTGATTGGAGATTG	pSOK4-lic
SOK5-GFP	F	TAGTTGGAATGGGTTCGAACCTTAACGATAAGAATTAAAGATACTCG	lic-pSOK5
	R	TTATGGAGTTGGGTTCGAACCTTTGTTCTTGTCTATGGAAAAGTG	pSOK5-lic
pSOK1-SOK1-YFP	F	TAGTTGGAATGGGTTCAATGAGTCGTTCCGTGGTAATCAATG	lic-SOK1
	R	TTATGGAGTTGGGTTCAACTCACTCTTGAGAGTAGTCGCAATACAG	SOK1-lic
pSOK1-SOK1-tdT	F	TAGTTGGAATGGGTTCAATGAGTCGTTCCGTGGTAATCAATG	lic-SOK1
	R	TTATGGAGTTGGGTTCAACTCACTCTTGAGAGTAGTCGCAATACAG	SOK1-lic
pSOK2-SOK2-YFP	F	TAGTTGGAATGGGTTCAATGCCGATTGATCTCGATAACAGAG	lic-SOK2
	R	TTATGGAGTTGGGTTCAACTTCCTTGATGAGATGATGACATTAAACACG	SOK2-lic
pSOK3-SOK3-YFP	F	TAGTTGGAATGGGTTCAATGAGTGTGAGATTCATTATCACCATCTCGA	lic-SOK3
	R	TTATGGAGTTGGGTTCAACAGGCTTCTGAAGGCACTTTCGA	SOK3-lic
pSOK4-SOK4-YFP	F	TAGTTGGAATGGGTTCAACTCTTCTGCTCAGCTGAGTGAGATAGAG	lic-SOK4
	R	TTATGGAGTTGGGTTCAACTGGTTGTCACCAACCACAGAAATTGG	SOK4-lic
pSOK5-SOK5-YFP	F	TAGTTGGAATGGGTTCAAACTAAAGTGTATGTGATACACACC	lic-SOK5

Chapter 3

Construct	F/R	Primer sequence	Purpose
pRPS5A-SOK1	R	TTATGGAGTTGGGTTCGAACCTGCTGCCACCATTTGTCCT	SOK5-lic
	F	TAGTTGGAATAGGTTCATGGAAAGTAATGGTGGAGGAGG	lic-SOK1
	R	AGTATGGAGTTGGGTTCACTCTTGTAGAGTAGTCGTC	SOK1-lic
pRPS5A-SOK1-YFP	F	TAGTTGGAATAGGTTCATGGAAAGTAATGGTGGAGGAGG	lic-SOK1
	F	CGGTATTGACGACTACTCTCAAAGAGATGACTAGTAAGGGCGAGGAGC	SOK1-YFP
	R	AGTATGGAGTTGGGTTCACTTGTACAGCTCGTCATGCC	YFP-lic
pRPS5A-SOK2-YFP	F	TAGTTGGAATAGGTTCATGGAAAGCTGAAGATGCAGAAGA	lic-SOK2
	F	CATCATCGAAGCAAATCAAGAAAATGACTAGTAAGGGCGAGGAGC	SOK2-YFP
	R	AGTATGGAGTTGGGTTCACTTGTACAGCTCGTCATGCC	YFP-lic
Myr-SOK1	F	TAGTTGGAATAGGTTCATGGGAGGATGCTTCTAAGAAGGAAAGTAATGGTGGAGGAGGAGAAG	lic-Myr-SOK1
SOK1-Myr	R	AGTATGGAGTTGGGTTCACTTCTAGAGAACGATCCTCCCTGTACAGCTCGTCATGCC	Myr-YFP
deletion ΔA	F	CGGCTAAACACCAGTATAAACCGAGGAAACCTGTTAACCC	pRPS5A
	R	GCCCTTACTAGTCATTAACCATTCTTCAC	SOK1-YFP
	F	GTGAAGAAATGGTTAATGACTAGTAAGGGC	SOK1-YFP
	R	GCGGACTCTAATCATAAAAACCCATCTCATAAATAACGTC	tNOS after YFP seq
	F	TAGTTGGAATAGGTTCATGGAAAGTAATGGTGGAGGAGG	lic-SOK1
	R	AGTATGGAGTTGGGTTCACTTGTACAGCTCGTCATGCC	YFP-lic
deletion ΔB	F	CGGCTAAACACCAGTATAAACCGAGGAAACCTGTTAACCC	pRPS5A
	R	GCCCTTACTAGTCATTAACCAGGAAACCTGTTAACCC	SOK1-YFP
	F	TCTGAGATTCTCTAATGACTAGTAAGGGC	SOK1-YFP
	R	GCGGACTCTAATCATAAAAACCCATCTCATAAATAACGTC	tNOS after YFP seq
	F	TAGTTGGAATAGGTTCATGGAAAGTAATGGTGGAGGAGG	lic-SOK1
	R	AGTATGGAGTTGGGTTCACTTGTACAGCTCGTCATGCC	YFP-lic
deletion ΔC	F	CGGCTAAACACCAGTATAAACCGAGGAAACCTGTTAACCC	pRPS5A
	R	GCCCTTACTAGTCATCGATCTCTGTGAGCA	SOK1-YFP
	F	TGCTCACAGAGATCGATGACTAGTAAGGGC	SOK1-YFP
	R	GCGGACTCTAATCATAAAAACCCATCTCATAAATAACGTC	tNOS after YFP seq
	F	TAGTTGGAATAGGTTCATGGAAAGTAATGGTGGAGGAGG	lic-SOK1
	R	AGTATGGAGTTGGGTTCACTTGTACAGCTCGTCATGCC	YFP-lic
deletion ΔD	F	CGGCTAAACACCAGTATAAACCGAGGAAACCTGTTAACCC	pRPS5A
	R	CCTACTAGTCATCTGGTCGACCGGA	SOK1-YFP
	F	TCGGTCGACCAAGTATGACTAGTAAGG	SOK1-YFP
	R	GCGGACTCTAATCATAAAAACCCATCTCATAAATAACGTC	tNOS after YFP seq
	F	TAGTTGGAATAGGTTCATGGAAAGTAATGGTGGAGGAGG	lic-SOK1
	R	AGTATGGAGTTGGGTTCACTTGTACAGCTCGTCATGCC	YFP-lic
deletion ΔE	F	CGGCTAAACACCAGTATAAACCGAGGAAACCTGTTAACCC	pRPS5A
	R	GCCCTTACTAGTCATCCCAGACCTAGACTT	SOK1-YFP
	F	AACTCTAGGCTGGATGACTAGTAAGGGC	SOK1-YFP
	R	GCGGACTCTAATCATAAAAACCCATCTCATAAATAACGTC	tNOS after YFP seq
	F	TAGTTGGAATAGGTTCATGGAAAGTAATGGTGGAGGAGG	lic-SOK1
	R	AGTATGGAGTTGGGTTCACTTGTACAGCTCGTCATGCC	YFP-lic
Template for ΔF-ΔL	F	CGGCTAAACACCAGTATAAACCGAGGAAACCTGTTAACCC	pRPS5A
	R	GCTCTCGCCCTACTAGTCATCTCTTGTAGAGTAGTCGTCATACACG	SOK1-YFP
	F	CGGTATTGACGACTACTCTCAAAGAGATGACTAGTAAGGGCGAGGAGC	SOK1-YFP
	R	GCGGACTCTAATCATAAAAACCCATCTCATAAATAACGTC	tNOS after YFP seq
deletion ΔF	F	TAGTTGGAATAGGTTCATGGCAGACGCAC	lic-SOK1
	R	AGTATGGAGTTGGGTTCACTTGTACAGCTCGTCATGCC	YFP-lic

SOSEKI polarity determinants reveal mechanisms of supra-cellular polarity in *Arabidopsis*

Construct	F/R	Primer sequence	Purpose
deletion ΔG	F	TAGTTGAAATAGGTTCATGAGCTCTCAAAG	lic-SOK1
	R	AGTATGGAGTTGGGTTCTTACTTGTACAGCTCGTCCATGCC	YFP-lic
deletion ΔH	F	TAGTTGAAATAGGTTCATGACGGCAACAC	lic-SOK1
	R	AGTATGGAGTTGGGTTCTTACTTGTACAGCTCGTCCATGCC	YFP-lic
deletion ΔI	F	TAGTTGAAATAGGTTCATGGTATCGTCTAC	lic-SOK1
	R	AGTATGGAGTTGGGTTCTTACTTGTACAGCTCGTCCATGCC	YFP-lic
deletion ΔJ	F	TAGTTGAAATAGGTTCATGGCTTTGGTCC	lic-SOK1
	R	AGTATGGAGTTGGGTTCTTACTTGTACAGCTCGTCCATGCC	YFP-lic
deletion ΔK	F	TAGTTGAAATAGGTTCATGCCTTCATGGC	lic-SOK1
	R	AGTATGGAGTTGGGTTCTTACTTGTACAGCTCGTCCATGCC	YFP-lic
deletion ΔL	F	TAGTTGAAATAGGTTCATGAGAAACATTCC	lic-SOK1
	R	AGTATGGAGTTGGGTTCTTACTTGTACAGCTCGTCCATGCC	YFP-lic
swap S2S1A	F	CGGCTAAACACCGTATAAACAGGGAACCTGTTAAACC	pRPS5A
	R	TGTGAGATAGTAAACAACCTGGACTCTTGTACTTCTCCCTCCACCATTTCTTCCAT	SOK1-SOK2
	F	ATGGAAAGTAATGGTGGAGGAGAGAAGTACGAAGAGTCCAAGTTGTTACTATCTCAC	SOK1-SOK2
	R	GGTGAACAGCTCCCTGCCCTACTAGTCATTTCTGATTGCTTCGATGATGACATTA	SOK2-YFP
	F	TTAATGTCATCATCGAAGCAAATCAAGAAAATGACTAGTAAGGGCGAGGAGCTGTTCAC	SOK2-YFP
	R	GCGGGACTCTAATCATAAAAACCCATCTCATATAAAACGTC	tNOS after YFP seq
	F	TAGTTGAAATAGGTTCATGGAAAGTAATGGTGGAGGAGG	lic-SOK1
	R	AGTATGGAGTTGGGTTCTTACTTGTACAGCTCGTCCATGCC	YFP-lic
	F	CGGCTAAACACCGTATAAACAGGGAACCTGTTAAACC	pRPS5A
swap S2S1B	R	GCTAAGGAATAAACTAAATTCACTCTTGTAAAATGGGTTCTTGTCTTGACCTCTTC	SOK2-SOK1
	F	GAAGAGGCTCAAGACAAGAACCCATTTCAGAAGAGTGAAATTAGTTAGTTAGTTCTTAGC	SOK2-SOK1
	R	TGGTCTGTCACATGTACTTCTGAAATTAGAAGATCTCAGATCCTTGTAGGACATA	SOK1-SOK2
	F	TATGTCCTCAAAGGATCTGAGATTCTCTAAATTCAAGAAGTACATGTAACAGACCA	SOK1-SOK2
	R	GGTGAACAGCTCCCTGCCCTACTAGTCATTTCTGATTGCTTCGATGATGACATTA	SOK2-YFP
	F	TTAATGTCATCATCGAAGCAAATCAAGAAAATGACTAGTAAGGGCGAGGAGCTGTTCAC	SOK2-YFP
	R	GCGGGACTCTAATCATAAAAACCCATCTCATATAAAACGTC	tNOS after YFP seq
	F	TAGTTGAAATAGGTTCATGGAAAGCTGTAAGATGCAAGAGAGG	lic-SOK2
	R	AGTATGGAGTTGGGTTCTTACTTGTACAGCTCGTCCATGCC	YFP-lic
swap S2S1C	F	CGGCTAAACACCGTATAAACAGGGAACCTGTTAAACC	pRPS5A
	R	CACATTAGGATAATCCTCTTGGAGAGCTGCGGTATTGAGATCCTTCAAGACATA	SOK2-SOK1
	F	TATGTCCTGAAAGGATCTGAAATCACCAGCAGCTCTCAAAGGAGGATTATCTAATGTG	SOK2-SOK1
	R	TACTTGCAAATCTGCTGTCTGGTCACTTAAGAACGAAACCTTCTGTTGTGGT	SOK1-SOK2
	F	ACCACGAACGAAGAAGGTTCTGTTCTAAGTTGACCAAGACAGAGCAAGATTGCAAGTA	SOK1-SOK2
	R	GGTGAACAGCTCCCTGCCCTACTAGTCATTTCTGATTGCTTCGATGATGACATTA	SOK2-YFP
	F	TTAATGTCATCATCGAAGCAAATCAAGAAAATGACTAGTAAGGGCGAGGAGCTGTTCAC	SOK2-YFP
	R	GCGGGACTCTAATCATAAAAACCCATCTCATATAAAACGTC	tNOS after YFP seq
	F	TAGTTGAAATAGGTTCATGGAAAGCTGTAAGATGCAAGAGAGG	lic-SOK2
swap S2S1D	R	AGTATGGAGTTGGGTTCTTACTTGTACAGCTCGTCCATGCC	YFP-lic
	F	CGGCTAAACACCGTATAAACAGGGAACCTGTTAAACC	pRPS5A
	R	CTGGCCGGAGACTGTTTCGGATCTGTTGTCGGTTTGTGATGATTCCATTGT	SOK2-SOK1
	F	ACAATGGAATCCACCGAACAAAAACCGAACAAACAAGATCCGAAACAGCTCTCCGGCCAG	SOK2-SOK1
	R	TCTCGGATTCATCACACTCGTGTGCGTAGTAGTTGTCGATGACACCACTCATCAA	SOK1-SOK2
swap S2S1D	F	TTGATGAAGTGTGGTGGTTGGACACAAACTACTACGCAACGGAGTGTGATGAATCCGAGA	SOK1-SOK2

Chapter 3

Construct	F/R	Primer sequence	Purpose
swap S2S1E	R	GGTGAACAGCTCGCCCTTACTAGTCATTTCTTGATTCGATGACATTAA	SOK2-YFP
	F	TTATGTCATCATCGAAGCAAATCAAGAAAATGACTAGTAAGGGCGAGGAGCTGTCACC	SOK2-YFP
	R	GCGGACTCTAATCATAAAAACCCATCTCATAAATAACGTC	tNOS after YFP seq
	F	TAGTGGATAGTTCATGGAAAGCTGTAAGATGCAGAAAGAGG	lic-SOK2
	R	AGATGGAGTTGGGTTACTTGTACAGCTGTCATGCC	YFP-lic
	F	CGGCTAAACACAGTATAAACCGAGGAACCTGTTAAC	prPS5A
	R	AGACTTATTCAAAGGCCAACATCGCGCTCTGGTGGCATGTGACCGCAAGAGATCAT	SOK2-SOK1
	F	ATGATCTCTGGGTACATGCCAACAGCAGCGCTATTGGTGCCTTGATAAGTCT	SOK2-SOK1
	R	TTACGCCGTGACTCGTCTGACTCACCGACGAGCATAATGGAGCCATGGAAGGCTGCT	SOK1-SOK2
	F	AGCAAGCCTCCATGGCTCATTATGCTCGTGGTGAAGTCAGGAACGAGTCACGGCTGAA	SOK1-SOK2
swap S2S1F	R	GGTGAACAGCTCTGCCCTTACTAGTCATTTCTTGATTCGATGACATTAA	SOK2-YFP
	F	TTATGTCATCATCGAAGCAAATCAAGAAAATGACTAGTAAGGGCGAGGAGCTGTCACC	SOK2-YFP
	R	GCGGACTCTAATCATAAAAACCCATCTCATAAATAACGTC	tNOS after YFP seq
	F	TAGTGGATAGTTCATGGAAAGCTGTAAGATGCAGAAAGAGG	lic-SOK2
	R	AGATGGAGTTGGGTTACTTGTACAGCTGTCATGCC	YFP-lic
	F	CGGCTAAACACAGTATAAACCGAGGAACCTGTTAAC	prPS5A
	R	CTTCTCAGGTTGAACAACCTCCACATTGCTCACCGATGCTCCGCTGAAATACTCTT	SOK2-SOK1
	F	AAAGAGTATTCAGCGGAAGCATCGTGGAGCAATGTTGGAGTTCAACACTGAGAAG	SOK2-SOK1
	R	GGTGAACAGCTCTGCCCTTACTAGTCATCTTGAGAGTAGTCGTCATACACGTTG	SOK1-YFP
	F	CAACGTATTGACGACTACTCTAAAGAGATGACTAGTAAGGGCGAGGAGCTGTCACC	SOK1-YFP
UAS::SOK1-YFP	R	GCGGACTCTAATCATAAAAACCCATCTCATAAATAACGTC	tNOS after YFP seq
	F	TAGTGGATAGTTCATGGAAAGCTGTAAGATGCAGAAAGAGG	lic-SOK2
	R	AGTATGGAGTTGGGTTACTTGTACAGCTGTCATGCC	YFP-lic
	F	TAGTGGATAGTTCATGGAAAGTAATGGTGGAG	LIC adaptor -SOK1
35S::SOK1DIX-YFP/ CFP BiFC	R	AGTATGGAGTTGGGTTCTCTGGAGAGCTTAG	YFP-LIC adaptor
	F	TAGTGGATAGTTCATGGAAAGTAATGGTGGAG	LIC adaptor -SOK1
	R	AGTATGGAGTTGGGTTCTCTGGAGAGCTTAG	DIX
	F	AGTATGGAGTTGGGTTCTCTGGAGAGCTTAG	SOK1 DIX-LIC
35S::SOK1DIX-n/ cYFP BiFC	R	AGTATGGAGTTGGGTTCTCTGGAGAGCTTAG	Adaptor
	F	AGTATGGAGTTGGGTTCTCTGGAGAGCTTAG	LIC adaptor -SOK1
	R	AGTATGGAGTTGGGTTCTCTGGAGAGCTTAG	DIX
	F	AGTATGGAGTTGGGTTCTCTGGAGAGCTTAG	SOK1 DIX-LIC
35S::n/cYFP- SOK1DIX BiFC	R	AGTATGGAGTTGGGTTCTCTGGAGAGCTTAG	Adaptor
	F	AGTATGGAGTTGGGTTCTCTGGAGAGCTTAG	LIC adaptor -SOK1
	R	AGTATGGAGTTGGGTTCTCTGGAGAGCTTAG	DIX
	F	AGTATGGAGTTGGGTTCTCTGGAGAGCTTAG	SOK1 DIX-LIC
swap A-E B	R	AGTATGGAGTTGGGTTCTCTGGAGAGCTTAG	Adaptor
	F	AGTATGGAGTTGGGTTCTCTGGAGAGCTTAG	LIC adaptor -SOK1
	R	AGTATGGAGTTGGGTTCTCTGGAGAGCTTAG	DIX
	F	AGTATGGAGTTGGGTTCTCTGGAGAGCTTAG	SOK1 DIX-LIC
swap A-E C	R	AGTATGGAGTTGGGTTCTCTGGAGAGCTTAG	Adaptor
	F	AGTATGGAGTTGGGTTCTCTGGAGAGCTTAG	LIC adaptor -SOK1
	R	AGTATGGAGTTGGGTTCTCTGGAGAGCTTAG	DIX
	F	AGTATGGAGTTGGGTTCTCTGGAGAGCTTAG	SOK1 DIX-LIC
swap A-E D	R	AGTATGGAGTTGGGTTCTCTGGAGAGCTTAG	Adaptor
	F	AGTATGGAGTTGGGTTCTCTGGAGAGCTTAG	LIC adaptor -SOK1
	R	AGTATGGAGTTGGGTTCTCTGGAGAGCTTAG	DIX
	F	AGTATGGAGTTGGGTTCTCTGGAGAGCTTAG	SOK1 DIX-LIC

Chapter 4

SOSEKI loss-of-function

Maritza van Dop¹, Saiko Yoshida^{1,2}, Jos Wendrich^{1,3}, Julius Durr⁴, Nosheen Hussain⁴,
Jose F. Gutierrez-Marcos⁴ and Dolf Weijers¹

¹Laboratory of Biochemistry, Wageningen University and Research. The Netherlands

²Present address: MPI for Plant Breeding Research, Cologne, Germany

³Present address: Department of Plant Biotechnology and Bioinformatics, Ghent University, Belgium

⁴School of Life Sciences, University of Warwick, United Kingdom

Abstract

Establishing directional axes and translating this polarity into sub-cellular processes is essential for plant development. Polarly localized membrane proteins use cell polarity to determine at which side of the cell they need to accumulate. Several of such proteins have been identified, but their localization is highly dependent on tissue context and cell identity. In addition, substrates, drugs and post-translational modifications easily disturb their polar accumulation. In contrast, the recently identified SOSEKI (SOK) family localizes very robustly to cell edges in the *Arabidopsis* embryo and root. Each of the 5 family members shows unique expression and localization patterns that partially overlap. SOKs contain a DIX-LIKE domain for protein clustering and a polarity domain for edge selection, yet their biological role remains unknown. Here, we aimed to generate mutants with reduced SOK function. We show that small mutations near the start site of *SOK1* can lead to fertility defects, but that partial or complete deletion of the gene does not result in a clear phenotype. *SOK4* is upregulated upon loss of *SOK1* in the root, which suggests the presence of a feedback loop or compensation mechanism. Based on expression and localization patterns of SOKs, additional potential redundancies were identified between SOK2 and 3 in the leaf and SOK2, 3 and 5 in the gynoecium.

Introduction

Seed plants start their life as a single-celled zygote, that grows out to form a complex organism with many different tissues and organs. Early in this process directional axes are established to guide development. Plant development relies on correct cell division orientation and expansion rather than cell movement, as a rigid wall fixes the cell directly after division. This means that directional axes need to be translated into polarity within each cell. Cell polarity is defined as the asymmetric distribution of proteins and organelles over the plasma membrane (PM) and throughout the cell following directional axes (reviewed in Nakamura & Grebe, 2018). Several proteins have been identified that localize in a polar manner. The function of these proteins is diverse: PIN proteins are involved in auxin transport and localize to polar cell faces (Gälweiler et al., 1998; Wisniewska et al., 2006); the Boron transporters BOR1 and NIP5;1 localize to inner lateral and outer lateral faces, respectively (Takano et al., 2010). A polar protein involved in asymmetric cell division is BASL, which functions during stomata formation. There, it localizes to one crescent face of the cell to regulate asymmetric division (Dong et al., 2009). BASL is required for proper localization of POLAR, which is also polarly localized in stomatal lineage cells, although its function remains unknown (Pillitteri et al., 2011). The outer-laterally localized SCHENGEN1 protein kinase is required for Caspary Strip formation, by influencing the position and integrity of the CASP protein ring on the plasma membrane (Alassimone et al., 2016).

Although more and more polarly localized proteins with diverse functions are being identified, it remains unclear how exactly these proteins 'read' cell polarity and how their localization is established accordingly. The localization of known polar proteins is highly dependent on tissue context or cell identity and the polar localization of many of these proteins is easily disturbed. For example, PIN2 localizes apically in epidermal root cells and basally in the cortex (Abas et al., 2006) and BASL switches polarity as stomata lineage cells divide (Dong et al., 2009). Both PIN and BOR1 polarity is highly sensitive to inhibition of vesicle trafficking pathways (Fujiwara et al., 2005; Geldner et al., 2001; Löfke et al., 2013; Tanaka et al., 2013), or their transport substrates auxin (Geldner et al., 2001; Paciorek et al., 2005) or Boron (Takano et al., 2010). Post-translational modifications such as palmitoylation and phosphorylation also have a great influence on localization and function of several polar proteins (Alassimone et al., 2016; Friml et al., 2004; Michniewicz et al., 2007; Zhang et al., 2015). Because of their context-dependence and conditional polar localization, known polar proteins may therefore not be part of the intrinsic cell polarity system.

Recently, we identified a novel family of polar proteins with unique localization and behavior: the SOSEKI (SOK, Möller et al., 2017, Chapter 3). These proteins were

discovered as downstream targets of the Auxin Response transcription Factor (ARF) MONOPTEROS, which is involved in embryo patterning (Hardtke & Berleth, 1998; reviewed in Smit & Weijers, 2015). SOK proteins accumulate in cell edges rather than faces, and integrate apico-basal and radial polarity to determine their localization. They have unique expression and localization patterns in the embryo and root tip, that can partially overlap. In roots, SOK1 is present in the youngest vascular cells and SOK2 accumulates in the endodermis. SOK3 is ubiquitously expressed, but most prominently marks the phloem, while SOK4 is weakly expressed in the vasculature. SOK5 is most highly expressed in the cortex and endodermis. SOK polarity is not altered by application of drugs and substrates that influence known polar markers. Only a change in the mechanical properties of the cell causes SOK to lose membrane localization and aggregate in the cytoplasm. Domain swap and deletion studies identified two functional domains: an unconserved polarity domain responsible for edge selection and a putative DIX protein-protein interaction domain necessary for SOK protein clustering. All these properties make SOKs interesting markers for polarity studies.

The unique localization and behavior of SOKs raised the question as to their biological function. All SOKs contain a DUF966 domain, which has not been characterized. They do not have any domains in common with other plant proteins and the N-terminal DIX-LIKE clustering domain is the only part of the protein with a potential structural counterpart outside the plant kingdom. It is therefore difficult to deduce potential SOK functions based on similarity. Mis-expression of SOK1 induced oblique divisions in roots and embryos, but whether SOKs are directly involved in cell division remains unknown. Here, we set out to unravel the biological function of SOKs by generating *Arabidopsis* mutants with reduced or complete lack of *SOK* expression. Phylogenetic analysis showed that *SOK1* is the most basal member of the family (see Chapter 5). In addition, it is expressed at sites of polarity establishment and dynamically regulated. Therefore, we focused mainly on *SOK1*. Here, we show that small mutations near the start site of *SOK1* can lead to fertility defects, but that partial or complete deletion of the gene does not result in a clear phenotype. *SOK4* is upregulated upon loss of *SOK1* in the root, which suggests the presence of a feedback loop or compensation mechanism. Based on expression and localization patterns, additional potential redundancies were identified between SOK2 and 3 in the leaf and SOK2, 3 and 5 in the gynoecium.

Results

Single sok insertion mutants do not show strong phenotypes

To investigate the biological role of SOKs, we aimed to obtain loss-of-function mutants. We set out to generate single mutants using two different approaches:

insertion lines and Clustered Regularly Interspaced Short Palindromic Repeats (CRISPR)/Cas9. First, we obtained publicly available T-DNA insertion lines of each *SOK* gene and genotyped these to confirm the insertion at the correct locus (Fig. 1a, Supplemental Table 1). Next, we generated lines homozygous for the insertion and determined the level of *SOK* transcripts by qPCR (Fig. 1a and b). Instead of the expected reduction in transcript levels, all *sok1* lines showed strong *SOK1* over-expression. We also examined the expression levels of *SOK3-5* in the *sok1-1* line to see how these genes react to changed *SOK1* levels. Interestingly, the three family members were also upregulated compared to WT, which indicates a potential feedback mechanism regulating *SOK* expression.

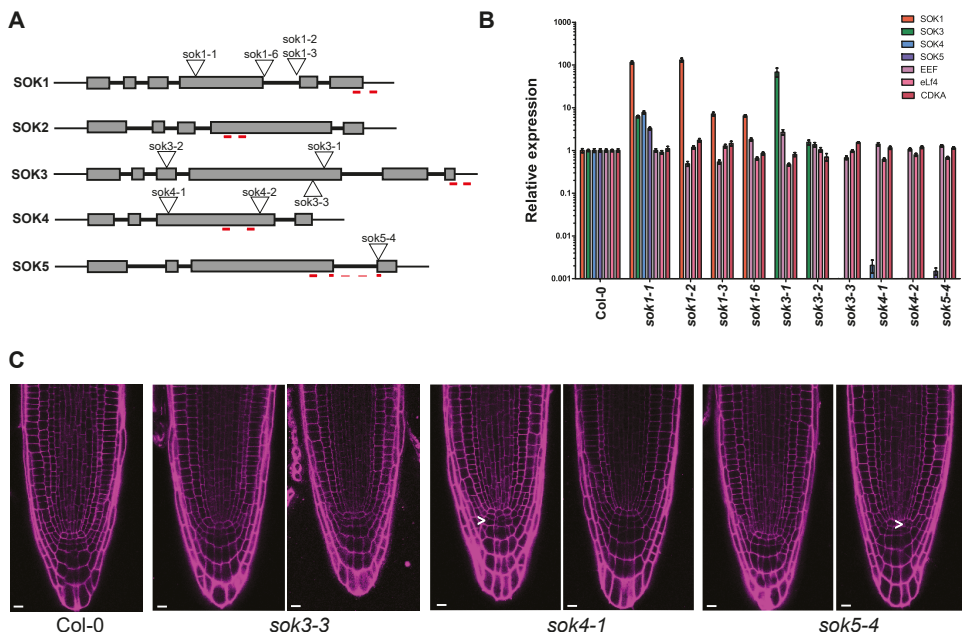


Figure 1. *SOK* insertion lines do not show a phenotype. (A) Schematic representation of *SOK* genes with position of insertions (triangles) and qPCR primers (red lines). (B) qPCR on insertion lines with three control genes (EEF, eLF4, CDKA). Col-0 expression levels were set as 1. Error bars represent Standard Error. (C) Roots of Col-0, *sok3-3*, *sok4-1* and *sok5-4*. White arrows indicate aberrant divisions. Scale bars represent 10 μ m.

In the *sok3-1* line, *SOK3* was strongly over-expressed, while *sok3-2* was 1.5 times WT levels and *sok3-3* line appeared to lack *SOK3* transcripts. Both tested *sok4* lines showed strong reduction in *SOK4* expression, although results for *sok4-1* were somewhat variable. The *sok5-4* line also completely lost expression of *SOK5*. None of the lines with reduced *SOK* expression showed any obvious growth phenotype under standard growth conditions. Likewise, we could not observe strong phenotypes in root anatomy in lines with reduced expression of *SOK3*, 4 or 5 (Fig. 1c). In some

individual roots, the QC or stem cells were slightly disorganized. These aberrant cell divisions occurred outside of the respective *SOK* expression domains and were similar regardless of which *SOK* gene was down-regulated. Such deviations could also occasionally be observed in control roots. Therefore, it is most likely that these divisions are a product of the background and/or growth conditions, rather than the loss of *SOK* function.

*Mutations close to the start site of *SOK1* and *2* can lead to reduced fertility*

Given that no lines with reduced *SOK1* or *SOK2* expression were obtained, we next used a CRISPR/Cas9 strategy to induce mutations in these two genes (Reviewed in Belhaj et al., 2015). In this approach, a DNA-cleaving Cas9 protein can be targeted to a specific genomic sequence (protospacer) by a guide RNA. This guide RNA is a 20 bp sequence that matches its genomic target region and is bound by Cas9. A Protospacer Adjacent Motif (PAM) sequence of NGG must be adjacent to the 3'end of the protospacer to allow Cas9 to cut the DNA, which limits the number and locations of available target sites. Cas9 cleaves both strands of its target DNA and incorrect repair of this break can result in addition or deletion of basepairs, which leads to a frameshift or early stop codon.

We targeted Cas9 to the first or second exon of the *SOK* gene using guide RNA's described in Figure 2 and Supplemental Table 2. The guide RNAs were targeted to the first exons of the genes to induce early stop codons. Such a short piece would likely not be functional and thus render the plant deficient of the targeted *SOK*. The exact sequence of the target site can greatly influence the efficiency of binding and cleaving. Therefore we used guide RNA prediction tools to select the best target sites based on location and predicted efficiency. Off-target activity can be a problem with the CRISPR/Cas9 system: DNA sequences similar to the intended target can get cleaved as well. To minimize the likelihood that sequences aside from the intended *SOK* were affected, we analyzed all guideRNAs *in silico* for potential off-target activity. Only those without predicted off-targets were used in our experiments. Mutation efficiency is not only influenced by the guideRNA and type of Cas9 protein. Also other components of the plasmid, such as the promoter and terminator, can have a profound effect. Therefore, we used three different plasmids in our experiments: pYB196 (Hyun et al. 2014), a PGG-Z03 based one (Lampropoulos et al., 2013) and pTTK312 (Tsutsui & Higashiyama, 2017). In all cases, Col-0 plants were used for transformation.

At first, we transformed Col-0 plants with pYB196 plasmids containing pICU2::Cas9 and a pU6 driven guide RNA that binds close to the start site of one of the *SOK*s (Fig. 2a, Sup. Table 2). We extracted DNA from leaves of T1 plants and amplified the genomic region surrounding the target site by PCR. The PCR fragments were

sequenced to identify mutations. Comparing the sequence traces to a WT sequence resulted in one candidate mutant for *SOK1* (F) and two for *SOK2* (I and P). For *SOK3-5*, no mutants were recovered. All three candidates showed double sequence peaks shortly after the target site, which indicates that plants are either heterozygous or chimaeric (Fig. 2b). We investigated the nature of the mutations with the BatchTide software (Brinkman et al., 2014), which compares the candidate sequencing traces to a WT one (Sup. Fig. 1). For all 3 candidates, the sequences start to deviate directly after the CRISPR cut site. This confirms that a mutation event happened.

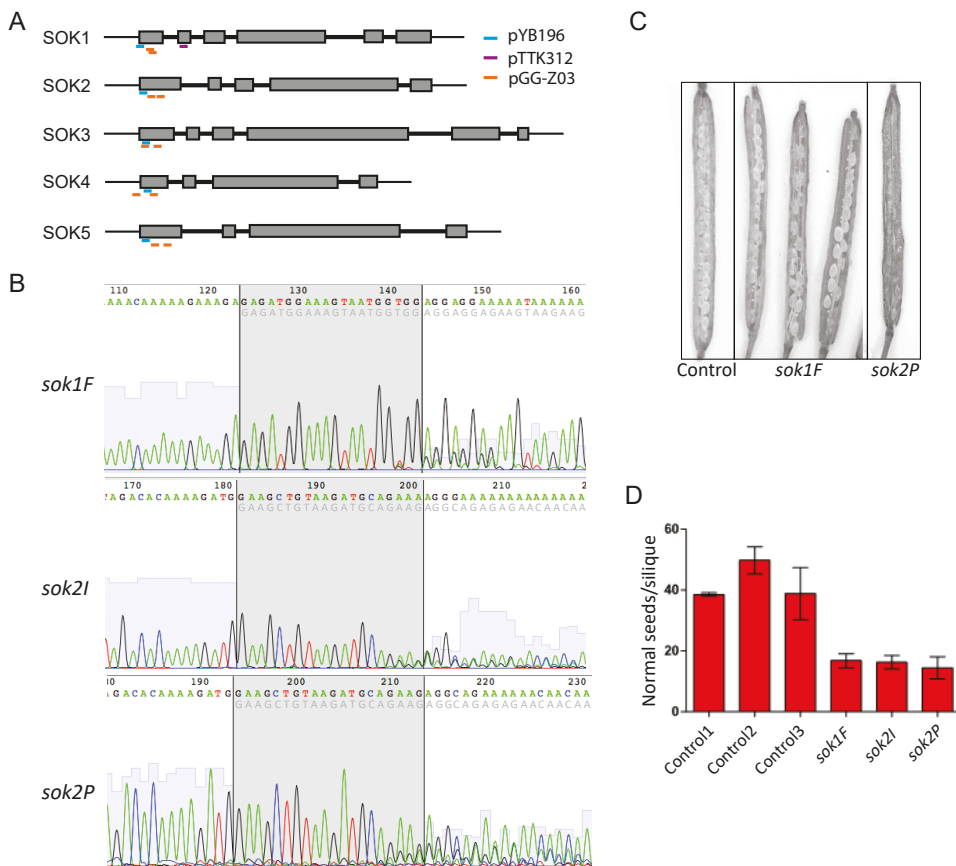


Figure 2. Mutations close to the start site of *SOK1* and 2 can lead to fertility defects. (A) Schematic representation of *SOK* genes with position of CRISPR target sequences. (B) Sequencing traces of *sok1* and 2 mutant candidates. Grey area indicates target sequence for the CRISPR guide. Light grey letters below the base calls represent the WT sequence before mutation. (C) Siliques of *sok1F*, *sok2P* and a WT sibling. (D) Number of normally developed seeds per siliques in the *sok* candidates (*n* of siliques is 8, 7, 9 respectively) and three random WT sibling plants (*n* of siliques is 4, 8, 7 respectively).

However, BatchTide was unable to reliably assign the mutations to a simple insertion or deletion event in one or both of the *sok* alleles. This suggests that the plants were chimaeras and/or contained more complex mutations. Phenotypic analysis revealed that all three candidates had strongly reduced fertility compared to the control (Fig. 2c and d). Many of the seeds were shriveled or undeveloped, while the other half looked similar to wildtype (WT). Sequencing of the progeny showed that all offspring was WT. These results suggest that the mutations near the start site of *SOK1* and 2 have a detrimental effect on fertility, both on the paternal and maternal side.

We also tested the same guideRNAs using an improved CRISPR vector (pTTK312) where the Cas9 was driven by the *pRP55A* promoter (Fig. 2a, Sup. Table 2). This time, plant apices were analyzed to ensure the mutation was present in the flowers, where it could be transferred to the progeny. This strategy resulted in 7 candidates with mutations in the first generation (not shown). This time, the plants did not show any obvious defects. However, similar to the previous experiment, no mutations was transmitted to the next generation. Thus, it seems that *sok1* mutations do not always result in visible defects in the mother plant, but that fertility or embryogenesis may still be affected.

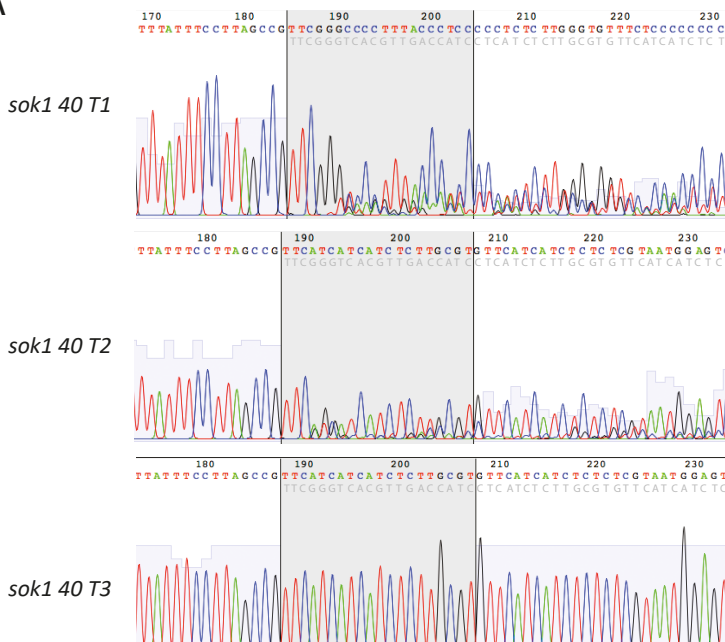
4 A larger deletion has no effect

In addition to the aforementioned plasmids, we tested a pGG-Z03 based plasmid, each containing a single pU6-26 driven guide RNA for one of the *SOK* genes (Fig. 2a, Sup. Table 2). In this case, Cas9 was expressed under control of a *PcUbi* promoter. One candidate mutant was recovered (*sok1-40*), whose sequence showed double peaks directly after the target site (Fig. 3a, Sup. Fig. 2a). Compared to *sok1F*, this plant had even more severe fertility problems and set very few seeds. Of the 16 offspring plants that were produced, 15 were WT and one had double peaks after the target site (Fig. 3a, Sup. Fig. 2a). This appeared to be a different, more complex mutation than the mother plant (Sup. Fig. 2a). Thus, the mutation in *SOK1* likely caused fertility defects and could not be transmitted to the next generation. As the CRISPR/Cas9 cassette was still present in the plant, a new mutation was introduced.

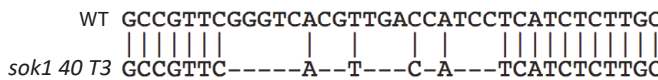
The newly mutated plant again showed fertility defects, with about half of the ovules aborted. We expected the progeny of this plant to be WT, as in the previous experiments. Surprisingly however, the mutation had been transmitted to the next generation (Fig. 3a, Sup. Fig. 2a). Of the 15 tested progeny, 4 were homozygous mutant, 6 heterozygous and 5 WT. The homozygous mutant plants were fully fertile and raised many viable offspring, which were again fully fertile. No defects were observed in the roots or other parts of the plants either (Sup. Fig. 2b).

The mutation is a deletion of 18 bp and insertion of 4 bp, which results in a predicted frameshift and early stop codon in the highly conserved first domain of the protein (Fig. 3b). This could cause only a small part of the original SOK1 protein being produced, which should not be functional given the effect that truncations have on SOK1 protein (Chapter 3). However, the occurrence of transmittance problems in many T1 mutants, but not *sok1-40* raises the question whether *sok1-40* truly completely lost SOK1 function. Alternatively, the use of alternative start sites downstream of the mutation (e.g. Fig 3c) could salvage the effect of the mutation.

A



B



C



Figure 3. A small deletion near the start site is transmittable and does not cause a phenotype. (A) Sequencing traces of *sok1* 40 T1-3. Grey area indicates target sequence for the CRISPR guide. Light grey letters below the base calls represent the WT sequence before mutation. (B) Alignment between a WT and *sok1* 40 T3 showing the deletion and insertion of basepairs. (C) Partial protein sequence of SOK1 in WT and *sok1* 40 T3. Red arrow indicates where the amino acids start to deviate from WT. Blue arrow indicates alternative start site.

*Loss of the entire *SOK1* gene leads to upregulation of *SOK4**

To unequivocally disrupt *SOK1* gene function, we used a double sgRNA construct to completely delete the *SOK1* gene. This construct contained Cas9 driven by the *EC1* promoter and sgRNAs under the control of pU6-26. The *EC1* promoter is active in the egg cell, zygote and earliest stages of embryogenesis (Wang et al., 2015). This should ensure that mutations are only induced at a very early stage of development and hopefully lead to a plant with the mutation in each cell, including those that generate the shoot meristem. The RNA guides were targeted 2.1 kb before the start and approximately 160 bp after the stop codon of the *SOK1* gene (Fig. 4a). A double cut should delete the entire *SOK1* gene.

The double CRISPR approach resulted in 7 plants with *SOK1* deletions in leaves, of which only one also carried the deletion in flowers. This shows that the *EC1* promoter is probably also active after the zygote stage and created chimaeric plants. The mutant candidate that had the deletion in the flowers did not show any fertility defects. PCR analysis of the progeny showed that the mutation was transmitted to the next generation in a mendelian manner. Sequencing of two homozygous progeny plants showed that the *SOK1* gene was fully deleted and that both plants carried the same mutation 'scar' (Fig. 4b). PCR on Δ *sok1* did not identify the *SOK1* gene anywhere else in the genome, and qPCR on Col-0 and Δ *sok1* confirmed that *SOK1* expression is completely lost in the mutant (Fig. 4c).

4 Phenotypic analysis of Δ *sok1* did not reveal any phenotype in rosette plants or root meristems (Fig. 4d). Occasionally, oblique divisions could be observed in the QC or root cap, although these occurred outside the expression domain of *SOK1* and could be observed in WT as well. This shows that the fertility phenotypes observed in the previously generated CRISPR mutant candidates had other causes than complete loss of *SOK1*. Observing embryos with DIC or confocal imaging did not reveal any consistent phenotypes either.

We did not observe any phenotype in Δ *sok1* roots under standard conditions. Therefore, abiotic stresses were applied to test whether Δ *sok1* roots had altered sensitivity to any of these conditions. As *SOK1* is regulated by the ARF MONOPTEROS (Möller et al., 2017), we supplied 5-day old roots with various concentrations of auxin and with the auxin transport inhibitor NPA for two days. In addition, previous work showed that *SOK1* protein loses its polar localization only upon mechanical perturbation of the cell. Therefore, we also tested the addition of salt, mannitol and isoxaben. None of these treatments resulted in a difference in root and root meristem length or meristem organization between WT and mutant (data not shown). This shows that *SOK1* is not necessary for root growth under auxin treatment or mechanical stress.

Interestingly, qPCR results showed that *SOK4* was upregulated in $\Delta sok1$ roots (Fig. 4c). This again suggests a feedback mechanism on *SOK* gene expression. *SOK4* is normally extremely weakly expressed in the same root tissues as *SOK1* (Fig. 4e). *SOK4* might be functionally redundant with *SOK1* and serve as a backup system. As such, upregulation of this gene in $\Delta sok1$ could be able to take over *SOK1* function.

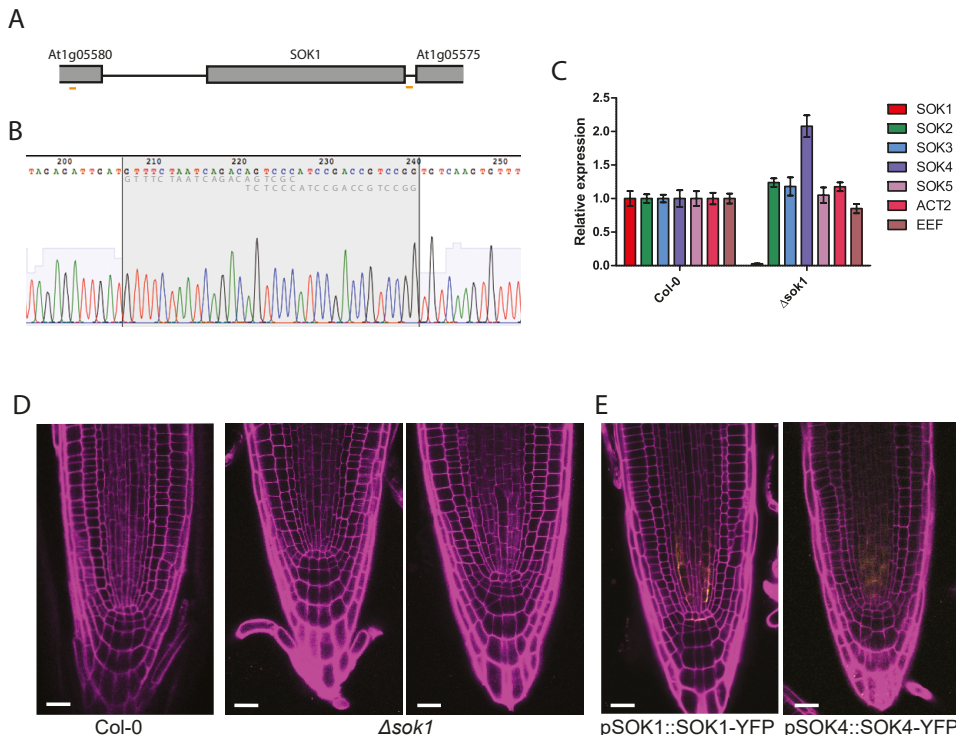


Figure 4. Complete loss of *SOK1* may be compensated by *SOK4*. A) Schematic representation of *SOK1* and surrounding genes with position of double-CRISPR target sequences in orange. B) Sequencing trace of a homozygous Δ sok1 plant. WT sequences in grey. C) qPCR on Δ sok1. Primer positions are indicated in Figure 1A and error bars represent Standard Error. D) Roots of Col-0 and Δ sok1. E) pSOK1::SOK1-YFP and pSOK4::SOK4-YFP. SOK4 is hardly visible, as it is extremely weak under standard conditions. Scalebar represents 20 μ m. Error bars represent Standard Error.

SOKs display polar localization throughout the plant

The potential redundancy between SOK1 and SOK4 raises the question whether SOK genes overlap only in the root or also in other places. To identify novel sites of SOK action and potential redundancies between family members, we investigated the expression and localization of SOK proteins throughout plant development. We found that each SOK has unique expression and localization patterns in many

different tissues. SOK4 was not studied, as fluorescence in SOK4-YFP lines was too weak to be reliably detected.

SOK2 and 3 are enriched facing stomata guard cells

We first addressed protein localization during vegetative growth of *Arabidopsis* by inspecting shoot apices of seedlings and leaves of 2 week-old plants. SOK1 was not observed in the shoot apex, while SOK2 was present in petioles and edges of young leaves, but also absent from the shoot apical meristem (SAM, Fig. 5a).

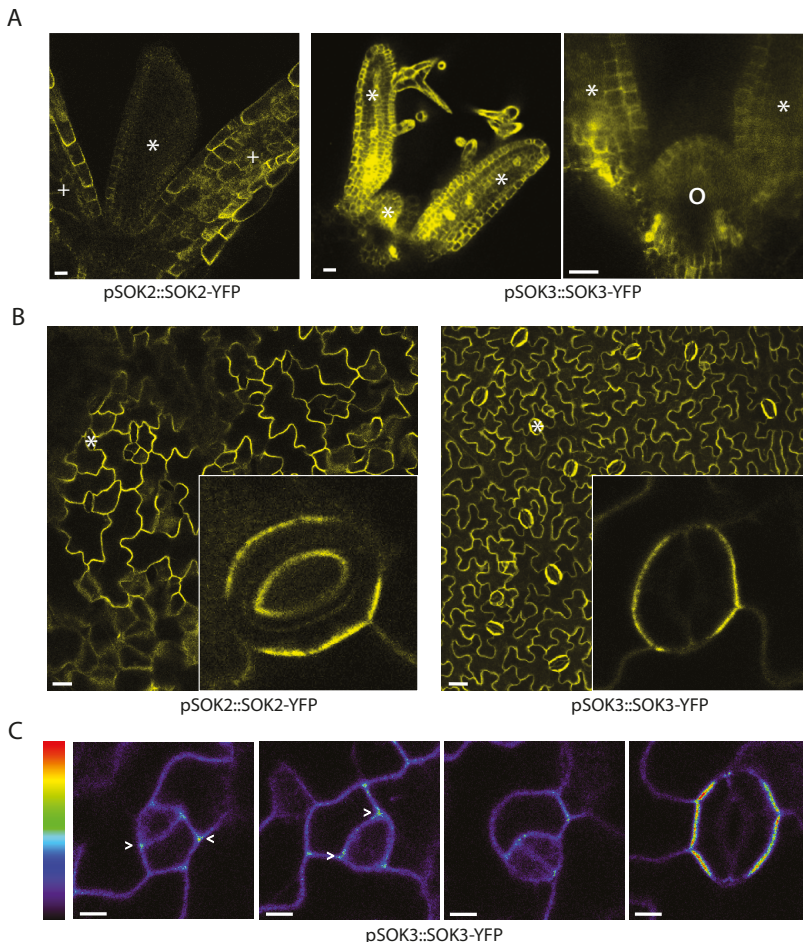


Figure 5. SOK2 and 3 are enriched facing stomata guard cells. (A) SOK2 and 3 in the seedling shoot apice. Stars indicate first leaves, plus sign stem of cotyledons and circle the shoot apical meristem. Scalebar 20 μ m. (B) SOK2 and 3 in young leaves. Inset: close-up of stomata. Stars indicate stomata. Scalebars 20 μ m. (C) SOK3 polarity in Stomata Lineage Cells. False colors indicate fluorescence intensity from low (dark blue) to high (red). Stars indicate SLCs. Scalebar represents 5 μ m.

SOK3 was found throughout the shoot apex, including the SAM (Fig. 5a). Young leaves lack SOK1 and 5, but show accumulation of SOK2 and 3 (Fig 5b). SOK2 accumulates weakly on the abaxial (bottom) side of the leaf and more strongly on the adaxial side, while SOK3 shows the opposite pattern. Both SOK2 and 3 are present in the cytoplasm and are enriched at the PM faces surrounding stomatal guard cells. SOK3 displays a dynamic pattern during stomatal development (Fig. 5c). In the meristemoid mother cell (MMC), SOK3 localizes to all corners. During amplifying divisions of the meristemoid cell, the protein remains corner-localized until the guard mother cell is specified. Shortly after division of the guard mother cell, polarity is lost from the corners and once the guard cells have formed, SOK3 polarity returns at the PM facing the guard cells. Although SOK2 and 3 are most strongly present at opposite sides of the leaf, their overlap in expression and localization indicates a potential redundancy between the two genes.

SOK1 is polar during male and female gametophyte development

Next, we investigated SOK protein accumulation in floral organs. Several CRISPR/Cas9 induced mutants in *SOK1* displayed fertility defects, suggesting that *SOK1* could play a role in gametophyte development and/or fertilization. Indeed, *SOK1* accumulates both in the male and female gametophyte. In the ovule, the window of *SOK1* accumulation is very brief and occurs only during embryo sac development (Fig. 6a). In the earliest stage of expression, the embryo sac is still a small cell and *SOK1* is mostly apolar. Localization quickly becomes polarized to the growing (chalazal) tip of the small cell and remains polar as the embryo sac expands. *SOK1* protein quickly disappears when growth of the embryo sac ceases. During male gametophyte development, *SOK1* is first visible as a ring-like structure in young microspores (Fig. 6b, c). This ring is probably related to the division of the microspore into a vegetative and generative cell, but it is unclear whether the ring forms before or after cell division. The *SOK1* ring rapidly turns into an invaginating patch, surrounding the generative cell as it becomes internalized. Throughout microgametogenesis, the *SOK1* promoter is only active in the vegetative cell (Fig. 6d), which means that the protein is polarized towards the generative cell rather than expressed inside it. *SOK1* remains on the membrane surrounding the generative cell after it divides into two sperm cells (Fig. 6b, c). When the pollen grains desiccate, the protein is found in large spots on the sperm cells. This localization often persists until pollen germination and pollen tube growth (Fig. 6c). Whether *SOK1* expression is still active during the fertilization process remains to be investigated. *SOK3* is also expressed in developing pollen, but in contrast to *SOK1*, it is localized in the cytosol and vegetative nucleus, while being excluded from the sperm cells (Fig. 6e). The

protein is also present throughout the ovules (Fig. 6e). No expression of SOK2 or 5 could be observed in microspores or the ovule. Taken together, these data show that SOK1 displays a unique and dynamic polar localization during male and female sporogenesis, during or shortly after symmetry breaking and at sites of directional growth and asymmetric division.

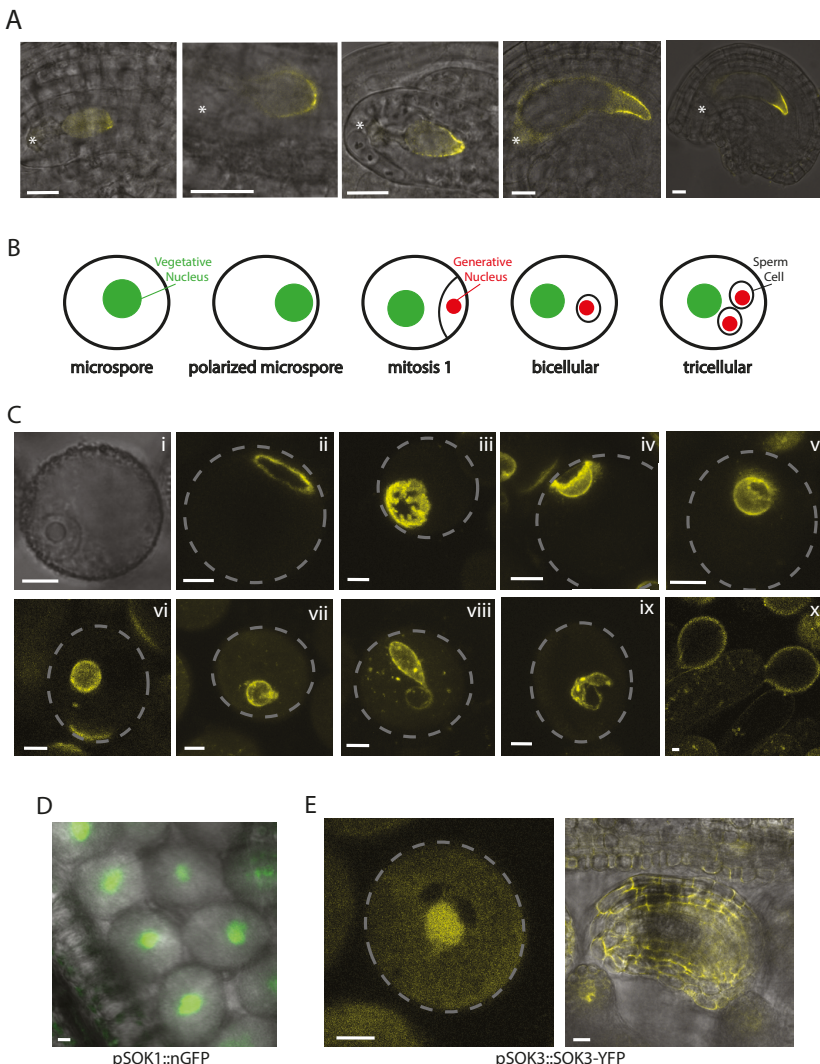


Figure 6. SOK1 is polar during male and female gametogenesis. (A) *pSOK1::SOK1-YFP* in the ovule as the embryo sac is established and expands. Stars indicate micropylar side and scalebar represents 10 μ m. (B) Schematic representation of microspore development. (C) maximum projections of *pSOK1::SOK1-YFP* localization in microspore development. I polarized microspore, ii polar ring, iii-v internalization of generative cell, vi-viii bicellular stage with elongating generative cell, ix tricellular stage, x pollen on the stigma after the sperm cells have been released. Scalebar represents 5 μ m. (D) *pSOK1::nGFP* in microspores. (E) *pSOK3::SOK3-YFP* in microspore (left) and ovule (right). Scalebar ovule 10 μ m, microspore 5 μ m.

Aside from microspores and ovules, some SOKs were also present in anther or gynoecium tissues. SOK1 is expressed in the vascular cells and the valve margin of the gynoecium (Fig. 7a). In the valve margins, SOK1 is enriched on the apical side of the cells. Like in other tissues, SOK3 is the most abundant family member in the gynoecium (Fig. 7b). It is most highly expressed in the epidermis and vasculature. The protein is polarized towards stomata guard cells and is enriched in every corner of most other cells. SOK2 and 5 are present in epidermal cells of the replum and style (Fig. 7c).

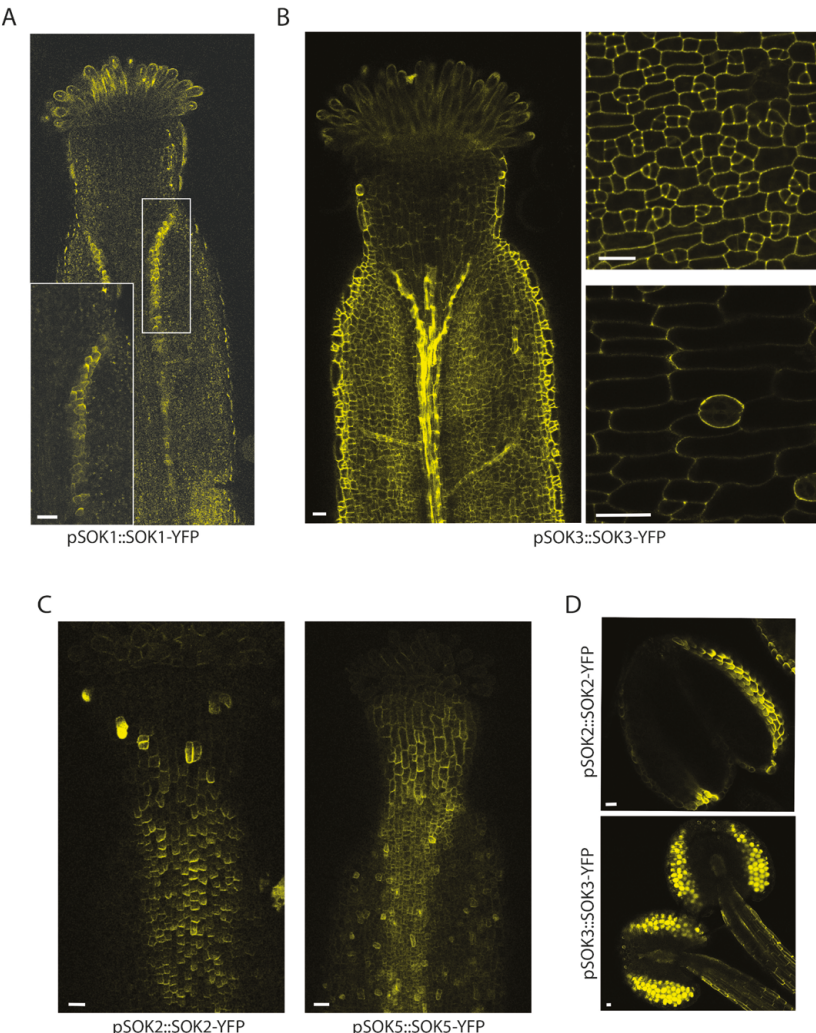


Figure 7. SOKs are expressed throughout the gynoecium and anther. (A) SOK1 polar localization in the valve margins. (B) SOK3 expression in the gynoecium. Overview (left), epidermis (top right), polar around stomata (bottom right). (C) SOK2 and 5 in the epidermis of the gynoecium. D) SOK2 (epidermis) and 3 (pollen) in anthers. Scalebar represents 20 μ m.

SOK2 is more highly enriched in some cells dotted over the style, while SOK5 displays this dotted pattern throughout the gynoecium epidermis. In contrast to the gynoecium, anthers lack expression of SOK1. In young anthers, polar SOK2 is present in the epidermis of the anther head (Fig. 7d). This quickly disappears as the anther matures and weak expression is found in the stamen filament instead. SOK3 is weakly present in the anther head, but more abundant in the stamen filament (Fig. 7d). Occasionally, weak signal of SOK5 could also be detected in the stamen (not shown).

Discussion

Translating tissue and cell polarity into sub-cellular processes is a vital, yet poorly understood process in plants. Several polar proteins with various functions have been reported, but their polarity is often easily disturbed. The recently described SOK family contains 5 members with unique expression and localization patterns in the root (Chapter 3). This localization is very robust, which makes SOKs interesting markers for polarity studies. Misexpression of SOK1 induces oblique divisions, but their exact biological function is unknown. Therefore, we generated CRISPR lines to knock out individual SOKs.

Interestingly, some mutations near the start site of *SOK1* lead to fertility defects in many candidate plants, while complete loss of *SOK* has no effect. It is unlikely that these defects were caused by off-target mutations, as the fertility problems only occurred in plants with a *sok1* mutation. Additionally, if the phenotypes were caused by another gene, the *sok1* mutations should have inherited independently. *SOK1* shows a unique polar localization in microspores and ovules, which explains that defects were observed in fertility and ovule/seed development. However, *SOK1* is not essential for microspore and ovule development, as complete loss of the gene leads to normal plants and gene transmission. Small mutations in the N-terminus of *SOK1* could create neomorphic, hypomorphic or hypermorphic effects, and this could turn the produced protein into a disruptive element rather than an inactive one. We also generated a *sok2* mutant candidate that displayed fertility defects like *sok1*. As we only obtained 1 candidate of *sok2*, it is not possible to tell whether affected fertility is a recurrent phenotype or caused by insertion position of the transgene.

Although complete loss of *SOK1* did not result in obvious phenotypes, qPCR revealed upregulation of *SOK4*. This suggests the presence of a feedback mechanism that monitors *SOK1* levels and regulates other *SOK* genes accordingly. *SOK4* is very weakly expressed in the root vasculature while *SOK1* is present in the first few vascular cells above the QC. Thus, if *SOK4* has a similar function as *SOK1*, increase of its expression might be able to compensate for loss of *SOK1* in the root. Polar edge polarity is important for *SOK1* function (Chapter 3). Because *SOK4* expression is

extremely weak, its polarity could not be determined. Expression of a SOK4 marker in $\Delta sok1$ should lead to higher protein levels, which would enable assessment of SOK4 polarity and whether it overlaps with SOK1. A double mutant among *SOK1* and 4 could reveal if this pair is truly functionally redundant.

It is interesting that specifically *SOK4* is upregulated in $\Delta sok1$, as *SOK3* is also present in the vascular tissues and in all edges of the cell. Expression of *SOK3* is hardly affected in $\Delta sok1$ and if *SOK3* was capable of taking over *SOK1* function, upregulation of *SOK4* would not be necessary. *SOK2* and *SOK5* are barely changed upon loss of *SOK1*. These two family members are normally not expressed in the vasculature. Clearly, the compensation mechanism favors upregulating a *SOK* that is already present in the vasculature over switching on *SOKs* that are not normally expressed there. This could amongst others imply differences in function, or tissue specificity of *SOK* gene regulation. Aside from the fact that MONOPTEROS is required for expression of *SOK1* and 5 (Möller et al., 2017), nothing is known about *SOK* gene regulation. Studying which transcription factors regulate *SOKs* in a spatial and temporal resolution would greatly enhance understanding *SOK* function and dynamics.

SOK patterns overlap both in the root and embryo. As *SOK1* and 4 form a potential redundant pair in the root, other *SOKs* might be redundant to each other as well. This redundancy can be tissue-specific, as expression patterns of genes can vary greatly from one tissue to another. For example, *SOK2* and 5 are both present in the root endodermis with a similar polar localization, but in the embryo their expression patterns are quite different (Chapter 3). In the gynoecium and stamen, *SOK1* and 5 show an overlapping expression and localization pattern. Thus, *SOK2* and 5 may be redundant in several places. *SOK3* is expressed almost everywhere, and at relatively high levels. As it is also present in every edge of the cell, *SOK3* might be redundant with any *SOK*. In leaves, *SOK3* accumulation is strikingly similar to *SOK2* around stomata guard cells. Although both proteins are most highly enriched at opposite sides of the leaf, redundancy is still possible. *SOK1* is the most dynamic family member with brief polar accumulation in the vasculature, microspore and embryo sac. Of the tested *SOKs*, only *SOK3* was present in microspore and ovule. However, its localization is very different from *SOK1* in these tissues, which makes it unlikely that *SOK3* can easily take over *SOK1* function there. Altogether, the potential redundancies between *SOKs* indicate that higher order mutants are likely necessary to reveal the biological function of *SOKs*.

In conclusion, we generated a *sok1* loss-of-function mutant that did not show a developmental phenotype, but displayed upregulation of *SOK4*. This revealed a feedback mechanism between *SOKs* and potential redundancy between *SOK1* and 4. Expression and localization analysis of *SOK1*, 2, 3 and 5 showed that redundancy

is also possible between SOK2 and 3 in leaves and between 2 and 5 in several other tissues. We have now identified SOK groups that can be targeted in generating higher order mutants. In addition, we highlighted genetic regulation of *SOK* genes as a promising avenue into understanding SOK dynamics and function.

Material and Methods

Plant material and growth conditions

Seeds were sterilized in 75% bleach / 25% ethanol for 8 minutes, washed twice in 70% ethanol and once in 96% ethanol. After drying they were plated on half strength Murashige and Skoog (1/2MS) medium, supplemented with 15mg/l phosphinothricin or 50mg/L kanamycin if selection was necessary. The seeds were incubated at 4°C for one or two days and cultured under long-day conditions (16h light, 8h dark) at 22°C and 75% humidity.

SOK insertion lines were obtained from the ABRC stock center. Each line was genotyped to validate the insertion at the correct locus using primers in Supplemental Table 1. Next, plants homozygous for the insertion were selected by genotyping with the same primers.

4

Abiotic stress treatments

Seeds of Col-0 and Δ sok1 were germinated on 1/2MS plates and grown vertically for 5 days. At day 5, 20 seedlings of each line were manually transferred to plates containing 1/2MS only, or 1/2MS plus NaCl (75 mM-250 mM), 2,4D (10-50 nM), IAA 100 nM, NAA 100 μ M, isoxaben 600 nM or mannitol 0.2-0.4 mM. Seedlings were grown for two more days, after which the plates were scanned. Root lengths were measured with ImageJ and images of the root tip were taken with a confocal microscope.

CRISPR GuideRNA selection

Selection of guideRNAs was performed using online tools:

<http://www.e-crisp.org/E-CRISP>, <http://crispr.mit.edu/>, http://bioinfogp.cnb.csic.es/tools/breakingcas/?gset=7x1_GENOMES_Eensembl_91 and <https://portals.broadinstitute.org/gpp/public/analysis-tools/sgrna-design>.

Generation of plasmids

Primers and guideRNAs used in this study are described in Supplemental Table 1 and 2.

The pYB196 constructs were created by amplifying the promoter and guide from a pPLV60 construct (unpublished). Next, the fragments were fused by fusion PCR and cloned into pYB196 with a SLICE reaction. For pTTK312, the two parts of the pU6-26-sg-guide-terminator fragment were amplified from pTTK194 and fused together by overlap-extension PCR. Next, the fragment was cloned into pTTK312 with SLICE. pGG-Z03 plasmids were ordered together with the Friml lab in Vienna. EC1-driven SOK1 deletion constructs were made as follows: guideRNAs were synthesized with respective overhangs. The two complementary oligos were annealed and inserted into pEN-2xChimera using BpiI and BsmBI restriction enzymes. The guide RNAs were then transferred into pUbiCAS9-Red (for protoplasts) or pEciCAS9-Red (for stable transformation in *A. thaliana*) by Gateway® single-site LR recombination-mediated cloning. Efficiency of the guides was tested in protoplasts: *Arabidopsis* mesophyll protoplasts for transient expression of the CRISPR/Cas9 construct (pUbiCAS9-Red) were prepared as described previously with minor modifications (Yoo et al 2007). Approximately 80,000 protoplasts were transformed with 16 µg of plasmid (pUbiCAS9-Red) and incubated for 48 h at 22°C under long photoperiod conditions (150 µmol/m²/s and 16 h/8 h light/dark cycles). DNA was isolated and concentrations adjusted before performing a semi-quantitative PCR using oligonucleotides flanking the region targeted for deletion.

Transformation and genotyping

Plasmids were generated/obtained as described above and transformed into *Arabidopsis* Col-0 plants via Agrobacterium-mediated transformation by floral dip as described in De Rybel et al., 2011. Transformed seeds were selected by antibiotic resistance or red seed coat fluorescence. DNA was extracted from leaves and/or flowers of the resulting plants with a CTAB (Cetyltrimethylammonium bromide) buffer (1% CTAB, 100 mM Tris-HCl pH8, 20 mM EDTA, 1.5 M NaCl). The DNA was then separated with chloroform, precipitated with isopropanol and washed with 70% ethanol. The area surrounding the sg target sites was amplified by PCR, using primers described in Supplemental Table2. The PCR product was precipitated with ammonium acetate and sequenced with the FW or RV PCR primer to identify mutations. A custom batch analysis version of the TIDE program (BatchTide, Brinkman et al., 2014) was used to analyze the nature of these mutations. Clustal-Omega (<https://www.ebi.ac.uk/Tools/msa/clustalo/>) and NCBI BLAST (<https://blast.ncbi.nlm.nih.gov/Blast.cgi>) were used to create alignments. Sequencing traces were displayed in APE-E <http://jorgensen.biology.utah.edu/wayned/ape/>. For the SOK1 deletion experiment, DNA was extracted as described above. Primers inside and surrounding the SOK1 gene were used for genotyping, see Supplemental Table 2. Plants homozygous for the deletion were sequenced as described above.

qRT-PCR

Primers for qRT-PCR were designed with BeaconDesigner 8 (Premier Biosoft International). Seedlings were grown on $\frac{1}{2}$ MS for 5 days in long day conditions. Roots were collected per line and snap frozen in liquid nitrogen. The material was ground using a Retch machine and RNA was isolated using TRIzol reagent (Invitrogen) and the RNAeasy kit (Qiagen). cDNA synthesis was performed on 0.5 μ g total RNA with the iScript cDNA Synthesis Kit (BioRad). qRT-PCR was performed as described previously (De Rybel et al., 2010) with iQ SYBR Green Supermix (BioRad) and measured on a CFX384 RT-PCR detection system (BioRad). Each reaction was done in triplicate. The data was analyzed using qBase, as described in Hellemans et al., 2007. Gene expression levels were normalized to ACT2, EEF α 4, eLF4 and CDKA.

Microscopy

To study embryos, ovules were cleared with chloral hydrate for at least 2 hours and observed with a Differential Interference Contrast (DIC) Leica DMR microscope as described in Llavata-peris et al., 2013.

For confocal imaging of roots, 5-day old seedlings were immersed in a drop of 20 μ g/ml Propidium Iodide solution and imaged with a confocal microscope after 5 minutes incubation. Embryos were observed by confocal microscopy as follows: ovules were isolated and mounted in a Renaissance staining solution (4%paraformaldehyde/5% glycerol/4% DMSO in 1x PBS with 1.5% SCRI Renaissance Stain R2200). Embryos were squeezed out of the ovules by gently tapping the coverslip with a pencil.

A Leica SP5 or SP8 confocal microscope was used for imaging plant tissues. The SP5 was equipped with an Argon laser and DSS561 diode laser, the SP8 with a pulsed white light laser. GFP was excited at 488 nm, YFP at 514 nm, Propidium Iodide at 561 nm and Renaissance at 504 nm. Hybrid detector filters were set at 495-520 nm for GFP, 520-550 nm for YFP, 600-650 nm for Propidium Iodide and 430-470nm for Renaissance.

Acknowledgements

Many thanks to Jos Wendrich's student Pieter Mijnhout for assisting with the generation of CRISPR materials. Tatyana Radoeva, thank you for helping with the embryo analysis. We'd also like to extend our appreciation to J.W. Borst for his help with the confocal microscope. This work was funded by a grant from the Netherlands Organization for Scientific Research (NWO; ALW-Topsector grant 831.13.001)

References

Abas, L., Benjamins, R., Malenica, N., Paciorek, T. T., Wiśniewska, J., Moulinier-Anzola, J. C. et al. (2006). Intracellular trafficking and proteolysis of the *Arabidopsis* auxin-efflux facilitator PIN2 are involved in root gravitropism. *Nature Cell Biology*, 8, 249–256.

Alassimone, J., Fujita, S., Doblas, V. G., Van Dop, M., Barberon, M., Kalmbach, L. et al. (2016). Polarly localized kinase SGN1 is required for Caspary strip integrity and positioning. *Nature Plants*, 2, 1–10.

Belhaj, K., Chaparro-Garcia, A., Kamoun, S., Patron, N. J., & Nekrasov, V. (2015). Editing plant genomes with CRISPR/Cas9. *Current Opinion in Biotechnology*, 32, 76–84.

Brinkman, E. K., Chen, T., Amendola, M., & Van Steensel, B. (2014). Easy quantitative assessment of genome editing by sequence trace decomposition. *Nucleic Acids Research*, 42, 1–8.

De Rybel, B., van den Berg, W., Lokerse, A. S., Liao, C.-Y., van Mourik, H., Moller, B., ... Weijers, D. (2011). A Versatile Set of Ligation-Independent Cloning Vectors for Functional Studies in Plants. *Plant Physiology*, 156, 1292–1299.

Dong, J., MacAlister, C. A., & Bergmann, D. C. (2009). BASL Controls Asymmetric Cell Division in *Arabidopsis*. *Cell*, 137, 1320–1330.

Friml, J., Yang, X., Michniewicz, M., Weijers, D., Quint, A., Tietz, O. et al. (2004). A PINOID-dependent binary switch in apical-basal PIN polar targeting directs auxin efflux. *Science*, 306, 862–865.

Fujiwara, T., Takano, J., Miwa, K., & Yuan, L. (2005). Endocytosis and degradation of BOR1, a boron transporter of *Arabidopsis thaliana* by boron availability. *PNAS*, 102, 12276–12281.

Gälweiler, L., Guan, C., Müller, a, Wisman, E., Mendgen, K., Yephremov, a, & Palme, K. (1998). Regulation of polar auxin transport by AtPIN1 in *Arabidopsis* vascular tissue. *Science*, 282, 2226–2230.

Geldner, N., Friml, J., Stierhof, Y. D., Jürgens, G., & Palme, K. (2001). Auxin transport inhibitors block PIN1 cycling and vesicle trafficking. *Nature*, 413, 425–428.

Hardtke, C. S., & Berleth, T. (1998). The *Arabidopsis* gene MONOPTEROS encodes a transcription factor mediating embryo axis formation and vascular development. *EMBO Journal*, 17, 1405–1411.

Hyun, Y., Kim, J., Cho, S. W., Choi, Y., Kim, J. S., & Coupland, G. (2014). Site-directed mutagenesis in *Arabidopsis thaliana* using dividing tissue-targeted RGEN of the CRISPR/Cas system to generate heritable null alleles. *Planta*, 241, 271–284.

Lampropoulos, A., Sutikovic, Z., Wenzl, C., Maegele, I., Lohmann, J. U., & Forner, J. (2013). GreenGate - A novel, versatile, and efficient cloning system for plant transgenesis. *PLoS ONE*, 8, e83043.

Löfke, C., Luschnig, C., & Kleine-Vehn, J. (2013). Posttranslational modification and trafficking of PIN auxin efflux carriers. *Mechanisms of Development*, 130, 82–94.

Michniewicz, M., Zago, M. K., Abas, L., Weijers, D., Schweighofer, A., Meskiene, I. et al. (2007). Antagonistic Regulation of PIN Phosphorylation by PP2A and PINOID Directs Auxin Flux. *Cell*, 130, 1044–1056.

Möller, B. K., ten Hove, C. A., Xiang, D., Williams, N., López, L. G., Yoshida, S. et al. (2017). Auxin response cell-autonomously controls ground tissue initiation in the early *Arabidopsis* embryo. *Proceedings of the National Academy of Sciences*, *114*, E2533–E2539.

Nakamura, M., & Grebe, M. (2018). Outer, inner and planar polarity in the *Arabidopsis* root. *Current Opinion in Plant Biology*, *41*, 46–53.

Paciorek, T., Zažímalová, E., Ruthardt, N., Petrášek, J., Stierhof, Y. D., Kleine-Vehn, J. et al. (2005). Auxin inhibits endocytosis and promotes its own efflux from cells. *Nature*, *435*, 1251–1256.

Pillitteri, L. J., Peterson, K. M., Horst, R. J., & Torii, K. U. (2011). Molecular Profiling of Stomatal Meristems Reveals New Component of Asymmetric Cell Division and Commonalities among Stem Cell Populations in *Arabidopsis*. *The Plant Cell Online*, *23*, 3260–3275.

Smit, M. E., & Weijers, D. (2015). The role of auxin signaling in early embryo pattern formation. *Current Opinion in Plant Biology*, *28*, 99–105.

Takano, J., Tanaka, M., Toyoda, A., Miwa, K., Kasai, K., Fuji, K. et al. (2010). Polar localization and degradation of *Arabidopsis* boron transporters through distinct trafficking pathways. *Proceedings of the National Academy of Sciences of the United States of America*, *107*, 5220–5225.

Tanaka, H., Kitakura, S., Rakusová, H., Uemura, T., Feraru, M. I., De Rycke, R. et al. (2013). Cell polarity and patterning by PIN trafficking through early endosomal compartments in *Arabidopsis thaliana*. *PLoS Genetics*, *9*, e1003540.

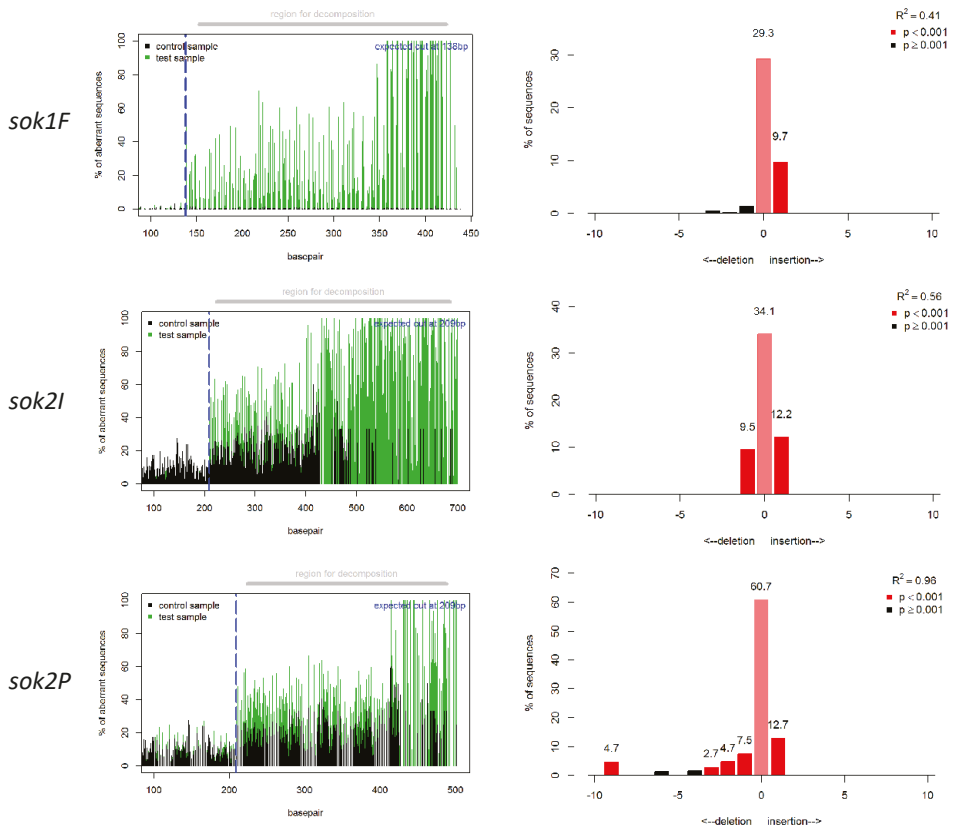
Tsutsui, H., & Higashiyama, T. (2017). PKAMA-ITACHI vectors for highly efficient CRISPR/Cas9-mediated gene knockout in *Arabidopsis thaliana*. *Plant and Cell Physiology*, *58*, 46–56.

Wang, Z. P., Xing, H. L., Dong, L., Zhang, H. Y., Han, C. Y., Wang, X. C., & Chen, Q. J. (2015). Egg cell-specific promoter-controlled CRISPR/Cas9 efficiently generates homozygous mutants for multiple target genes in *Arabidopsis* in a single generation. *Genome Biology*, *16*, 1–12.

Wisniewska, J., Xu, J., Seifertova, D., Brewer, P. B., Ru, K., Scheres, B. et al. (2006). Polar PIN Localization Directs Auxin, *312*, 883.

Zhang, Y., Wang, P., Shao, W., Zhu, J. K., & Dong, J. (2015). The BASL Polarity Protein Controls a MAPK Signaling Feedback Loop in Asymmetric Cell Division. *Developmental Cell*, *33*, 136–149.

Supplemental information

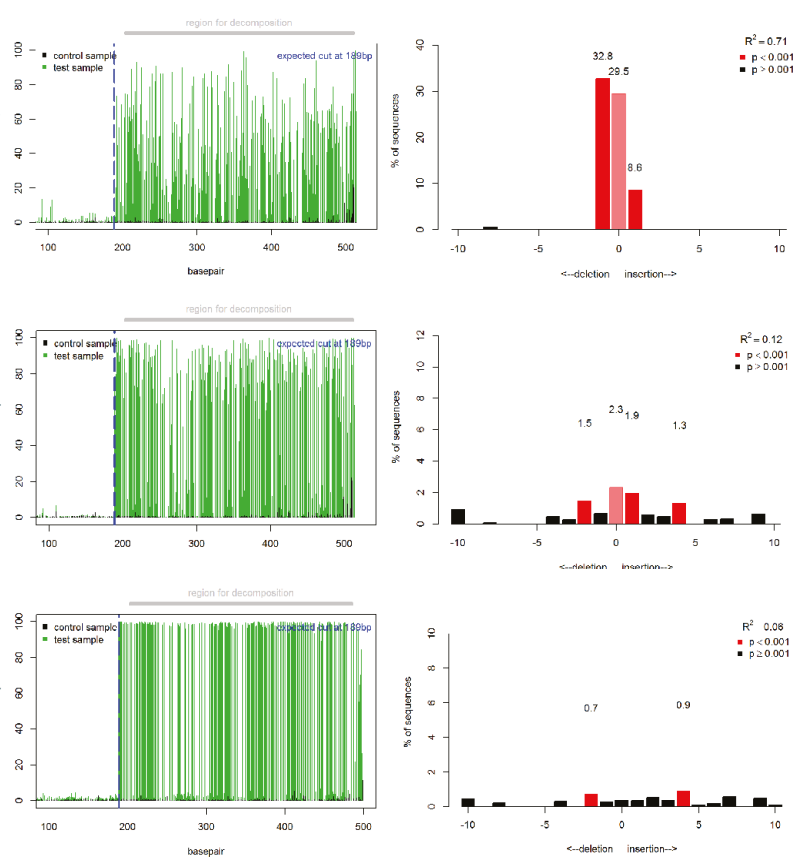


Supplemental Figure 1. A) BatchTide analysis of the *sok1* 40 mutations. Green graphs show the immediate and strong deviation of the candidate sequence after the cut site (dashed line). Red graphs display the percentage of sequence traces that showed an insertion or deletion of x basepairs. R^2 signifies how well the data can be predicted by the given graph.

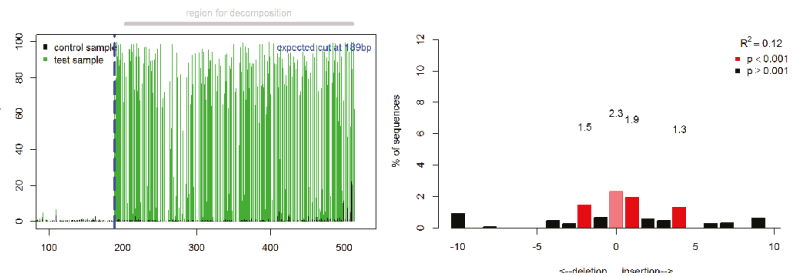
Chapter 4

A

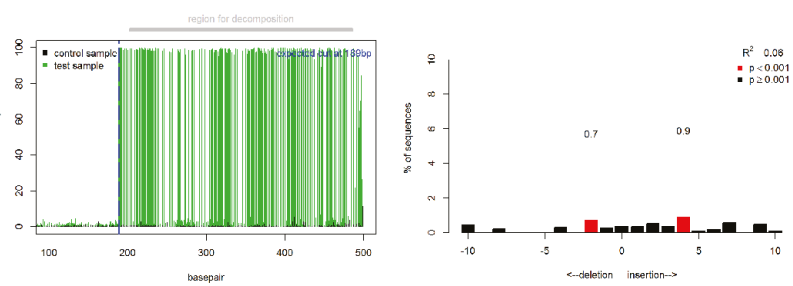
sok1 40 T1



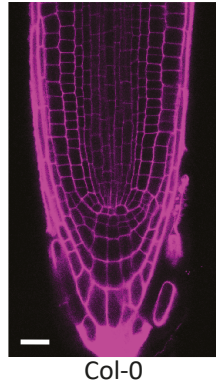
sok1 40 T2



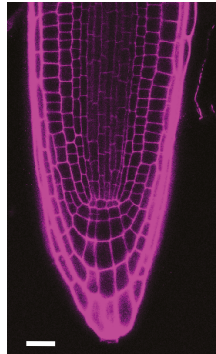
sok1 40 T3



B



Col-0



sok1 40

Supplemental Figure 2. A) BatchTide analysis of the *sok1 40* mutations. Green graphs show the immediate and strong deviation of the candidate sequence after the cut site. Red graphs display the percentage of sequence traces that showed an insertion or deletion of x basepairs. R^2 signifies how well the data can be predicted by the given graph. B) Col-0 and *sok1 40* roots stained with Propidium Iodide. Scalebar represents 20 μ m.

Supplemental Table 1: Primers used in this study

Genotyping insertion lines			
Line	Insertion line	Background	Primer 1
sok1-1	SAIL_1283_E07	Col-0	TCGAGTTATATCAAGAATAAGAGCTATCGAGC
sok1-2	SM_3_36648	Col-0	AGCTTTACATAGACTAAGAC
sok1-3	SM_3_36651	Col-0	AGCTTTACATAGACTAAGAC
sok1-6	SALK_036308	Col-0	AAAGAGTCTCCGGTCTTCTGC
sok3-1	FLAG_477B10	ws	CGTCTTCTCTGAATGAATCGG
sok3-2	SALK_042424	Col-0	TAGCGTCTCGAGAATCAGGAG
sok3-3	GABI_223C03	Col-0	AAGCTGTGATTTGGCACAAG
sok4-1	SALK_051352	Col-0	ACATTAATGGCGTTGGTGAATTC
sok4-2	GT_3_10797	ler	AACTCGTAAACTCTCGATGGATG
sok5-4	SALK_106678	Col-0	TGTCGTTAAAGAATGTGGGC
Line	Primer 2	General primer	
sok1-1	AGCAGAGCTTACGAGCATAATGGAGC	GCCTTTTCAGAAATGGATAAATAGCCTGCTCC	
sok1-2	GGATAATCCTCTGTTTTGAGAAAC	CTTATTCAGTAAGAGTGTGGGTTTG	
sok1-3	GGATAATCCTCTGTTTTGAGAAAC	CTTATTCAGTAAGAGTGTGGGTTTG	
sok1-6	ATGCTCCCTCGAAGCTTTTC	ATTTGCCGATTCGGAAC	
sok3-1	AACCGATGAAACTGTGAGTGG	CGTGTGCCAGGTGCCACGGAATAGT	
sok3-2	CCAAGAACGTCAACTTGAGC	ATTTTCCGATTCGGAAC	
sok3-3	AACCGATGAAACTGTGAGTGG	ATATTGACCATCATACTCATTGC	
sok4-1	GTTGATTAATATGCCATTAGC	ATTTTCCGATTCGGAAC	
sok4-2	GAATCGTTATTGTGGATTCC	ACCCGACCGGATCGTATCGGT	
sok5-4	ATCGTGCCGTTTTGTACTG	ATTTTCCGATTCGGAAC	
CRISPR cloning primers pYB196			
LIC-U6-F	TAGTTGGAATGGGTTCGAAGAATGATTAGGCATCGAACCT		
LIC-sg-R	TTATGGAGTTGGGTTCGAACATAATCAATGTCAACGCG		
SOK1 FW	GAGATGGAAAGTAATGGTGGGTTTAGAGCTAGAAATAGCAA		
SOK1 RV	CCACCATTACTTCCATCTCACAACTACTACTTCGACTCTAGCT		
SOK2 FW	GAAGCTGTAAGATGCAGAAGGTTTAGAGCTAGAAATAGCAA		
SOK2 RV	CTTCTGCATCTTACAGCTTCACAATCACTACTTCGACTCTAGCT		
SOK3 FW	GTCCAGACTTTGCTCTCGTTAGAGCTAGAAATAGCAA		
SOK3 RV	GAGAGAGCAAAGTCTGGACACAATCACTACTTCGACTCTAGCT		
SOK4 FW	CGCAAGACTCAAAACCCCTCCGTTAGAGCTAGAAATAGCAA		
SOK4 RV	GGAGGGTTTGAGTCTGCGACAATCACTACTTCGACTCTAGCT		
SOK5 FW	AACACCAGATAACAACATTGTTAGAGCTAGAAATAGCAA		
SOK5 RV	AATAGTTGTTATCTGGTGTACAATCACTACTTCGACTCTAGCT		

CRISPR cloning primers pTTK312

U6-F-Slice	TTACTAGATCACTAGTGCGGCCGCTCGTTGAACAACGGAAACTCG
guide-R-Slice	GCTTGAGCTCTCCATATGGTCGACCGAATTGAGCTCGGTACCC
SOK1_guide-F	AAATGGTTAGCAGACGCACGGTTTAGAGCTAGAAATAGC
SOK1-U6-sg-R	CGTGCCTGCTAACCATTAAATCACTACTTCGACTCTAG

CRISPR cloning primers SOK1 deletion

sgRNA AT1G05577 A1 fw	ATTGCCGGACGGTCGGATGGGAGA
sgRNA AT1G05577 A1 rv	AAACTCTCCCATCCGACCGTCCGG
sgRNA AT1G05577 B1 fw	ATTGTCTCTGCCTCTGGTCAAATA
sgRNA AT1G05577 B1 rv	AAACTATTGACCAGAGGCAGAGA
sgRNA AT1G05577 B2 fw	ATTGGTTCTAATCAGACAGTCGC
sgRNA AT1G05577 B2 rv	AAACGCGACTGTCTGATTAGAAC

CRISPR genotyping primers

pYB196, pTTK312, pGG-Z03

sok1 FW	GCCCTTGTAGTCCGATCC
sok1 RV	CCATTCTTCACATCTGCG
sok2 FW	CCCATTGTACCATCAGGTAG
sok2 RV	CTCTTAACCGGAGAGGCTGG
sok3 FW	CTGTCTCTCCATTAAATCTCCACTG
sok3 RV	AAGCCTCTATAACATCTGC
sok4 FW	CCTCGTCATTATGTCAGACAA
sok4 RV	CCATTCCATTGCCTCGTAGATC
sok5 FW	GCCCTTGTCTCTCGCATCC
sok5 RV	CGTGGGAAGAGAGAGTGAC

sok1 deletion genotyping primers

Deletion band FW	CTCGCTGACCGGAAACTGTA
Deletion band RV	GCGTTTGCATAAGCCAA
WT band FW	CTCGCTGACCGGAAACTGTA
WT band RV	AGCATGGAGTGGCATAAAGATGAAAGAG

Primers used in qPCR

SOK1 qPCR FW	GGAAATCCATTGGGACATC
SOK1 qPCR RV	TTCACGAACTAGCAAACAG
SOK2 qPCR FW	AGAGGAAGAAGATGGAGAG
SOK2 qPCR RV	GAGAACAGCGAGATTGAG
SOK3 qPCR FW	TCAGAAGAGCCTTAACCAAGT
SOK3 qPCR RV	GTTGCCGCCACAATACAA
SOK4 qPCR FW	CATTGATGAGAGCAGATG
SOK4 qPCR RV	CTATAATTCCCTGTTCCCTC
SOK5 qPCR FW	GAGGAGCAGAGGATAATG
SOK5 qPCR RV	CATTCTGAACACCTGTC

Supplemental Table 2. GuideRNAs used in this study

pYB196		pGG-Z03	
SOK1	GAGATGGAAAGTAATGGTGG	SOK1 clone 39	AACGGCTAAGGAAATAAAGT
SOK2	GAAGCTGTAAGATGCAGAAG	SOK1 clone 40	GATGGTCAACGTGACCCGAA
SOK3	GTCCAGACTTTGCTCTCTC	SOK2 clone 45	AAAGTCCAGAGAGGATCATA
SOK4	CGCAAGACTCAAACCTCC	SOK2 clone 46	ACTTGGACTCTCGGAAAAT
SOK5	AACACCAGATAACAACATT	SOK3 clone 43	GTCCAGAGAGAGCAAAGTC
		SOK3 clone 44	ATGCTCAAGTTGACGATTCT
pTTK312		SOK4 clone 41	CCGAACAAACATTAATGGCGT
SOK1	AAATGGTTAGCAGACGCACG	SOK4 clone 42	GGGGACTATCGTTCCCTGG
		SOK5 clone 47	GCTCAGACCAGATTGGTTA
		SOK5 clone 48	GATGGTCAAGCTGACCATTG

SOK1 deletion

	<i>EC1 construct 1</i>		<i>EC1 construct 2</i>
Guide A1	CCGGACGGTCGGATGGGAGA	Guide A1	CCGGACGGTCGGATGGGAGA
Guide B2	GTTTCTAATCAGACAGTCGC	Guide B1	TCTCTGCCTCTGGTCAAATA

Chapter 5

Deep evolutionary origin of the polymerizing DIX domain in locally focused protein assemblies

Maritza van Dop¹, Sumanth Kumar Mutte¹, Marc Fiedler², Kuan-Ju Lu¹,
Jeroen de Keijzer^{3,4}, Marcel E. Janson³, Mariann Bienz², Dolf Weijers¹

¹Laboratory of Biochemistry, Wageningen University and Research, Wageningen, The Netherlands

²MRC Laboratory of Molecular Biology, Cambridge, United Kingdom.

³Laboratory of Cell Biology, Wageningen University and Research, Wageningen, The Netherlands.

⁴Present address: Department of Crop Genetics, John Innes Center, Norwich, United Kingdom.

Abstract

When plants evolved from simple water-dwelling algae to complex land plants, more elaborate regulatory mechanisms were required to guide their development relative to fixed light and gravity vectors, as well as to the 3D body surface. Polarity is one of these mechanisms essential for morphogenesis. Specialized membrane proteins use cell polarity cues to establish polar localization and carry out local functions. The *Arabidopsis* SOSEKI (SOK) protein family members localize robustly to subcellular domains, including cell edges in the embryo and root. Here, we investigated the evolutionary history of SOK protein sequences, properties and subcellular polarity. We found that an ancestral SOK gene first arose in basal land plants. We identified 5 conserved domains within SOK proteins, and based on these domains, divided SOKs into an ancestral and a more recently evolved type. Almost all major clades in land plants contain at least one ancestral type SOK, while vascular plants have both types. Localization to cell edges is one of the most striking features of *Arabidopsis* SOK proteins. We assessed the evolutionary conservation of this polarity in the moss *Physcomitrella patens*, which contains 9 SOK genes that all derived from moss-specific gene duplication events. One of the four tested PpSOKs showed edge polarity in the gametophore, suggesting that edge polarity of SOK proteins is an ancient property. Furthermore, we found that misexpression of the only SOK in the liverwort *Marchantia polymorpha* induced defects in gemma shape, likely by altering cell shape and/or division plane, as in *Arabidopsis*. Thus far, DIX domains have only been found in animal proteins, where they represent a polymerization domain in Axin, Dixin and Dishevelled proteins, thus forming local foci of Wnt signalling (signalosomes). We extended our phylogenetic analysis and found that DIX(-LIKE) domains occur in animals, plants as well as the SAR group, presumably representing a common ancestry that was lost in many Eukaryotic clades. DIX sequence and (predicted) structure is similar between these groups, and we used in vitro experiments to show that the capacity to polymerize is conserved in these three lineages. Taken together, our work showed that plant-specific SOK proteins use an ancient polymerization domain to generate local foci of high protein concentrations, culminating in edge localization of *Arabidopsis* SOK proteins.

Introduction

In multi-cellular organisms, polarity is necessary for establishing shape and for guiding local processes relative to organismal axes and/or external vectors. As land plants developed from simpler form, represented by extant algal morphologies, to complex 3-dimensional structures, translating organismal and tissue polarity into sub-cellular processes must have accompanied the evolution of anatomical complexity. However, it remains unclear how these translation mechanisms work and how they evolved. Studies in flowering plants identified membrane proteins that use polarity information to direct their sub-cellular localization. In roots, these proteins localize to one face of the cell and are absent from others (reviewed in Nakamura & Grebe, 2018). Leaf pavement cells have a more complex jigsaw puzzle shape, which leads polar proteins to accumulate in the necks or lobes (Fu, et al., 2002; Li et al., 2011). In stomatal lineage cells, several polar proteins can be found in the edge opposing a newly formed division plane (Dong, et al., 2009). Aside from cell faces, specific local accumulations of membrane proteins have also been reported. Examples are the medial CASP ring during Caspian Strip formation (Roppolo et al., 2011), the ROP island prior to root hair formation and accumulation of many proteins at the growing tip of root hairs (Jones, 2002; Molendijk et al., 2001; Stanislas et al., 2015). Much less is known about locally accumulated membrane proteins in basal land plants or beyond. Polar tip growth is a commonly used mechanism in for example rhizoids and protonema, and some proteins have been found to localize at the tips (Honkanen & Dolan, 2016; Ito et al., 2014; Vidali et al., 2009; Vidali et al., 2010). Both structures consist of only a single filamentous cell file and as such have a relatively simple polarity. Three-dimensional plant tissues require integration of polarity from 3 dimensions. So far, information about polarly localized membrane proteins in more complex structures of basal plants is extremely limited. A recent study showed that PIN auxin transporters may localize polarly in the moss *Physcomitrella patens*, as they do in the flowering plant *Arabidopsis thaliana* (Bennett et al., 2014). Whether there are more polar membrane proteins in *Arabidopsis* that share their polarity with basal land plants remains to be investigated, and likewise, it remains to be seen if there are universal mechanisms for polar protein localization in land plants.

We previously identified a novel family of five polar proteins in *Arabidopsis* that does not localize to cell faces, but to the edges in various tissues (Chapter 3). Each of these SOSEKI (SOK) proteins has its own expression and localization pattern. SOK proteins integrate apico-basal and lateral information to guide their localization. They contain a region required for polar edge selection and a highly conserved N-terminal domain that mediates protein clustering. Homology modelling suggested that the latter domain is structurally related to a DIX domain. DIX domains have never been described in plants before, but in animals they are well studied. In animals,

DIX is found in several proteins in the Wnt signalling pathway - Dishevelled and Axin, (reviewed in Bienz, 2014). One branch of Wnt signalling regulates planar cell polarity, and in some cases involves polar localization of the Disheveled (Dvl) protein (Axelrod, 2001). The DIX domain acts as a protein-protein interaction domain that can form head-to-tail polymers (Schwarz-Romond et al., 2007). DIX polymerization is a dynamic process that depends on protein concentration (Schwarz-Romond et al., 2007). Ubiquitination of this domain can negatively affect the capacity of DIX to polymerize, and as such forms a mechanism to regulate polymer size and stability (Madrzak et al., 2015). Although the SOK DIX-LIKE domain is predicted to be structurally very similar to animal DIX (Chapter 3), there are no other sequence or structural similarities between SOK and animal proteins containing DIX.

SOKs form a unique family of plant proteins in *Arabidopsis*, but it is unknown whether their polarity and function is conserved in other land plants. Therefore, we assessed the evolutionary conservation of SOK sequence, structure and polarity. We found that SOK proteins first arose in early land plants. The edge localization found in *Arabidopsis* SOK is also present in a moss SOK, which suggests that edge localization may be an ancestral trait. We assessed the evolutionary trajectory of the DIX domain across eukaryotes and identified DIX-LIKE in all three major kingdoms. Not only DIX-LIKE structure is highly conserved, we also showed that DIX-LIKE can polymerize like animal DIX. Our work revealed that SOKs are an ancient family of land plant proteins and that the DIX protein polymerization module is used in different pathways in different branches of the evolutionary tree.

Results

5

SOKs originated in the common ancestor of all land plants

Arabidopsis thaliana contains five paralogs within the SOK family, that each have unique expression and polarity patterns. This fascinating family has not been described in any plant species before, yet the presence of 5 paralogs in *Arabidopsis* suggests that common ancestors may be present earlier in land plant evolution. We therefore asked when SOK originated and how it evolved.

To understand the evolution of SOKs, we used the OneKP (One Thousand Plants; Matasci et al., 2014; www.onekp.com) dataset. This dataset includes over 1300 RNAseq-based transcriptomes, with multiple transcriptomes from every major clade in red algae, green algae and land plants. We used a strategy that we developed earlier to reconstruct auxin response system evolution (Mutte & Kato et al., 2018). Briefly, we used all five *Arabidopsis* SOK protein sequences as well as the single SOK in the liverwort *Marchantia polymorpha* as query sequences to search against a BLAST database of individual transcriptome. Next, all scaffolds with BLAST hits

were extracted and translated to protein sequences using TransDecoder. The longest protein sequence for each scaffold, that also showed orthology with *A.thaliana* SOKs in a reciprocal BLAST was used for phylogenetic analysis in PhyML. Based on this phylogenetic analysis (Fig. 1; Fig. S1), we concluded that the SOK protein was not found in red algae or green algae. SOK first emerged in basal land plants: the bryophytes. We found that all bryophytes (liverworts, hornworts and mosses) and lycophytes had only one SOK in their ancestral state, while species-specific duplications have resulted in varied gene copy numbers in each species. As a result, all bryophyte SOK genes are co-orthologous to all *Arabidopsis* SOK genes. The first duplication in the SOK family that was retained in descendant species is observed in ferns. One daughter of this duplication event led to *Arabidopsis* SOK1, while the other further expanded in gymnosperms and angiosperms and gave rise to SOK2-5 in *Arabidopsis*.

Domain organization of SOK proteins

SOK proteins were previously annotated as “Domain of Unknown Function 966 proteins (DUF966)” and no further structural or functional information was available. We recently used deletion and domain-swap experiments to identify two functional domains within SOK1: a conserved N-terminal DIX-LIKE domain for polar edge protein clustering, and a non-conserved region involved in edge selection (Chapter 3). To provide a more complete annotation of all SOK proteins and identify putative functional domains, we further analyzed the domains and/or motifs present in this gene family. We used all land plant SOK protein sequences that were used for phylogenetic analysis, to identify conserved domains using the MEME motif finder (Bailey et al., 2009). Five domains were identified (Domain-I to -V; Fig. 1), however not all domains were identified in all the different sub-classes of SOK (Fig. 1; Fig. S1). Domain-I is the DIX-LIKE domain described previously. Domain-II is a DAxtqt motif, which strongly resembles the (D)KxTQT motif bound by Dynein Light Chain (DLC) in humans (Rapali et al., 2011). The human motif is variable, which suggests that the SOK Domain II could be a DLC-binding motif in plants. Domain-III includes a CG motif that is very highly conserved. This domain falls within the region that is required for polar membrane localization of SOK1 and 2 (Chapter 3). Cysteines can be palmitoylated: a post-translational modification that can attach proteins to the membrane and/or target them to specific membrane domains (reviewed in Hurst & Hemsley, 2015). Thus, the conserved CG site may be palmitoylated to aid SOK localization. We also identified a KEYFSGS motif of unknown function as Domain-IV, and Domain-V is a Zinc Finger-like (ZnF) domain.

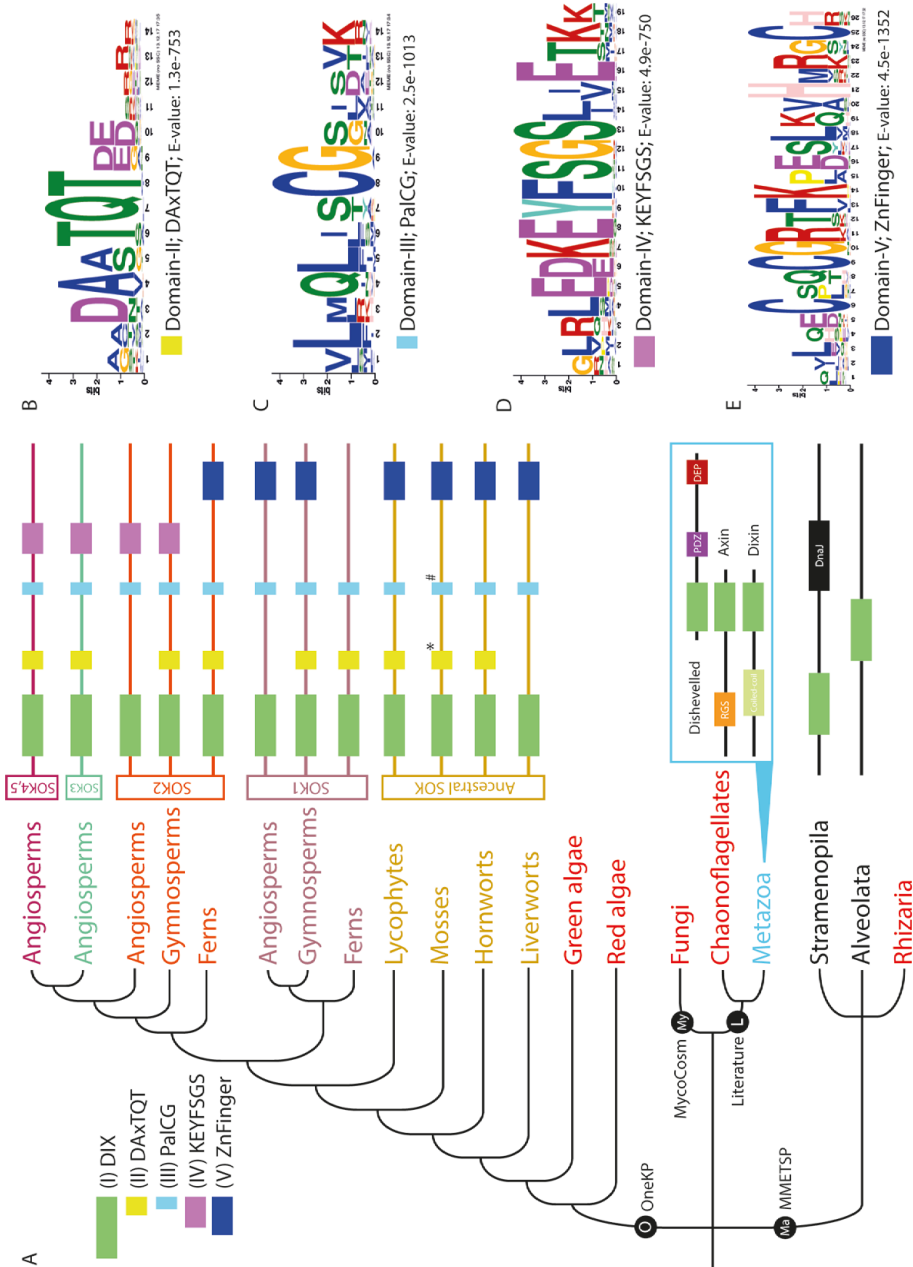


Figure 1. Phylogeny and motif distribution of SOKs: (A) Summary of phylogenetic distribution of SOK orthologs. Clades shown in red indicate the absence of SOK/DIX(-LIKE) domain. On the right, domain distribution is shown for the respective clades. * indicates the modification of Domain-II. # indicates the modification of Domain-III to CRG. (B-E) The amino acid profile of each conserved domain, represented along with the E-values from MEME suite.

Domain-I (DIX-LIKE) is not only common to all SOKs but is also the most highly conserved domain among the others. No other *Arabidopsis* proteins contain this domain, nor was it found outside the SOK family in land plants. Almost all land plant SOK proteins contain Domain-II as well. Bryophytes generally have Domain-I (DIX-LIKE), Domain-II (DAxTQT), Domain-III (PalCG) and Domain-V (Zn-Finger), which indicates that this probably was the configuration of the ancestral SOK gene. In Liverworts, Domain-II has been lost. Mosses do not have the canonical Domain-II and -III, but derivatives of these: The DLC-binding domain contains a SQT motif instead of TQT. As DLC can interact with variable motifs in humans (Rapali et al., 2011), the SQT motif might still be able to bind DLC. The PalCG site of Domain-III has been altered into CRG in mosses. Lycophytes have Domain-I (DIX-LIKE), Domain-II (DAxTQT) and Domain-III (PalCG). However, Domain-V (ZnF) is only observed in very few species.

The duplication in ferns that gave rise to *Arabidopsis* SOK1 contains Domains-I, -II, -III and -V, and thus resembles the ancestral SOK. Only ferns lack Domain-V in this clade, which could be the result of a fern-specific loss that probably happened after divergence from the ancestor of gymnosperms, as gymnosperms and angiosperms in the SOK1 clade do contain Domain-V. Surprisingly, in the other sub-clade that gave rise to *Arabidopsis* SOK2-5, ferns alone have Domain-V. In contrast, all gymnosperms and angiosperms lost this domain and gained Domain-IV, while still containing Domains -I to -III. The origin of domain -IV is unclear, as we did not find this domain in any other proteins in any plant species. Taken together, these results clearly indicate that SOK1 is retained as ancestral copy with the ‘original’ domains, while the SOK2-5 clade was modified in gymnosperms and angiosperms.

The conserved CG motif in SOK1 contributes to polar localization

The phylogenetic analysis revealed 5 conserved domains in SOK. Deletions in the SOK1 protein and domain swap between SOK1 and 2 had already shown that the DIX-LIKE (Domain I) was required for polar clustering of SOK. Furthermore, SOK1 mis-expression caused aberrant divisions and polar edge localization was necessary for inducing this division phenotype (Chapter 3). We re-analyzed the deletion and swap data in light of the more detailed phylogeny-based motif analysis.

Neither SOK1 nor SOK2 have Domain-II. However, they do have a conserved Domain-III (PalCG). This putative Palmitoylation site is located in what was identified as the domain responsible for polar edge selection (Chapter 3). Palmitoylation is a reversible process that can anchor a protein to the plasma membrane and target it to specific sub-domains of the membrane. Whether SOK is directly attached to the membrane or is sequestered there by other proteins is unknown. Therefore, we asked whether the CG site is necessary for polar localization of SOK. Mutation of G234

(Gly) to W (Trp) resulted in strongly reduced polarity of AtSOK1-YFP, although membrane association was not lost (Fig. S3A). The oblique division phenotype induced by SOK1 in RPS5A-misexpression lines was absent in lines misexpressing SOK1 G234W mutant protein. Thus, G234 is not required for membrane attachment per se, but is required for precise polar localization and for biological function as inferred from misexpression. Ancestral SOK proteins have a C2H2 ZnF-like domain (Domain-V) at their C-terminus, while the duplicated copy in angiosperms and gymnosperms instead contain Domain IV. Removal of domain V in SOK1 did not result in change of polar localization, nor in loss of the mis-expression phenotype (Chapter 3). Thus, the ZnF in SOK1 is not involved in polar localization or induction of oblique divisions. Domain swaps were not informative in studying the function of Domain-IV, as this domain was present in the same fragment as part of the polarity domain (Swap S1S2E, Chapter 3). As a result, this swap showed a mixture of SOK1 and SOK2 localization. Taken together, our analysis showed that the PalCG domain is necessary for polar localization and that the ZnF is not required for localization or induction of oblique divisions.

Edge localization is an ancient SOK protein property

One of the most striking features of the *Arabidopsis* SOK proteins is their robust polar edge localization. We inferred that the SOK protein originated in the common ancestor of the Bryophytes, but it is unknown whether SOKs are polar in these plants. To investigate this, we made use of a well-established Bryophyte model plant, the moss *Physcomitrella patens*. This moss diverged from the common ancestor of other land plants more than 400 million years ago and is a good model system for microscopy due to its thin tissues. It also has a highly efficient homologous recombination (HR) system, which allows direct fluorescent tagging of endogenous genes. A *Physcomitrella* colony starts from a spore or shred of tissue. From this initial, filamentous protonema grow in a radial pattern by apical tip growth and transverse divisions. Protonema are present in two forms: the chloronema with large chloroplasts and caulinema with few, poorly developed chloroplasts. As the colony matures, buds form on the protonema, which grow out into 3D structures that form gametophores (Fig. 2B, C). The gametophore consists of a meristem and leaf-like blades of one cell layer thickness. The moss can propagate by forming a sporophyte on top of the gametophore, or by tissue explants.

The *Physcomitrella* genome contains 8 full-length SOK proteins and 1 truncated version (Fig. 2A). These 9 *PpSOKs* evolved from a single ancestral gene by gene and genome duplication, and are thus co-orthologous to all *Arabidopsis* SOK genes. Using the *Physcomitrella patens* genome and sequencing data, we selected four *PpSOKs* of which we could predict the start and stop sites with most confidence: *PpSOKa-d*.

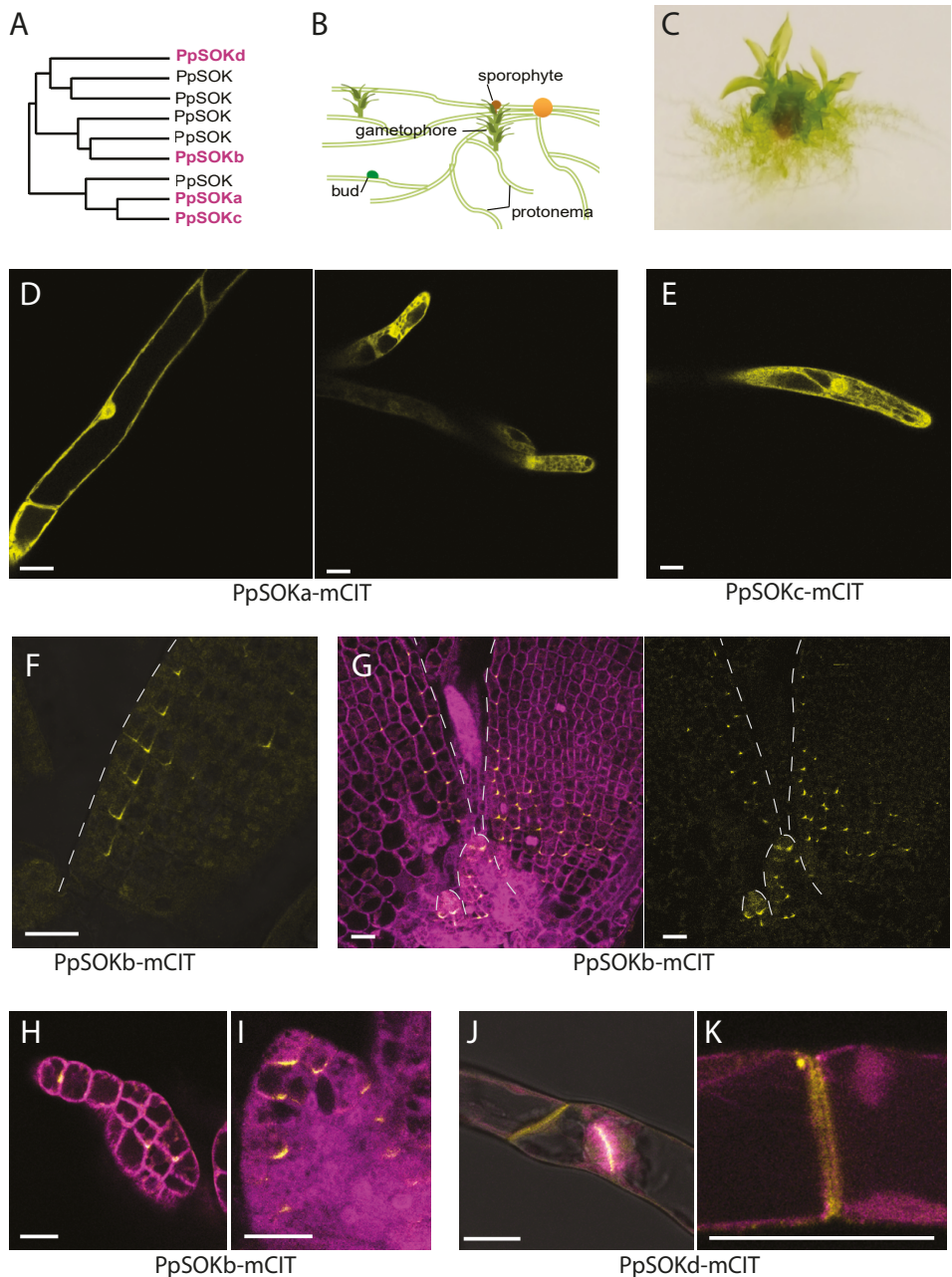


Figure 2. Localization of four PpSOKs. (A) Phylogeny of PpSOK. (B) Schematic representation of *Physcomitella patens*. (C) Picture of *Physcomitrella* grown on plate. No sporophytes are present on this plant. (D) Localization of PpSOKa in protonema. (E) Localization of PpSOKc in protonema. (F-I) Polar edge localization of PpSOKb in young leaf (F), two young leaves and two small initials (G), gametophore bud (H) and newly initiated leaf (I). (J-K) Localization of PpSOKd on the cell plate in protonema.

Next, we tagged these four genes at their C-terminus with mCITRINE (mCIT) by HR. Candidate transformants were screened for successful HR by genotyping the flank of the insert and *SOK* gene with PCR. Protonema and gametophore leaves of successful recombinants were then observed for mCIT fluorescence. Two full-length SOKs (PpSOKa; Pp3c14_23220 and PpSOKc; Pp3c17_23930) were present in the single-cell-file protonema and localize to the cytoplasm and nucleus (Fig. 2D, E). PpSOKd (Pp3c18_11140), which has a truncated C-terminus, localizes to the phragmoplast and both sides of recently formed cell plates in protonema (Fig. 2J, K). In contrast to the protonema SOKs, PpSOKb (Pp3c2_20380) was only present in the gametophore. the protein was already present in young protonema buds that were induced with BAP (Fig. 2H). In the gametophore, PpSOKb was found in the youngest leaves and localized in an edge towards the leaf base (Fig. 2F, G). In the tip cell of the most recently initiated leaf, the protein localized basally towards the longitudinal axis or towards one or both of its lower neighbours (Fig. 2I). It accumulated in the inner basal edge (relative to the central longitudinal leaf axis) in cells at the edge of the leaf blade. Slightly older leaves displayed patches of PpSOKb expression, often near the leaf base, with a clear inner basal edge polarity (Fig. 2F, G). These results show that one of the four PpSOK proteins localizes to a polar edge, like its *Arabidopsis* orthologs. This localization may have evolved independently in both species, or it could have been derived from a polar ancestor. In the latter case, PpSOK1, 3 and 4 might have lost the polarity, or the single cell files they are expressed in do not contain enough information for polar localization.

To study the biological function and activity of the ancestral SOK protein, we used *Marchantia polymorpha*. This liverwort contains only a single SOK gene, which represents the ancestral copy. *Marchantia* is a dioecious plant that grows as a thick, flat thallus anchored by rhizoids (Fig. 3A). It bifurcates during growth and produces umbrella-like gametophores for sexual reproduction. Asexual reproduction is possible thanks to the generation of gemmae, which are flat disc-like structures produced in gemma cups on the dorsal side of the thallus. They contain a meristem on each lateral side that can grow to form a new thallus when the gemma is placed on suitable medium. We first asked where the MpSOK gene was expressed in gemmae. We used 3.8kb upstream of the start codon of MpSOK as promoter and fused this promoter with nuclear TdTOMATO (nTdTOM). Expression of the promoter was present both in the meristems and in the rest of the thallus (Fig. 3B).

Over-expression of MpSOK causes morphological defects

We next asked whether MpSOK controls development by misexpression of MpSOK using the *EF1* promoter. The *EF1* promoter is most strongly expressed in the meristems and expressing MpSOK from *pEF1* led to morphological defects in gemmae, such

as extra lobes and meristem-like invaginations (Fig. 3C, D). The severity of this phenotype varied per line, from near-WT to strongly deformed. After 10 days of growth, the plants of severely affected lines curled down into the agar, while WT continued to grow flat and slightly upwards (Fig. 3E). While it remains to be seen if the cellular basis of this phenotype is similar to the defect in *Arabidopsis* plants misexpressing AtSOK1, it is clear that in both species, the proteins have the capacity to deregulate normal development.

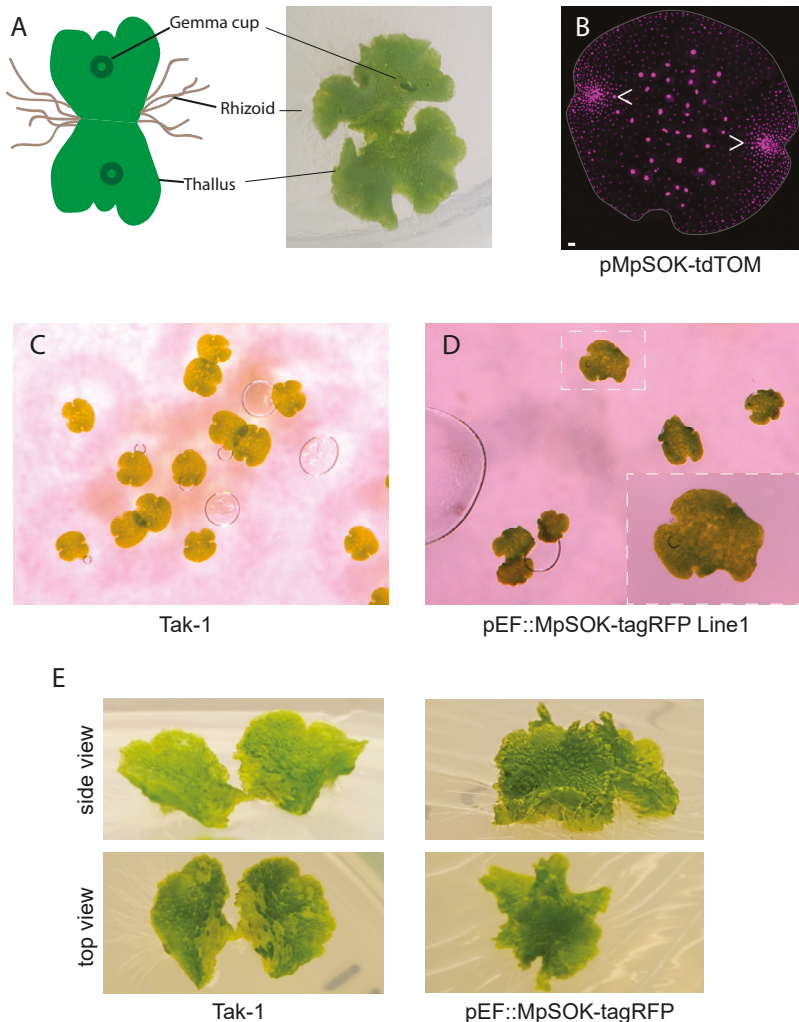


Figure 3. SOK in *Marchantia polymorpha*. (A) Schematic representation and picture of thallus. (B) pMpSOK-TdTOM expression in gemma. White arrows indicate the meristems. (C) WT gemmae. (D) gemmae of a MpSOK over-expression line with a more severe phenotype, to illustrate the morphological defects. (E) young thallus of WT and MpSOK over-expression line 1.

Deep evolutionary origin of the DIX domain

Our phylogenetic analysis shows that the DIX-LIKE domain is the most highly conserved domain in plant SOK proteins. The DIX domain was originally described in animals, where it is involved in protein clustering in Wnt signalling. In plants, it is essential for polar edge clustering of SOK proteins. This is a striking resemblance in DIX domain function, despite their presence in completely different proteins and species. In addition, the predicted structure of plant DIX-LIKE is very similar to DIX (Chapter 3), while the amino acid sequence shows variation (Fig. 4). Therefore, we asked whether the DIX(-LIKE) domain in plants and animals have a common ancestor, and where these domains first arose in evolution.

To answer this question, we searched for DIX-LIKE domains in all the major kingdoms in Eukaryotes. Beyond the previously discovered DIX(-LIKE) domains in Metazoa and Viridiplantae, we discovered DIX(-LIKE) domains in the SAR (Straminopila, Alveolata and Rhizaria) group of basal Eukaryotes. Interestingly, not all the species/classes of the SAR group have DIX-LIKE proteins. Using the Marine Microbial Eukaryotic Transcriptome Sequencing Project (MMETSP) data (Keeling et al., 2014), we found that among the Straminopila, only Labrynthulomycetes, Phaeophytes and Dictyophytes have a DIX-LIKE domain. Among the Alveolata, only Dinoflagellates contain DIX-LIKE. None of species of Rhizaria were found to have the domain, which could also be attributed to the fact that limited data was available. In the Ophisthokonta group, Fungi seem to lack DIX-LIKE, while the Metazoans contain the DIX domain. Among the Streptophytes, green algae do not have DIX-LIKE while land plants do. We compared the protein sequences of DIX(-LIKE) domains within these groups, and it is evident that the secondary structural elements are conserved but most amino acids are not completely conserved (Fig. 4).

The DIX domain contains a ubiquitin-like fold. A similar fold is found in the Phox and Bem1 (PB1) domain, which is structurally similar to the DIX domain. Similar to DIX, PB1 is also capable of forming head-to-tail interactions (reviewed in Bienz, 2014). Given this resemblance, we tested whether the sequences that we considered for phylogeny are indeed DIX-like domains rather than PB1. To this end, we took several species of animals and plants that contained a PB1 domain, and several species from animals, plants and SAR that had a DIX(-LIKE) domain. A phylogenetic tree of both domains clearly showed that PB1 and DIX form completely separate groups (Fig. S2). Thus, PB1 and DIX are distinct domains and our phylogenetic analysis of DIX(-LIKE) only contained DIX and not PB1. Taken together, these results show that the DIX(-LIKE) domain is clearly distinguishable from the very similar PB1 in our phylogenetic analysis. Additionally, the phylogeny showed an independent monophyletic origin of DIX in Viridiplantae, Metazoa and SAR.

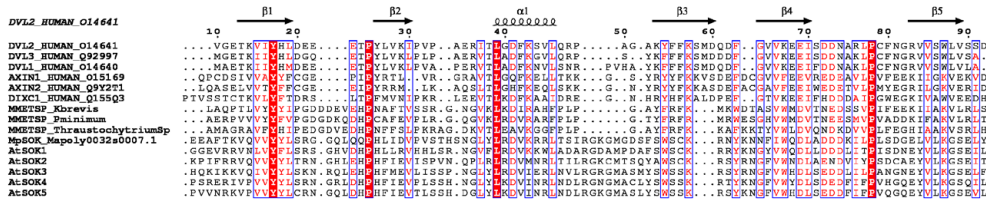


Figure 4. Alignment of DIX(-LIKE) domains from Human, SAR group and land plants. Secondary structures on the top are based on the crystal structure of Human DVL2. Alignment is numbered corresponding to AtSOK1. Kbrevis, Karenia brevis; Pminimum, *Prorocentrum minimum* belongs to Dinoflagellata (Alveolates) and *Thraustochytrium* belongs to Labrynthulomycetes (Stramenopiles). MpSOK, *Marchantia polymorpha*; AtSOK, *Arabidopsis thaliana*.

DIX domain polymerization is conserved in plants and SAR

The DIX(-LIKE) domain is present in three highly diverse groups, yet both in animals and plants it is involved in clustering of proteins (Chapter 3, reviewed in Bienz, 2014). The animal DIX domain is capable of oligomerizing head-to-tail in a concentration-dependent manner (Schwarz-Romond et al., 2007). FRET-FLIM and BiFC studies showed that *Arabidopsis* DIX-LIKE can dimerize (Chapter 3). However, the exact mechanism of DIX-LIKE interaction is not yet known, nor is it clear if higher-order complexes can be formed. To investigate whether plant DIX-LIKE can only dimerize or also form larger polymers like their animal counterparts, we purified the DIX-LIKE domains of *Arabidopsis* SOK1-4, *Physcomitrella* SOKb and the *Marchantia* SOK protein. *In vitro* gel-filtration experiments showed that all tested plant DIX-LIKE can indeed form higher order polymers (Fig. 5A,B; Fig. S4). AtSOK1 DIX-LIKE formed a complex up to about 292 kDa, which corresponds to a polymer of 12 subunits. An additional small peak was present with the size of a monomer. The majority AtSOK3 protein eluted very closely to the void volume, which indicates that it might have been misfolded and aggregated. However, it showed the typical right-tailed slope of a polymer and dilution of the sample lead to movement of part of the peak to smaller sizes (not shown). This could either mean that there were very large polymers present in the original sample, or that dilution allowed misfolded proteins to refold properly. A second, smaller peak of AtSOK3 was present around the size of a 137 kDa 6-mer, and two more at the size of a dimer and monomer. AtSOK4 polymerized to a complex of up to 418 kDa, which is about an 18-mer, and a small fraction of the sample contained dimers or monomers. The *Marchantia* and *Physcomitrella* DIX-LIKEs also polymerized well. *Marchantia* DIX-LIKE formed complexes up to 827 kDa, which is about 36 subunits. A sub-fraction contained monomers. *Physcomitrella* polymerized up to a 21-mer of 491 kDa.

Some species in the SAR group have DIX-LIKE-domain containing proteins, but the function and localization of these proteins is unknown. As both plant and animal DIX polymerize, we asked whether this trait was shared with the SAR group as well. We tested the DIX-LIKE domains of *Ectocarpus siliculosus* (a Brown Alga), *Cryptosporidium parvum* (an Apicomplexan) and *Paramecium tetraurelia* (a Ciliate). All three showed polymer formation of very similar size: approximately 10-mer for *E.S.*, 11-mer for *C.p.* and 8-mer for *P.t.* (Fig. 5). Unlike the plant and animal versions, *Cryptosporidium* and *Paramecium* measurements lacked the right-tailed slope. This suggests that DIX-LIKEs of these two species have less variability in their polymer size. *Ectocarpus* showed more of a tailed slope and thus a greater tendency to form polymers of varying size. Taken together, these results show that not only the (predicted) structure, but also polymerization is shared between DIX and DIX-LIKE across the three kingdoms.

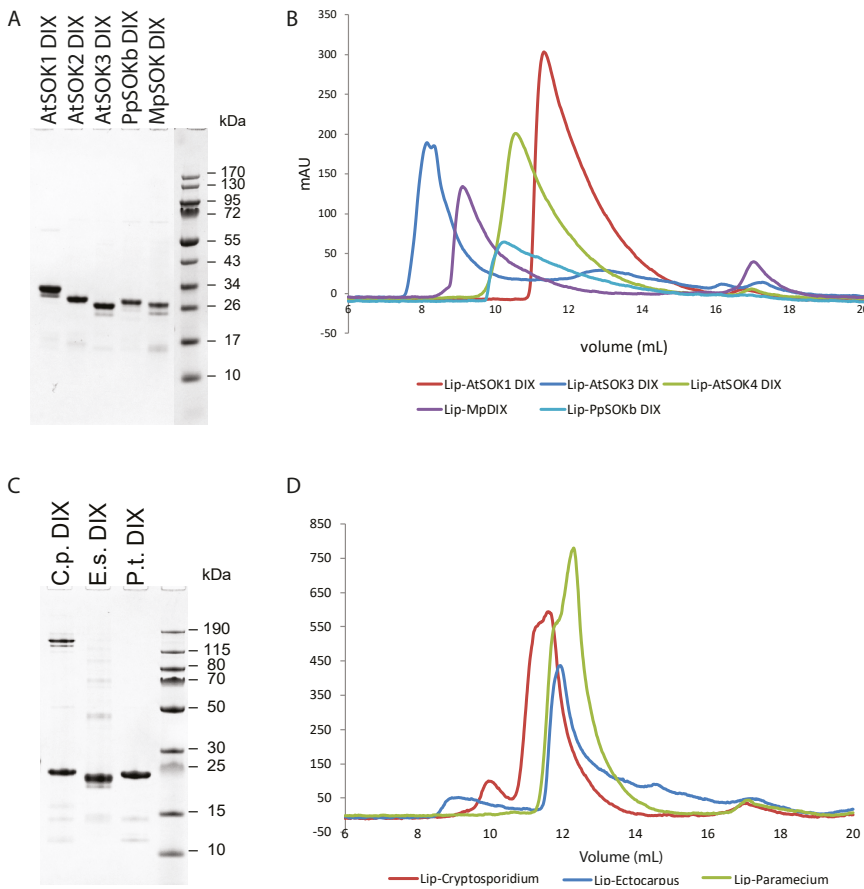


Figure 5. *In vitro* polymerization of DIX-LIKE. (A) Purification of plant DIX domains. (B) Filtration spectra of the plant DIX-LIKE domains. (C) Purification of SAR DIX-LIKE. (D) Filtration spectra of SAR DIX-LIKE.

Discussion

The evolution of SOK proteins

Polarity is essential for plant morphogenesis and survival. In this study, we investigated the evolutionary conservation of the polar SOK proteins found in *Arabidopsis*. We used data from the 1KP project to identify SOK protein sequences and discovered that SOK first arose in the ancestor of land plants. This suggests that it might have been important for the transition from simple aquatic organisms to more complex land dwellers. Up to the Lycophytes, there was a single ancestral copy of SOK. The ancestral SOK duplicated in ferns, and one of the branches further duplicated in the ancestor of Gymnosperms and Angiosperms. Strikingly, the branch that gave rise to AtSOK1 did not give rise to duplications. We identified five domains in SOK: Domain-I (DIX-LIKE), Domain-II (DAxTQT), Domain-III (PalCG), Domain-IV (KEYFSGS) and Domain-V (ZnFinger). The ancestral SOK probably contained Domain-I to -IV. Later in evolution, a new type of SOK arose where Domain-IV was replaced with Domain-V. We could not find any plant gene that contained Domain-IV, until the domain appeared in Euphyllophytes, and its origin is thus an open question.

Almost all land plants contain at least one ancestral type SOK, which suggests the strong selection pressure on this type. An exception to this rule are the Lycophytes, where only few species contain domain-IV. It would therefore be informative to investigate whether SOK has a different function in Lycophytes without Domain-IV. Gymnosperms and Angiosperms have at least one ancestral type and one duplication copy, indicating that Domain-IV and-V have unique and important functions in these clades. However, further studies are needed to elucidate the functions of these novel protein domains.

Domain-II is a putative binding site for DLC, and binding of DLC next to a dimerization domain is thought to stabilize protein dimers in humans (Rapali et al., 2011). Domain-II was not identified in Liverworts and the SOK1 and 2 clades in Angiosperms. This suggests that Domain-II, and thus potential binding of DLC is not essential for function of all SOKs. Domain-III is present in all plant groups, with a small modification in mosses. The motif is located in a region that we previously identified as important for membrane attachment and polar edge selection in *Arabidopsis* (Chapter 3). The CG site is potentially Palmitoylated. Palmitoyl chains can anchor a protein in the membrane. In addition, it can cause proteins to be localized to specific lipid rafts on the membrane. As Palmitoylation is reversible, membrane localization of Palmitoylated proteins can be highly dynamic (reviewed in Hurst & Hemsley, 2015). Mutation of G into W in the PalCG site resulted in reduction, but not complete loss of SOK1 polarity. Thus, this amino acid is important for polar localization, but not for membrane attachment. Palmitoylation modifies

cysteines and mutation of the C in the PalCG should reveal whether it is essential for polar localization. Taken together, SOKs contain highly conserved domains, but their exact function remains elusive. Thus, a detailed study of the SOK domains in diverse plant species would provide a new avenue into understanding SOK function and localization throughout evolution.

The most highly conserved domain in SOKs is Domain-I (DIX-LIKE). As both Viridiplantae and Metazoa contain a DIX(-LIKE) domain, we investigated whether these have a common ancestor. Aside the aforementioned groups, we also identified DIX-LIKE domains in some species of the SAR group. Our data suggest that there is a strong selection pressure in multicellular lineages (Viridiplantae and Metazoa) to keep the DIX-LIKE domain-containing proteins. In the SAR group there appears to be less selective pressure on DIX-like, as only few sub-classes contain DIX-LIKE domain containing proteins. DIX-LIKE domains are present in Viridiplantae and Metazoa, but not in other ancestral lineages of multicellular organisms, such as Fungi and Charophytes. Thus, retention of a DIX-LIKE domain is not absolutely required for a multicellular lifestyle.

In animals, DIX acts as a head-to-tail polymerization domain (Schwarz-Romond et al., 2007) and here we showed that land plant DIX-LIKE can polymerize as well. Already in early land plants such as *Marchantia* and *Physcomitrella*, DIX-LIKE has strong clustering capabilities. DIX-LIKE was capable of polymerizing without the presence of DLC or Domain II. This shows neither are essential for polymerization, but rather might have a regulatory or stabilizing role. Interestingly, the liverwort *Marchantia* shows the largest DIX-like polymers compared to the other tested plant DIX, followed by the moss *Physcomitrella*, while *Arabidopsis* DIX-LIKEs form relatively the smallest complexes. These findings suggest that there may be a decrease in polymerization capability over evolutionary time. Two of the tested SAR species, and the third to a lesser extent, showed a strong tendency to form DIX-LIKE polymers of a specific size, while polymer sizes of plant and animal DIX(-LIKE) were more variable. DIX-LIKE of a *Tetrahymena* species shows similar behaviour (Marc Fiedler, personal communication, not shown). Thus, having a strong optimum in polymer size may be a trait commonly found in the SAR group. A study of more DIX-LIKE domains in other species will show whether the behaviour reported here applies to plants and SAR in general. Detailed analysis of DIX-LIKE structures will provide insights into the biochemical basis of polymer variation.

Given that the DIX(-LIKE) domains are present in all three major lineages of Eukaryotes and show similar polymerization behaviour, it is plausible to infer that this domain evolved from a common Eukaryotic ancestor. The domain could also have been passed from one lineage to another by horizontal gene transfer. However, phylogenetic analysis showed that Metazoa, Viridiplantae and SAR DIX(-LIKE) are

in clearly distinct clades. In addition, the emergence times and rates of evolution of these clades are very different. Therefore, we have no evidence that would support horizontal gene transfer. Convergent evolution could also have led to presence of a DIX(-LIKE) domain in three clades, yet we did not find convincing evidence supporting this theory.

Despite having very similar behaviour in SAR, plants and animals, the context of the DIX-domain is completely different. Aside from the DIX domain, there are no other similarities in protein domain architecture. The domain must act in different pathways in the different lineages, as no components of the Wnt signalling pathway are present in plants. Yet, in both animal and plant lineages DIX(-LIKE) domains can operate in a polarity system. The autocatalytic, self-reinforcing property of oligomerization might be useful to achieve high local concentrations of proteins. Such local accumulations may in turn be advantageous in a signalling and polarity context. Perhaps this is the reason why it has been retained in Metozoa, Viridiplantae and SAR.

SOK polarity and function in basal plants

The SOK protein sequence and DIX-LIKE polymerization capability are highly conserved amongst land plants. As one of the most striking features of SOKs in *Arabidopsis* is polar localization, we investigated whether this polarity was already present in basal land plants. The moss *Physcomitrella patens* has 10 SOK orthologs, of which we selected 4 for localization studies. Three of the SOKs were expressed in the filamentous protonema. PpSOKa and -c localized in the cytoplasm and nucleus, while PpSOKd accumulated at the cell plate. PpSOKd is a truncated SOK that lacks the Domain-II to -IV, and whether it is a functional protein is unknown. PpSOKb was expressed in the gametophore, usually at the base of the leaf. Here, the protein showed a distinct basal edge localization.

All four tested PpSOKs lacked Domain-II and -III, yet PpSOKb is edge localized. This shows that presence of the complete domains II and III are not essential for SOK polar localization, at least in *Physcomitrella*. While the tested PpSOK proteins don't contain the putative palmitoylation site CG, PpSOKb has the amino acids CRK and PpSOKd has CTA in the region where SOK proteins of other plants have CG. PpSOKa and c do not contain any Cysteine in that area and localize to the cytoplasm. If CG is a palmitoylation site, perhaps the Cysteines in the PpSOKb and d motifs can be palmitoylated as well, as PpSOKc and d localize to the membrane/cell plate.

PpSOKb faces towards the central axis of the leaf and is always basal. These findings suggest that PpSOKb may use radial and apico-basal information to direct its edge polarity, like AtSOK1. The fact that *Physcomitrella* contains at least one polar SOK

suggests several possible scenarios: polarity could have evolved independently in both *Arabidopsis* and *Physcomitrella*, or this polarity was already present in the ancestral SOK, but got lost in PpSOKa and -c. Alternatively, PpSOKa and -c may still be capable of polar localization, but the filamentous protonema may lack the necessary spatial/mechanical cues.

Polar SOK accumulation is the result of DIX-LIKE polymerization. In animals, DIX(-LIKE) containing proteins accumulate in puncta (Schwarz-Romond et al., 2007). Study of SOK in various plant species may reveal whether polar localization and puncta formation was present throughout evolution. The liverwort *Marchantia polymorpha* is a promising candidate for such a study, as this basal plant only has one SOK. Our promoter fusion showed that MpSOK is expressed throughout gemmae. Analysis of growing thallus, rhizoids and sexual organs is necessary to identify additional sites of MpSOK action. Over-expression of MpSOK in the meristematic zones resulted in gemma shape phenotypes. These phenotypes could be caused by cell division and/or expansion defects, similar to AtSOK1 over-expression. However, no fluorescent signal was observed, and further analysis is required to ensure that at least the full MpSOK protein is produced. In addition, mutagenesis of the single MpSOK gene is a promising avenue into understanding more about SOK function in basal land plants.

In this work, we showed that SOK is an ancient land plant specific family that shows polar localization in both *Arabidopsis* and a moss. We provide a comprehensive annotation for the conserved domains of SOK. Additionally, we show that DIX domain polymerization must be a useful module that is conserved in three major clades of Eukaryotes.

5

Material and Methods

Plant material and growth conditions

Arabidopsis was grown and transformed as described in Chapter 3. *Physcomitrella patens* plants were grown on BCDT medium under continuous light until transformation. PpSOK constructs were linearized and introduced into a pEF1::mCherry-tubulin (Kosetsu et al., 2017) containing *Physcomitrella* line by PEG-mediated protoplast transformation, as described in Yamada et al., 2016. Transformants were selected on BCDT supplemented with Kanamycin and genotyped for successful homologous recombination using primers described in Supplemental Table 2. After selection of the transformants, the plants were grown under long-day conditions as described above. Plants were propagated by cutting up a piece of the colony with a razor blade and plating the fragments on fresh BCD or BCDT plates. For imaging, plants were grown on BCD medium.

Marchantia polymorpha Tak-1 was used as WT in this study. Plants were grown on half strength B5 medium, supplemented with 100mg/L cefotaxim and 10mg/L Hygromycin B for selection of transformants if necessary. The plants were grown in continuous light conditions, as described in (Kato et al., 2015). Plant transformation was performed as described in (Kubota et al., 2013). Plants were propagated by plating gemma of the parental plant on fresh ½B5 medium. If a plant did not produce gemma, small pieces of thallus were broken off the parental plant and placed on fresh medium.

Generation of plasmids

Primers used in this study are described in Supplemental Table 2.

Arabidopsis G233W

SOK1 was amplified from a SOK1 cDNA plasmid in two halves, with primers containing the G233W mutation. Both fragments were stitched together with fusion PCR and cloned into pRPS5a::LIC (pPLV28).

Physcomitrella plasmids

Four *PpSOK* genes were selected based on the confidence of the genome assembly and annotation. This analysis was based on *P. patens* genome V6.

Physcomitrella can be transformed by homologous recombination. To target mCITRINE to the C-terminus of the endogenous SOK genes, ~1kb of the genomic region before the stop codon and ~1kb after the stop codon was amplified with restriction sites and cloned into the pCTRN-nptII vector (Hiwatashi et al., 2014) by ligation. The left flank was cloned with restriction sites KpnI and Xho for left *PpSOKa*, ApaI and ClaI for *PpSOKb*, ApaI and HindIII for *PpSOKc* and KpnI and XhoI for *PpSOKd*. SmaI and NotI were used to clone all right flanks.

Marchantia Cellular markers

The genomic region of the promoter (3.8 kb) or promoter plus gene was amplified by PCR and cloned into a pENTR/D-TOPO plasmid by TOPO reaction (Invitrogen). To create the final vectors, a LR reaction (Invitrogen) was performed to clone the insert into pMpGWB116 (for pMpSOK::nTdTOM), pMpGWB106 (for p35S::MpSOK-Citrine), pMpGWB108 (for pEF::MpSOK-Citrine), or pMpGWB127 (for pEF::Mp-TagRFP).

In vitro expression

DIX domain sequences were amplified from cDNA and cloned into a pLipK vector.

Microscopy

Marchantia gemma and young thalli were observed with a Leica epifluorescence microscope. If the plants were too big for this microscope, pictures were taken with a Samsung A3 or Galaxy S6 smartphone camera.

Confocal images were taken on a Leica SP5 or SP8 confocal microscope. The SP5 was equipped with an Argon laser and DSS561 diode laser, the SP8 with a pulsed white light laser. YFP was excited at 514nm and TagRFP, TdTOMATO and mCherry at 561nm. Crystal filters were set at 520-550nm for YFP and 570-630 nm for mCherry, TdTOMATO and TagRFP.

Data for phylogenomic study

CDS and protein sequences encoding all the orthologous genes in SOK gene family from *Marchantia polymorpha*, *Physcomitrella patens*, *Amborella trichopoda*, *Oryza sativa*, *Zea mays*, *Solanum lycopersicum* and *Arabidopsis thaliana* were obtained from Phytozome ver11 (phytozome.jgi.doe.gov/pz/portal.html). Various DIX domain containing proteins from *H. sapiens*, *M. musculus*, *C. elegans*, *D. rerio* etc. were obtained from UniProt database (www.uniprot.org; Sup. Table1 with ID's used). tBLASTn module at JGI MycoCosm (<https://genome.jgi.doe.gov/fungi>) was used to search for DIX-domain containing proteins in Fungi using both plant (*A. thaliana*) and animal (*H. sapiens*) DIX domains as query sequences. Data access to 1000 plant transcriptomes was provided by the OneKP consortium (www.onekp.com; Matasci et al., 2014). To understand the presence and evolution of SOKs in SAR group, Marine Microbial Eukaryotic Transcriptome Sequencing Project (MMETSP) data (Keeling et al., 2014) was used and a similar analysis procedure was followed as for OneKP data.

Phylogenetic analysis

BLAST database for all species from both the transcriptome datasets (OneKP and MMETSP) were generated using 'makeblastdb' module in BLAST + v2.2.28 (Camacho et al., 2009). Protein sequences from *A. thaliana*, *M. polymorpha* and *P. patens* were used to query each database independently for each gene family using tBLASTn. All the scaffolds with the BLAST hits were extracted from the respective transcriptomes and further translated using TransDecoder (ver2.0.1; <http://transdecoder.github.io>). This provided the CDS and protein sequences of all the scaffolds of the BLAST hits to any of the query sequences. The protein sequences were run through the InterProScan database (ver5.19-58.0; <http://www.ebi.ac.uk/interpro/>) to look for conserved domains. Filtered sequences were further confirmed by BLASTx

search against *A. thaliana* proteome to confirm orthologous relationship. MAFFT (ver7.123b; Katoh & Standley, 2013) iterative refinement algorithm (E-INS-i) was used to align the protein sequences. Alignment positions with more than 70% gaps were removed using the Phyutility program (ver2.2.6; Smith & Dunn, 2008) before the phylogeny construction. PartitionFinder (ver2.1.1; Lanfear et al., 2017) was used to identify the most suitable evolutionary model using the trimmed alignments on all the domains. Maximum likelihood algorithm implemented in PhyML (ver3.1; Guindon et al., 2010) with Jones-Taylor-Thornton (JTT) model of evolution with 100 bootstraps was used for the phylogenetic analysis. Obtained trees were visualized using the iTOL (ver4; <http://itol.embl.de/>) phylogeny visualization program. Phylogenetic trees were cleaned up manually for misplaced sequences as well as for clades with long branch attraction.

Domain/motif identification in SOKs

Protein sequences of all the transcripts that were used in the phylogenetic tree construction were also used for domain finding in MEME motif discovery program with default settings and additional parameters “-mod zoops -nmotifs 15 -minw 10”(ver 4.12.0; Bailey et al., 2009). Among the 15 motifs identified, four motifs were spanned over a stretch of first 100 N-terminal residues, which all together taken as DIX-LIKE domain. Motifs that were specific to a certain clade or motifs that did not show specificity in certain amino acids were discarded for further analysis. In total apart from DIX domain, four other conserved domains were identified and represented as domains-II to -V.

Protein purification and size exclusion analysis

Plant DIX domains were expressed with an N-terminal 6xHisLipoyl-tag (followed by a TEV cleavage site) in *E. coli* BL21-CodonPlus(DE3)-pRARE2 cells. Cells were grown at 37 °C in LB to OD₆₀₀ of 0.8, and the temperature was dropped to 24 °C before isopropyl-β-D-thiogalactoside induction for overnight. Cells were pelleted, resuspended in 25 mM Tris (pH 8), 200 mM NaCl, 10 mM imidazole supplemented by one complete EDTA-free protease inhibitor cocktail tablet (Roche), lysed by passing twice through an EmulsiFlex-C5 (Avestin) and spun down at 50,000g for 30 min. The supernatant was incubated with Ni-NTA Sepharose resin (Qiagen) followed by multiple washes and imidazole elution. The eluted 6xHisLip-tagged DIX domains were diluted to 5 mg/ml and 100 µl was injected onto the gel filtration column (Superdex 200 Increase 10/300 GL; GE Healthcare) using PBS as running buffer. Protein size estimations were calculated based on the Gel Filtration Standard (Bio-Rad) with molecular weights of 670, 158, 44, 17 and 1.4 kDa.

Acknowledgements

The authors would like to thank Hirotaka Kato for introducing them to *Marchantia polymorpha* and for his advice on cultivation and analysis of the liverwort. Thanks also to J.W. Borst for his assistance with the confocal microscope. We would also like to express our appreciation to the 1KP consortium for providing the transcriptome data.

References

Axelrod, J. D. (2001). Unipolar membrane association of Dishevelled mediates Frizzled planar cell polarity signaling, 1182–1187.

Bailey, T. L., Boden, M., Buske, F. A., Frith, M., Grant, C. E., Clementi, L. et al. (2009). MEME Suite: Tools for motif discovery and searching. *Nucleic Acids Research*, 37, 202–208.

Bennett, T. A., Liu, M. M., Aoyama, T., Bierfreund, N. M., Braun, M., Coudert, Y. et al. (2014). Plasma membrane-targeted PIN proteins drive shoot development in a moss. *Current Biology*, 24, 2776–2785.

Bienz, M. (2014). Signalosome assembly by domains undergoing dynamic head-to-tail polymerization. *Trends in Biochemical Sciences*, 39, 487–495.

Camacho, C., Coulouris, G., Avagyan, V., Ma, N., Papadopoulos, J., Bealer, K., & Madden, T. L. (2009). BLAST+: Architecture and applications. *BMC Bioinformatics*, 10, 1–9.

Dong, J., MacAlister, C. A., & Bergmann, D. C. (2009). BASL Controls Asymmetric Cell Division in Arabidopsis. *Cell*, 137, 1320–1330.

Fu, Y., Li, H., & Yang, Z. (2002). The ROP2 GTPase Controls the Formation of Cortical Fine F-Actin and the Early Phase of Directional Cell Expansion during Arabidopsis Organogenesis. *The Plant Cell*, 14, 777–794.

Guindon, S., Dufayard, J.-F., Lefort, V., Anisimova, M., Hordijk, W., & Gascuel, O. (2010). New Algorithms and Methods to Estimate Maximum-Likelihood Phylogenies: Assessing the Performance of PhyML 2.0. *Systematic Biology*, 59, 307–321.

Hiwatashi, Y., Sato, Y., & Doonan, J. H. (2014). Kinesins Have a Dual Function in Organizing Microtubules during Both Tip Growth and Cytokinesis in *Physcomitrella patens*. *The Plant Cell*, 26, 1256–1266.

Honkanen, S., & Dolan, L. (2016). Growth regulation in tip-growing cells that develop on the epidermis. *Current Opinion in Plant Biology*, 34, 77–83.

Hurst, C. H., & Hemsley, P. A. (2015). Current perspective on protein S-acylation in plants: More than just a fatty anchor? *Journal of Experimental Botany*, 66, 1599–1606.

Ito, K., Ren, J., & Fujita, T. (2014). Conserved function of Rho-related Rop/RAC GTPase signaling in regulation of cell polarity in *Physcomitrella patens*. *Gene*, 544, 241–247.

Jones, M. A. (2002). The Arabidopsis Rop2 GTPase Is a Positive Regulator of Both Root Hair Initiation and Tip Growth. *The Plant Cell Online*, 14, 763–776.

Kato, H., Ishizaki, K., Kouno, M., Shirakawa, M., Bowman, J. L., Nishihama, R., & Kohchi, T. (2015). Auxin-Mediated Transcriptional System with a Minimal Set of Components Is Critical for Morphogenesis through the Life Cycle in *Marchantia polymorpha*. *PLoS Genetics*, 11, 1–26.

Katoh, K., & Standley, D. M. (2013). MAFFT multiple sequence alignment software version 7: Improvements in performance and usability. *Molecular Biology and Evolution*, 30, 772–780.

Keeling, P. J., Burki, F., Wilcox, H. M., Allam, B., Allen, E. E., Amaral-Zettler, L. A. et al. (2014). The Marine Microbial Eukaryote Transcriptome Sequencing Project (MMETSP): Illuminating the Functional Diversity of Eukaryotic Life in the Oceans through Transcriptome Sequencing. *PLoS Biology*, 12, e1001889.

Kosetsu, K., Murata, T., Yamada, M., Nishina, M., Boruc, J., Hasebe, M. et al. (2017). Cytoplasmic MTOCs control spindle orientation for asymmetric cell division in plants. *Proceedings of the National Academy of Sciences*, 114(, E8847–E8854.

Kubota, A., Ishizaki, K., Hosaka, M., & Kohchi, T. (2013). Efficient Agrobacterium -Mediated Transformation of the Liverwort *Marchantia polymorpha* Using Regenerating Thalli. *Bioscience, Biotechnology, and Biochemistry*, 77, 167–172.

Lanfear, R., Frandsen, P. B., Wright, A. M., Senfeld, T., & Calcott, B. (2017). Partitionfinder 2: New methods for selecting partitioned models of evolution for molecular and morphological phylogenetic analyses. *Molecular Biology and Evolution*, 34, 772–773.

Li, H., Lin, D., Dhonukshe, P., Nagawa, S., Chen, D., Friml, J. et al. (2011). Phosphorylation switch modulates the interdigitated pattern of PIN1 localization and cell expansion in *Arabidopsis* leaf epidermis. *Cell Research*, 21, 970–978.

Madrzak, J., Fiedler, M., Johnson, C. M., Ewan, R., Knebel, A., Bienz, M., & Chin, J. W. (2015). Ubiquitination of the Dishevelled DIX domain blocks its head-to-tail polymerization. *Nature Communications*, 6, 1–11.

Matasci, N., Hung, L., Yan, Z., Carpenter, E. J., Wickett, N. J., Mirarab, S. et al. (2014). Data access for the 1 , 000 Plants (1KP) project. *Gigascience*, 3, 1–10.

Molendijk, A. J., Bischoff, F., Rajendrakumar, C. S. V., Friml, J., Braun, M., Gilroy, S., & Palme, K. (2001). *Arabidopsis thaliana* Rop GTPases are localized to tips of root hairs and control polar growth. *EMBO Journal*, 20, 2779–2788.

Nakamura, M., & Grebe, M. (2018). Outer, inner and planar polarity in the *Arabidopsis* root. *Current Opinion in Plant Biology*, 41, 46–53.

Rapali, P., Szenes, Á., Radnai, L., Bakos, A., Pál, G., & Nyitrai, L. (2011). DYNLL/LC8: A light chain subunit of the dynein motor complex and beyond. *FEBS Journal*, 278, 2980–2996.

Roppolo, D., De Rybel, B., Tendon, V. D., Pfister, A., Alassimone, J., Vermeer, J. E. M. et al. (2011). A novel protein family mediates Casparyan strip formation in the endodermis. *Nature*, 473, 381–384.

Schwarz-Romond, T., Fiedler, M., Shibata, N., Butler, P. J. G., Kikuchi, A., Higuchi, Y., & Bienz, M. (2007). The DIX domain of Dishevelled confers Wnt signaling by dynamic polymerization. *Nature Structural and Molecular Biology*, 14, 484–492.

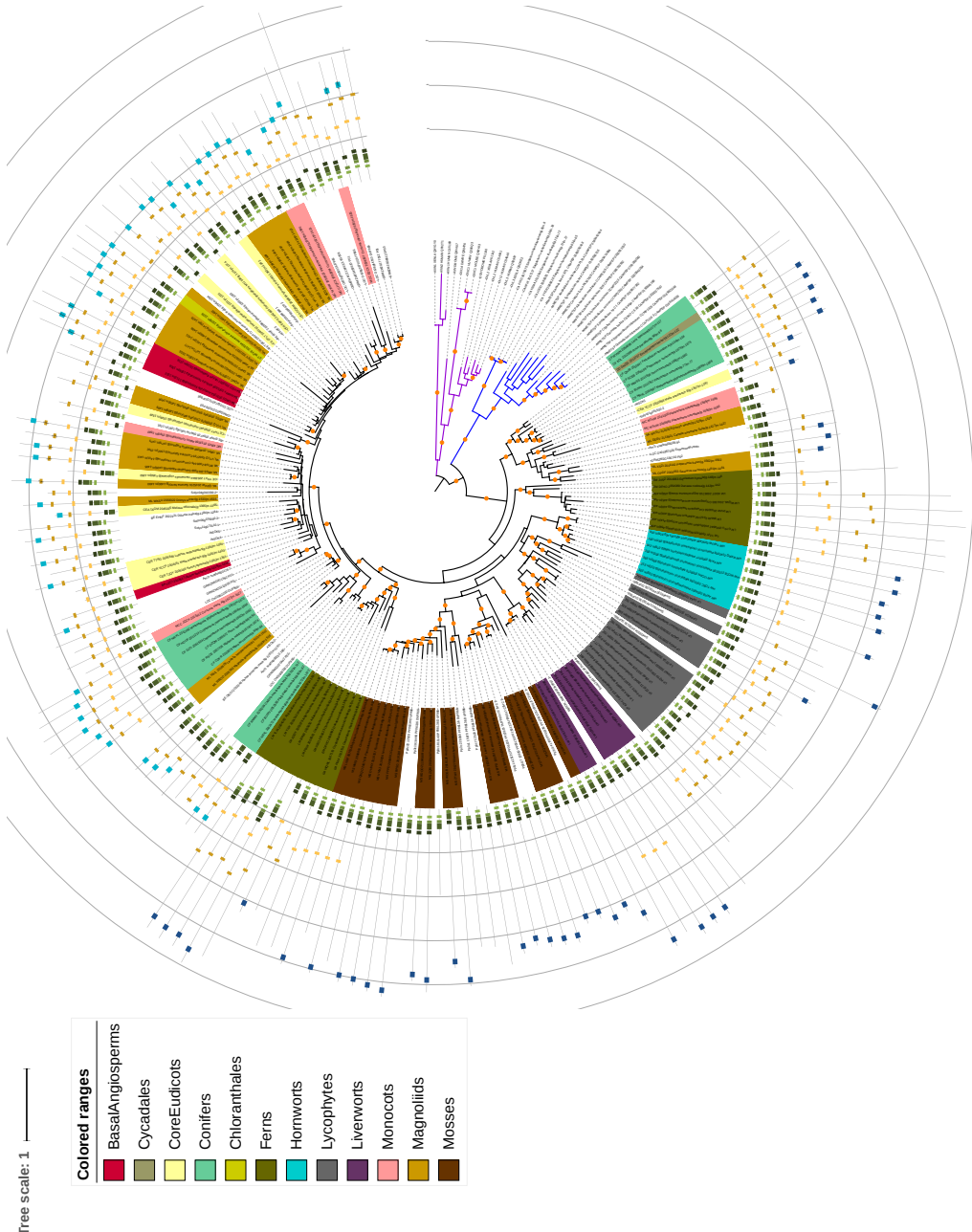
Smith, S. A., & Dunn, C. W. (2008). Phyutility: A phyloinformatics tool for trees, alignments and molecular data. *Bioinformatics*, 24, 715–716.

Stanislas, T., Hüser, A., Barbosa, I. C. R., Kiefer, C. S., Brackmann, K., Pietra, S. et al. (2015). *Arabidopsis* D6PK is a lipid domain-dependent mediator of root epidermal planar polarity. *Nature Plants*, 1, 1–9.

Vidali, L., Burkart, G. M., Augustine, R. C., Kerdavid, E., Tüzel, E., & Bezanilla, M. (2010). Myosin XI Is Essential for Tip Growth in *Physcomitrella patens*. *The Plant Cell*, 22, 1868–1882.

Vidali, L., van Gisbergen, P. A. C., Guerin, C., Franco, P., Li, M., Burkart, G. M. et al. (2009). Rapid formin-mediated actin-filament elongation is essential for polarized plant cell growth. *Proceedings of the National Academy of Sciences*, 106, 13341–13346.

Supplemental information

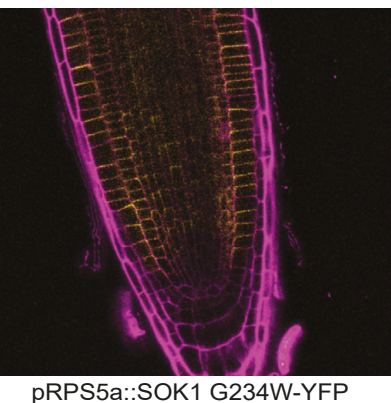


Supplemental Figure 1. Complete phylogeny of DIX(-LIKE) from land plant SOKs along with animal and SAR group counterparts. Orange circles indicate the branches with bootstrap support above 60. Label colors are indicated in the legend for the respective clades. Purple branches indicate the animal DIX domains and blue branches indicate the SAR group.



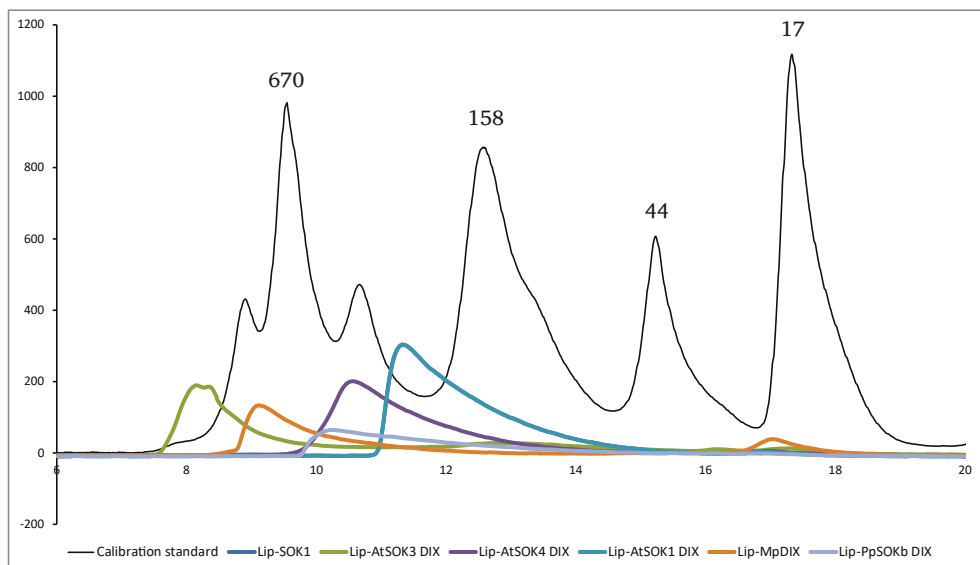
Supplemental Figure 2. DIX and PB1 phylogeny. Phylogenetic tree of DIX and PB1 domains. Four groups are shown the tree: Black, Animalia PB1 domains; Red, Plantae PB1 domains; Orange, SAR group DIX domains; Blue, Animalia DIX domains; and Green, Land plant DIX-LIKE domains of SOKs. Numbers on the phylogenetic tree indicate the bootstrap values calculated from the maximum likelihood method using LG model with GAMMA rate distribution implemented in RAxML.

A



pRPS5a::SOK1 G234W-YFP

Supplemental Figure 3. (A) Localization of mis-expressed SOK C234W in the root.



Supplemental Figure 4. Calibration curve of in vitro DIX(-LIKE) polymerization. Numbers above peaks are protein (complex) size in kDa.

Supplemental Table 1: Protein name, Species and UniProt ID of the animal DIX domains used in this study. FW: forward primer. RV: reverse primer.

ProteinName	Species	UniprotID	ProteinName	Species	UniprotID
DVL1	MOUSE	P51141	AXIN2	MOUSE	O88566
DVL2	MOUSE	Q60838	AXIN1	HUMAN	O15169
DVL3	MOUSE	Q61062	AXIN2	HUMAN	Q9Y2T1
DVL1	HUMAN	O14640	AXIN1	DANRE	P57094
DVL2	HUMAN	O14641	AXIN1	CHICK	O42400
DVL3	HUMAN	Q92997	AXIN1	XENLA	Q9YGY0
DVL2	XENLA	P51142	AXN	DROME	Q9V407
DVL3	XENLA	Q6DKE2	AXN-PRY1	CAEEL	O62090
DSH	DROME	P51140	DIXC1	MOUSE	Q80Y83
DSH-MIG5	CAEEL	Q22227	DIXC1	HUMAN	Q155Q3
DSH	DANRE	F1QM97	DIX1A	DANRE	Q804T6
AXIN1	MOUSE	O35625			

Supplemental Table 2: primers used in this study.

Marchantia cellular markers	
pMpSOK F	CACCGCGGAATAGTGGAACGGCAG
pMpSOK R	GCCACCGAACGTCCTACCTCG
MpSOK CDS F	CACCATGGTCTGGTAGGTCAAGG
MpSOK CDS R	TTGCAGTCGAGTCCGTATGG
Physcomitrella cellular markers	
PpSOKa-LF-F-KpnI	GGGGTACCCGCAGAACGAGAACAGTTGACACC
PpSOKa-LF-R-XhoI	CCGCTCGAGGCATCGGACCACATGCGG
PpSOKa-RF-F-SmaI	GGGATTCTGTTATTGTGCGGCTGG
PpSOKa-RF-R-NotI	AGAACGGCCGTTGGTCTGCTCCCTCCATCG
PpSOKb-LF-F-ApaI	ACCGGGGCCACCAGAACAAAGTCACAGGGAGG
PpSOKb-LF-R-ClaI	CCATCGATTGCAGTATCAAATCCTTGGAGATTG
PpSOKb-RF-F-SmaI	GGGATGCTCGTAAGTGCCTCATTCAG
PpSOKb-RF-R-NotI	AGAACGGCCGATGCAACATGGCGGATACAG
PpSOKc-LF-F-ApaI	ACCGGGGCCATTGCATTCTCCTCCCTGTG
PpSOKc-LF-R-HindIII	CCCAAGCTCGAAGCTCGAGATCGGACGACG
PpSOKc-RF-F-SmaI	GGGCTTTCTGACTGCCGATTGAG
PpSOKc-RF-R-NotI	AGAACGGCCGCTACATTCTGCCCACGTCC

Physcomitrella cellular markers

PpSOKd-LF-F-KpnI	GGGGTACCTGCACACAATCTCCACTCTC
PpSOKd-LF-R-XhoI	CCGCTCGAGTTTTGATACTCTGATCCTGTTAAGG
PpSOKd-RF-F-SmaI	GGGCCTAGGTATTGAATTCTGAAGTATCC
PpSOKd-RF-R-NotI	AGAACGGCCGCGGTGTCGATGCCTCTTCGATTG

LF: left flank, RF: right flank

Genotyping Physcomitrella

Physco genotyping mCIT RV standard	GCCGGACACGCTGAACCTTGTG
Physco genotyping T35S F standard	TGCTAAGGCAGGGTGGTTACG
Physco genotyping PUFa FW before	GTCAGTGAACAGGCTTCAC
Physco genotyping PUFa RV after	GGTCGAAATCACTTCCGG
Physco genotyping PUFb FW before	CAGACGATCAATAAGGAGGGCACC
Physco genotyping PUFb RV after	GTCGAGTAGGGTGCAGGGAG
Physco genotyping PUFc FW before	GCCGACATCCCAGAAATCTGCC
Physco genotyping PUFc RV after	GTTGGCCTTGTATTCAATAAAG

C234W Arabidopsis

C233A fusion RV	TGTGTCCAACCACCAGCCTTCATCAAGTTCCG
G234W fusion FW	AACTTGATGAAGTGTGGGGTTGGACACAAAC

DIX purification

Arabidopsis thaliana SOK1:

Lip-SOK1t: CGAAAACCTGTACTTCCAGATGGAAAGTAATGGTGGAGG

Lip-SOK1b: GCTGCCGCTGCCGCCAGATTATTCTTCTCACATTAGGATAATCC

Arabidopsis thaliana SOK3:

Lip-SOK3t: CGAAAACCTGTACTTCCAGgggAAGTATCATCAAAAGATCAAG

Lip-SOK3b: GCTGCCGCTGCCGCCAGATTAATCTGAATTGGATTCAAA

Arabidopsis thaliana SOK4:

Lip-SOK4t: CGAAAACCTGTACTTCCAGTCCAGGGAACGGATAG

Lip-SOK4b: GCTGCCGCTGCCGCCAGATTAGTCGAGAATTGAGAGCC

Physcomitrella patens:

Lip-PhyscoT: CGAAAACCTGTACTTCCAGAGCGAAAGCTATCATAAAAT

Lip-PhyscoB: GCTGCCGCTGCCGCCAGATTAATCCATCACTCCAGCG

Marchantia polymorpha:

Lip-MarchT: CGAAAACCTGTACTTCCAGgggACCAAAGTGCAGGTGG

Lip-MarchB: GCTGCCGCTGCCGCCAGATTATTCCGCTTTCTGAAAG

DIX purification

Ectocarpus siliculosus: Brown algae

Lip-EctoT: CGAAAACCTGTACTTCCAGATGATCCGCTATTATTCCAGC

Lip-EctoB: GCTGCCGCTGCCGCCAGATTAGTCCGACAACCTCGTATTGGCCGTAAACAC

Cryptosporidium parvum: Apicomplexan

Lip-CryptoT: CCGCGAAAACCTGTACTTCCAGaacaacGAGGGTCTTATCACTGTG

Lip-CryptoB: GCTGCCGCTGCCGCCAGATTAGTTGATACGAAGAACCTTGGCG

Zea mays:

Lip-ZeaDIXt: CGAAAACCTGTACTTCCAGATGGGGGGCGCGAAGTGC GCCGCATTAACGTG
GTGTAT

Lip-ZeaDIXb: GCTGCCGCTGCCGCCAGATTAGCGTTGGGTCTGGCTGCCGCCGGCG
GGGTGCCGCGCACATCGCTCCCTTCAGCACATATCGTTATC

Paramecium tetraurelia: Ciliate

Lip-ParaT: CGAAAACCTGTACTTCCAGATGAAGCAATTACGCTGATT

Lip-ParaB: GCTGCCGCTGCCGCCAGATTAGCTAATACGTGTCGCCCTTAATAAG

Chapter 6

SOSEKI proteins form a polar scaffold that recruits interactors to cell edges

Maritza van Dop¹, Charlotte Siemons^{1,2}, Dominique Hagemans^{1,3},
Richard Benders¹ and Dolf Weijers¹

¹Laboratory of Biochemistry, Wageningen University and Research, Wageningen, The Netherlands

²Present address: Plant Developmental Systems, Wageningen University and Research, Wageningen, The Netherlands

³Present address: Laboratory of Biomolecular Mass Spectrometry and Proteomics, Utrecht University, Utrecht, The Netherlands

In plants, polarity is essential for local subcellular processes, such as morphogenesis and directional transport of solutes. Cell polarity is used to orient the division plane, especially in cases where a deviation from symmetry is required. In addition, localization of polar membrane proteins requires translation of cell polarity into targeted delivery, retention and recycling. Yet, it remains unclear how directional cues are translated to these sub-cellular processes. The recently identified SOSEKI (SOK) proteins robustly localize to cell edges, where they use an N-terminal DIX-like domain to cluster together. Mis-expression of SOK1 resulted in oblique divisions in the embryo and root. However, the molecular function and localization mechanism of SOK remained unknown. Here, we used a biochemical and cell biological approach to address these questions. We identified unique and shared interactors of SOK1, SOK2 and SOK3, and we showed that SOK proteins can form heteromeric complexes. At least one of the interactors was recruited to the polar SOK1 site, and complex formation depended on the DIX-like domain. An extended network of interaction partners of SOK interactors showed links with cytoskeletal regulation. Based on these results, we propose that SOK polymerization creates a polar subcellular scaffold that may be stabilized by one of the interactors, Dynein Light Chain1. This polar scaffold then recruits interactors for local tasks, which may entail modification of the cytoskeleton during normal growth and during changes in mechanical stress.

Introduction

In seed plants, a single-celled zygote grows out to form an organism with complex tissue and cell patterns. To establish such patterns, directional information, or polarity, needs to be integrated and translated into cellular processes. One of these processes is cell division. Control of cell division plane orientation is of crucial importance, as plants cannot easily migrate or replace cells like animal cells do: A rigid cell wall forms soon after cell division, which fixes the new cell permanently to its neighbors. Regulation of oriented cell division is especially important in early embryos and stem cell niches (meristems), as these tissues lay the foundations for all future organs. Particularly in the flowering plant *Arabidopsis thaliana*, the embryo consists of very few cells and each cell has its own specific function and destiny (Reviewed in Lau et al. 2012; De Smet et al., 2010). Defects in the embryonic cell pattern are therefore detrimental for post-embryonic development, as they result in missing or deformed organs. For example, mutants in the *WUSCHEL RELATED HOMEOBOX (WOX)* and *MONOPTEROS (MP)* genes display abnormal orientations of cell division planes in the embryo, which causes deformations, organ fusions or missing organs (Berleth & Jürgens, 1993; Breuninger et al., 2008). Likewise, if stem cell niches fail to divide in the proper direction, this can result in absent tissue layers or impaired development of secondary organs such as flowers and lateral roots (Fisher & Turner, 2007).

Experiments and computational modeling showed that if no directional cue is provided, topological and geometrical properties of the cell are used to position the cell division machinery (Besson & Dumais, 2011; Minc, et al., 2011; Minc & Piel, 2012; Sahlin & Jönsson, 2010). It has been proposed that dynamic probing of the cell geometry by Microtubules (MT) favors the shortest possible connections between the nucleus and cell periphery. This results in division through the center of mass along the shortest route possible, often on alternating planes (Besson & Dumais, 2011). Yet, the shortest path theory is not always able to explain division orientations found in nature. Anisotropic tensile stresses predict division plane position better in tissues with more complex shape, such as the shoot apex (Louveau et al., 2016). Such a default division patterns will still not result in the highly ordered cell division planes that accompany the formation of new organs or cell layers, thus a cell needs to have some alternative sense of directionality or at least axiality to determine in which way it should divide. In embryos, auxin was shown to cause cell division to deviate from the default symmetry (Yoshida et al., 2014), although how auxin affects directional cues or their interpretation remains to be determined.

The directional cue for oriented cell division is thought to be provided by cell polarity (Jürgens, 2003). Cell polarity is defined as the asymmetrical distribution of proteins and organelles over the plasma membrane (PM) and throughout the cell

following directional axes (Reviewed in Nakamura & Grebe, 2018). The cell polarity hypothesis is supported by recent work on stomatal development where polarity switching, mediated by the polarly localized BREAKING OF ASYMMETRY IN THE STOMATAL LINEAGE (BASL) protein (Dong et al., 2009) is crucial for generating the proper pattern of stomata and their neighboring cells (Robinson et al., 2011). As exciting as this finding is, BASL-like genes have only been found in close *Arabidopsis* relatives (Vatén & Bergmann, 2012) and are only active in stomatal lineage cells (Dong et al., 2009). In essence, while oriented cell divisions are deeply conserved in plants (Harrison, et al., 2009) it is unknown how polarity controls cell division plane.

Cell polarity is not only instructive for cell division orientation, but also for other processes that require directionality, such as localization of polar membrane proteins. These proteins localize to only one part the cell membrane, such as PIN-FORMED (PIN; upper or lower cell face, Gálweiler et al., 1998; Wisniewska et al., 2006), BORON TRANSPORTER1 (BOR1; inner lateral, Takano et al., 2002, 2010), NIP5;1 (outer lateral, Takano et al., 2010) and SCHENGEN1 (SGN1; outer lateral, Alassimone et al., 2016) in the root. Previous studies have addressed the localization mechanism of some of these polarly localized proteins. Polar localization can be accomplished by polar delivery, selective retention, restriction of lateral diffusion and/or local endocytosis (Langowski et al., 2016). Protein modifications such as phosphorylation and palmitoylation can have a profound effect on polar localization. For example, PIN phosphorylation status determines which cell face the protein is targeted to (Friml et al., 2004; Kleine-Vehn et al., 2009; Michniewicz et al., 2007). Phosphorylation of NOD26-LIKE INTRINSIC PROTEIN5;1 (NIP5;1) is important for polar localization (Wang et al., 2017), and palmitoylation of SGN1 is required for polar membrane accumulation(Alassimone et al., 2016). BOR1, NIP5;1 and PIN rely on endocytosis to maintain their polar localization (Kleine-Vehn et al., 2011; Mravec et al., 2011; Wang et al., 2017; Yoshinari et al., 2016). Some polar proteins appear to be limited in their lateral diffusion, which helps sustain their strict polar accumulation (Kleine-Vehn et al., 2011; Langowski et al., 2016). All these observations help explain how proteins are recycled on the membrane and how their polarity is restricted. However, it is still unclear how polar proteins select the correct cell face for localization.

We recently identified the SOSEKI (SOK) family of polar proteins as downstream targets of the embryo patterning transcription factor MP (Chapter 3). These proteins robustly localize towards cell edges in the root rather than cell faces (Chapter 3). SOKs contain a highly conserved DIX-like domain (Domain-I) that mediates protein clustering, and a polarity domain for edge selection (Chapter 3 and 5). In addition, through deep phylogenetic analysis, we identified a putative Dynein Light Chain (DLC)-binding motif, a putative palmitoylation motif within the polarity domain

and two C-terminal domains (Chapter 5). Each SOK contains only one of these two domains: either a Zinc-finger-like domain (Domain-IV), or a KEYFSGS motif (Domain-V) (Chapter 5). Mis-expression of SOK1 leads to aberrant cell divisions in both embryo and root (Chapter 3). As such, SOK may influence cell division, but its exact molecular function remains unknown. Additionally, it remains unclear how exactly SOK selects its specific polar edge and finds its way there. Therefore, we studied the molecular context of SOK1-3 in more detail, by combining proteomics with cell biology in the *Arabidopsis* root. We found that SOK proteins can interact with each other and share several interactors. They form a polar scaffold that recruits interactors in a DIX-like domain-dependent manner. Based on the function and behavior of proteins in the SOK complex, we propose two models for SOK complex function in cytoskeleton regulation.

Results

SOK proteins share interaction partners

The molecular function of SOK proteins have so far remained elusive. Therefore, we aimed to gain a better understanding of the proteins on a molecular level. Identification of interaction partners could provide a hint as to which pathways or processes SOKs are involved in. Here, we used immuno-precipitation coupled with mass-spectrometry (IP-MS/MS), followed by quantitative statistical analysis to identify molecular interactors of SOK1-3 in *Arabidopsis* roots. As protein levels of endogenous promoter lines were too low to be recovered by IP-MS (Fig. 1A), roots of pRPS5A::SOK-YFP lines were used. The RPS5A promoter is active throughout the root meristem, which results in mis-expression and higher levels of the SOK proteins. Each experiment was repeated at least once to guarantee reproducibility of the results. After the statistical analysis, the results were manually screened for “sticky” proteins often found in IP-MS experiments using GFP- or YFP-tagged proteins in *Arabidopsis*. In addition, we excluded general transcription and translation machinery proteins, as they are often sticky and not likely to interact with membrane-associated proteins. If proteins were only found in one IP per SOK, but for multiple SOK proteins, they were included in the study.

In each IP-MS experiment, the target SOK was amongst the most strongly enriched proteins, indicating that the approach was successful (Fig. 1). We identified several proteins that were uniquely found for one of the three tested SOK proteins (Table S1, Fig. 1, Table1): A BTB/NON PHOTOTROPIC HYPOCOTYL 3 (NPH3) family protein of unknown function (SOSEKI Interacting BTB/NPH3 1; SIB1) was found as unique putative interactor of SOK1. Two Protein Phosphatase 2a B regulatory subunits alpha and beta (PP2a B α and PP2a B β) were solely present in SOK2 samples. We also identified a Dynein Light Chain (DLC2) as putative interactor of SOK3.

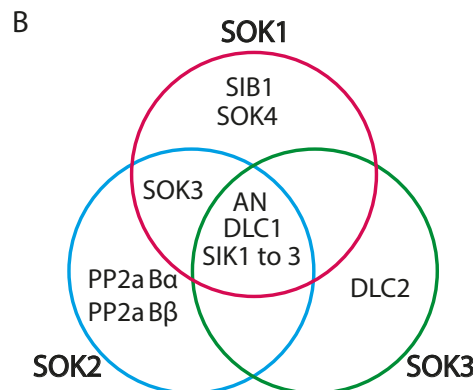
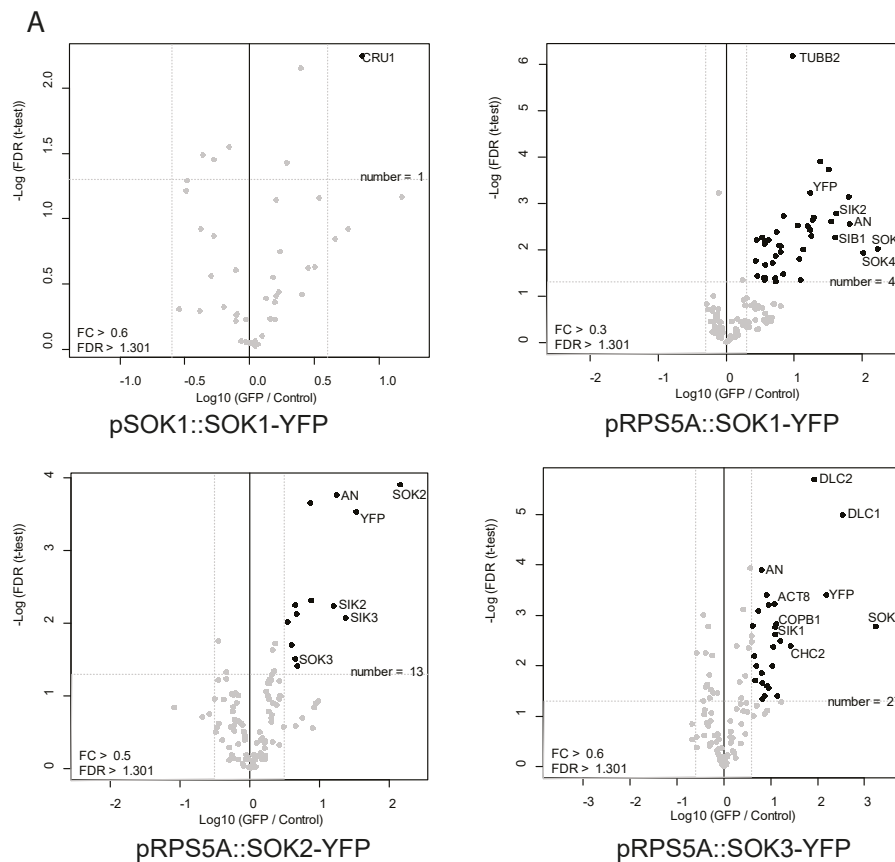


Figure 1. *SOK* proteins have shared and unique interactors. (A) Example volcano plots of IP-MS experiments on *pSOK1::SOK1-YFP*, *pRPS5A::SOK1-YFP*, *pRPS5A::SOK2-YFP* and *pRPS5A::SOK3-YFP*. (B) Venn-diagram showing the unique and shared interactors of *SOK1-3* as identified by IP-MS.

The BTB/NPH3 family protein SIB1 has no assigned function, but homologs of this gene are involved in development, phototropism and PIN localization (Cheng et al., 2007; Christie et al., 2017; Furutani et al., 2007, 2011; Stogios et al., 2005; Wan et al., 2012). NPH3 itself has been shown to interact with CULLIN3 (CUL3), which is part of a ubiquitin ligase complex (Roberts et al., 2011). SOK2-interacting PP2a has been implicated in a wide variety of functions, from protein localization to cell division (e.g. Michniewicz et al., 2007; Spinner et al., 2013). The two regulatory subunits identified in this study are essential for activation of Nitrate reductase and a double mutant is lethal (Heidari et al., 2011). Whether they have additional functions is unknown. In most eukaryotes, Dynein Light Chains are part of the Dynein microtubule motor. However, plants do not contain Dynein Heavy Chains, which are the motor part of the complex, and the function of Light Chains in plants remains to be investigated (Yamada & Goshima, 2017).

In addition to proteins associating with only one of the SOK proteins, several putative interactors were identified as shared between all three (Table S1, Fig. 1, Table1): A Dynein Light Chain (DLC1) that is the closest homolog of DLC2, three closely related kinases (SOSEKI INTERACTING KINASE; SIK1-3) and ANGUSTIFOLIA (AN). Tubulin was also recovered in many IPs, but as Tubulin is highly abundant in cells, and is recovered often in IP-MS experiments, it is difficult to determine whether it was recovered by specific interaction.

Table 1. Names, description and AGI numbers of new candidate interactors of SOKs identified by IP-MS.

Name	Description	AGI #
ANGUSTIFOLIA	Ct-bars protein	At1g01510
SIB1	BTB/NPH3 family protein	At1g30440
DLC1	Dynein Light Chain	At4g15930
DLC2	Dynein Light Chain	At1g23220
SIK1	Ser/Thr protein kinase	At1g73450
SIK2	Ser/Thr protein kinase	At1g73460
SIK3	Ser/Thr protein kinase	At3g17750
PP2a B α	PP2a regulatory subunit	At1G51690
PP2a B β	PP2a regulatory subunit	At1G17720

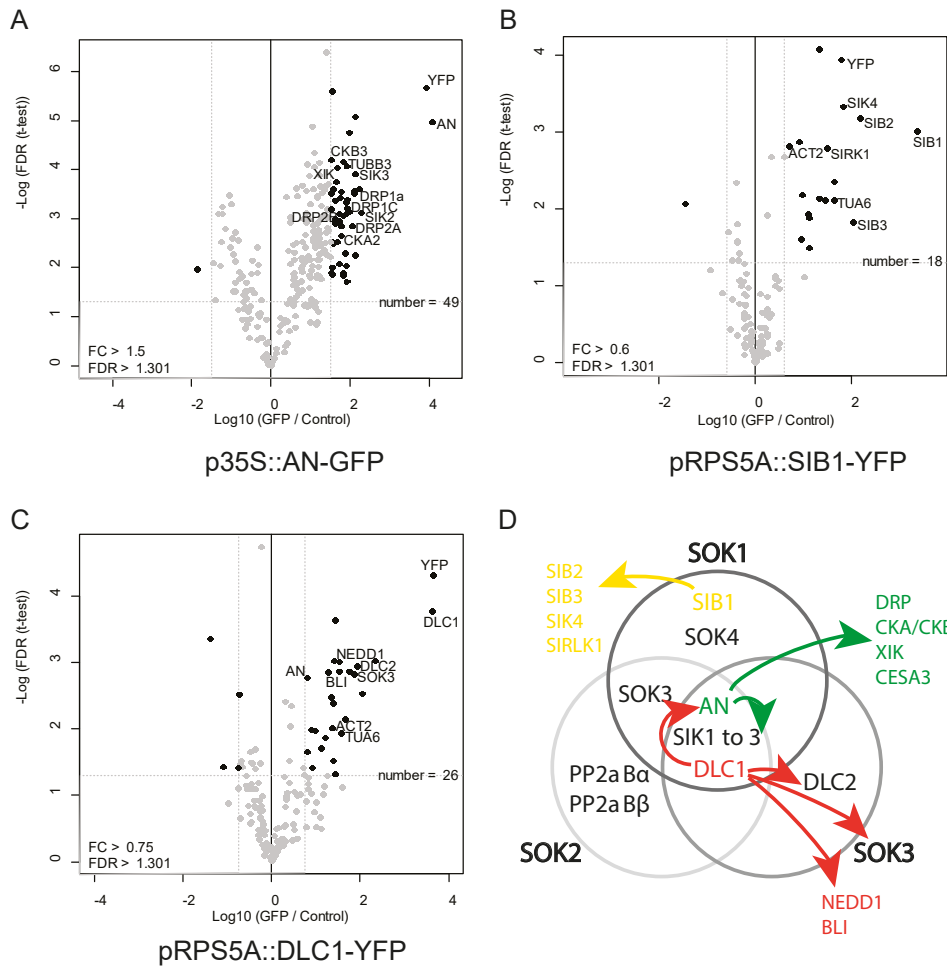
It is striking that DLCs were recovered both as shared interactor and as unique interactor of SOK3. During our phylogenetic analysis of SOK, we identified a DAxTQT motif (Domain II) that was part of the ancestral SOK and conserved in most land plants (Chapter 5). This motif is very similar to the (D)KxTQT dynein light chain

binding motif found in animals (Reviewed in Rapali et al., 2011). The identification of DLCs as SOK interactors suggests that the Domain II motif may indeed be bound by DLCs. So far, nothing has been published about the biological role of SIK1-3. A recent study also showed interaction between SIK1 (AIK1) and AN in a yeast-two-hybrid assay (Bhasin & Hülskamp, 2017). SIK1 to 3 are part of the Dual-specificity tyrosine-regulated kinases (DYRK) protein kinase family of which only one member has been studied in plants (Shiu et al., 2004). This *AtYAK* gene encodes a dual specificity protein kinase that phosphorylates amongst others annexins and tubulin (Kim et al., 2015). AN is the best studied protein in our interactome. It is involved in MT organization, stress response, tissue morphogenesis and trans-Golgi vesicle shape (Bhasin & Hülskamp, 2017; Folkers et al., 2002; Kim et al., 2002; Minamisawa et al., 2011). However, its exact molecular function remains to be determined. Strikingly, when one SOK was used as a bait, other SOK family members could be recovered in the IP. This is an indication that SOKs do not only homo-di/polymerize, but might also form heteromeric complexes.

The extended interactor network reveals potential function in cytoskeleton organization and stress

After identification of primary SOK interactors, we expanded the interaction network to gain better understanding of which processes SOKs could be involved in. To this end, we focused on candidate interactors that were shared between SOK1-3 or unique for SOK1: AN, SIB1 and DLC1. We generated pRPS5A::SIB1/DLC1-YFP mis-expression lines to use as bait for IP-MS. For AN, we used the previously published p35S::AN-GFP line (Kim et al., 2002; Fig. S1). Next, IP-MS was performed on roots as described above. Identified interactors are described in Table 2 and Fig. 2.

In the pull-down with AN (Table 2, Fig. 2A, D), we recovered SIK1 to 3. Actin and associated Dynamin Related Proteins (DRP) and Myosin XIK were also identified. In addition, Casein kinases, Tubulin, and CELLULOSE SYNTHASE3 (CESA3) were present in the IP sample. DRP1 and 2 are involved in vesicle pinching during endocytosis, post-Golgi trafficking and polar localization of PIN and BOR1 (Huang et al., 2015; Mravec et al., 2011; Yoshinari et al., 2016). Myosin XIK functions mostly in organelle motility, cytoplasmic streaming, cell morphogenesis and actin remodeling (Avisar et al., 2018; Ojangu et al., 2007; Peremyslov et al., 2010; Ueda et al., 2010). These results show that AN is not only involved with MT, but also has a link to Actin and sub-cellular transport. Casein kinases are widely implied in many developmental and stress response processes (Mulekar & Huq, 2014). The presence of many kinases in the AN complex suggests that either AN is phosphorylated by several kinase groups, or that AN mediates phosphorylation of other proteins. AN association with CESA components has been reported previously (Consortium, 2011), although the function of such an interaction remains to be investigated.



IP-MS on SIB1 resulted in the identification of two closely-related BTB/NPH3 family members (hereby named SIB2 and SIB3. Table 2, Fig. 2B, D). These have not been assigned a function. The pull-down also revealed a kinase (SIK4) and Leucine Rich Repeat Receptor-Like kinase (SIRLK1). The function of all these proteins remains to be investigated.

Lastly, DLC1 interacted with its closely related family member DLC2, that was also identified in the SOK3 IPs (Table 2, Fig. 2C, D). SOK3 itself was also found amongst the interactors. Thus, DLC1, 2 and SOK3 clearly form an interaction cluster. In addition, AN, NEDD1 and BLISTER were identified as putative interaction partners. NEDD1 regulates MT nucleation and has an important role in mitotic spindle organization, cell plate and phragmoplast assembly, and pollen and embryo sac development (Walia et al., 2014; Zeng et al., 2009). BLISTER regulates stress responses and is involved in development and differentiation, although its exact function in the latter processes is unknown (Kleinmanns et al., 2017; Schatlowksi et al., 2010). Taken together, these results reveal a completely novel interaction network with a potential link between SOKs and cytoskeleton organization. Several first and second degree interactors are implied in stress responses, and therefore SOKs might play a role in such processes as well.

Table 2. Names and AGI numbers of candidate-interactors of AN, SIB1 and DLC1 as identified by IP-MS.

AN			SIB1		
Name	Description	AGI #	Name	Description	AGI #
SIK2	Ser/Thr protein kinase	At1g73460	SIB2	BTB/NPH3 family	At3g44820
SIK3	Ser/Thr protein kinase	At3g17750	SIB3	BTB/NPH3 family	At5g66560
DRP1a	Dynamin Related Protein	At5g42080	SIK4	Ser/Thr protein kinase	At2g40980
DRP1c	Dynamin Related Protein	At1g14830	SIRK1	Receptor-like kinase	At1g12460
DRP2a	Dynamin Related Protein	At1g10290	DLC1		
DRP2b	Dynamin Related Protein	At1g59610	Name	Description	AGI #
CKA2	Casein Kinase	At3g50000	DLC2	Dynein Light Chain	At1g23220
CKB3	Casein Kinase	At3g60250	SOK3	SOSEKI3	
XIK	Myosin	At5g20490	AN	ANGUSTIFOLIA	At1g01510
CESA3	Cellulose Synthase	At5g05170	BLI	BLISTER	At3G23980
			NEDD1	NEDD1	At5G05970

DLC1 interacts directly with SOK

IP-MS techniques identify proteins that are retained in a complex, but do not provide information about whether these interactions are direct or indirect. We aimed to gain more information about direct associations, because this would help establishing the structure of the complex. Förster Resonance Energy Transfer- Fluorescence Lifetime Imaging (FRET-FLIM) in protoplasts was mostly unsuccessful, as SOK1 lost membrane localization when the cell wall is removed and forms aggregates in the cytoplasm. Therefore, Bi-molecular Fluorescence Complementation (BiFC) in *Nicotiana benthamiana* (tobacco) was used to study the direct molecular interaction between SOKs and their candidate interactors.

We previously showed that SOK proteins contain a DIX-like domain, which strongly interacts with itself in FRET-FLIM and BiFC assays (Chapter 3). This domain was used as a positive control in our assay.

First, YFP fusions of SOK proteins were expressed in tobacco to study their localization (Fig. 3). This would help predicting where interaction could take place. If interaction was found in an unexpected location, this could suggest that an interactor is recruited or that both proteins move to a new location upon interaction. SOK1 is normally not present in *Arabidopsis* pavement cells, while SOK2 and 3 are expressed there (Chapter 4). When expressed in tobacco, SOK1 localized to the cell periphery, where it accumulated more in some lobes and necks than in others (Fig. 3A). SOK2 was weakly present at the cell periphery and accumulated slightly more around mature stomata (Fig. 3B). SOK3 was most strongly enriched around stomata, while relatively little was present at the rest of the cell periphery (Fig. 3C). The uneven accumulation of SOK1 at the cell periphery suggests that it responded to local polarity or mechanical cues, rather than a more tissue-wide signal. SOK2 and 3 patterns resemble the way they localize in *Arabidopsis* leaves, which suggests that mechanisms that guide localization are conserved across eudicots.

Next, we studied the localization of the putative interactors (Fig. 3). AN and DLC1 were both present in the cytoplasm and nucleus (Fig. 3D, E). Interestingly, DLC1 signal was stronger surrounding stomata than in other parts of the cytoplasm, which is reminiscent of SOK3 localization. While AN was partially nuclear in tobacco, in *Arabidopsis* this protein was excluded from the nucleus. SIB1 showed a patchy localization, which seemed to be coordinated on both sides of the cell wall (Fig. 3E). 3D imaging and plasmolysis showed that the protein was mostly secreted and stuck to the cell wall (not shown). This behavior is very different from *Arabidopsis*, where SIB1 was membrane localized and directly became cytoplasmic upon plasmolysis (not shown). As most of the protein was secreted in tobacco, it was unlikely to be available for interaction with SOKs.

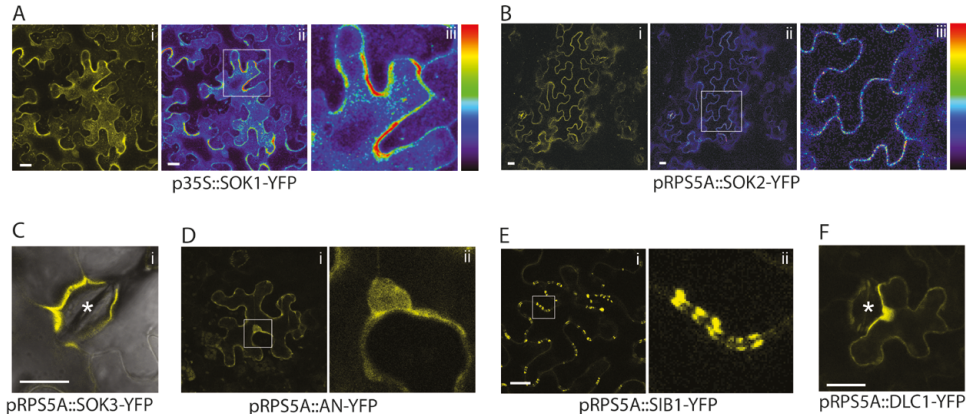


Figure 3. *SOK1*, *3* and *DLC1* show polar localization in tobacco leaf pavement cells. (A, B) *SOK1* and *2*-YFP in tobacco leaf pavement cells. i: protein fusion of *SOK1* or *2* with YFP, ii: false-colored intensity representation of the YFP signal with blue as low intensity and red as high. White box: area that is shown in higher magnification in iii. (A) is a maximum projection to better show uneven enrichment of *SOK1*. (C) protein fusion of *SOK3* with YFP in tobacco leaf pavement cells. (D, E) Resp. *AN* and *SIB1* in tobacco leaf pavement cells. i: protein fusion with *AN* or *SIB1* and YFP. White box: area that is shown in higher magnification in ii. (F) protein fusion of *DLC1* with YFP in tobacco leaf pavement cells. Star indicates the stomata. Scalebar represents 20 μ m.

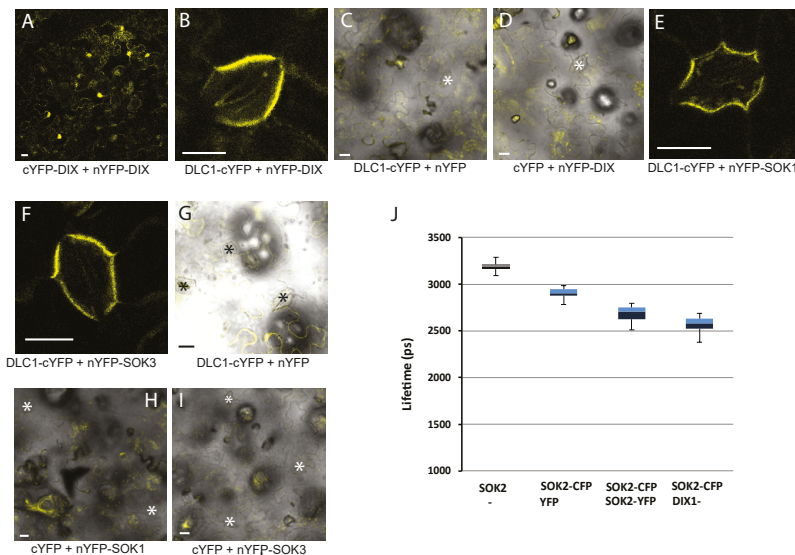


Figure 4. BiFC and FLIM reveal interactions with *DLC1* in tobacco leaf pavement cells. (A) Positive control of *DIX*-like + *DIX*-like in tobacco leaf pavement cells. (B) BiFC of *DLC1* and *DIX*-like in close up of stomata. (C, D) Negative controls of resp. *DLC1* and *DIX*-like. (E, F) BiFC between *DLC1* and resp. *SOK1* or *SOK3* in close up of stomata. (G-I) Negative controls of resp. *DLC1*, *SOK1* and *SOK3*. (G) The negative control of *DLC1* occasionally shows some YFP signal in the cytoplasm and nucleus, but never polar around stomata. (J) FRET-FLIM results of *SOK2* alone, *SOK2* with YFP, *SOK2* with *SOK2* and *SOK2* with *DIX*-like in protoplasts. Stars indicate stomata in the negative controls. Scalebar represents 20 μ m.

Finally, BiFC was performed with YFP halves fused to the C- (protein-xYFP) or N-terminus (xYFP-protein) of the proteins. We tested every possible combination of interaction pair and tag position for the constructs we had available. The positive control of DIX-like (xYFP-DIX or DIX-xYFP) showed a clear YFP signal for all tag positions and combinations, which indicated that our assay was functional (Fig. 4A). Of the shared interactor candidates, DLC1 interacted with all three SOKs and with xYFP-DIX-like (Fig. 4B-F). Strikingly, BiFC signal with both DIX-like and full-length SOKs was almost uniquely visible surrounding the stomata, while the individual proteins also overlap in other parts of the cell. As expected, no interaction was observed between SIB1 and SOK1 or DIX-like. AN did not show interaction with the full-length SOKs, nor with the DIX domain only. These results show that DLC1 directly interacts with SOKs around stomata, while the individual proteins are also present at the cell periphery. This suggests that specific factors or cues mediating interaction are present at the cell faces around stomata, that are absent elsewhere.

None of SOK1 to 3 showed any interaction with themselves or the other family members, nor with the DIX-like domain of SOK1, regardless of tag position and combination. This could be due to tags not being able to reach each other to create the full YFP, or that the cellular environment was not suitable for SOK-SOK interaction. Co-factors or specific membrane structures might be missing in this heterologous system, for example. With FRET-FLIM, we were able to show homodimerization of SOK2, and interaction between SOK2 and the DIX domain of SOK1 (Fig. 4J), confirming the ability to form heteromeric complexes.

SIB1 and interactors form a lateral interaction module

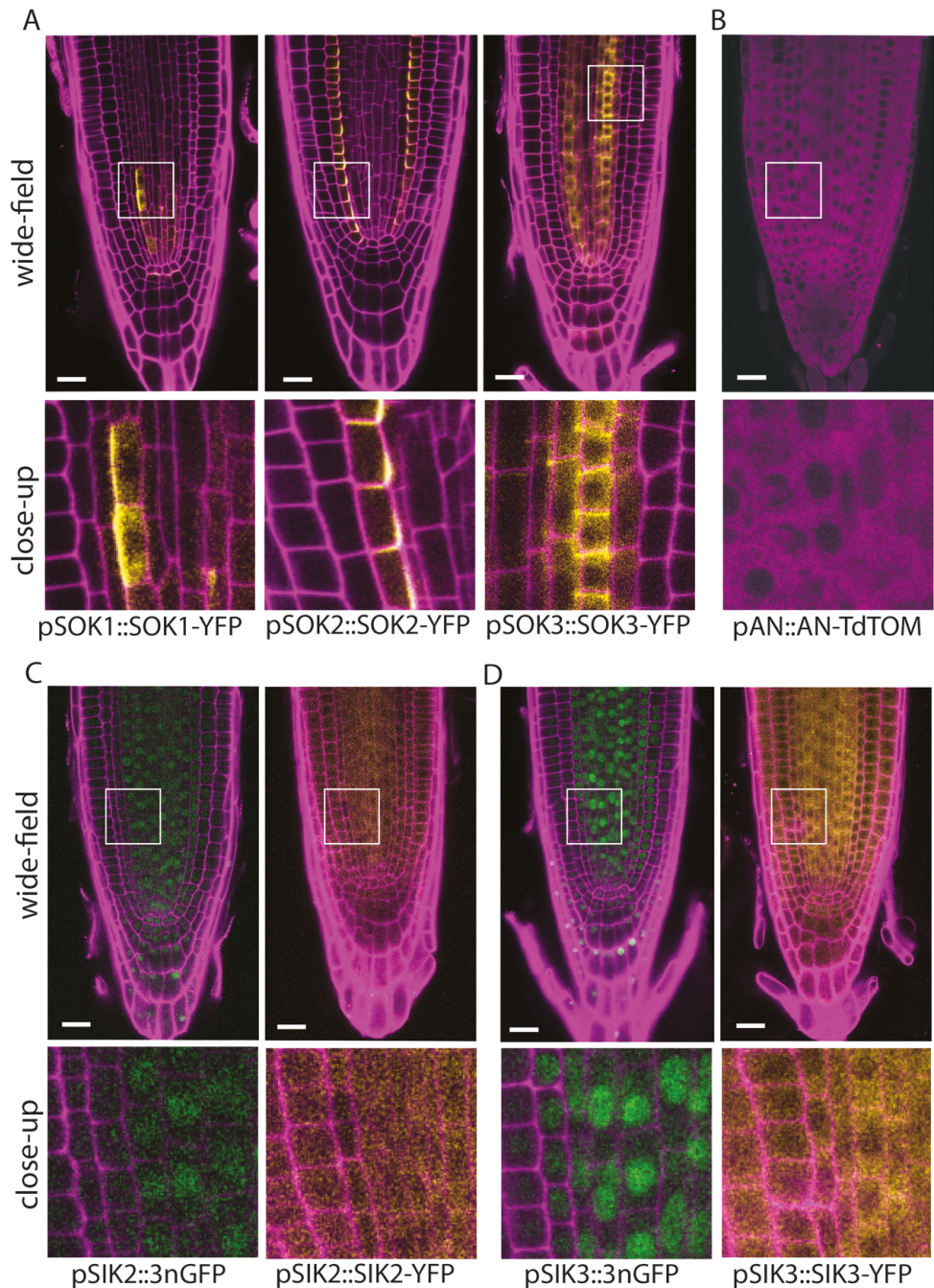
The candidate interactors were identified using mis-expression lines of the SOK bait and BiFC experiments showed which partners can physically interact. However, it is unknown which interactors would actually be able to meet each other in a WT root. Therefore, we analyzed the expression and localization patterns of the interactors in *Arabidopsis* roots to determine if any of the proteins was a false positive.

To this end, we generated candidate-interactor promoter fusion lines expressing the 2-3kb genomic region upstream of the start codon fused to a nuclear triple-GFP (pINTERACTOR::n3GFP). Protein fusions were made by fusing the genomic promoter and coding region to a YFP (pINTERACTOR::INTERACTOR-YFP) or TdTOMATO (pINTERACTOR::INTERACTOR-TdTOM). When expressed under their endogenous promoter, SOK1 localized to the outer apical cell edges in the first vascular cells and SOK2 to the inner basal edges of the endodermis. SOK3 is present in all edges in all cells and is most strongly expressed in the phloem (Chapter 3; Fig. 5A). AN was present in the cytoplasm throughout the root meristem and could therefore interact with all three SOKs (Fig. 5B). This localization is in agreement

with the published p35S::AN-GFP line (Kim et al., 2002, Fig. S1), although we did not observe the aggregation in dots in our TdTOM line that was reported for the p35S::AN-GFP version. Expression of the kinases SIK2 and 3 was very weak. Both were expressed throughout the root meristem, most strongly in the vasculature, and localized in the cytoplasm (Fig. 5C, D). This shows that interaction of AN, SIK2 and SIK3 with all three SOK proteins is indeed possible. None of the aforementioned interactors showed any polar localization. This could mean that interactions with SOK are brief and/or that not many of the interactor proteins are recruited to the SOK complex. Interaction might also depend on a condition or circumstance that we miss during imaging.

Of DLC1, we were only able to obtain the promoter fusion (Fig 6A). The endogenous promoter fusion showed expression exclusively in the phloem, where SOK3 is present, but SOK1 and 2 are not. Unless DLC1 is a mobile protein, it therefore most likely interacts with SOK3 and not with SOK1 and 2 in the root. DLC1-YFP driven by pRPS5A localizes in the cytoplasm and nucleus (Fig. S1), and probably does the same under its normal promoter. SIB1 is expressed most strongly in the vasculature and lateral root cap, and weakly in the epidermis-cortex-endodermis. The protein fusion is present in almost every cell in the root tip (Fig. 6B). The SIB1 protein localizes to a lateral side of the cell, although there is also cytoplasmic signal in most roots. In the epidermis and cortex, SIB1 localizes to the inner lateral face of the cell. In the stele, polarity is much more difficult to determine. The polar fraction is strictly lateral. SIB1 is hardly expressed in the endodermis, but in several roots that did express some SIB1 in the endodermis, the protein appeared to face to the endodermis-cortex junction (Fig. 6C), which suggests that SIB1 may be outer-lateral in the stele. Interestingly, this flip in lateral polarity is highly reminiscent of mis-expressed SOK1. Thus, SIB1 overlaps with SOK1 in the early vascular cells and may be a true interaction partner *in vivo*. The SIB1 interactor SIK4 showed a similar polar localization pattern (Fig. 6D, E). The RLK SIRK1 was not studied here, but closely-related family members are known to show a polar lateral localization as well (Jaimie van Norman, personal communication). Thus, SIBs form a lateral polar interaction module together with SIK4 and probably SIRK1.

Figure 5 (right page). Expression and localization of SOK and interactors in the root. (A) Protein fusions of SOK1, 2 and 3 with YFP under their endogenous promoter. (B) Protein fusion of AN with TdTomato under its endogenous promoter. (C) left: SIK2 promoter fusion with 3nGFP, right: SIK2 protein fusion with YFP under its endogenous promoter. (D) left: SIK3 promoter fusion with 3nGFP, right: SIK3 protein fusion with YFP under its endogenous promoter. White box: area that is enlarged in the close-up below. Roots were counterstained with PI (purple), except for pAN::AN-TdTOM. Scalebar represents 20 μ m.



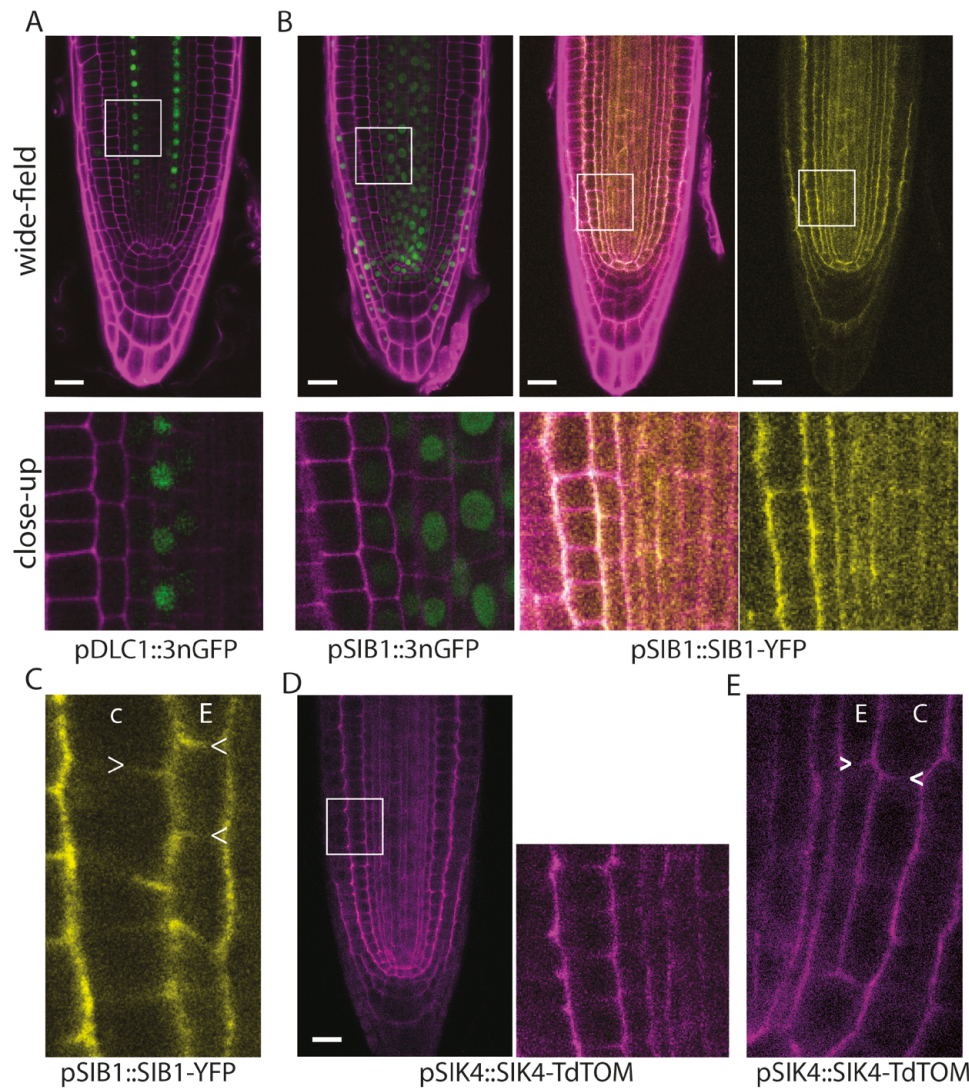


Figure 6. *DLC1*, *SIB1* and *SIK4* in the root. (A) *DLC1* promoter fusion with 3nGFP. (B) left: *SIB1* promoter fusion with 3nGFP, middle and right: *SIB1* protein fusion with YFP under its endogenous promoter. Middle image shows overlay with PI stain, right image without. (C) close-up of cortex (c) and endodermis (e) of a root expressing pSIB1::SIB1-YFP. White arrows indicate presence of *SIB1* facing endodermis/cortex junction. (D) *SIK4* protein fusion with TdTomato under its endogenous promoter. (E) close-up of cortex (c) and endodermis (e) of a root expressing pSIK4::SIK4-YFP. White arrows indicate presence of *SIK4* facing endodermis/cortex junction. White box: area that is enlarged in the close-up below (A, B) or to the right (D). Roots in (A) and (B) were counterstained with PI (purple). Scalebar represents 20 μ m.

AN and potentially SIB1 are recruited to SOK1

The interaction and localization data showed that AN and SIB1 are promising interactors of SOK1. However, AN does not show enrichment at polar SOK1 sites under standard conditions. To study whether AN can get recruited by SOK1 in the root, we made use of the pRPS5A::SOK1-YFP over-expression lines. In these lines, polar SOK1 is present in most cells in the root tip and at higher levels compared to endogenous expression. Transforming these lines with pAN::AN-TdTOM resulted in partial recruitment of AN to the polar edge where SOK1 was present (Fig. 7A, B). This recruitment was best visible when SOK1 expression was high and AN expression relatively low. These results show that SOK1 can recruit AN, but that few molecules are recruited and/or that interaction is brief.

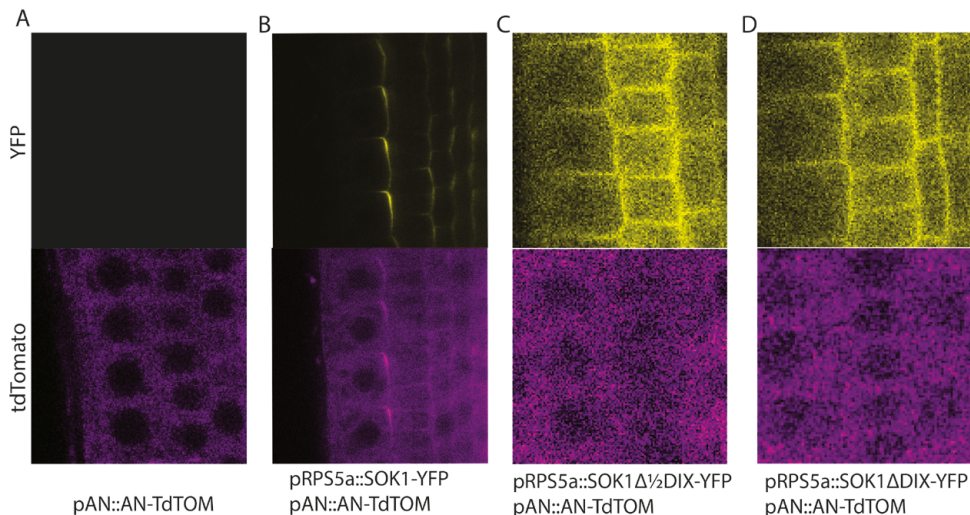


Figure 7. Close-ups of AN recruitment by SOK1 in root cells. (A) Localization of AN protein fusion with TdTomato in wild-type roots. (B) Localization of AN protein fusion with TdTomato in roots mis-expressing SOK1-YFP. (C-D) Localization of AN protein fusion with TdTomato in roots mis-expressing SOK1 lacking half (C) or the entire (D) DIX-LIKE domain. SOK-YFP protein fusions are displayed in the top panels, AN protein fusions in the same cells in the bottom panels.

BiFC was unsuccessful to show interaction between SIB1 and SOK1 or the SOK1 DIX-like domain, possibly because SIB1 was secreted. However, we found a hint for interaction during our attempts at FRET-FLIM. As reported, SOK1 directly formed aggregates in protoplasts. When expressed by itself, SIB1 localized smoothly throughout the cytoplasm (Fig. 8). However, when it was co-expressed with SOK1, SIB1 was drawn into the SOK1 aggregates. This was specific for SIB1, as DLC1 did not get recruited. Thus, SIB1 can be recruited by SOK1 aggregates in protoplasts. SIB1 and over-expressed SOK1 show a very similar localization in the root, which makes study of (partial) recruitment nearly impossible.

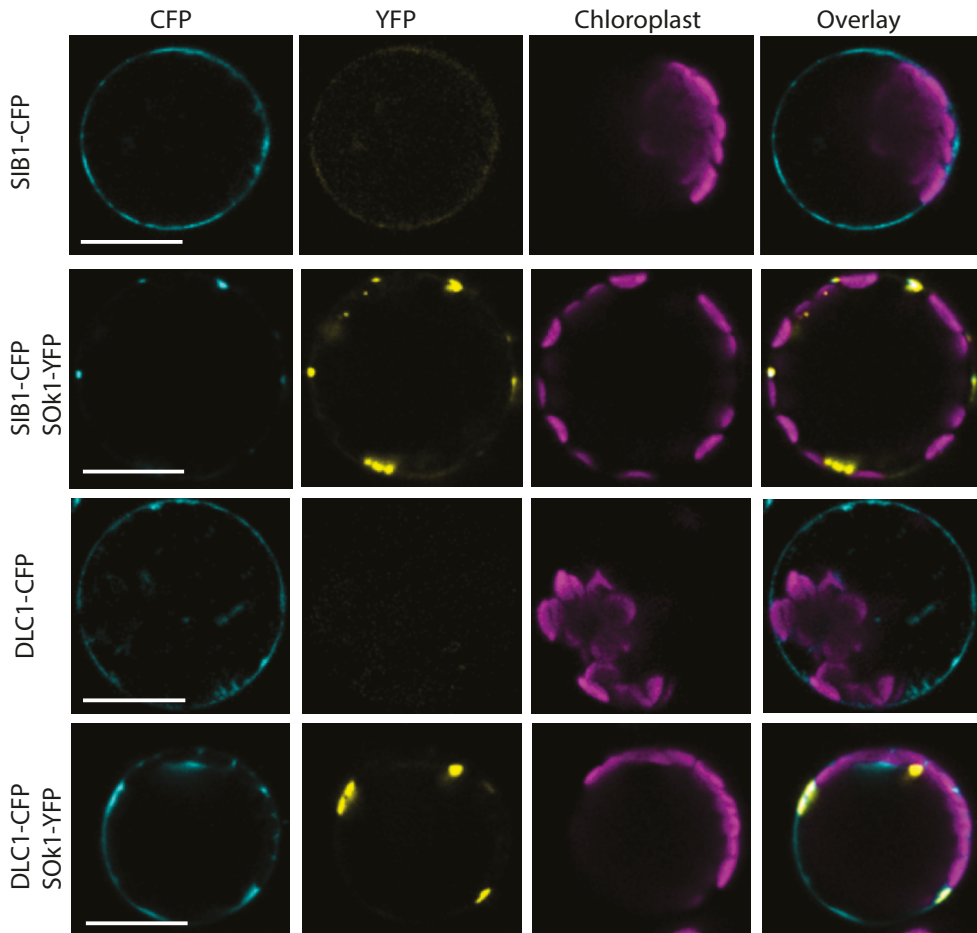


Figure 8. *SIB1* recruitment to *SOK1* in protoplasts. Top row: protein fusion of *SIB1* with CFP in protoplast. Second row: *SIB1*-CFP co-expressed with *SOK1* fused to YFP in protoplast. Third row: protein fusion of *DLC1* with CFP in protoplast. Bottom row: *DLC1*-CFP co-expressed with *SOK1*-YFP in protoplast. Scalebar represents 20 μ m.

The DIX-like domain is necessary for complex formation and recruitment

Many of the interactors identified by IP-MS are shared between *SOK1*-3. This suggests that the domains/motifs these interactor complexes attach to could be conserved amongst the *SOK*s. We previously showed that all *SOK*s contain a DIX-like interaction domain, which is necessary for polar *SOK* clustering and function (Chapter 3, 5). This is the most highly conserved domain in *SOK1*-3, and its clustering properties could provide a scaffold for complex formation. In that case,

removal of the DIX-like domain should result in disruption of the complex. When we performed IP-MS on a pRPS5a::SOK1 Δ DIX-YFP line, all interactors were lost, which indicates that the DIX domain is indeed important for complex formation (Fig. S1). To confirm the importance of DIX-like for complex formation *in vivo*, we created double marker lines of pAN::AN-TdTOM with SOK1 lacking half or the entire DIX-like domain (pRPS5a::SOK Δ 1/2DIX or Δ DIX-YFP). In these lines, AN recruitment was no longer visible (Fig. 7C, D). Taken together, these results show that SOKs provide a DIX-like-dependent polar scaffold to recruit interactors to cell edges.

Discussion

Polarly localized proteins carry out essential local functions within the cell and their localization is often dynamically controlled. The recently identified SOSEKI family has a striking polar localization, but molecular function remained unknown. All SOKs contain a DIX-like protein-protein interaction domain, that is necessary for polar SOK clustering and function (Chapter 3). In this study, we aimed to gain more insight into the function and localization mechanism of SOKs by investigating their interactome. By IP-MS, we identified interactors of SOK1 to 3.

SOK proteins may interact with each other

SOK 1 to 3 share some interactors. Interestingly, amongst those shared interactors were other SOK family members: One of the two SOK1 IPs recovered SOK4, and both SOK1 and 2 interacted with SOK3. This interaction likely depends on the DIX-like domain. The DIX-like domain is similar for all SOKs, which makes interaction and thus formation of heteromeric complexes physically possible. This raises the question whether there is a specificity of interaction, or if each SOK interact with all others if given the chance. Do SOK proteins form heteromeric complexes with each other in a wild-type root, and which SOKs have such interactions with each other? Do their specific polarities prevent/facilitate interaction? BiFC failed to show hetero-dimers, potentially because of technical limitations of the method. FRET-FLIM revealed dimerization of SOK2, and interaction between SOK2 and DIX-like of SOK1. Other methods could be used to study interaction of SOKs expressed by their endogenous promoter directly in the root. The possibility of interaction between different SOK proteins also raises questions about the function and necessity of such complexes. Removal of SOK1 or strong decrease of SOK3, 4 or 5 does not lead to a phenotype (Chapter 4). This shows that one SOK can be absent from a potential heteromeric complex without negative consequences. Higher order mutants combined with cell biology studies will provide more insight into the occurrence, dynamics and function of SOK cross-interaction.

Interactors are involved in cytoskeleton, stress and endomembrane trafficking

Aside from SOK proteins, we found many unstudied proteins in our direct interactome and expanded interaction network of SOK1-3. Therefore, SOK proteins may be involved in a process that was previously unknown. Here, we will discuss the interactors in more detail.

SOK1 was found to interact with SIB1, which is a BTB/NPH3 domain protein. In turn, SIB1 interacted with two closely-related family members. Homologs of these three, named NAKED PINS IN YUC MUTANTS (NPYs), act in polar localization of PINs, although it is unclear how exactly (Furutani et al., 2011). Another homolog, NPH3 is part of a ubiquitin ligase complex and acts during light signaling (Roberts et al., 2011; Wan et al., 2012). The patterns of SOK1, its behavior and its other interactors make it unlikely that SOK1 is involved in light signaling, although we did not specifically test for it. However, ubiquitination of SOK1 is very well possible. SOK1 is the most dynamically expressed and localized of the SOK proteins. This requires quick production and likely also fast removal of the protein. Ubiquitination could be a mechanism to ensure that SOK1 removal. Additionally, animal DIX domains are ubiquitinated to decrease the stability of polymers (Madrzak et al., 2015). Ubiquitinating the SOK1 DIX-like domain could therefore help with quick relocation or removal of SOK1.

AN and its interacting kinases SIK1 to 3 form a module that is shared between SOKs. We found that AN is expressed throughout the root meristem (this Chapter) and many other tissues of the plant (not shown). It localizes in the cytoplasm and as such is indeed available to interact with all SOK proteins. AN is a CtBP gene, but unlike its animal counterparts, its main function does not seem to be transcriptional regulation. Instead, it is involved in microtubule arrangement, morphogenesis, (a)biotic stress and trans-Golgi vesicle shape. AN contains a Casein kinase phosphorylation site, but the motif is not essential for *Arabidopsis* AN function (Minamisawa et al., 2011). However, our identification of Casein Kinases in complex with AN reveals that the motif could actually be functional. Several studies reported the role of AN in MT organization (Folkers et al., 2002; Kim et al., 2002). Surprisingly, we also identified actin and its associated motor protein myosin XIK as interactors of AN. XIK is involved in endomembrane shape and transport, and actin remodeling (Avisar et al., 2012; Duan & Tominaga, 2018; Ojangu et al., 2007; Peremyslov et al., 2010; Ueda et al., 2010). This suggests that AN may be involved in actin organization and/or endomembrane transport. The identification of several membrane-pinching Dynamin Related Proteins as AN interactors supports this hypothesis. This would explain the Golgi transport and vesicle shape defects observed in the AN mutant (Minamisawa et al., 2011).

AN forms an interaction module with SIK1 to 3, which are DYRK kinases (Shiu et al., 2004). These kinases could be in the complex via AN, or (also) interact with SOKs directly. Like AN, SIK1-3 are expressed throughout the root tip and localize to the cytoplasm. This makes interaction with both SOKs and AN a possibility. The only DYRK member described in plants is YAK1, which phosphorylates annexins and tubulin (Kim et al., 2015). SIK1-3 may have a similar function and as such could help AN modify the MT array. In yeast, DYRKs have a role in cell cycle progression and polar growth. They phosphorylate proteins with functions in cell growth and cytoskeleton dynamics (e.g. Kettenbach et al., 2015; Soppa & Becker, 2015). In mammals, DYRKs are negative regulators of the cell cycle during development and stress. They can also regulate gene transcription, protein degradation, chromatin remodeling, circadian rhythm and various other functions (reviewed in Aranda et al., 2011). Phosphorylation assays are required to identify whether SOKs or other proteins are phosphorylated by SIK1-3 and Casein kinases, and what the function of this phosphorylation is. Two PP2a phosphatase subunits were identified in IPs with SOK2. These phosphatases may counteract the phosphorylation by SIKs or other, unidentified kinases. The PP2a phosphatases are involved in a wide variety of functions. Amongst others, they dephosphorylate PINs to turn them to a basal localization (Michniewicz et al., 2007). As such, if phosphorylation state directs SOK2 localization, dephosphorylation of SOK2 may keep it in the basal edge of the cell. Alternatively, SOK2 may provide a platform for PP2a to dephosphorylate other targets.

The last shared interactor of SOKs is DLC1. DLC1 localizes to the cytoplasm and nucleus in an over-expression line, and BiFC showed that interaction is possible with SOK 1 to 3. However, the promoter fusion shows that DLC1 is expressed in the phloem. If the protein is immobile, this would mean it could only interact with SOK3. DLC1 is predicted to have a MW of 15kDa and this would be small enough to freely diffuse through the plasmodesmata in the root tip (Oparka et al., 1999) if its movement is not regulated. If such diffusion takes place, DLC1 could interact with other SOKs as well and may even provide a spatial or directional signal. A protein fusion of DLC1 is necessary to show whether DLC1 moves freely or not. Interestingly, DLC1 was enriched on the cell faces surrounding stomata in tobacco, just like SOK1-3. This was the only site where interaction took place in BiFC, although the proteins also overlapped elsewhere. Perhaps SOK and DLC1 localization and interaction depends on a mechanical cue or a biological signal coming from stomata.

Land plants do not contain a Dynein Heavy Chain (Yamada & Goshima, 2017) and therefore DLCs must have other functions than MT motor component. In animal literature, various other functions for DLCs have been described. For example, DLCs have been implied in actin regulation and clathrin-mediated endocytosis (Chuang et al., 2005; Farrell et al., 2017). DLC1 interacts with NEDD1 in our IPs. NEDD1

function in MT nucleation and cytokinesis hints that DLC1 in *Arabidopsis* could function in MT dynamics (Walia et al., 2014; Zeng et al., 2009). Human DLCs are also known to bind to unstructured regions of proteins that contain a (D)KxTQTx motif, although the motif can vary a bit (reviewed in Rapali et al., 2011). This motif is often found close to dimerization domains and the current hypothesis is that DLC promotes and stabilizes dimerization. SOKs contain a DAxTQT (Domain II) motif, which very closely resembles the DLC-binding motif in humans (Chapter 5). Domain II is located in the unstructured region near the DIX polymerization domain. IP showed that SOK can interact with DLC1. It is therefore possible that the DAxTQT motif is indeed bound by DLC1/2, which could influence polymerization of the DIX-like domain. However, only SOK3 contains the canonical Domain II (Chapter 5), yet BiFC showed interaction with SOK1 and 2 as well. Removal of the DIX domain resulted in loss of DLC1 interaction with SOK1. Additionally, BiFC between DIX-like and DLC1 showed interaction. Thus, DLC1 (also) interacts with the DIX-like domain itself. The DIX-like domain is capable of polymerizing by itself, without Domain II or presence of DLCs (Chapter 5). Thus, the DLCs probably have a more stabilizing/regulatory role in DIX-like polymerization rather than being absolutely required. To gain more insight into which parts of SOK interact with DLC, additional interaction and mutation studies in Domain II and DIX-like are required. This could also provide more insight into the influence of DLCs on SOK polymerization.

SOKs form a polar scaffold that recruits interactors and may modify the cytoskeleton

6

DIX-like-mediated polymerization of SOKs in their polar edge is essential for SOK function, as SOK1 without DIX-like is unable to induce aberrant cell divisions. Here, we showed that lack of DIX-like results in loss of all interactors in IP-MS. AN, and potentially SIB1, is recruited to the SOK polar site in a DIX dependent manner. Taking these results together, we propose SOK proteins as polar scaffolds (Fig. 9). SOK proteins polymerize in their polar corner, potentially with the help of DLC1/2. The polymerized lattice then recruits the other interaction partners to perform local functions. Hardly anything is known about the significance of cell edges or the processes that take place there, but the SOK interactors provide clues as to what they might entail. The options are numerous, so we will focus on two models that are best supported by our data.

A local function in the cell edge could entail modifying the cytoskeleton, as many interactors are linked to MT and/or actin regulation. It is notoriously difficult for cytoskeletal filaments to bend, especially around sharp corners. The SOK complex might help cortical filaments to bend around the corner, or nucleate new ones using the corner as an anchor point. In addition, cell edges receive relatively little mechanical stress compared to cell faces (e.g. Hervieux et al., 2017). Changes in

this stress pattern could for example indicate tissue damage, drought or cell growth. The SOK complex could monitor these changes in mechanical stress and adjust the cytoskeleton, and perhaps other proteins, accordingly.

Both filament bending and mechanical stress models would work for stomata as well. SOK2 and 3 are present in cells around stomata and face the guard cells in the leaf. These cell faces are very rounded, and cortical cytoskeleton may need help to bend along this curve. It may also be important to nucleate and/or anchor filaments that radiate out from the stomata-facing side. Guard cells open and close to regulate gas exchange, which causes large mechanical changes in the cells surrounding the stomata. Similar to in the root, SOK 2 and 3 complexes could monitor these changes and regulate the cytoskeleton to deal with these changing stress patterns.

Many studies have been performed on the cytoskeleton. However, the many cell layers in the root made it difficult to study these fine filaments in detail. Similarly, in leaves most studies focus on the MT on the surface, while little is known about the cytoskeleton along cross walls. To assess whether the SOK complexes influence the cytoskeleton, more detailed knowledge is needed about cytoskeleton localization and dynamics in cell edges.

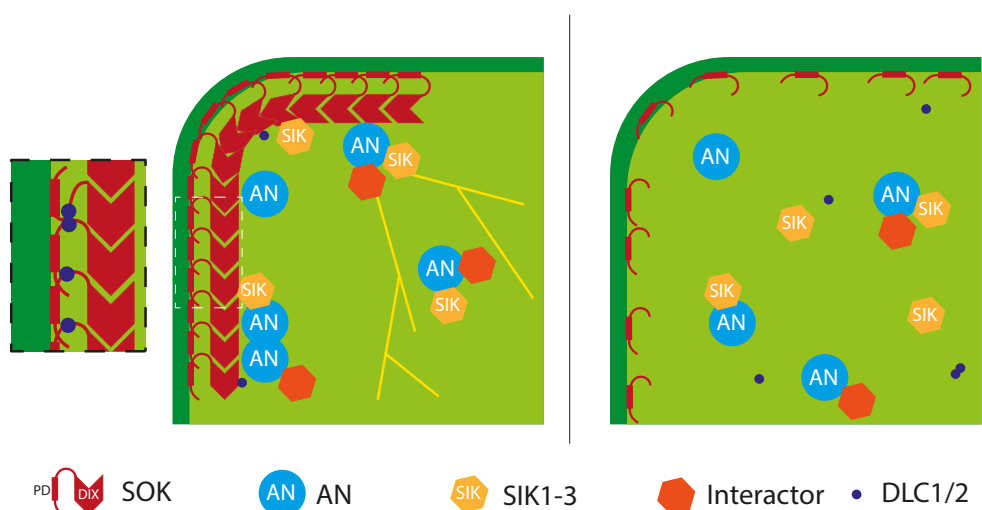


Figure 9. Model of SOK and interactors. Left: SOK with DIX-LIKE domain. The DIX domain mediates clustering of SOK at the cell edge. This may provide a scaffold that recruits interactors to the polar domain. DLC may bind the putative DLC-binding motif near DIX-LIKE and/or interact with DIX-LIKE. Right: Without DIX domain, the interactor complex falls apart. Clustering is no longer possible and SOK spreads over the membrane. Symbols: SOK with Polarity domain PD and DIX-LIKE domain (Red), AN (Blue), SIK1 to 3 (Orange), other AN interactors (Brown), DLC1 or 2 (Dark blue), cytoskeleton (Yellow lines).

In conclusion, we identified the interactome of SOK1 to 3 and showed that SOK proteins form a polar scaffold that can recruit interactors to carry out local tasks. We revealed that DLCs likely help with polymerization of SOK proteins. Based on the function of the interactors in *Arabidopsis* and animal model systems, we propose two potential functions for SOK complexes: 1. SOK proteins could regulate the cytoskeleton during normal development, amongst others by helping the filaments bend around corners or by nucleating new ones there. 2. Sensing changes in mechanical stress and regulating the cytoskeleton accordingly. We highlight detailed studies of protein modification, cytoskeleton and membrane trafficking in cell edges as promising fields of further study.

Material and Methods

Plant materials and growth conditions

All used SOK transgenic lines have been described previously in Chapter 3. The Δ sok1 mutant has been described in Chapter 4. The p35S::AN-GFP line was kindly provided by the Hirokazu Tsukaya lab (Kim et al., 2002).

Arabidopsis seeds were sterilized in 25% bleach, 75%EtOH for 7-10 minutes, followed by 2 wash steps in 70% EtOH and one wash step in 96% EtOH. After drying, seeds were plated on half strength Murashige and Skoog (MS) medium with 10g/L sucrose. For T1 selection, plates were supplemented with 50mg/L Kanamycin or 15mg/L Phosphinotricin. For IP experiments, plates were used without sucrose. After 24-48 hours of incubation at 4°C plants were grown under long-day conditions (16h light, 8h dark) at 22°C and 75% humidity. Plant transformation was performed by floral dipping, as described in De Rybel et al., 2011.

Generation of plasmids

Primers used in this study are described in Sup. Table 2. Promoter fusion constructs were generated by amplifying the genomic promoter of 3kb or up to the upstream gene and cloning this into pPLV04 (De Rybel et al., 2011). Protein fusions contained the promoter plus the coding region of the gene cloned into pPLV16 (YFP) or pPLV23 (TdTomato, De Rybel et al., 2011). For the over-expression constructs, the coding sequence was amplified from cDNA and cloned into a pPLV28 containing YFP. BiFC plasmids were made by amplifying the coding region from cDNA or existing plasmids and cloning this into modified pPLV26, which contained either the n-terminal or c-terminal half of YFP. FLIM constructs were generated similarly, but using pMON CFP or YFP as final vector. All cloning reactions were performed with LIC or SLICE (De Rybel et al., 2011; Zhang et al., 2012).

IP-MS

IP-experiments were performed as described in Wendrich, Boeren, Möller, Weijers, & Rybel, 2017 on pRPS5a::SOK1-YFP, pRPS5a::SOK2-YFP, pRPS5a::SOK3-YFP, pRPS5a::SOK1ΔDIX-YFP, p35S::AN-GFP, pRPS5a::BTB/NPH3-YFP or pRPS5a::DYN-YFP. Within each IP, root samples of equal weight were used (1.2 to 1.8g, depending on experiment; See M&M Table 1). Protein complexes were isolated by incubating a total root extract with anti-GFP magnetic beads (Milteny Biotech) for two hours and applying the mixture to magnetic columns (Milteny Biotech). Transgenic samples were compared to replicates of non-transgenic Col-0 samples. MS and statistical analysis were performed with MaxQuant and Perseus.

M&M Table 1. Number of replicates and sample weight per IP. Blocks of white/gray indicate which experiments were done in one run.

Line and experiment	# replicates within IP	Sample weight
SOK1 IP 1	3	1.5g
SOK1 IP 2	3	1.5g
SOK2 IP 1	2	1.5g
SOK2 IP 2	2	1.5g
SOK3 IP 1	3	1.5g
SOK2 IP 3	3	1.8g
SOK3 IP 2	2	1.8g
SOK1ΔDIX IP	3	1.4g
AN	3	1.2g
SIB1	3	1.3g
DLC1	3	1.3g

Microscopy

A Leica SP5 or SP8 confocal microscope was used for imaging. The SP5 was equipped with an Argon laser and DSS561 diode laser, the SP8 with a pulsed white light laser. GFP was excited at 488nm, YFP at 514nm, and Propidium Iodide and TdTomato at 561nm. Filters were set at 500-550 for GFP, 520-550nm for YFP, 570-600 for TdTomato and 600-650 nm for Propidium Iodide. If samples contained multiple fluorescent markers, sequential scanning was used to prevent bleed-through.

BiFC

Agrobacterium containing BiFC plasmids were grown overnight in 5ml LB + 20mg/L Gentamycin, 50mg/L Kanamycin, 25mg/L Rifampicin and 2mg/L Tetracyclin. Cultures were spun down at 4000rpm for 10 minutes and the bacterial pellet was resuspended in 1 mL MMAi (5g/L MS salts without vitamins, 2g/L MES, 20g/L sucrose, pH 5.6, 0.2 mM Acetosyringone). The OD₆₀₀ was measured with a spectrophotometer. The infiltration samples were mixed 1:1 at a total OD₆₀₀ of 0.8. Samples were incubated at room temperature (RT) for 2 hours and infiltrated into the underside of *Nicotiana benthamiana* leaves with a 1mL syringe. After two days, leaf samples were cut out with a razor blade and imaged with a confocal microscope.

FLIM

Protoplast transfection and FLIM measurements were performed as described in Rios et al., 2017.

Acknowledgements

We'd like to express our thanks to J.W. Borst for his help with FRET-FLIM and confocal imaging. Also, thanks to S. Boeren for his advice on Mass-Spec preparation and for measuring the IP samples, and Mark Roosjen for assisting with data analysis and the volcano plots. Our appreciation also goes to C-Y. Liao for providing the pRPS5a::LIC-YFP cloning vector and Hirokazu Tsukaya for sending the 35S::AN-GFP line. This work was funded by a grant from the Netherlands Organization for Scientific Research (NWO; ALW-Topsector grant 831.13.001)

References

Alassimone, J., Fujita, S., Doblas, V. G., Van Dop, M., Barberon, M., Kalmbach, L. et al. (2016). Polarly localized kinase SGN1 is required for Casparyan strip integrity and positioning. *Nature Plants*, 2, 1–10.

Aranda, S., Laguna, A., & de la Luna, S. (2011). DYRK family of protein kinases: evolutionary relationships, biochemical properties, and functional roles. *The FASEB Journal*, 25, 449–462.

Avisar, D., Abu-Abied, M., Belausov, E., & Sadot, E. (2012). Myosin XIK is a major player in cytoplasm dynamics and is regulated by two amino acids in its tail. *Journal of Experimental Botany*, 63, 241–249.

Berleth, T., & Jürgens, G. (1993). The role of the monopteros gene in organising the basal body region of the *Arabidopsis* embryo. *Development*, 118, 575–587.

Besson, S., & Dumais, J. (2011). Universal rule for the symmetric division of plant cells. *Proceedings of the National Academy of Sciences of the United States of America*, 108, 2011.

Bhasin, H., & Hülskamp, M. (2017). ANGUSTIFOLIA, a Plant Homolog of CtBP/BARS Localizes to Stress Granules and Regulates Their Formation. *Frontiers in Plant Science*, 8, 1–17.

Breuninger, H., Rikirsch, E., Hermann, M., Ueda, M., & Laux, T. (2008). Differential expression of WOX genes mediates apical-basal axis formation in the *Arabidopsis* embryo. *Developmental Cell*, 14, 867–876.

Cheng, Y., Qin, G., Dai, X., & Zhao, Y. (2007). NPY1, a BTB-NPH3-like protein, plays a critical role in auxin-regulated organogenesis in *Arabidopsis*. *Proceedings of the National Academy of Sciences*, 104, 18825–18829.

Christie, J., Suetsugu, N., Sullivan, S., & Wada, M. (2017). Shining Light on the Function of NPH3/RPT2-like Proteins in Phototropin Signalling. *Plant Physiology*, pp.00835.2017.

Chuang, J. Z., Yeh, T. Y., Bollati, F., Conde, C., Canavosio, F., Caceres, A., & Sung, C. H. (2005). The dynein light chain tctex-1 has a dynein-independent role in actin remodeling during neurite outgrowth. *Developmental Cell*, 9, 75–86.

Consortium, A. I. M. C. (2011). Evidence for Network Evolution in an *Arabidopsis* Interactome Map, 334, 1372–1378.

De Rybel, B., van den Berg, W., Lokerse, A. S., Liao, C.-Y., van Mourik, H., Moller, B. et al. (2011). A Versatile Set of Ligation-Independent Cloning Vectors for Functional Studies in Plants. *Plant Physiology*, 156, 1292–1299.

De Smet, I., Lau, S., Mayer, U., & Jürgens, G. (2010). Embryogenesis - The humble beginnings of plant life. *Plant Journal*, 61, 959–970.

Dong, J., MacAlister, C. A., & Bergmann, D. C. (2009). BASL Controls Asymmetric Cell Division in *Arabidopsis*. *Cell*, 137, 1320–1330.

Duan, Z., & Tominaga, M. (2018). Actin-myosin XI: An intracellular control network in plants. *Biochemical and Biophysical Research Communications*, 1–6.

Farrell, K. B., McDonald, S., Lamb, A. K., Worcester, C., Peersen, O. B., & Di Pietro, S. M. (2017). Novel function of a dynein light chain in actin assembly during clathrin-mediated endocytosis. *The Journal of Cell Biology*, 216, 2565–2580.

Fisher, K., & Turner, S. (2007). PXY, a receptor-like kinase essential for maintaining polarity during plant vascular-tissue development. *Current Biology*, 17, 1061–1066.

Folkers, U., Kirik, V., Schöbinger, U., Falk, S., Krishnakumar, S., Pollock, M. A. et al. (2002). The cell morphogenesis gene *ANGUSTIFOLIA* encodes a CtBP/BARS-like protein and is involved in the control of the microtubule cytoskeleton. *The EMBO Journal*, 21, 1280–1288.

Friml, J., Yang, X., Michniewicz, M., Weijers, D., Quint, A., Tietz, O. et al. (2004). A PINOID-dependent binary switch in apical-basal PIN polar targeting directs auxin efflux. *Science*, 306, 862–865.

Furutani, M., Kajiwara, T., Kato, T., Treml, B. S., Stockum, C., Torres-Ruiz, R. A., & Tasaka, M. (2007). The gene MACCHI-BOU 4/ENHANCER OF PINOID encodes a NPH3-like protein and reveals similarities between organogenesis and phototropism at the molecular level. *Development*, 134, 3849–3859.

Furutani, M., Sakamoto, N., Yoshida, S., Kajiwara, T., Robert, H. S., Friml, J., & Tasaka, M. (2011). Polar-localized NPH3-like proteins regulate polarity and endocytosis of PIN-FORMED auxin efflux carriers. *Development*, 138, 2069–2078.

Gälweiler, L., Guan, C., Müller, a., Wisman, E., Mendgen, K., Yephremov, a., & Palme, K. (1998). Regulation of polar auxin transport by AtPIN1 in *Arabidopsis* vascular tissue. *Science*, 282, 2226–2230.

Harrison, C. J., Roeder, A. H. K., Meyerowitz, E. M., & Langdale, J. a. (2009). Local cues and asymmetric cell divisions underpin body plan transitions in the moss *Physcomitrella patens*. *Current Biology*, 19, 461–471.

Heidari, B., Matre, P., Nemie-Feyissa, D., Meyer, C., Rognli, O. A., Møller, S. G., & Lillo, C. (2011). Protein phosphatase 2A B55 and A regulatory subunits interact with nitrate reductase and are essential for nitrate reductase activation. *Plant Physiology*, 156, 165–172.

Hervieux, N., Tsugawa, S., Fruleux, A., Dumond, M., Routier-Kierzkowska, A. L., Komatsuzaki, T. et al. (2017). Mechanical Shielding of Rapidly Growing Cells Buffers Growth Heterogeneity and Contributes to Organ Shape Reproducibility. *Current Biology*, 27, 3468–3479.

Huang, J., Fujimoto, M., Fujiwara, M., Fukao, Y., Arimura, S. I., & Tsutsumi, N. (2015). *Arabidopsis* dynamin-related proteins, DRP2A and DRP2B, function coordinately in post-Golgi trafficking. *Biochemical and Biophysical Research Communications*, 456, 238–244.

Jürgens, G. (2003). Growing up green: cellular basis of plant development. *Mechanisms of Development*, 120, 1395–1406.

Kettenbach, A. N., Deng, L., Wu, Y., Baldissard, S., Adamo, M. E., Gerber, S. A., & Moseley, J. B. (2015). Quantitative Phosphoproteomics Reveals Pathways for Coordination of Cell Growth and Division by the Conserved Fission Yeast Kinase Pom1. *Molecular & Cellular Proteomics*, 14, 1275–1287.

Kim, D., Ntui, V. O., Zhang, N., & Xiong, L. (2015). *Arabidopsis* Yak1 protein (AtYak1) is a dual specificity protein kinase. *FEBS Letters*, 589(21), 3321–3327.

Kim, G. T., Shoda, K., Tsuge, T., Cho, K. H., Uchimiya, H., Yokoyama, R. et al. (2002). The *ANGUSTIFOLIA* gene of *Arabidopsis*, a plant CtBP gene, regulates leaf-cell expansion, the arrangement of cortical microtubules in leaf cells and expression of a gene involved in cell-wall formation. *EMBO Journal*, 21, 1267–1279.

Kleine-Vehn, J., Huang, F., Naramoto, S., Zhang, J., Michniewicz, M., Offringa, R., & Friml, J. (2009). PIN Auxin Efflux Carrier Polarity Is Regulated by PINOID Kinase-Mediated Recruitment into GNOM-Independent Trafficking in *Arabidopsis*. *The Plant Cell*, 21, 3839–3849.

Kleine-Vehn, J., Wabnik, K., Martinière, A., Langowski, L., Willig, K., Naramoto, S. et al. (2011). Recycling, clustering, and endocytosis jointly maintain PIN auxin carrier polarity at the plasma membrane. *Molecular Systems Biology*, 7, 1–13.

Kleinmanns, J. A., Schatłowski, N., Heckmann, D., & Schubert, D. (2017). BLISTER Regulates Polycomb-Target Genes, Represses Stress-Regulated Genes and Promotes Stress Responses in *Arabidopsis thaliana*. *Frontiers in Plant Science*, 8, 1–14.

Langowski, L., Wabnik, K., Li, H., Vanneste, S., Naramoto, S., Tanaka, H., & Friml, J. (2016). Cellular mechanisms for cargo delivery and polarity maintenance at different polar domains in plant cells. *Cell Discovery*, 2.

Lau, S., Slane, D., Herud, O., Kong, J., & Jürgens, G. (2012). Early embryogenesis in flowering plants: setting up the basic body pattern. *Annual Review of Plant Biology*, 63, 483–506.

Louveaux, M., Julien, J.-D., Mirabet, V., Boudaoud, A., & Hamant, O. (2016). Cell division plane orientation based on tensile stress in *Arabidopsis thaliana*. *Proceedings of the National Academy of Sciences*, 113, E4294–E4303.

Madrzak, J., Fiedler, M., Johnson, C. M., Ewan, R., Knebel, A., Bienz, M., & Chin, J. W. (2015). Ubiquitination of the Dishevelled DIX domain blocks its head-to-tail polymerization. *Nature Communications*, 6, 1–11.

Michniewicz, M., Zago, M. K., Abas, L., Weijers, D., Schweighofer, A., Meskiene, I. et al. (2007). Antagonistic Regulation of PIN Phosphorylation by PP2A and PINOID Directs Auxin Flux. *Cell*, 130, 1044–1056.

Minamisawa, N., Sato, M., Cho, K. H., Ueno, H., Takechi, K., Kajikawa, M. et al. (2011). ANGUSTIFOLIA, a plant homolog of CtBP/BARS, functions outside the nucleus. *Plant Journal*, 68, 788–799.

Minc, N., Burgess, D., & Chang, F. (2011). Influence of cell geometry on division-plane positioning. *Cell*, 144, 414–426.

Minc, N., & Piel, M. (2012). Predicting division plane position and orientation. *Trends in Cell Biology*, 22, 193–200.

Mravec, J., Petrášek, J., Li, N., Boeren, S., Karlova, R., Kitakura, S. et al. (2011). Cell plate restricted association of DRP1A and PIN proteins is required for cell polarity establishment in *arabidopsis*. *Current Biology*, 21, 1055–1060.

Mulekar, J. J., & Huq, E. (2014). Expanding roles of protein kinase CK2 in regulating plant growth and development. *Journal of Experimental Botany*, 65, 2883–2893.

Nakamura, M., & Grebe, M. (2018). Outer, inner and planar polarity in the *Arabidopsis* root. *Current Opinion in Plant Biology*, 41, 46–53.

Ojangu, E. L., Järve, K., Paves, H., & Truve, E. (2007). *Arabidopsis thaliana* myosin XIK is involved in root hair as well as trichome morphogenesis on stems and leaves. *Protoplasma*, 230, 193–202.

Oparka, K. J., Roberts, A. G., Boevink, P., Cruz, S. S., Roberts, I., Pradel, K. S. et al. (1999). Simple, but not branched, plasmodesmata allow the nonspecific trafficking of proteins in developing tobacco leaves. *Cell*, 97, 743–754.

Peremyslov, V. V., Prokhnevsky, A. I., & Dolja, V. V. (2010). Class XI Myosins Are Required for Development, Cell Expansion, and F-Actin Organization in *Arabidopsis*. *The Plant Cell*, 22, 1883–1897.

Rapali, P., Szenes, Á., Radnai, L., Bakos, A., Pál, G., & Nyitrai, L. (2011). DYNLL/LC8: A light chain subunit of the dynein motor complex and beyond. *FEBS Journal*, 278, 2980–2996.

Rios, A. F., Radoeva, T., Rybel, B. De, Weijers, D., & Borst, J. W. (2017). FRET-FLIM for Visualizing and Quantifying Protein Interactions in Live Plant Cells, 1497, 135–146.

Roberts, D., Pedmale, U. V., Morrow, J., Sachdev, S., Lechner, E., Tang, X. et al. (2011). Modulation of Phototropic Responsiveness in *Arabidopsis* through Ubiquitination of Phototropin 1 by the CUL3-Ring E3 Ubiquitin Ligase CRL3NPH3. *The Plant Cell*, 23, 3627–3640.

Robinson, S., Barbier de Reuille, P., Chan, J., Bergmann, D., Prusinkiewicz, P., & Coen, E. (2011). Generation of spatial patterns through cell polarity switching. *Science*, 333, 1436–1440.

Sahlin, P., & Jönsson, H. (2010). A modeling study on how cell division affects properties of epithelial tissues under isotropic growth. *PloS One*, 5, e11750.

Schatlowski, N., Stahl, Y., Hohenstatt, M. L., Goodrich, J., & Schubert, D. (2010). The CURLY LEAF Interacting Protein BLISTER Controls Expression of Polycomb-Group Target Genes and Cellular Differentiation of *Arabidopsis thaliana*. *The Plant Cell Online*, 22, 2291–2305.

Shiu, S., Karlowski, W., & Pan, R. (2004). Comparative analysis of the receptor-like kinase family in *Arabidopsis* and rice. *The Plant Cell*, 16, 1220–1234.

Soppa, U., & Becker, W. (2015). DYRK protein kinases. *Current Biology*, 25, R488–R489.

Spinner, L., Gadeyne, A., Belcram, K., Goussot, M., Moison, M., Duroc, Y. et al. (2013). A protein phosphatase 2A complex spatially controls plant cell division. *Nature Communications*, 4, 1863.

Stogios, P. J., Downs, G. S., Jauhal, J. J. S., Nandra, S. K., & Privé, G. G. (2005). Sequence and structural analysis of BTB domain proteins. *Genome Biology*, 6, R82.

Takano, J., Noguchi, K., Yasumori, M., Kobayashi, M., Gajdos, Z., Miwa, K. et al. (2002). *Arabidopsis* boron transporter for xylem loading. *Nature*, 420, 337–340.

Takano, J., Tanaka, M., Toyoda, A., Miwa, K., Kasai, K., Fuji, K. et al. (2010). Polar localization and degradation of *Arabidopsis* boron transporters through distinct trafficking pathways. *Proceedings of the National Academy of Sciences of the United States of America*, 107, 5220–5225.

Ueda, H., Yokota, E., Kutsuna, N., Shimada, T., Tamura, K., Shimmen, T. et al. (2010). Myosin-dependent endoplasmic reticulum motility and F-actin organization in plant cells. *Proceedings of the National Academy of Sciences*, 107, 6894–6899.

Vatén, A., & Bergmann, D. C. (2012). Mechanisms of stomatal development: an evolutionary view. *EvoDevo*, 3, 11.

Walia, A., Nakamura, M., Moss, D., Kirik, V., Hashimoto, T., & Ehrhardt, D. W. (2014). GCP-WD mediates γ -TuRC recruitment and the geometry of microtubule nucleation in interphase arrays of *arabidopsis*. *Current Biology*, 24, 2548–2555.

Wan, Y., Jasik, J., Wang, L., Hao, H., Volkmann, D., Menzel, D. et a. (2012). The Signal

Transducer NPH3 Integrates the Phototropin1 Photosensor with PIN2-Based Polar Auxin Transport in Arabidopsis Root Phototropism. *The Plant Cell*, 24, 551–565.

Wang, S., Yoshinari, A., Shimada, T., Hara-Nishimura, I., Mitani-Ueno, N., Feng Ma, J. et al. (2017). Polar Localization of the NIP5;1 Boric Acid Channel Is Maintained by Endocytosis and Facilitates Boron Transport in Arabidopsis Roots. *The Plant Cell*, 29, 824–842.

Wendrich, J. R., Boeren, S., Möller, B. K., Weijers, D., & Rybel, B. De. (2017). In Vivo Identification of Plant Protein Complexes Using IP-MS/MS. *Plant Hormones: Methods and Protocols, Methods in Molecular Biology*, 1497, 147–158.

Wisniewska, J., Xu, J., Seifertova, D., Brewer, P. B., Ru, K., Scheres, B. et al. (2006). Polar PIN Localization Directs Auxin, 312, 2006.

Yamada, M., & Goshima, G. (2017). Mitotic Spindle Assembly in Land Plants: Molecules and Mechanisms. *Biology*, 6, 6.

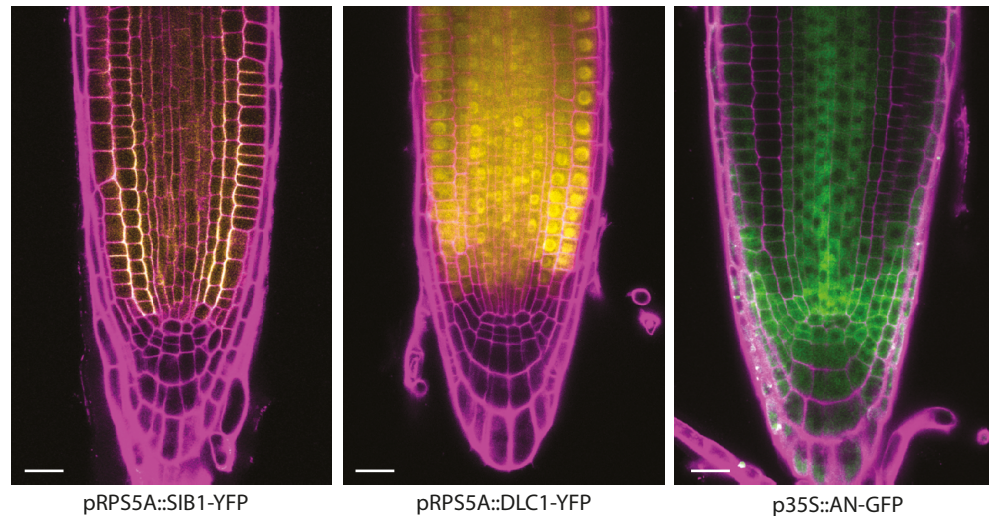
Yoshida, S., Reuille, P. B. De, Lane, B., Bassel, G. W., Prusinkiewicz, P., Smith, R. S., & Weijers, D. (2014). Genetic Control of Plant Development by Overriding a Geometric Division Rule. *Developmental Cell*, 29, 75–87.

Yoshinari, A., Fujimoto, M., Ueda, T., Inada, N., Naito, S., & Takano, J. (2016). DRP1-dependent endocytosis is essential for polar localization and boron-induced degradation of the borate transporter BOR1 in arabidopsis thaliana. *Plant and Cell Physiology*, 57, 1985–2000.

Zeng, C. J. T., Lee, Y.-R. J., & Liu, B. (2009). The WD40 Repeat Protein NEDD1 Functions in Microtubule Organization during Cell Division in Arabidopsis thaliana. *The Plant Cell*, 21, 1129–1140.

Zhang, Y., Werling, U., & Edelmann, W. (2012). SLiCE: A novel bacterial cell extract-based DNA cloning method. *Nucleic Acids Research*, 40, 1–10.

Supplemental information



Supplemental Figure 1. Over-/misexpression lines of *SOK* interactors. Protein fusions of interactors with YFP or GFP.

Supplemental Table 1. Number of IPs interactors have been identified in \ number of IPs performed.

Interactor	Gene #	Bait		
		<u>SOK1</u>	<u>SOK2</u>	<u>SOK3</u>
AN	at1g01510	2 \ 2	3 \ 3	2 \ 2
SOK4	At3g46110	1 \ 2	0 \ 3	0 \ 2
SIK1/2	AT1G73460/50	2 \ 2	3 \ 3	2 \ 2
SIK3	AT3g17750	1 \ 2	2 \ 3	1 \ 2
SIB1	At1g30440	2 \ 2	0 \ 3	0 \ 2
DLC1	At4g15930	1 \ 2	1 \ 3	2 \ 2
SOK3	At2g28150	2 \ 2	2 \ 3	x
PP2aB beta	AT1G17720	0 \ 2	2 \ 3	0 \ 2
PP2aB alpha	AT1G51690	0 \ 2	2 \ 3	0 \ 2
DLC2	At1g23220	0 \ 2	0 \ 3	2 \ 2

Supplemental Table 2. Primers used in this study.

<i>Genomic fusions</i>	
AN FW	tagttgaaatgggttctacaaccaaatcgaccaca
AN RV	ttatggagttgggttccatcgatccaacgtgtatac
SIB1 FW	tagttgaaatgggttcagaatctaaagacataagg
SIB1 RV	ttatggagttgggttcccctcagaactaatgctcg
SIK2 FW	tagttgaaatgggttcacaactgggtctttactta
SIK2 RV	ttatggagttgggttccagcagagattgggtcgat
SIK3 FW	tagttgaaatgggttctacatccaccggaaaaaaca
SIK3 RV	ttatggagttgggttccggcagatatgggtcgtag
DLC1 FW	tagttgaaatgggttctttatattatacacaag
DLC1 RV	ttatggagttgggttccaccgacttgaagagcagc
SIK4 FW	tagttgaaatgggttcggcagagaaccttatgagt
SIK4 RV	ttatggagttgggttctgcctgaagattcaatttttc
<i>Over-expression</i>	
FW primers were the same as the FLIM FW primers.	
ANGUSTIFOLIA RV	agtatggagttgggttcgcacatcgatccaacgtgtatacc
DLC1 RV	agtatggagttgggttcgcacccgacttgaagagcagcacag
SIB1 RV	agtatggagttgggttcgcctctcagaactaatgctcg
<i>Promoter fusions</i>	
DLC1 promoter FW	tagttgaaatgggttcaaagagagaaaaggaaagag
DLC1 promoter RV	ttatggagttgggttcttttttttcagtttcctc
SIB1 promoter FW	tagttgaaatgggttcagaatctaaagacataag
SIB1 promoter RV	ttatggagttgggttctttcttcaccagaattc
SIK3 AT3G17750 promoter FW	tagttgaaatgggttcgattctgtattttttg
SIK3 AT3G17750 promoter RV	ttatggagttgggttctcccaaatctctagaac
SIK2 AT1G73460 promoter FW	tagttgaaatgggttcccttagtttgtcatttg
SIK2 AT1G73460 promoter RV	ttatggagttgggttacaatatacaggagaag

FLIM

DIX1 FW	tagttggaatagggtcatggaaagtaatggtggag
DIX1 RV	agtatggagttgggttcctccttggagagcttag
SOK1 FLIM FW	tagttggaatagggtcatggaaagtaatggtggaggag
SOK1 FLIM RV	agtatggagttgggttcctccttggagagcttag
SOK2 FLIM FW	tagttggaatagggtcatggaaagctgtaaagatgcagaag
SOK2 FLIM RV	agtatggagttgggttcctccttggagagcttag
ANGUSTIFOLIA FLIM FW	tagttggaatagggtcatggaaagatccgtcgatc
ANGUSTIFOLIA FLIM RV	agtatggagttgggttcctccttggagagcttag
DLC1 FLIM FW	tagttggaatagggtcatggaaacccgacttggaggagaaag
DLC1 FLIM RV	agtatggagttgggttcctccttggagagcttag
SIB1 FLIM FW	tagttggaatagggtcatggaaacccgacttggaggagaaag
SIB1 FLIM RV	agtatggagttgggttcctccttggaggagaaag

BiFC*C-terminal fusions*

FW primers were the same as FLIM FW primers

DIX BifC RV	agtatggagttgggttcactccttggagagcttag
SOK1 BifC RV	agtatggagttgggttcactccttggagagcttag
SOK2 BifC RV	agtatggagttgggttcactccttggagagcttag
ANGUSTIFOLIA BifC RV	agtatggagttgggttcactccttggagagcttag
DLC1 BifC RV	agtatggagttgggttcactccttggagagcttag
SIB1 BifC RV	agtatggagttgggttcactccttggagagcttag

N-terminal fusions

FW primers were the same as FLIM FW primers

SOK3 for BiFC FW	tagttggaatagggtcatggaaagcgaggatgaagaag
SOK1 N-term BiFC RV	agtatggagttgggttcactccttggagagcttag
SOK2 N-term BiFC RV	agtatggagttgggttcactccttggagagcttag
SOK3 N-term BiFC RV	agtatggagttgggttcactccttggagagcttag
AN N-term BiFC RV	agtatggagttgggttcactccttggagagcttag
SIB1 N-term BiFC RV	agtatggagttgggttcactccttggagagcttag
DLC1 N-term BiFC RV	agtatggagttgggttcactccttggagagcttag
DIX N-term BiFC RV	agtatggagttgggttcactccttggagagcttag

Chapter 7

General Discussion

General Discussion

Generating, interpreting and translating cell polarity information is essential for plant morphogenesis and survival (reviewed in Nakamura & Grebe, 2018; Van Norman, 2016). However, how these processes are accomplished largely remains a mystery. In **Chapter 1 and 2**, we discussed the *Arabidopsis* embryo as a model to study cell polarity. The embryo develops from a single-celled zygote that depolarizes after fertilization and subsequently re-establishes apico-basal polarity (Faure et al., 2002; Ueda et al., 2011). The first cell divisions are predictable, and recent work revealed the stages where cell starts to deviate from geometrically-defined cell division planes, probably by integrating cell polarity into the division (Yoshida et al., 2014). Incorrect establishment and translation of polarity has a great impact on embryogenesis, as it leads to incorrect divisions and often lethality (Lukowitz et al., 2004; Ueda et al., 2011; Wang et al., 2007; Yoshida et al., 2014). Thus, mutants that are affected in fundamental polarity pathways are not likely to survive past the young embryo stage, which makes the embryo an attractive model for identifying and studying polarity factors. Polarly localized proteins provide an essential tool for studying mechanisms underlying cell polarity in the embryo and throughout the plant. As we summarize in **Chapter 1**, several polar proteins have been identified, but the unstable nature of their localization makes them less suitable for devising the underlying fundamental polarity principles. In **Chapter 3**, we identified a family of five polar proteins that robustly localize to cell edges. These SOSEKI (SOK) proteins had not been described before and their function was unknown. Therefore, we set out to unravel the localization mechanism, function and evolution of these proteins.

Transcriptional regulation of SOK genes

The SOK protein family was discovered in a transcriptome profiling experiment aimed at identifying downstream targets of the auxin-dependent transcription factor ARF5/MONOPTEROS (MP) in the embryo. Two *SOK* genes were downregulated in this experiment: *SOK1* (7.5 fold) and *SOK5* (2.4 fold, **Chapter 3**). Expression of *SOK1* in lines with locally inhibited MP was greatly reduced (Möller et al., 2017) and its expression pattern overlaps with MP both in the embryo and root (Rademacher et al., 2011). This suggests that *SOK1* could be a direct target of MP. Yet, *SOK1* expression is restricted to the vascular initials in the heart stage embryo, while MP expression is much broader. Therefore, either other transcription factors are involved in controlling *SOK1* expression, or the *SOK1* gene is only activated in cells within the MP expression domain with the highest auxin levels, and thus maximal MP activity. *SOK5* expression only partially overlaps with MP in the embryo and root, and the other *SOK* family members show partial overlap or none at all. In **Chapter 4**, we further explored SOK expression patterns in various parts of the

plant. We discovered the presence of SOK2 and 3 in the leaf epidermis, yet MP was only reported to be expressed in mesophyll cells (Zhang et al., 2014), and thus MP-dependent expression is likely to be restricted only to some family members. QPCR analysis of the *sok1* deletion mutant revealed upregulation of mainly *SOK4* in the root, which might be a compensation mechanism (Chapter 4). This potential feedback loop suggests the presence of a mechanism that monitors SOK expression and/or protein levels or activity and modifies expression of other SOK family members. Interestingly, *SOK4* is very weakly expressed in the vasculature, like *SOK1*. *SOK3* is also present in the vasculature, yet expression of this gene remained unchanged. Thus, the feedback mechanism shows a preference for upregulating a specific SOK family member. It is unknown how this specificity is accomplished and which transcription factors are involved. Taken together, SOK transcriptional regulation requires additional or alternative transcription factors than MP. These transcription factors may be of the ARF family, but promoter analysis might reveal binding elements for other transcription factors as well. SOK is also expressed in moss and liverwort (Chapter 5), yet their transcriptional control remains to be investigated. Both basal lineages contain ARFs, which may be involved in regulating SOK transcription (Mutte et al., 2018).

Finding the edge

The SOK family is not only striking because the proteins all localize to cell edges in the embryo and root, but even more so because most family members only select one edge out of the multiple available ones in *Arabidopsis* (Chapter 3). This behavior leads to the question how SOK proteins are localized. In most cells, SOK seems to appear directly in its polar domain, rather than being broadly targeted to the PM and then restricted. Disruption of canonical sub-cellular trafficking pathways and the cytoskeleton did not alter SOK localization (Chapter 3). This suggests that SOK does not depend on pathways commonly used for localization of polar proteins. The direct interactome of SOK1 to 3 did not reveal any candidates with a known role in protein transport or localization in plants (Chapter 6). The extended network contained several proteins involved in cytoskeleton dynamics and transport. However, as SOK edge localization does not depend on the cytoskeleton, these interactors probably act downstream or in independent processes.

Unfortunately, very little is known about the properties of cell edges in plants and how they could influence protein localization. That edges are significant for protein localization is not only indicated by SOK, but also by several other proteins. Microtubule-associated protein CLASP for example has been reported to localize at cell edges (Ambrose et al., 2011). In addition, the Ras-like small GTPase RAB-A5c localizes in vesicles that are relatively immobile at, and thus potentially attached

to, the cell edges in young meristematic cells (Kirchhelle et al., 2016). The plasma membrane (PM) at cell edges is strongly curved, which presents an environment with different mechanical properties than cell faces. In addition, (phospho)lipids and other molecules could preferentially accumulate in these curved areas, which would provide local signaling or anchor points, or differences in PM charge. All these properties would enable distinction between cell faces and edges, and allow proteins to localize to all edges. Several phosphoinositides (PIs) are an important part of the PM and can influence membrane charge and mechanical properties, such as membrane curvature. They are amongst others involved in sub-cellular trafficking and localization of proteins (reviewed in Noack & Jaillais, 2017). PI(4)P was shown to drive the electrostatic field across the PM, which in turn is required for PM localization of the membrane proteins PID and MAKR2 (Simon et al., 2016). Available markers for specific PI species did not show any preferential accumulation in cell edges (Simon et al., 2014). This suggests that PIs cannot provide the information required for edge localization of proteins. However, it is possible that subtle but biologically significant differences in PI distribution are not revealed by current methods. Inhibition of PI3K and PI4K with Wortmannin (Matsuoka et al., 1995) did not alter SOK localization (**Chapter 3**), which suggests that PI(3)P and PI(4)P are not involved in SOK localization. Sterols are another class of molecules that form an integral part of the PM. Correct membrane sterol composition has been shown to be required for correct polar PIN2 localization by influencing endocytosis (Men et al., 2008). Inhibition of endocytosis did not influence SOK localization (**Chapter 3**), and it has not been shown that cell edges form distinct sites of sterol accumulation (reviewed in Valitova et al., 2016). Reports on consistent edge accumulation of other small PM molecules are also lacking. Taken together, aside from membrane curvature, it remains unclear if and what additional properties allow proteins to distinguish between cell faces and cell edges.

Four out of five *Arabidopsis* SOK proteins and the polar *Physcomitrella* SOK accumulate at a specific cell edge, while AtSOK3 localizes to all edges (**Chapter 3, 5**). As such, SOK3 may use a relatively simple mechanism for its localization, while the other SOK proteins must further refine their localization to accumulate in only one edge. We showed that SOK1 integrates apico-basal with lateral polarity cues to guide its localization (**Chapter 3**) and other SOK family members may use a similar mechanism. The moss experiments in **Chapter 5** revealed that at least one of the *Physcomitrella* SOKs also localizes to one cell edge, which implies that the underlying polarity mechanism is conserved throughout evolution. The information that polarity integration should lead to edge localization of SOK is encoded in a region in the middle of the protein, at least in *Arabidopsis* (**Chapter 3**). This region is very different between the SOK family members, which could explain the differences in localization. The SOK localization domain contains a putative palmitoylation site, which could target SOK to the membrane (**Chapter 5**). However, it remains unclear

how this protein region directs localization to a certain cell edge. The domain may for example be involved in sub-cellular trafficking of the protein, interaction with other polarly localized proteins or direct interaction with the PM. If SOK depends on yet unknown delivery, retention and/or recycling mechanisms, the localization domain may determine which pathway is taken. How these pathways distinguish between the different membrane edges then becomes the next question. SOK may also select its edge by interacting with proteins that are already localized at said edge. Our IP-MS experiments did not reveal any interactors that showed the same robust polar localization as the SOK proteins (Chapter 6). However, these experiments probably did not cover all SOK interactors. Especially those that are in low abundance or difficult to pull down may not have shown in our results.

Whether it is SOK or an interactor that localizes to a specific cell edge first, the protein and/or delivery mechanism must be able to distinguish between the different cell edges. This hypothesis implies that each edge can consistently be distinguished from the other. The simple fact that the membrane is curved at a cell edge cannot be sufficient for selection of one edge, as this curvature applies to all cell corners. The angle of curvature is also not instructive enough, as these angles can be quite different in different cells, yet SOK polarity is consistent in a given plane. In addition, mis-expression of SOK1 showed that the protein always has the same polarity in the endodermis and cortex, regardless of whether oblique divisions generated cells with sharp or shallow angles (Chapter 3). If membrane curvature cannot be the determining factor for localization, local PM charge, mechanical properties or composition may be important. However, as discussed before, it is unknown whether lipids or other molecules accumulate preferentially in certain cell edges. An alternative model for specific edge selection of SOK does not involve asymmetry in the cell edges, but relies on sensing and interpreting mobile cytoplasmic signals from neighboring cells, such as hormones. An example of such a mechanism is the establishment of a polar domain involved in root hair formation. Here, directional transport of the hormone auxin is thought to provide a gradient within the cell, which is used to position the ROP domain (Fischer et al., 2006; Payne & Grierson, 2009). SOK uses both lateral and apico-basal information to determine its localization (Chapter 3). This could entail integration of two gradients of mobile signals, one originating from lateral transport and one from apical or basal transport. SOK or proteins involved in SOK localization may sense these gradients and position SOK e.g. towards or away from them. However, most cells that contain SOK are relatively small, which would not allow large differences in gradient. Additionally, cytoplasmic streaming will probably move and mix up the signals, which will make the directional information unreadable.

Taken together, cell edges are significant for the localization and function of certain proteins, yet they have been poorly studied. Their small size and the fact that they are often embedded in tissues and organs makes detailed investigation difficult. Yet, the constant improvement of experimental techniques and use of new model systems will hopefully shed more light on the properties of cell edges and processes that occur there.

The endodermis-cortex junction as a positional cue

In **Chapter 3**, we showed that SOK1 localizes to the outer-apical edge in young vascular cells. When mis-expressed, it uses the endodermis-cortex junction as a positional cue: in the epidermis and cortex the protein flips towards the inner-apical edge of the cell. Interestingly, we identified a module of laterally-localizing proteins as putative interactors of SOK1 (**Chapter 6**). SIB 1 localizes to the inner side of the cell in the epidermis and cortex. In other tissue layers, the polarity is difficult to determine, as the localization of SIB1 is fuzzy and strictly lateral if polar. Often, SIB1 was observed facing both sides of the endodermis-cortex junction, which suggests that it may make a similar polarity flip as SOK1. The secondary interactor SIK4 behaved in the same way. We did not analyze SIRLK1, but family members of this Receptor-Like Kinase localize laterally and use the endodermis-cortex junction as an orientation point (Jaimie van Norman, personal communication). In addition, the laterally-localized SGN1 kinase also faces the endodermis-cortex junction when mis-expressed (Alassimone et al., 2016). Taken together, these findings suggest the presence of a radial polarity field that can be read and interpreted by a variety of laterally-localized proteins. This polarity field uses the cortex-endodermis junction as a focal point, which raises the question how this focal point is established. Whatever mechanism is responsible, it likely involves a signal that spans more than just the endodermis and cortex. It is unknown whether there is a difference in for example composition between the cortex-endodermis junction and other junctions that can be sensed and relayed. Alternatively, these junctions may simply happen to be the point where unknown radial signals converge. Mechanical forces may play a role, but little is known about such forces across the root. Gradients of hormones or other mobile factors might also be instructive. As several proteins respond to a polarity cue in the same way, the underlying mechanism that translates this polarity in localization might be shared. Unraveling the nature of the radial polarity field and the mechanisms that use this field to guide polar localization would provide a great insight into plant polarity.

Clustering to achieve high local protein concentrations

Delivering a protein to the correct part of the PM is a first step towards establishing polar localization. Once on the membrane, spreading of the protein outside of its intended domain must be prevented. This can be achieved by restriction of lateral diffusion and/or protein recycling at the edges of the polar domain. Physical barriers may prevent lateral diffusion, but evolution also devised another way: protein clustering. Sticking proteins or protein complexes together generates larger protein patches that are less likely to diffuse. These patches recruit more proteins, which reinforces polar localization. In plants, the CASPs are an excellent example of such a process. CASP family members interact with each other, polymerize into patches and capture more CASP proteins as they arrive, which results in an immobile ring-shaped lattice (Roppolo et al., 2011). Our experiments revealed that SOK uses a similar mechanism to achieve its robust polar localization, as we identified a domain responsible for SOK clustering. Without this DIX-LIKE domain, SOK spreads out over the membrane, which shows that there are no other strong barriers to its lateral diffusion (**Chapter 3**). The DIX-LIKE domain is the most highly conserved domain in plant SOKs and is also found in animal and SAR group proteins. In animals, DIX polymerizes in an autocatalytic fashion (Schwarz-Romond et al., 2007). We showed that the DIX-LIKE has very similar polymerization behavior in plants and the SAR group (**Chapter 5**). The autocatalytic polymerization of DIX-LIKE ensures formation of a high local concentration of SOK proteins. Although docking on and off the polymer may be a dynamic process, the overall result is a patch of proteins that is difficult to move or disrupt compared to other polar plant proteins. DIX-LIKE-mediated clustering is also essential for SOK function, as removal of DIX-LIKE domain results in loss of interactors (**Chapter 6**) and of the oblique cell division phenotype (**Chapter 3**). A similar case was observed in animals, where over-expression of DIX-containing Dvl resulted in the formation puncta and formation of these local highly concentrated protein assemblies was required for Dvl function in signaling (Schwarz-Romond et al., 2007). Thus, the autocatalytic clustering of DIX(-LIKE) can be useful in a variety of contexts where local high concentrations of proteins are required, such as polarity and signaling. Yet, many organisms lack DIX-LIKE domains. It is likely that other domains or strategies are used to assemble protein polymers. There are two other domains that interact head-to-tail like DIX: PB1 and SAM. The PB1 domain is structurally similar to DIX and can be found in animals, plants, fungi and amoebas. Not all PB1 domains form polymers, but they mediate several protein-protein interactions, some of which are involved in polarity (reviewed in Bienz, 2014). The SAM domain structure is different from DIX and PB1. This domain is present in all eukaryotic phyla and some bacteria and acts amongst others in signaling and transcriptional silencing (reviewed in Bienz, 2014). DIX, PB1 and SAM are versatile ‘polymerization blocks’ that can be found in various proteins within the same species, which enables interaction between different kinds

of proteins. As generating high local protein concentrations can be useful in various cellular processes, there may be additional common or protein-specific domains that mediate polymerization.

Molecular contexts as an indication for function

Functional analysis of proteins usually starts with mutagenesis and complementation of the corresponding gene. If the gene is picked up in a mutagenic screen, this process is relatively straightforward. However, new genes of interests are often picked up in other experiments, such as micro-arrays and IP-MS. Then, obtaining a mutant, especially one with a phenotype, can become quite the challenge. As we found out for our SOK genes (**Chapter 4**), insertion lines often do not have reduced mRNA levels. The number of insertion lines for a given gene is limited, and the large insertions make it difficult to predict how mRNA levels will be affected. Other ‘classical’ strategies, such as microRNA knockdown and TILLING have varying rates of success. CRISPR-Cas9 promises to be a great new tool for mutagenesis with its precise targeting and ability to introduce relatively small alterations to the DNA. Unfortunately, CRISPR proved to be surprisingly difficult in *Arabidopsis* compared to other species. Seemingly minor alterations, such as in the exact guideRNA composition (e.g. Liang et al., 2016), promoter sequence (e.g. Tsutsui & Higashiyama, 2017) and growth temperature (Le Blanc et al., 2017) can have a large effect on the CRISPR mutagenesis efficiency. In the past few years, a large body of publications provided the scientific community with for example improved vectors, better guideRNA efficiency predictions and kits to assemble multiple guides in one vector (reviewed in Ma et al., 2016). The latter allowed targeting multiple genes or gene sub-regions at the same time, thus improving the chance at mutagenesis and even higher order mutants. It is owing to all these improvements that we were able to obtain the *sok1* deletion mutant. Yet, gene redundancy probably caused the absence of a plant phenotype (**Chapter 4**). Multi-site CRISPR of the remaining SOK genes in the *sok1* deletion background will hopefully address this problem.

As mutagenesis of SOK proved to be a challenge, we addressed the molecular context of this protein family in **Chapter 6**. Such a strategy may not reveal the effect of SOKs on the plant level, but leads to a greater understanding of the cellular mechanisms SOK proteins are involved in. By using IP-MS, we identified a SOK interactome of mostly unstudied proteins. This shows that IP-MS can be a great tool to help identify novel pathways. Combining biochemistry with cell biology revealed that SOK proteins act as a polar scaffold that recruit other proteins to their domain in a DIX-LIKE dependent manner. The moss *Physcomitrella patens* has several SOK proteins, and at least one of them localizes to a cell edge (**Chapter 5**). *Marchantia polymorpha* contains a single copy of the ancestral SOK. It is not yet known if this

SOK has polar localization, accumulates in patches or puncta or shows an entirely different localization. Its DIX-LIKE domain is capable of polymerizing, which makes SOK complexes likely *in vivo*. At least several of the AtSOK interactors, such as AN, DLC and DYRK kinases are present in *Marchantia* and *Physcomitrella* as well (<https://phytozome.jgi.doe.gov>). IP-MS and cell biology studies with MpSOK and PpSOK will reveal whether they are capable of forming a complex with these putative interactors and whether the scaffolding-recruitment mechanism is conserved. Based on what is known about the interactors and their orthologs in other species, we proposed that SOK may be involved in organization of the cytoskeleton and/or mechanical stress. These hypotheses and interactors provide a great starting point to further elucidate the function of the SOK family, not only in *Arabidopsis* but also in more basal plants. Thus, although mutant studies are required for understanding the biological role of SOK and other proteins, unraveling the molecular mechanism provides valuable insight into how this role is accomplished on a cellular level throughout evolution.

Future impact of SOK investigations on cell polarity research and biotechnology

Unraveling the function of SOK is of great interest, but the protein family can also be used as tools to understand other biological processes. So far, only few polarly localized proteins have been identified in plants. In this thesis, we used IP-MS to identify interactors of three SOK family members (Chapter 6). Interestingly, one of these interactors showed a laterally polar localization. Thus, by using one polar protein as a bait, we found a new polar protein. When we used the polar interactor as bait to expand the interaction network, we identified yet another polar protein, and several others that are likely polar as well. These results show that IP-MS can be an excellent method to find polarly localized proteins. Tandem IP-MS and protein localization experiments could be used to expand and study the polar proteome, perhaps for other PM subdomains as well. This could lead to greater understanding of the establishment and maintenance of cell polarity, as well as of the function of proteins localizing to PM subdomains.

Plant polarity establishment and translation are not only processes of fundamental interest, but are also relevant issues for plant breeding and agriculture. For example, these processes are essential for regeneration of tissue cultures into new plants. Sometimes, generation of new crops or multiplication of existing ones is impeded by failing regeneration. The robust polar localization of SOK proteins makes them excellent markers for polarity and might be useful to investigate if and how polarity is established in crops. Naturally, similar experiments can be performed in model systems used in the lab. In *Arabidopsis*, SOK proteins switch polarity when a lateral root is formed, which indicates that they are able to follow a newly established

polar axis. Therefore, SOK may be used to study polarity switches in other tissues or model plants as well. In addition, little is known about the mechanism of polarity establishment and polar localization. Mutagenesis screens on plants expressing SOK and other polar markers could identify novel players in polar localization pathways.

In conclusion, establishment of plant cell polarity and its translation into sub-cellular processes are still poorly understood. This thesis introduces the novel SOSEKI (SOK) family of proteins that shows a polar localization to cell edges and recruits interactors to their polar domain. Our work indicates that robust polar axes are present in the plant, which proteins use to determine their sub-cellular localization. We showed that autocatalytic polymerization is useful both in a polarity and signaling context, and that it can be essential for protein function. Lastly, this work provided tools and techniques to improve our understanding of establishment and translation in the context of plant evolution.

References

Alassimone, J., Fujita, S., Doblas, V. G., Van Dop, M., Barberon, M., Kalmbach, L. et al. (2016). Polarly localized kinase SGN1 is required for Caspary strip integrity and positioning. *Nature Plants*, 2, 1–10.

Ambrose, C., Allard, J. F., Cytrynbaum, E. N., & Wasteneys, G. O. (2011). A CLASP-modulated cell edge barrier mechanism drives cell-wide cortical microtubule organization in *Arabidopsis*. *Nature Communications*, 2, 412–430.

Bienz, M. (2014). Signalosome assembly by domains undergoing dynamic head-to-tail polymerization. *Trends in Biochemical Sciences*, 39, 487–495.

Fischer, U., Ikeda, Y., Ljung, K., Serralbo, O., Singh, M., Heidstra, R. et al. (2006). Vectorial Information for *Arabidopsis* Planar Polarity Is Mediated by Combined AUX1, EIN2, and GNOM Activity. *Current Biology*, 16, 2143–2149.

Kirchhelle, C., Chow, C. M., Foucart, C., Neto, H., Stierhof, Y. D., Kalde, M. et al. (2016). The Specification of Geometric Edges by a Plant Rab GTPase Is an Essential Cell-Patterning Principle During Organogenesis in *Arabidopsis*. *Developmental Cell*, 36, 386–400.

Le Blanc, C., Zhang, F., Mendez, J., Lozano, Y., Chatpar, K., Irish, V., & Jacob, Y. (2017). Increased efficiency of targeted mutagenesis by CRISPR/Cas9 in plants using heat stress. *The Plant Journal*, 9, 377–386.

Liang, G., Zhang, H., Lou, D., & Yu, D. (2016). Selection of highly efficient sgRNAs for CRISPR/Cas9-based plant genome editing. *Scientific Reports*, 6, 21451.

Lukowitz, W., Roeder, A., Parmenter, D., & Somerville, C. (2004). A MAPKK Kinase Gene Regulates Extra-Embryonic Cell Fate in *Arabidopsis*. *Cell*, 116, 109–119.

Ma, X., Zhu, Q., Chen, Y., & Liu, Y. G. (2016). CRISPR/Cas9 Platforms for Genome Editing in Plants: Developments and Applications. *Molecular Plant*, 9, 961–974.

Matsuoka, K., Bassham, D. C., Raikhel, N. V., & Nakamura, K. (1995). Different sensitivity to wortmannin of two vacuolar sorting signals indicates the presence of distinct sorting machineries in tobacco cells. *Journal of Cell Biology*, 130, 1307–1318.

Men, S., Boutté, Y., Ikeda, Y., Li, X., Palme, K., Stierhof, Y. D., ... Grebe, M. (2008). Sterol-dependent endocytosis mediates post-cytokinetic acquisition of PIN2 auxin efflux carrier polarity. *Nature Cell Biology*, 10, 237–244.

Möller, B. K., ten Hove, C. A., Xiang, D., Williams, N., López, L. G., Yoshida, S. et al. (2017). Auxin response cell-autonomously controls ground tissue initiation in the early *Arabidopsis* embryo. *Proceedings of the National Academy of Sciences*, 114, E2533–E2539.

Mutte, S. K., Kato, H., Rothfels, C., Melkonian, M., Wong, G. K.-S., & Weijers, D. (2018). Origin and evolution of the nuclear auxin response system. *eLife*, 7, e33399.

Nakamura, M., & Grebe, M. (2018). Outer, inner and planar polarity in the *Arabidopsis* root. *Current Opinion in Plant Biology*, 41, 46–53.

Noack, L. C., & Jaillais, Y. (2017). Precision targeting by phosphoinositides: how PIs direct endomembrane trafficking in plants. *Current Opinion in Plant Biology*, 40, 22–33.

Payne, R. J. H., & Grierson, C. S. (2009). A theoretical model for ROP localisation by auxin in *arabidopsis* root hair cells. *PLoS ONE*, 4, e8337.

Rademacher, E. H., Möller, B., Lokerse, A. S., Llavata-Peris, C. I., Van Den Berg, W., & Weijers, D. (2011). A cellular expression map of the *Arabidopsis* AUXIN RESPONSE FACTOR gene family. *Plant Journal*, 68, 597–606.

Roppolo, D., De Rybel, B., Tendon, V. D., Pfister, A., Alassimone, J., Vermeer, J. E. M. et al. (2011). A novel protein family mediates Casparyan strip formation in the endodermis. *Nature*, 473, 381–384.

Schwarz-Romond, T., Fiedler, M., Shibata, N., Butler, P. J. G., Kikuchi, A., Higuchi, Y., & Bienz, M. (2007). The DIX domain of Dishevelled confers Wnt signaling by dynamic polymerization. *Nature Structural and Molecular Biology*, 14, 484–492.

Simon, M. L. A., Platret, M. P., Assil, S., Van Wijk, R., Chen, W. Y., Chory, J. et al. (2014). A multi-colour/multi-affinity marker set to visualize phosphoinositide dynamics in *Arabidopsis*. *Plant Journal*, 77, 322–337.

Simon, M. L. A., Platret, M. P., Marquès-Bueno, M. M., Armengot, L., Stanislas, T., Bayle, V. et al. (2016). A PtdIns(4)P-driven electrostatic field controls cell membrane identity and signalling in plants. *Nature Plants*, 2(7), 1–10. <https://doi.org/10.1038/NPLANTS.2016.89>

Tsutsui, H., & Higashiyama, T. (2017). PKAMA-ITACHI vectors for highly efficient CRISPR/Cas9-mediated gene knockout in *Arabidopsis thaliana*. *Plant and Cell Physiology*, 58, 46–56.

Ueda, M., Zhang, Z., & Laux, T. (2011). Transcriptional Activation of *Arabidopsis* Axis Patterning Genes WOX8/9 Links Zygote Polarity to Embryo Development. *Developmental Cell*, 20, 264–270.

Valitova, J. N., Sulkarnayeva, A. G., & Minibayeva, F. V. (2016). Plant Sterols: Diversity, Biosynthesis, and Physiological Functions. *Biochemistry. Biokhimiia*, 81, 819–834.

Van Norman, J. M. (2016). Asymmetry and cell polarity in root development. *Developmental Biology*, 419, 165–174.

Wang, H., Ngwenyama, N., Liu, Y., Walker, J. C., & Zhang, S. (2007). Stomatal Development and Patterning Are Regulated by Environmentally Responsive Mitogen-Activated Protein Kinases in *Arabidopsis*. *The Plant Cell*, 19, 63–73.

Yoshida, S., Barbier de Reuille, P., Lane, B., Bassel, G. W., Prusinkiewicz, P., Smith, R. S., & Weijers, D. (2014). Genetic control of plant development by overriding a geometric division rule. *Developmental Cell*, 29, 75–87.

Zhang, J.-Y., He, S.-B., Li, L., & Yang, H.-Q. (2014). Auxin inhibits stomatal development through MONOPTEROS repression of a mobile peptide gene STOMAGEN in mesophyll. *Proceedings of the National Academy of Sciences*, 111, E3015–E3023.

Summary

The evolution of multi-cellular plants went hand in hand with the establishment of a complex polarity system to guide development and survival. Within the cell, polarity cues need to be established, read and translated into sub-cellular processes. Yet, the exact mechanisms that translate polarity into sub-cellular processes remain elusive. In **Chapter 1**, we discuss polarity and several proteins that use polar information to guide their localization. The *Arabidopsis* embryo is introduced as an excellent model for studying cell polarity.

In **Chapter 2**, we take a closer look at development of the *Arabidopsis* embryo. Hereby we focus specifically on how oriented divisions are generated by developmental regulators and the division machinery. Recent advancement in 3D imaging of the embryo revealed that cell division abides to a ‘smallest plane’ rule, and that auxin can prevent adherence to this rule. Studying how auxin effectors are linked to cell division regulators and cell polarity may provide a greater understanding of oriented cell division in the embryo.

Using the *Arabidopsis* embryo as model for auxin-regulated development, we identify a novel family of polarly localized proteins in **Chapter 3**. Unlike previously published polar proteins, this new family shows a robust localization to specific cell edges, which coined the name SOSEKI (SOK, Japanese for cornerstone). SOK localization is guided by integration of plant-wide apico-basal and radial polarity. Pharmacological inhibition of pathways commonly used by polarly localized proteins showed that SOK is localized through a novel mechanism. Mis-expression of *SOK1* caused oblique cell divisions and polar localization was required for this activity. We identified a highly conserved N-terminal domain that structurally resembles the DIX domain found in Wnt polarity signalling proteins in animals (Ehebauer & Arias, 2009; Schwarz-Romond et al., 2007). In animals, this domain shows autocatalytic polymerization. SOK1 DIX-LIKE can dimerize and is required for polar edge clustering and biological activity, which shows that the fundamental function of DIX is conserved. Taken together, this chapter revealed a compass of polar axes that guides SOK polar edge localization. In addition, we showed that both plants and animals use the DIX domain in the context of polarity.

SOK showed striking localization and behavior, but nothing was known about the function of this protein family. In **Chapter 4**, we studied SOK function by generating *sok* mutants. We found that small mutations near the N-terminal end of *SOK1* sometimes caused fertility defects, but that larger deletions had no effect. The *sok1* deletion mutant showed upregulation of the *SOK4* gene, which suggests that there may be a compensation mechanism or feedback loop. The potential redundancy between SOK1 and SOK4 led to further investigation of SOK expression

and localization throughout the plant. Based on our findings, SOK2 and 3 may be redundant in the leaf, while SOK2, 3 and 5 overlap in the gynoecium.

As SOK was a completely novel protein family with unknown origin, we aimed to learn more about its evolutionary history. Therefore we investigated the protein sequence, properties and polar localization throughout plant evolution in **Chapter 5**. We showed that SOK first arose in early land plants, and that they contain several conserved domains that separate SOKs in an ancestral and a more recently evolved type. To assess the conservation of polarity, we studied four SOKs in the moss *Physcomitrella patens*. One of these tested PpSOKs showed polar edge accumulation in the gametophore, which suggests that edge polarity of SOK proteins is conserved throughout evolution. Next we performed phylogenetic and functional analysis on the DIX domain, which is the most highly conserved domain of SOK. Our results revealed that DIX is present in land plants, animals and the SAR group, and that it is capable of polymerization in all these clades.

The molecular context of a protein can reveal how it functions within the cell and how it obtains its localization. To address these questions in **Chapter 6**, we combined biochemistry and cell biology and identified shared and unique interactors of SOK1, SOK2 and SOK3. At least one of these interactors was recruited to the polar SOK1 site in a DIX-LIKE-dependent manner. We extended the network of interaction partners and found that SOK1 interacts with a network of laterally-polar proteins. The secondary interactors revealed links with amongst others the cytoskeleton. Based on these findings, we propose that DIX-like-mediated polymerization creates a polar scaffold that recruits interactors for local tasks. Such tasks may be modification of the cytoskeleton during cell growth or mechanical stress.

To conclude this thesis, the context and implications of our results were discussed in **Chapter 7**. In this discussion, we also provide an outlook for the future and suggestions for application of our results in research and biotechnology.

Nederlandse samenvatting

De evolutie van meercellige planten ging hand in hand met de ontwikkeling van een complex polariteitssysteem dat ontwikkeling stuurt. In de cel moeten polariteitssignalen worden geproduceerd, gelezen en vertaald naar sub-cellulaire processen. De exacte mechanismen die polariteit vertalen naar sub-cellulaire processen zijn echter nog niet bekend. In **Hoofdstuk 1** bespreken we polariteit en diverse eiwitten die polariteit gebruiken om hun lokalisatie te bepalen. Het embryo van *Arabidopsis* wordt geïntroduceerd als een excellent model om celpolariteit te bestuderen.

In **Hoofdstuk 2** kijken we in meer detail naar de ontwikkeling van het embryo in *Arabidopsis*. We focussen hierbij vooral op hoe georiënteerde celdeling wordt gestuurd door eiwitten die ontwikkeling regelen en door het celdelingsapparaat. De recente vooruitgang in 3D-imaging van het embryo liet zien dat celdeling zich houdt aan een ‘kleinste delingsvlak’ regel, en dat auxine kan voorkomen dat de cel zich aan deze regel houdt. De studie naar hoe auxine is gelinkt aan regulatoren van celdeling en celpolariteit kan leiden tot een beter begrip van georiënteerde celdeling in het embryo.

Door het embryo als een model te gebruiken voor auxine-gereguleerde ontwikkeling identificeren we een nieuwe familie van polair gelokaliseerde eiwitten in **Hoofdstuk 3**. In tegenstelling tot al bekende polaire eiwitten lokaliseert deze eiwitfamilie robuust in specifieke hoeken van de cel. Dit gedrag inspireerde hun naam: SOSEKI, wat Japans is voor hoeksteen. SOK lokalisatie wordt bepaald door integratie van apicaal-basale en radiale polariteit. Verstoring van mechanismen die de lokalisatie van andere polaire eiwitten reguleren liet zien dat SOK eiwitten een nieuw lokalisatiemechanisme gebruiken. Mis-expressie van SOK1 resulteerde in afwijkende celdelingen. Polaire lokalisatie was een voorwaarde voor deze activiteit. We hebben een sterk geconserveerd N-terminaal domein geïdentificeerd dat qua structuur lijkt op het DIX domein, dat onderdeel is van eiwitten betrokken bij Wnt polarity signalling in dieren (Ehebauer, & Arias, 2009; Schwarz-Romond et al., 2007). In dieren kan dit domein uit zichzelf polymeriseren. SOK1 DIX-LIKE kan dimeriseren en is nodig voor polaire clustering en biologische activiteit. Dit laat zien dat de fundamentele functie van DIX is geconserveerd. Alles bij elkaar genomen onthult dit hoofdstuk een kompas van polariteitsassen die nodig zijn voor SOK lokalisatie. Daarnaast hebben we laten zien dat zowel planten als dieren het DIX domein gebruiken in de context van polariteit.

SOK eiwitten hebben een opmerkelijke lokalisatie en gedrag, maar er was niets bekend over de functie van deze familie. In **Hoofdstuk 4** hebben we de functie van SOK bestudeerd door mutanten te maken van SOK. We vonden dat kleine mutaties

in de buurt van de N-terminus van SOK1 soms fertilitetsdefecten veroorzaakten. Grottere deleties hadden daarentegen geen effect. SOK4 had verhoogde expressie in de *sok1* deletiemutant, wat suggereert dat er een compensatiemechanisme of feedback loop is. De mogelijke redundantie tussen SOK1 en SOK4 leidde tot verder onderzoek naar SOK expressie en lokalisatie in de plant. Hieruit concludeerden we dat er mogelijke redundantie bestaat tussen SOK2 en 3 in het blad, en SOK2, 3 en 5 in het gynoecium.

SOK was een compleet nieuwe eiwitfamilie van onbekende afkomst, dus wilden we meer weten over de evolutionaire geschiedenis. Daarom hebben we de evolutie van de eiwitsequentie, eigenschappen en polaire lokalisatie onderzocht in **Hoofdstuk 5**. SOKs ontstonden in de eerste landplanten, en hebben verscheidene geconserveerde domeinen die SOK eiwitten verdelen in een ancestraal en meer recent type. Om de conservatie van polariteit te onderzoeken hebben we vier SOK eiwitten in het mos *Physcomitrella patens* bestudeerd. Een van deze vier had een polaire lokalisatie in de hoek van de cel, wat suggereert dat hoeklokalisatie van SOK eiwitten is geconserveerd in de evolutie. Vervolgens hebben we een fylogenetische en functionele analyse gedaan op het DIX domein, het meest geconserveerde domein in SOK. Onze resultaten lieten zien dat DIX aanwezig is in landplanten, dieren en de SAR groep, en in al deze groepen kan polymeriseren.

De moleculaire context van een eiwit kan onthullen hoe het eiwit werkt in de cel en hoe het zijn lokalisatie bepaalt. In **Hoofdstuk 6** combineerden we biochemie en celbiologie om deze vragen te beantwoorden. Deze aanpak identificeerde gedeelde en unieke interactoren van SOK1, SOK2 en SOK3. Ten minste een van deze interactoren werd gerekruiteerd naar de polaire SOK1. Hiervoor was het DIX domein nodig. Het interactor netwerk werd verder uitgebreid en hieruit bleek dat SOK1 interacteert met een netwerk van lateraal gelokaliseerde eiwitten. De secundaire interactoren zijn gelinkt aan onder andere het cytoskelet. Gebaseerd op deze bevindingen hebben we een model opgesteld: polymerisering van het DIX domein creëert een platform dat interactoren rekruiteert om lokaal taken uit te voeren, zoals wijziging van het cytoskelet tijdens celgroei of mechanische stress.

Als afsluiting van de thesis worden de context en implicaties van de resultaten besproken in **Hoofdstuk 7**. In deze discussie kijken we ook naar de toekomst en geven we suggesties voor toepassing van onze resultaten in onderzoek en biotechnologie.

Acknowledgements

Most people start their acknowledgements with their PhD. However, I will go a bit further back, because I have some people to thank that I started this amazing journey in the first place! Remko Offringa and team, thank you for introducing me to the wonderful world of plants and polarity. Niko Geldner, Joop Vermeer and all the team members in Lausanne, thank you so much for the great time and for inspiring me to do a PhD. It was one of the best decisions of my life.

Dolf, I do not know where to start thanking you. When we met during my search for a lab to write a grant proposal with and discussed the SOK project, I immediately knew that I wanted to work in your group. Your constant support, enthusiasm, input and dedication have been invaluable, and your dedication both to science and to your group are a great inspiration. I will fondly remember many little interactions, such as our chats during my regular visits to the drop candy jar in your office. Thanks for accepting me in your group and helping me grow into the scientist I am now.

The next person to thank is Sacco. Dag meneer! You were department head during the first years of my PhD. Together we enjoyed not only chats and discussions in the lab, but also a flight in your plane and a PhD trip to Barcelona. Thanks for everything.

They say today's new friend is tomorrow's family, and nothing could be more true about the Plant Development group. I could write an entire book about all the great moments that we shared. I immensely enjoyed the discussions, activities, chatter and support during my PhD. You are really a group that extends far beyond the lab and office. Our many amazing BBQs, poker nights, deep conversations, house warmings, lab weekends, filming crews, dinners and many more social activities are proof of that!

A special thanks goes to my colleagues and paranympths Tanya and Kuan-Ju. Tanya, you are a great friend and have been a wonderful support during my entire PhD. Thank you so much for your friendship, your help and patience. I am happy we get to work in the same place for another year! Kuan-Ju, I am so glad I met you. We started soon after each other, which was great for sharing experiences and support. You are a lovely friend and I wish you all the best in your personal and scientific life.

The Cool Office also deserves tons of my appreciation for their help, company and discussions. Margo, I loved our talks and wish you lots of fun building your future, both in Lego and in real life. Thijs, your calm company and support was much appreciated. Prasad, I was floored by your ability to endure my chatter in the office

Acknowledgements

and I really enjoyed our little jokes and conversations. My salutations also to Mark, we had many fun moments together. Thanks for all your help with the IP analysis.

To all my other colleagues in the group and the department: thank you so much for the great time, support, laughter, fun, help and all the experiences we shared, both personal and scientific. I learned a lot from everyone and will remember you with great fondness. Of course all former colleagues that already left the lab are included in this! Without this great environment my PhD would not have been half as enjoyable. Saiko, thank you for introducing me to the SOK project and helping me get started. I want to thank Jan Willem for all his help with confocal microscopy, the discussions and jokes. Also great appreciation for Laura. What would we do without your patient support?! Thanks to Sjef for all the mass-spec work and to Casper for diligently taking care of our precious plants. During my project, I got to work together with several people from other labs. I wish to thank them all for the pleasant collaboration, the discussions and great science.

Of course I will not forget to thank my wonderful students. It has been a joy to supervise you and help you to develop your scientific skills. Each of you made a great contribution to my project. I wish you all the best for the future!

During my PhD I received a lot of support from my friends. Especially Esther, Mariska and Jason, I cannot thank you enough for your patience and encouragement. For listening to my rants and celebrating the happy moments. You are amazing! All the people from Stedelijke Harmonie Wageningen also played a big part in keeping me happy and sane. Sharing my passion for music was a great way to relax and connect with a bunch of wonderful people.

Lieve familie. Jullie steun, aanmoediging en luisterend oor zijn de afgelopen jaren van onschabare waarde geweest. Ik moest zo nodig naar de universiteit en een PhD doen, en jullie hebben altijd achter me gestaan. Verhuizen naar Zetten was een klus, maar door de vele bezoekjes en tefeloontjes was ik nooit echt ver weg. Ontzettend bedankt voor al jullie liefde, interesse en geduld!

Curriculum vitae

Maritza van Dop was born on the 25th of November, 1988 in De Lier, The Netherlands. She went to High School in Delft, where she graduated at Grotius College. In 2007 she started a Bachelor in “Pedagogiek” in Leiden, but soon discovered that her true call lied in studying the inner workings of animals and plants. In 2008, she started a Bachelor in Biology in Leiden, followed by a Msc focused on Molecular and Cellular Bioscience at the same university. Research on plants had caught her interest, and her first MSc thesis in the Plant Developmental Genetics group of Prof. Dr Remko Offringa introduced her to the field of cell polarity. Fascinated by polar proteins, she pursued an internship in group of Prof. Dr Niko Geldner at the Department of Plant Molecular Biology, Lausanne University in Switzerland. Here, she studied the polarly localized SGN1 kinase. In 2013, Maritza obtained her MSc degree. Her passion for research and cell polarity led her to join the EPS Graduate Programme, in which she wrote a PhD grant together with Prof. Dr Dolf Weijers. This grant was awarded to her and early 2014, Maritza started her PhD project on the edge localized SOSEKI proteins in the Laboratory of Biochemistry, Wageningen University. The results of this project are presented in this thesis.



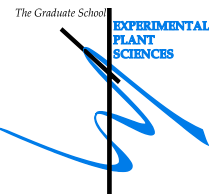
Publications

Publications

Yoshida, S. , **van Dop, M.**, van der Schuren, A., van Galen, L., Saiga, S., Adibi, M., Möller, B., Marhavy, P., Smith, R., Friml, J. & Weijers, D. (2018). SOSEKI polarity determinants reveal mechanisms of supra-cellular polarity in *Arabidopsis*. *Submitted*.

Alassimone, J., Fujita, S., Doblas, V. G., **Van Dop, M.**, Barberon, M., Kalmbach, L., Vermeer, J. E. M., Rojas-Murcia, N., Santuari, L., Hardtke, C. S., Geldner, N. (2016). Polarly localized kinase SGN1 is required for Casparyan strip integrity and positioning. *Nature Plants*, 2, 1–10.

van Dop, M., Liao, C. Y., & Weijers, D. (2015). Control of oriented cell division in the *Arabidopsis* embryo. *Current Opinion in Plant Biology*, 23, 25–30.



Education Statement of the Graduate School

Experimental Plant Sciences

Issued to: Maritza van Dop
 Date: 07 September 2018
 Group: Laboratory of Biochemistry
 University: Wageningen University & Research

1) Start-up phase	<u>date</u>
► First presentation of your project Shouting from the corner: directing cell polarity and oriented division	Dec 2013
► Writing or rewriting a project proposal Shouting from the corner: directing cell polarity and oriented division	Nov 2013
► Writing a review or book chapter Review: Control of oriented cell division in the Arabidopsis embryo. Current Opinion in Plant Biology, (2015) 23:25-30, DOI: 10.1016/j.pbi.2014.10.004	Feb 2015
► MSc courses	
► Laboratory use of isotopes	
► Laboratory use of isotopes	

Subtotal Start-up Phase 13.5 credits*

2) Scientific Exposure	<u>date</u>
► EPS PhD student days EPS PhD day 'Get2Gether' 2015, Soest, NL EPS PhD day 'Get2Gether' 2016, Soest, NL	29-30 Feb 2015 15-16 Feb 2018
► EPS theme symposia EPS theme 1 'Developmental biology of plants', Leiden, NL EPS theme 1 'Developmental biology of plants', Wageningen, NL EPS theme 1 'Developmental biology of plants', Wageningen, NL	08 Jan 2015 21 Jan 2016 30 Jan 2018
► National meetings (e.g. Lunteren days) and other National Platforms Annual meeting 'Experimental Plant Sciences', Lunteren, NL Annual meeting 'Experimental Plant Sciences', Lunteren, NL Annual meeting 'Experimental Plant Sciences', Lunteren, NL Annual meeting 'Experimental Plant Sciences', Lunteren, NL	14-15 Apr 2014 13-14 Apr 2015 11-12 Apr 2016 10-11 Apr 2017
► Seminars (series), workshops and symposia Seminar: Dr. Alexis Maizel Seminar: Dr. Ivonne Stahl Seminar: Dr. George Bassel Seminar: Dr. Jennifer Nemhauser Seminar: Dr. Cyril Zipfel Seminar: Dr. Doris Wagner Seminar: Dr. Saijaliisa Kangasjärvi Seminar: Dr. Martin Jinek Seminar: Dr. François Parcy Seminar: Dr. Julia Santiago	08 Mar 2014 11 Mar 2014 24 Apr 2014 20 Mar 2014 04 Jun 2014 11 Dec 2014 28 May 2015 06 Jun 2015 15 Oct 2015 12 Nov 2015

Education Statement

<i>Seminar:</i> Dr. Mark Estelle	07 Apr 2016
<i>Seminar:</i> Dr. Jill Harisson	12 May 2016
<i>Seminar:</i> Dr. Helene Robert	03 Jun 2016
<i>Seminar:</i> Dr. Jose Gutierrez-Marcos	07 Mar 2016
<i>Seminar:</i> Dr. Chun-Ming Liu	21 Jun 2016
<i>Seminar:</i> Dr. Sabine Müller	09 Sep 2016
<i>Seminar:</i> Dr. Lars Ostergaard	21 Dec 2016
<i>Seminar:</i> Dr. Gerd Jürgens	11 May 2017
<i>Seminar:</i> Dr. Katharina Bürstenbinder	01 Jun 2017
<i>Seminar:</i> Dr. Arnold Boersma	19 Jun 2017
<i>Seminar:</i> Dr. Manuel Juette	05 Sep 2017
<i>Joint Meeting:</i> groups of prof. Dolf Weijers and prof. Ben Scheres, Wageningen, NL	25 Sep 2015
<i>Joint Meeting:</i> groups of prof. Dolf Weijers and prof. Ben Scheres, Wageningen, NL	22 Jan 2016
<i>Symposium:</i> Systems biology for Food, Feed and Health, Wageningen, NL	24 Jun 2014
► Seminar plus	
► International symposia and congresses	
EMBO Conference Series 'Interdisciplinary Plant Development', Cambridge, UK	21-24 Sep 2014
Gordon Research Conference on Plant Cell Walls, Waltham, MA, USA	12-17 Jul 2015
EMBO workshop 'New model systems for early land plant evolution', Vienna, Austria	22-24 Jun 2016
Annual meeting programme SEB, Gothenburg, Sweden	03-06 Jul 2017
► Presentations	
<i>Talk:</i> Graduate School Uitgangsmaterialen proposal defense: Shouting from the corner: directing cell polarity and oriented division	18 Nov 2013
<i>Talk:</i> Netwerkdag TKI Uitgangsmaterialen: Regulatoren van polariteit en celdeling in de hoek gezet	12 May 2014
<i>Talk:</i> Haigerloch 4.0 Embryo meeting: Where cell polarity meets oriented cell division	12 May 2015
<i>Talk:</i> Annual Meeting 'Experimental Plant Sciences' 2017: Shouting from the corner - a novel family of polar proteins	11 Apr 2017
<i>Talk:</i> Invited speaker John Innes Center, Norwich, UK	05 Jun 2017
<i>Talk:</i> Annual meeting programme SEB Gothenburg: Dissection of a novel plant cell polarity pathway	03 Jul 2017
<i>Talk:</i> EPS Theme 1 'Developmental biology of plants': Characterization of SOSEKI polar proteins	30 Jan 2018
<i>Poster:</i> EMBO workshop 'New model systems for early land plant evolution': Deep conservation of a family of unique polar proteins	22 Jun 2016
► IAB interview	
► Excursions	
EPS excursion to Enza Zaden	12 Jun 2015

Subtotal Scientific Exposure

*20.1 credits**

3) In-Depth Studies

► EPS courses or other PhD courses	<i>date</i>
Postgraduate Course 'Microscopy and Spectroscopy in Food and Plant Sciences', Wageningen, NL	06-09 May 2014
Postgraduate Course 'Transcription Factors and Transcriptional Regulation', Wageningen, NL	12-14 Dec 2016
6th International Advanced Course Proteomics, Wageningen, NL	01-04 May 2017
► Journal club	
Weekly Journal club, Laboratory of Biochemistry	2014-2018
► Individual research training	

*Subtotal In-Depth Studies 6.6 credits****4) Personal development**

► Skill training courses	<i>date</i>
Project and Time Management, Wageningen, NL	Mar-May 2015
SciFund Challenge online course: Outreach	Oct-Nov 2015
Scientific Artwork with Photoshop and Illustrator, Wageningen, NL	19-20 Sep 2016
Microsoft online course: Introduction to R for Data Science	Dec 2017
► Organisation of PhD students day, course or conference	
► Membership of Board, Committee or PhD council	

*Subtotal Personal Development 3.6 credits****TOTAL NUMBER OF CREDIT POINTS*** 43.8

Herewith the Graduate School declares that the PhD candidate has complied with the educational requirements set by the Educational Committee of EPS which comprises of a minimum total of 30 ECTS credits

* A credit represents a normative study load of 28 hours of study.

The research presented in this thesis was performed at the Laboratory of Biochemistry, Wageningen University & Research, and was financially supported by a grant from the Netherlands Organization for Scientific Research (NWO; ALW-Topsector grant 831.13.001).

Financial support from the Laboratory of Biochemistry for printing this thesis is gratefully acknowledged.

Cover design: AgileColor Design Studio/Atelier || AgileColor.com
Layout design: Tatyana Radoeva, Maritza van Dop
Printed by: GVO drukkers & vormgevers, Ede (NL) || gvo.nl

